2018-04-30

Identification of dipeptidase-1 as an organ-selective adhesion receptor utilized by neutrophils and metastatic cancer cells in the liver and lungs

Roy Choudhury, Saurav

UNIVERSITY OF CALGARY

Identification of dipeptidase-1 as an organ-selective adhesion receptor utilized by neutrophils

and metastatic cancer cells in the liver and lungs

by

Saurav Roy Choudhury

A THESIS

SUBMITTED TO THE FACULTY OF GRADUATE STUDIES

IN PARTIAL FULFILMENT OF THE REQUIREMENTS FOR THE

DEGREE OF DOCTOR OF PHILOSOPHY

GRADUATE PROGRAM IN MEDICAL SCIENCE

CALGARY, ALBERTA

APRIL, 2018

Abstract

Lungs and liver are two major sites of neutrophil trafficking and inflammatory disease. Neutrophil recruitment in response to an inflammatory cue is a sequentially coordinated process where adhesion molecules expressed on the endothelium of a given organ mediate different steps in the classical leukocyte recruitment cascade [1]. However, molecules identified as being central in the canonical schema of neutrophil recruitment to different organs (mesentery, skin, and cremaster muscle) are not required in the inflamed pulmonary and hepatic vasculatures [2-8]. Using an unbiased functional screen *in vivo,* we isolated a peptide-displaying phage that homed to the liver and lungs of mice treated with a bacterial inflammatory stimulus (lipopolysaccharide). Employing intravital microscopy, we found that this phage, or its corresponding displayed-peptide, termed LSALT herein, inhibited the adhesion of neutrophils in the inflamed lungs and liver vasculatures in response to LPS. The corresponding synthetic peptide also reduced the metastatic colonization of melanoma cells to the lungs in human xenograft and immunocompetent mouse models. Using biochemical, genetic and confocal intravital imaging approaches we identified dipeptidase-1 (DPEP1) as the functional target of this peptide and established its role as a physical adhesion receptor for neutrophil and metastatic cancer cell adhesion independent of its enzymatic activity. Importantly, genetic ablation or functional peptide blocking of DPEP1 significantly reduced neutrophil recruitment and cancer metastasis to the lungs and liver, and in models of Acute Respiratory Distress Syndrome (ARDS), prevented septic lung injury and mortality. This study identified DPEP1 as an organ-selective vascular endothelial adhesion receptor for the recruitment of neutrophils and metastatic cancer cells to the lungs and liver and identifies DPEP1 as a novel therapeutic target for systemic inflammatory disorders as well as organ-selective metastatic diseases.

Graphical abstract
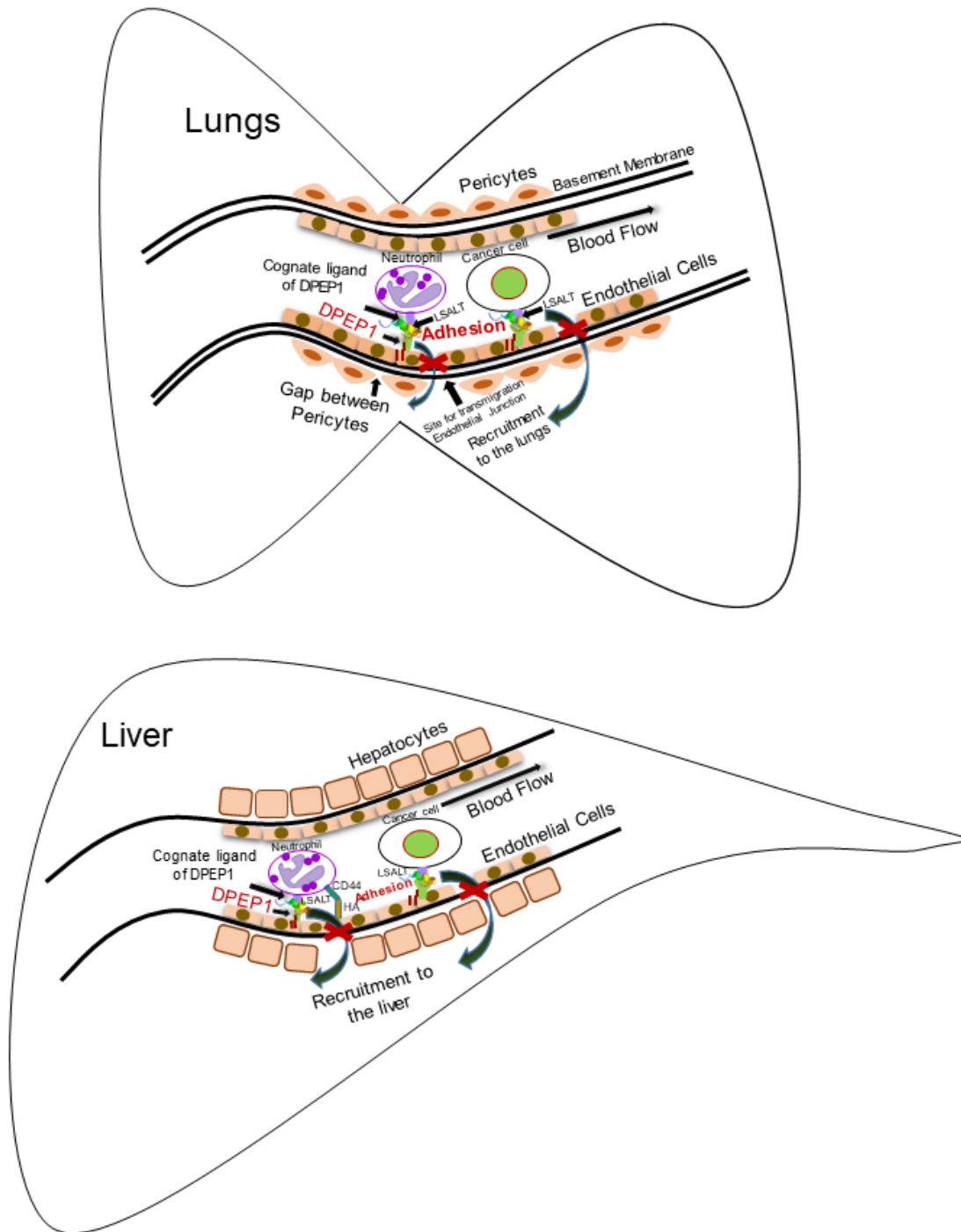
Thesis Objective

At the time when this thesis project was initiated, the underlying mechanism of cell recruitment to the lungs and liver were unknown. This study was initiated and driven based on an observation that lungs and liver use additional (non-canonical) adhesion molecules for organ selective endothelial binding and recruitment. Despite the established role of classical adhesion receptors (selectins and integrins) in the neutrophil recruitment cascade in the mesentery, skin and cremaster muscle, studies as well as observations by Dr. Paul Kubes and colleagues at the University of Calgary demonstrated that the recruitment of neutrophils were not impaired in the lungs and liver of mice that were deficient in either of these families of classical adhesion receptors. These observations led to the notion that, there are additional molecules involved in the lungs and liver vascular beds that mediate the recruitment of neutrophils to these organs. In 2008, McDonald et al. provided evidence that the interaction of neutrophil-CD44 and endothelial-hyaluronan is a dominant mechanism for the sequestration of neutrophils to the inflamed hepatic sinusoids [3]. These observations provided the initial foundation of this study focusing on the central objective to identify novel adhesion molecules expressed on the surface of inflamed pulmonary and hepatic vascular beds that play a requisite role in the recruitment of neutrophils to these organs in response to inflammation. Employing biochemical, genetic and confocal intravital imaging approaches this study has identified DPEP1 as a major adhesion receptor for the organ-selective recruitment of neutrophils and metastatic cancer cells to the lungs and liver.

Preface

A major part of the work presented in this thesis was recently submitted to *Cell* and is currently under revision.

1. ***In vivo screen identifies Dipeptidase-1 as a major adhesion receptor for organ-selective neutrophil recruitment in inflamed pulmonary and hepatic vasculatures.***

Saurav Roy Choudhury, Liane Babes, Jennifer J. Rahn, Bo Young Ahn, Kimberly-Ann R. Goring, Xiaoguang Hao, Andrew K. Chojnacki, Ajitha Thanabalasuriar, Arthur Lau, Erin F. McAvoy, Sébastien Tabariès, Kamala D. Patel, Peter M. Siegel, Daniel A. Muruve, Bryan G. Yipp, Paul Kubes , Stephen M. Robbins and Donna L. Senger *(under revision in Cell)*

In addition to this study, a second manuscript is also presently in preparation. This study demonstrates a novel role of a lung and liver homing peptide (termed LSALT herein) in organ-selective metastatic disease in pre-clinical mouse models. In addition, the findings of this study also identified Dipeptidase-1 as novel mediator of organ-selective metastasis in the lungs and liver. The significant part of this manuscript is presented in different sections of this thesis.

2. ***Dipeptidase-1, a central mediator of organ-selective metastasis to the lungs and liver.***

Saurav Roy Choudhury, Jennifer J. Rahn, Xiaoguang Hao, Xueqing Lun, Liane Babes, Bo-Young Ahn, Kimberly-Ann R. Goring, Ngoc Ha Dang, Jennifer King, Sébastien Tabariès, Peter M. Siegel, Stephen M. Robbins and Donna L. Senger *(in preparation)*

3. *Immune Surveillance by Renal Phagocytes and Tubular Dipeptidase-1 are Essential for Contrast-Induced Acute Kidney Injury.*

Arthur Lau, Hyun Jae Chung, Takanori Komada, Jaye M. Platnich, Christina F. Sandall, Saurav R. Choudhury, Justin Chun, Victor Naumenko, Bas G.J. Surewaard, Michelle C. Nelson, Annegret Ulke-Lemée, Paul L. Beck, Hallgrimur Benediktsson, Anthony M. Jevnikar, Sarah L. Snelgrove, Michael J. Hickey, Donna L. Senger, Matthew T. James, Justin A. Macdonald, Paul Kubes, Craig N. Jenne, Daniel A. Muruve (*resubmitted to Journal of Clinical Investigation)*

Acknowledgements

The scientific observations presented in this thesis represent a phenomenon that goes beyond the biological parameters. The results unveiled here in this thesis was only feasible from the enormous support and immense dedication from a long list of individuals over the last few years. First and foremost, I would like to express my sincere gratitude to my supervisor Dr. Donna Senger, for her guidance, patience, support, advice and constant encouragement throughout the course of this thesis. Despite the regular complexities in a scientific pursuit, Donna has always inspired me with a positive attitude to consider the 'big picture' situations. The extended list of things that I had learned from Donna over the years is difficult to elucidate. To mention a few: '*science is all about troubleshooting*', '*three most important things to remember in science: What (research question), Why (rationale), and How (experiments)*, '*PhD is not about doing experiments and getting data, it's about thinking differently*'. The following quote of Socrates may summarize my learnings from Donna: *"understanding a question is half an answer"-Socrates, Essential Thinker.* I want to express my deepest appreciation to Dr. Stephen Robbins for his invaluable guidance and motivational suggestions during the course of my PhD tenure. His innovative ideas and thoughtful interpretations about diverse scientific questions has helped me to learn and acquire divergent thinking.

I would also like thank my supervisory committee members, Drs. Kubes, Morris and Schriemer for providing me the valuable guidance and helpful suggestions throughout my PhD tenure. This thesis would never have been possible without the indispensable collaborative contributions from several laboratories within the Cumming School of Medicine at the University of Calgary. The invaluable collaboration with Dr. Paul Kubes provided me the platform to perform my intravital microscopy imaging studies throughout my PhD. In addition, collaborations with Dr.

Bryan Yipp's and Dr. Daniel Muruve's, laboratories had also provided important insights with regards to my thesis project during the course of my PhD tenure. I thank Dr. Kamala Patel and Dr. Peter Siegel for their collaborations. I would also like to thank the Live Cell Imaging facility within the Snyder Institute for Chronic diseases for providing me the opportunity to perform my imaging experiments. I would like to acknowledge Kids Cancer Care Foundation for providing me with a graduate studentship during my PhD tenure.

I am grateful to Dr. Jennifer Rahn, a teacher in every aspect who has helped in numerous different areas during my PhD tenure. I would like to thank Dr. Liane Babes for dedicating her countless hours for assisting me in my intravital imaging experiments throughout my PhD. I would also like to thank Mana Alshehri, Dr. Astrid De Boeck and Dr. Bo Young Ahn for their constant help and support during my PhD tenure. I am also grateful to the all the lab members that have passed through the Senger and Robbins laboratories during the course of my PhD: Wale Olyeusi, Jun Zhang, Xiaoguang Hao, Eva Ujack, Juan Carlos Corredor, Xiuling Wang, Ngoc Ha Dang, Kevin Zhou, Kimberley-An Ruth Goring, Charlotte D'Mello, Jennifer King, Lauren Wierenga, Xueging Lun. I would also like to thank my friends, Satbir, Soumya, Kunal, Ranjan, Abhishek, Manoj and their extended families whose support has helped me immensely during my stay in Calgary. I would like to express my deepest gratitude to my mother whose values and infectious attachment with my education has inspired me to always achieve the impossible from my childhood days. I would not be what I am today without the love, teachings, dedication and support of my late father and grandmother. Finally, I would like to thank my wife Debarati for being an incredible friend and partner, her perseverance, sacrifices and dedication during the course of my finishing years in PhD is unexplainable.

Dedication

To my father

Table of Contents

List of Tables

List of Figures and Illustrations

Chapter One: General Introduction

1.1 Immune cell recruitment in inflammation: Initial observations and the era of Cohnheim and Metchnikoff.

Recruitment of innate immune sentinels to a site of injury or infection as a key process during inflammation was conceived and established in the nineteenth century [9-10]. Despite several limitations, scientists in the nineteen hundreds were able to visualize the emigration of white blood cells from the vasculature to an inflamed tissue [11]. However, initial intravital microscopy using trans-illumination only allowed limited understanding of the recruitment process in certain organs (such as the mesentery). Due to the limitations, visualization and understanding of cellular infiltration in other major organs (such as lungs and liver) during inflammation was not feasible for a number of years. A significant advancement in *in vivo* imaging in the past two decades have provided substantial progress in the molecular understanding of cell recruitment [12-14]. This study was originated and focused to understand the underlying mechanisms of cell recruitment to the lungs and liver.

The concept of inflammation dates back to the ancient Egyptian and Greek cultures. Hippocrates, a Greek physician considered to be the 'father of medicine' first introduced the term 'edema' in the 5th century BC and described inflammation as a process of tissue healing after injury [15]. Aulus Cornelius Celsus, a roman encyclopeadist, first described the cardinal features of inflammation in the first century AD and *rubor et tumor cum calore et dolore* (redness and swelling with heat and pain) were the first documented signs of inflammation [16-18]. Galen and then Virchow in the third century AD provided the humoral aspects of inflammation and in 1871 the fifth cardinal feature of inflammation- 'function laesa' (loss of function) was added [17-18]. As mentioned, a real acceleration in our cell-based understanding of inflammation occurred upon the development of microscopic techniques. Julius Cohnheim, a German pathologist, first described

the physiological basis of inflammation when he visualized the emigration of white blood cells from the blood vessels into a tissue during an inflammatory response in the mesentery of a frog tongue pinned on a corkboard [11]. His seminal observations included the dilation of blood vessels, adhesion of transparent white blood cells on the surface of endothelial cells and their subsequent transmigration during an inflammatory response thus establishing some of the fundamental basis of inflammation [9]. Based on these observations, he proposed extravasation of white blood cells was a consequence of an inflammatory insult in the blood vessel wall that is generated by either an irritant or an infectious stimulus. To further investigate this idea he studied ischemia reperfusion injury and suggested that leukocyte extravasation was a result of tissue autonomous inflammation and stated "inflammation is a result of molecular change in the vessel wall" [19]. Inflammation (from the latin word *inflammare* meaning 'to set on fire') was later defined as a protective response triggered to either a foreign pathogenic substance or to a sterile injury insult resulting in the recruitment of subpopulations of activated immune sentinels from the blood to a tissue that results in the generation of heat, redness, swelling and pain. Based on a number of characteristics and the cell types involved, inflammation was divided into two broad sub-categories, acute and chronic. Acute inflammation is short-term and in most cases lasting for a few days. Neutrophils, known as the soldiers of the immune system, are the primary innate immune sentinels in acute inflammation. In contrast, chronic inflammation is a long-lasting ongoing inflammatory response that is primarily characterized by tissue infiltration of other immune cell types such as monocytes and lymphocytes.

Beside Cohnheim's early studies, a significant contribution of another pathologist named Elie Metchnikoff (also known as Ilya Mechnikov), a Russian zoologist/pathologist were influential in uncovering some fundamental aspects of inflammation [20]. Metchnikoff, considered to be the father of cellular immunology, initially described phagocytosis as the process of tissue digestion.

Based on his experimental observations later, he described phagocytosis as a general mechanism of host defense [20-24]. He termed the white corpuscles in lymphoid glands as "lymphocytes" and the other blood cells and exudates as "macrophages (monocytes)" and microphages (granulocytes). In his experimental observations he witnessed that in inflamed tissues, macrophage and neutrophils can phagocytose crystals and bacteria. He also observed that the injection of bacilli into the blood stream significantly enhanced the number of circulating neutrophils [23-24]. In addition, Metchnikoff and colleagues observed the chemotactic behavior of neutrophils either in the presence of an inflammatory stimulus or in response to a bacterial infection in frogs and Mexican salamander (*Ambystoma mexicanum*) that helped provide a substantial insight into the overall understanding of inflammation [22-24]. He described leukocyte trafficking through the vessel wall as a process that consisted of chemotactic behavior, adhesive cellular and molecular interactions between immune cells with the vascular endothelium, and emigration of leukocytes from the vessel wall to tissues in response to inflammation, the first documented steps now known as the classical leukocyte adhesion cascade [23-24].

1.2 The classical neutrophil recruitment cascade during inflammation.

The sequential recruitment of leukocytes across a vessel wall and into an inflamed tissue was first described in the late nineteenth century when three major steps of the leukocyte adhesion cascade were identified as rolling, adhesion and transmigration [22-24]. Over the past three decades the identification of adhesion molecules and their respective ligands that mediate each of these events has enhanced the overall understanding of inflammation [1, 25]. Neutrophils are the most predominant type of granulocytes/polymorphonuclear leukocytes in mammals. These white blood cells are invariably the first leukocyte cell populations that are recruited to the site of injury or infection [1, 26]. Proteins involved in this process were discovered through the assessment of

neutrophil recruitment in the skin, mesentery and cremaster and have formulated our understanding of the classical recruitment cascade [27-29]. This process begins when neutrophils bind to the selectins (P-selectin, E-selectin), a family of glycoprotein-cell adhesion molecules stored within the endothelial cell granules (Weibel-Palade bodies) [30-31] that are expressed on the luminal endothelial surface in response to inflammatory cues (interstitially released cytokines, chemokines, bacterial endotoxins, cysteinyl leukotrienes from tissue resident leukocytes in the presence of an infection) [25]. Interaction of the selectins or "tethering" occurs through binding of the selectin to their corresponding ligand (PSGL1) present on the surface of circulating neutrophils, and a process termed 'rolling' is initiated [25] where the neutrophil rolls along the vessel wall in the direction of blood flow [25]. Heparin sulfate proteoglycans, a family of extracellular matrix proteins composed of a complex of negatively charged polysaccharide chains, capture the interstitially released/secreted positively charged chemokines that are presented across the endothelium to the apical endothelial cell surface by a process termed transcytosis [25]. Subsequent activation of G-protein coupled chemokine receptors on neutrophils induce a conformational change in integrin structure on the surface of neutrophils that changes the inactive bent confirmation of the integrin to a more active and open confirmation necessary for ligand binding [32]. Activation and subsequent binding of neutrophil integrins (LFA1 and Mac1) to their corresponding ligands (ICAM1, ICAM2) present on the inflamed endothelial cells leads to a state where neutrophils strongly attach/bind to the endothelial cell surface without rotational movement [1]. This strong covalent attachment in affinity (avidity) results in adhesion. The firmly adhered neutrophil then crawls along the endothelium in an elongated manner for transmigration [25]. The exact molecular mechanism of crawling under shear is poorly understood but occurs at least in part through the interaction of Mac-1 and ICAM-1 by VAV-1, a Rho GTPase [33-34]. Crawling of

neutrophils also involves mechanotactic mechanisms as the neutrophil senses the shear force [32-34]. CDC42, a cell cycle regulator, has been shown to play a crucial role in the migration and polarization of neutrophils [34]. Although it is necessary for the neutrophil to release some of the adhesive bonds at this stage in order to move, they remain firmly adhered to the endothelium with the interaction of integrins (high affinity confirmation) with the actin cytoskeleton forming the foundation of crawling under shear stress.

Next, to transmigrate, the neutrophil undergoes a sequence of events that involves crossing the endothelial barrier and the basement membrane. Transmigration of neutrophils is largely governed by the interaction of integrins with various cell adhesion molecules (ICAM-1, ICAM-2, and VCAM-1) expressed on the endothelium [25] as well as the junctional adhesion molecules (JAMs) and platelet/endothelial cell adhesion molecule-1 (PECAM-1) present along the junctions of the endothelial cells [25]. Most neutrophils follow the paracellular route of diapedesis and transmigrate between two endothelial cells [35] through tri-cellular junctions [36-37]. Although paracellular transmigration has been shown by a number of *in vitro* paradigms, *in vivo* evidence of this route of transmigration remains elusive. Since few junctional proteins are present *in vitro* and the endothelial cell organization does not mimic the more complex *in vivo* scenario, *in vivo* imaging studies will be essential to elucidate these behaviors and to understand the molecular basis of paracellular transmigration. An alternative pathway for neutrophil transmigration is the transcellular route where neutrophils pass through a single endothelial cell. This involves the formation of a cup like projection on the top of a neutrophil called a dome [38]. ICAM-1 and VCAM-1 enriched microvilli-like protrusions are essential to form these dome like structures around the adherent neutrophil in an LFA-1 and VLA-4 dependent manner [39-40]. This process also depends on the leukocyte specific protein (LSP-1), an intracellular F-actin binding protein

expressed by resting endothelial cells [39]. Although, a number of *in vitro* observations have suggested the formation of domes in transcellular diapedesis [39], these observations still need to be confirmed *in vivo*. Rearrangement of the actin cytoskeleton in neutrophils, and their subsequent association with the extracellular matrix by focal adhesion proteins, connects the endothelial cells to the extracellular matrix [41-42]. Expression of neutrophil proteases such as matrix metalloproteinases (MMP-9), and serine proteases (neutrophil elastase) assist in degradation of the basement membrane [41-42] thereby allowing the neutrophil to migrate between the pericyte-wrapped endothelial cells, crawling actively by a Mac-1/LFA-1-ICAM-1 dependent manner in order to hunt for gaps through which they can leave the vasculature [43].

Although the well-documented steps of classical recruitment of neutrophils (within the mesentery and then in the skin and muscle) during inflammation were established as early as the nineteenth century, recruitment of neutrophils to other organs such as the lungs and liver have been understudied due to the limitations of high resolution imaging and the lack of advanced microscopic techniques. Based on several observations using monoclonal antibodies and gene knockout mouse models, together with intravital imaging, support for the existence of a non-canonical neutrophil recruitment mechanism within the inflamed pulmonary and hepatic vasculatures are beginning to emerge [44-45].

1.3 Adhesion molecules in leukocyte recruitment and inflammation.

Monoclonal antibody directed identification of adhesion molecules contributed significantly to the discovery of adhesion receptors that mediate the classical recruitment of leukocytes in response to various inflammatory stimuli. From the pioneering work of Julius Cohnheim and Elie Metchnikoff, it was well-established that leukocytes bind to the surface of inflamed endothelial cells prior to their transit from the blood to tissues during inflammation [23-

20

24]. However, the identification of the molecular players involved in the sequential series of events that occurred during leukocyte adhesion was largely unknown. In the 1980's several research groups started investigating the molecular basis underlying leukocyte adhesion with a major impetus on identifying molecules that mediate the different steps of leukocyte recruitment. To identify cell surface molecules that mediate adhesion and homing of lymphocytes, Gallatin and Butcher generated a monoclonal antibody (Mel-14) against a high endothelial venule (HEV) binding lymphoma [46]. This antibody was shown to functionally inhibit the homing and adhesion of lymphocytes in the peripheral lymph node HEV and the binding of lymphoma cells *in vitro* through its recognition of an antigen present on the surface of the lymphocytes and lymphoma cells [47]. Several years later it was determined that Mel-14 recognized a cell surface glycoprotein expressed on the majority of leukocytes and hence was named 'Leukocyte selectin' or L-selectin. L-selectin, also known as CD62L, LAM-1, LECAM-1, gp90MEL, DREG, is the sole example of a selectin that mediates leukocyte recruitment in lymphatic tissues. Using a similar strategy, Bevilacqua and Gimbrone reported the generation of two monoclonal antibodies called H18/7 and H4/18 that recognized an antigen on the surface of cytokine and endotoxin-stimulated human endothelial cells (HUVEC) *in vitro* but not their unstimulated counterparts [48]. As these monoclonal antibodies were found to inhibit the adhesion of polymorphonuclear leukocytes, and HL-60 human promyelocytic leukemia cell line, to stimulated HUVEC monolayers *in vitro*, the name endothelial-leukocyte adhesion molecule 1 (ELAM-1) was proposed for the antigenic epitope of these antibodies [49]. ELAM-1 later known as E-selectin, CD62E, and LECAM-2 is expressed predominantly by endothelial cells and is regulated transcriptionally by pro-inflammatory cytokines IL-1β and TNF-α [50]. Three years later, Rodger McEver's group at the University of Oklahoma, described an unique adhesion process of neutrophils mediated by a

protein they named GMP-140 (Granule Membrane Protein-140) [51]. This molecule was found to be localized on the plasma membrane of endothelial cells upon activation (PMA and histamine) and degranulation [50]. In this study, Geng et al. showed that neutrophils, and HL-60 cells, bound to both COS cells expressing GMP-140 and activated HUVEC in *in vitro* adhesion assays [52]. Interestingly, GMP-140 shared significant structural homology and functional similarities with the molecules identified by Gallatin and Butcher, and Bevilacqua and Gimbrone, and thus, GMP-140 was later named P-selectin (a.k.a CD62P, PADGEM, and LECAM-3) [50] becoming the 3rd member of the selectin family of adhesion proteins based on structural similarities consisting of a core basic structure containing a lectin-like domain at the NH_2 terminus, followed by an EGF-like domain, and a number of consensus repeats [53]. Soon after the identification of the selectins, enormous effort was devoted to identifying their corresponding ligands. Initial studies suggested that all selectins could bind to the carbohydrate sialyl lewis^x (sLe^X), a tetrasaccharide attached to the cell surface o-glycans [54]. Studies in subsequent years however, identified P-selectin glycoprotein ligand (PSGL1) expressed on the surface of myeloid, lymphoid and dendritic cells as the specific ligand for P-selectin [30-31]. Apart from PSGL1, P-selectin has also been shown to bind to CD24, another GPI-anchored glycoprotein expressed on neutrophils [55]. Subsequently, E-selectin glycoprotein ligand (ESL1) was identified as the ligand for E-selectin, while L-selectin was shown to bind GlyCAM-1, MAdCAM-1, CD34 and Sgp200 [56-57]. By exploiting monoclonal antibody-mediated blocking strategies and selectin knockout mouse models, several *in vitro* and *in vivo* observations have established the involvement of selectins in tethering and rolling of leukocytes to the endothelium during inflammation [27, 58]. For example, Mayadas et al. showed the involvement of P-selectin in the rolling of leukocytes in the mesenteric venules in response to LPS [59].

At the time when the role of selectins was being demonstrated, the involvement of other adhesion receptors of the immune system were being elucidated. While determining the mechanisms underlying immune cell adhesion during immune surveillance, Timothy Springer at Harvard reported the generation of monoclonal antibodies that recognized a human leukocyte differentiation antigen family with a distinct α-subunit and a common β-subunit [60]. The molecules in this protein family were later identified as lymphocyte function-associated antigen-1 (LFA-1) and Mac-1/OKM1 and an unnamed protein called p150, 95 [61]. This interesting observation led Kishimoto and Springer to clone the β-subunit of human LFA-1, Mac-1, and p150, 95 proteins in the leukocyte integrin family [62]. Serendipitously, these proteins were the homologues of the CSAT complex of avian fibroblasts and the putative fibronectin receptor on human platelets called the GPIIβ/IIIα discovered by Richard Hynes's laboratory at the Massachusetts Institute of Technology (MIT) [63]. Irrespective of species, parallel observations by these two research groups together with David Philips's laboratory in California, identified this family of adhesion receptors and collectively called them 'integrin's'. In the intervening years, considerable effort was made to characterize the different subunits of these heterodimeric proteins [64-66]. Law et al. purified and resolved the primary structure of the β-subunit of the heterodimeric protein complex from spleen [67]. Around the same time, a second group of heterodimers, that were distinct from the heterodimeric proteins identified by Timothy Springer, were biochemically characterized. These proteins were called very late antigen complexes (VLA-1 and VLA-2) and their carbohydrate profile, antibody binding sites, and protein subunits were characterized in the subsequent years [68]. Martin Hemler identified three members in the VLA protein family that were structurally different from LFA-1 and Mac-1, although they shared a common β-subunit and

a number of α-subunits [69]. These VLA proteins were later identified and characterized as the human β1-integrins.

Around this time, compelling evidence established the corresponding receptors of leukocyte integrins (reviewed in [70-71]). VLA-4 expressed by lymphocytes was identified as the ligand of VCAM-1 (Vascular Cell Adhesion Molecule) on activated endothelial cells. This study showed for the first time that surface expression of VLA-4 on K562 cells allows these cells to specifically adhere to VCAM-1 expressed on the activated endothelium and that a monoclonal antibody directed against VLA-4 could inhibit this interaction [72]. Steven Marlin and Timothy Springer identified ICAM-1 (Intracellular Cell Adhesion Molecule) expressed by the endothelial cells as the receptor of leukocyte integrin called LFA-1[73]. Studies in the following years showed that neutrophils could also adhere to ICAM-1 in a Mac-1 (CD11b/CD18) dependent manner [73]. Several laboratories began to question the underlying cause of patients with recurrent bacterial infection and discovered that a primary attribute was a defect in adherence properties in their granulocyte population in the blood [74-77]. These leukocyte adhesion deficient (LAD) patients were found to lack a number of high molecular weight proteins referred to as LFA-I, CR3/Mac- 1, Mo1, pfSO, 95/CR4 or CD11, CD18. This direct clinical involvement of leukocyte integrins in LAD syndrome led an extended era of integrin research and uncovered several molecular aspects underlying leukocyte adhesion deficiencies [71]. Based on a number of *in vitro* and *in vivo* observations that suggested the indispensable involvement of the selectins and integrins in the recruitment of leukocytes in the mesentery, skin and cremaster muscle, proteins in these two super-families are considered essential adhesion molecules in the classical leukocyte recruitment process. Moreover, studies in the last three decades have provided evidence for the existence of

several non-canonical cell surface proteins/enzymes involved in leukocyte adhesion and are discussed in the following sections of this thesis.

Pericytes
Basement membrane
Endothelial cells

Circulating neutrophil | Tethering | Rolling | Full arrest | Firm Adhesion | Intraluminal crawling | Paracellular Transmigration

Blood Flow

| Selectin ligand | Active integrin | Chemokine receptor |
| Selectin | Integrin ligand | Chemokine |

Extravasated Neturophil

Or

Pericytes
Basement membrane
Endothelial cells

Intraluminal crawling | Transcellular transmigration

Blood Flow
Dome formation

Extravasated neturophil

26

Figure 1.1: Schematic representation of the classical neutrophil recruitment cascade. Shown here are the sequential steps/events involved in the recruitment of neutrophils from the blood to a tissue in response to an inflammatory stimulus. Upon inflammation or infection, a circulating neutrophil tethers and rolls (PSGL-1, ESL-1 on the neutrophil binds to P and E selectin on the endothelium) on the vascular endothelium towards the direction of blood flow. Subsequent chemokine-mediated activation and arrest of the rolling neutrophil results in a process called firm adhesion that is mediated by the integrins (Mac-1, LFA-1, VLA4 on the neutrophil binds to ICAM-1/2, VCAM-1 on the endothelium). The firmly adhered neutrophil then actively crawls (Mac-1 on the neutrophil binds to ICAM-1 on the endothelium) towards the endothelial junctions and transmigrates either via a paracellular or transcellular route in a process known as diapedesis. A detailed description of adhesion molecules that mediate these steps in the recruitment process are summarized in section 1.3.

1.4 Vascular zip codes as a determinant of organ-selective cell recruitment.

The monolayer of cells forming the inner endothelial lining of blood vessels exhibits significant structural and functional diversity and heterogeneity in different organs [78]. These diverse characteristics of the vascular endothelium determine the fate of many cellular and physiological processes in health and disease [79-81]. Examples of these include circulation/flow of blood, coagulation, metabolism, immune responses in inflammatory processes and infection, angiogenesis and dissemination of cancer cells from the circulation to a distant tissue [82].

Organ selective recruitment of cells has been widely documented and investigated with respect to leukocytes and cancer cells [83-84]. The mechanistic observations underlying this organ-selective homing, adhesion and subsequent recruitment of leukocytes and metastatic cancer cells has led to the idea that organ-specific vascular addresses or 'zip codes' exist on organ endothelium [85-88]. Bacteriophage display technologies have aided in the identification of these subtle differences on the endothelium. The pioneering work of Errki Ruoslahti and colleagues at the Burnham Institute in California, has remained one of the most powerful unbiased approaches for the identification of molecular signatures on a given endothelium as it employs rapid *in vivo* screening of ~$3x10^{10}$ unique peptides displayed on the bacteriophage and as the bacteriophage act as inert particles in mammalian systems [89-90]. Using this strategy, studies have not only identified organ-specific adhesion molecules utilized by leukocytes and metastatic cancer cells but have also provided important insights into the tissue specific vascular signatures that exist within a given organ [90]. For example, metadherin, a surface protein expressed on breast cancer cells was identified using a phage display library made from cDNA generated from a metastatic breast cancer [91]. A peptide corresponding to a portion of the metadherin protein was found to bind lung endothelium and metadherin antibodies or siRNA knockdown in breast cancer cells inhibited the

development of metastasis in an experimental model of lung metastasis [91]. These data suggest that identification and elucidation of tissue specific binding partners between circulating cells and the vascular endothelium of a given organ that facilitate adhesion and extravasation of leukocytes and metastatic cancer cells, may provide molecular targets that could therapeutically inhibit organ-selective leukocyte recruitment and metastatic disease.

1.5 Unique pulmonary and hepatic endothelium requires a distinct neutrophil recruitment paradigm.

Observations in recent years have suggested that liver and lungs employ unique mechanisms of neutrophil recruitment as both of these organs use unique, non-canonical adhesion molecules expressed on their respective endothelia [44-45]. Based on the relatively small luminal diameters of lung capillaries, studies have proposed that the sequestration of neutrophils within the inflamed pulmonary vascular beds is a result of 'physical trapping' [92-94]. This observation has been challenged in recent years as the ability to image and visualize neutrophil trafficking within the very small lung capillaries in a live breathing mouse by intravital spinning disk microscopy has dramatically improved our ability to assess neutrophil behaviour. Real-time *in vivo* imaging of the mouse lungs has revealed neutrophil behavior consistent with the presence of lung adhesion mechanisms. This imaging demonstrates that not only are neutrophils adhered in vessels too large to cause mechanical trapping, but that the adhered neutrophils are able to use ameboid migration to move through small diameters [12].

The uniqueness of the pulmonary endothelium is a consequence of its function and location as it is strategically positioned to filter the blood before it enters into the circulation [95]. The lungs receive the entire cardiac output every heartbeat and the large surface area of the pulmonary endothelium (about 120m^2) allows the vast majority of immune cells to interact with molecules

expressed on the surface of the endothelial lining [96]. In the lungs, the blood pressure is low and oxygen concentration is high which allows for the exchange of gases between alveolar structures. The thin layers of smooth muscle cells surrounding the arteries and veins within the pulmonary vasculature help maintain a fine-vessel architecture that is in contrast to other high blood pressure vascular beds. Pulmonary endothelial cells reside on a basement membrane that is thicker compared to other organs and is continuous, unlike other vascular compartments such as the hepatic endothelium [97]. This unique ultrastructure of the lung endothelium governs the exchange of fluids and nutrients and hence maintains a normal vascular tone/permeability in the circulatory system [98-99]. Independent of its respiratory function, these salient attributes make the lung the frontline organ to defend against bacterial infections of the cardiovascular system [100-101], these same characteristics however also impact the development of pathologies such as acute lung injury and lung infections [95, 102].

From an immune standpoint, the lungs are comprised of a repertoire of innate immune cells with specialized functions, containing one of the highest populations of leukocytes including neutrophils, alveolar macrophage and dendritic cells under normal physiological condition (reviewed in [103]). Similar to other organs, recruitment of certain innate immune subpopulations to the pulmonary vasculature is a hallmark of lung inflammation and this excessive sequestration of immune sentinels has been implicated in a number of different lung inflammatory diseases such as asthma, COPD etc [104].

Despite a significant progress in *in vivo* imaging, visualizing neutrophil behavior in the lungs has been challenging due to the limitations of imaging techniques to visualize neutrophil recruitment *in vivo* in real time. Thus the majority of the studies have depended on histological analysis, flow cytometry, or myeloperoxidase activity assays to assess neutrophil recruitment in

the lungs. Although extensive research has been dedicated to identifying lung adhesion molecules, the molecular players underlying neutrophil recruitment within the lungs still remains largely unidentified. Although a few reports have implicated neutrophil integrins such as CD11b/CD18 and endothelial ICAM-1/2 in aerosolized-LPS mediated murine models of inflammation within the alveolar compartments of the lungs [105], a number of other studies have shown neutrophil recruitment in the pulmonary vasculature to be independent of the classical adhesion molecules [4-8, 106-108] (**Table 1**).

Similar to the pulmonary endothelium, the hepatic vascular beds have also been shown to have distinct anatomical and functional features with the liver containing the largest network of endothelial cells in the body that house a large number of immune sentinels with defined functions for the detection and clearance of pathogens from blood [109-110]. In contrast to the lungs, the endothelium within the hepatic sinusoids is discontinuous and does not have a well-structured and organized basement membrane. This anatomical characteristic forms an opening between the endothelial cells and the hepatocytes around the endothelial cells which is termed the 'space of Disse' [97]. This anatomical gap results in the formation of a fenestrated endothelium that is structured in an orderly fashion in clusters known as the sieve plates [111]. These unique features are critical in mediating the transport of accessory molecules in the liver [112]. The endothelial cells in the liver sinusoids expresses a wide variety of pattern recognition receptors, such as the toll like receptors (TLR's) [113]. Expression of these receptors on the endothelial cells enables them to recognize a wide array of microbial pathogens for capture and clearance by resident macrophage cells known as Kupffer cells [103]. A number of scavenger receptors and mannose receptors are also expressed on the endothelial cells. This unique topography of the hepatic vascular endothelium helps facilitate the recruitment of immune cells to the liver. In addition, the

liver has other specialized cell types such as hepatocytes, hepatic stellate cells, dendritic cells and liver resident lymphocytes that mediate a number of essential functions [103].

Like the lungs, the recruitment of cells into the liver in response to inflammation, in the most part, does not utilize the classical adhesion molecules. For example, neutrophils have been shown to bypass the requirement for selectins including the absence of selectin-mediated rolling within the hepatic vascular beds [44-45]. Instead as described previously, the interaction of CD44 with hyaluronan represents one of the predominant mechanisms for the adhesion of neutrophils in the sinusoidal endothelium of liver [3]. Apart from CD44, Vascular Adhesion Protein-1 (VAP-1) has also been shown to play a specific role in the recruitment of Th2 lymphocytes to inflamed liver sinusoids [114].
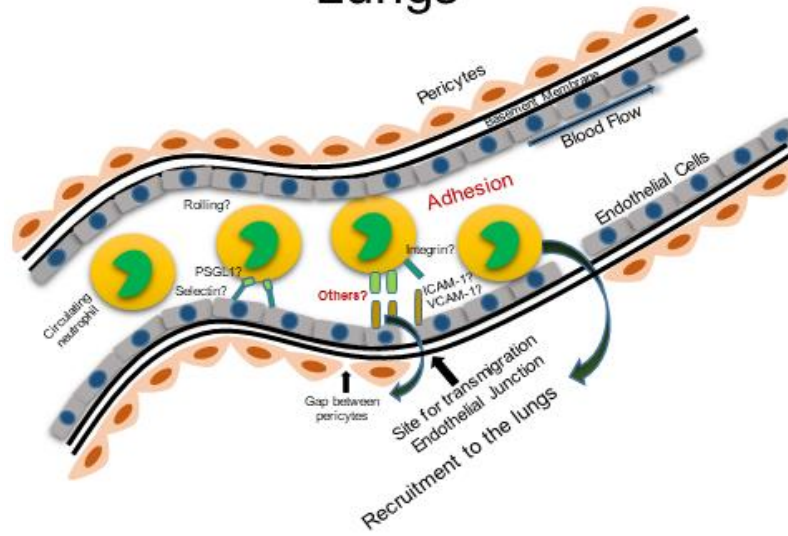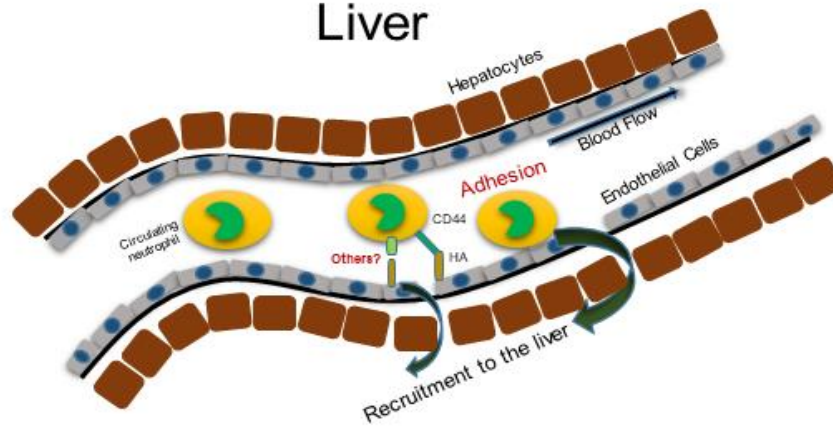
Figure 1.2: Non-canonical neutrophil recruitment paradigm in the lungs and liver. Liver and lungs use additional adhesion molecules for the recruitment of neutrophils in inflammation. The classical adhesion molecules that mediates the recruitment of neutrophils to the many vascular beds have minimal involvement in the recruitment of neutrophils to the lungs and liver. While a single adhesion molecule is yet to be identified that mediates neutrophil adhesion to the lungs, CD44-HA interaction is the only known example of a non-canonical neutrophil adhesion mechanism within the liver sinusoids during inflammation.

Molecules either on the endothelium or on the neutrophil	Method of assessment	Phenotype	References
P-selectin, L-selectin, E-selectin	Knockout mice, monoclonal antibody *in vitro* and *in vivo*	No reduction in neutrophil recruitment	Doerschuk et al. [94]
CD11b, CD18	Monoclonal antibody *in vivo* and Knockout mice	No reduction in neutrophil recruitment	Mizgerd et al. [106], Burns et al.,Doerschuk et al.[108]
VLA4, VLA5	Monoclonal antibody *in vivo*	No inhibition in neutrophil recruitment	Burns et al. [108]
ICAM-1 and ICAM-2	Monoclonal antibody and knockout mice	Not required for neutrophil entrapment and sequestration	Petrovich et al., [115], Doerschuk et al, [107]
CD44	Monoclonal antibody and knockout mice	No reduction in neutrophil recruitment	Yipp and Kubes et al. Unpublished observations

Table 1: Adhesion molecules investigated for the recruitment of neutrophils to lungs.

1.6 Non-canonical adhesion receptors as mediators of neutrophil recruitment during inflammation.

Although the classical adhesion receptors have been studied extensively in neutrophil recruitment, the role of other proteins expressed on a given organ endothelium have lacked attention. As mentioned, in contrast to the canonical neutrophil recruitment process present in the vascular beds of the mesentery, skin and muscle, recruitment to pulmonary and hepatic vasculatures are believed to be unique as both of these organs found to utilize non-canonical adhesion molecules [2-8, 45]. Also, the role of a number of ectoenzymes have been implicated in the recruitment of lymphocytes and leukocytes during inflammation in recent years and are discussed in the next section of this thesis.

1.7 Cell surface enzymes as mediators of neutrophil recruitment during inflammation.

Alternative mechanisms of leukocyte recruitment are beginning to be elucidated including several cell surface ectoenzymes, a group of enzymes with their catalytic domain in the extracellular space [116-117]. These ectoenzymes belong to diverse families of membrane proteins and can regulate leukocyte trafficking either by acting as direct adhesion receptors (through physical binding) or indirectly via their enzymatic activity and have been shown to regulate many steps within the leukocyte adhesion cascade [116-117]. For example, several studies demonstrated the involvement of the cell surface amine oxidase VAP-1, also known as amine oxidase copper containing-3 (AOC3) in rolling, adhesion and transmigration of leukocytes [118-120]. Since its discovery more than twenty years ago as a mediator of lymphocyte recruitment in humans [120], VAP-1 has been the most well-characterized ectoenzyme shown to mediate leukocyte recruitment. Using monoclonal antibodies as well as knockout mouse models, independent studies have shown the crucial role of this protein for leukocyte and lymphocyte recruitment [114, 120-121]. Although,

VAP-1 was initially shown to mediate recruitment of lymphocytes by acting as a physical adhesion receptor, subsequent studies in recent years have also identified the importance of its catalytic activity in the migration of lymphocytes [119]. Using VAP-1 endothelial cell knockout mice as well as selective inhibitors of VAP-1 catalytic activity, studies have demonstrated the requirement of VAP-1 catalytic activity in leukocyte recruitment *in vitro* and *in vivo* [122-123]. Recently, the corresponding ligand for VAP-1 on leukocytes was identified as Siglec-10 (human) and shown to be essential for the VAP-1 mediated adhesion of leukocytes [124]. Aalto et al. have also found that Siglec-9, another protein in the same family, can bind to VAP-1 *in vitro* and *ex-vivo* [125].

Similar to the amine oxidases, the involvement of other ectoenzymes, in particular ADP-ribosyl transfereases, 5′-nucleotidases, and peptidases, are beginning to be implicated in the recruitment of leukocytes during inflammation [117]. CD38 (a ADP-ribosyl transferase), a glycoprotein expressed on the surface of leukocytes has been shown to regulate chemotaxis and thus control various steps in the leukocyte recruitment cascade [116, 126]. Using CD38 deficient mice, two independent studies highlighted the role of this ectoenzyme in leukocyte adhesion and migration. Partida-Sánchez et al. demonstrated that deficiency of CD38 induced susceptibility of mice to bacterial infections due to a lack of directional movement of neutrophils towards the site of infection [126]. They also showed that CD38 could regulate the trafficking of dendritic cells through a chemokine receptor mediated signal [127]. Moreover, CD38 is thought to regulate leukocyte trafficking by controlling the functional consequences of leukocyte integrins [128-129] and has been shown to bind platelet/endothelial cell adhesion molecule (PECAM). CD157, another ADP-ribosyl transferase, has also been shown to be involved in leukocyte adhesion. Similar to CD38, this GPI anchored protein regulates leukocyte adhesion by modulating chemotaxis via a β-

integrin mediated crosstalk (when it localizes in GM-1 enriched lipid raft microdomains in the cell membrane) [130].

Apart from ADP-ribosyl transferases, the crucial role of 5′-Nucleotidases has been implicated in the adhesion and transmigration of leukocytes in response to an inflammatory stimulus. CD73, another GPI-anchored glycoprotein is the most well studied example in this family of ectoenzymes. CD73 was first identified to be involved in the adhesion of lymphocytes by Airas et al. where they generated a monoclonal antibody (4G4) by immunizing mice with endothelial cell extracts prepared from inflamed human synovia [131]. CD73 was initially named L-VAP-1 (lymphocyte VAP-2). Subsequent studies by the same group showed that this monoclonal antibody could inhibit the adhesion of lymphocytes to COS cells transfected with CD73 cDNA [132]. Based on these observations, a number of studies in the past decade have shown the functional importance of CD73 using knockout mice. Eltzschig, H. K. et al. showed enhanced recruitment of leukocytes in conditions with low atmospheric oxygen in mice that were deficient for CD73, while Koszalka, P. et al. demonstrated that targeted disruption of CD73 in mice induced increased binding of leukocytes to inflamed endothelium. These studies have demonstrated that the dephosphorylation of AMP to adenosine by CD73 activate the adenosine receptors A2AR and A2BR on the surface of neutrophils and this adenosine act as an anti-adhesive signal for the binding of neutrophils [133]. These two important observations have suggested the functional relevance of CD73 in leukocyte adhesion *in vivo* [133-134].

Similar to other ectoenzymes, the increased expression and activity of ectopeptidases and proteases at inflammatory sites has been shown to regulate leukocyte trafficking. Emerging evidence from a number of studies supports the involvement of CD10, CD13, CD26, and CD156b as well as matrix metalloproteases [116-117]. Most of these ectoenzymes have been shown to

regulate leukocyte recruitment either by activating or inactivating the accessory molecules such as the chemokines and/or other adhesion receptors. For example, CD10 was shown to modulate the inflammatory peptides such as metenkephalin and f-MLP [135] while CD13 was shown to degrade interleukin-8 (IL-8) thereby inactivating its chemotactic activity [136]. Moreover, targeted deletion of CD10 in mice induced granulocyte infiltration and exacerbated inflammation in the intestine in response to *Clostridium difficile A* [137]. Further, dipeptidyl peptidase-4, also known as CD26, is expressed by activated T cells, B cells, NK cells and endothelial cells, and can cleave dipeptides with a number of cytokine and chemokines acting as substrates [138-139]. Enzymatic function of CD26 has also been implicated in leukocyte trafficking *in vivo*. Kruschinski et al. showed loss of CD26 induced the recruitment of T cells in rat model of asthma [140]. In addition, using CD26 deficient mice Busso et al. showed that CD26 can regulate active stromal cell-derived factor-1 (SDF-1) [141]. CD156b has also been shown to cleave CD62L from the leukocyte surface by acting as a sheddase [142]. Apart from CD156b, a number of matrix metalloproteinases can also cleave adhesion molecules from the surface of leukocytes and thus regulate leukocyte trafficking at inflammatory sites [143-145]. Together, these evidences suggest an important role of ectopeptidases in the regulation (via their catalytic activity) of leukocyte recruitment during inflammation.
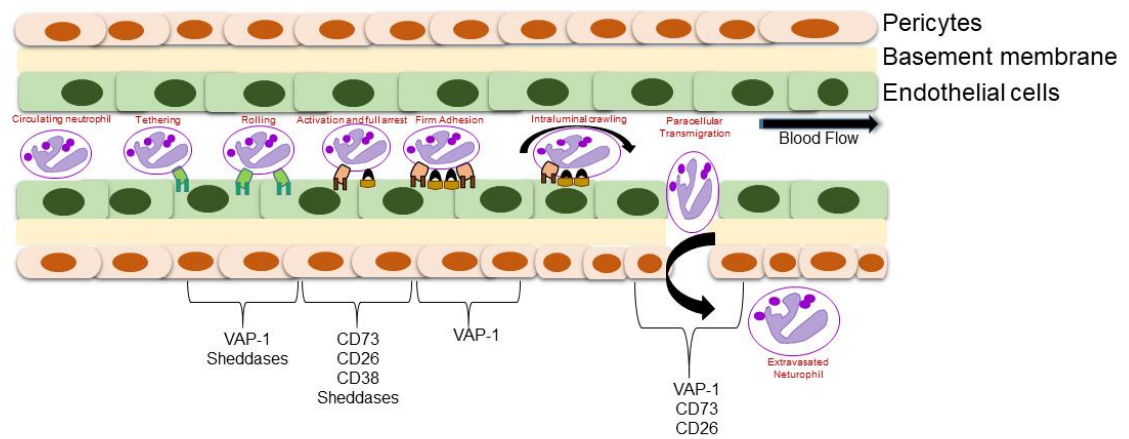
Figure 1.3: Involvement of ectoenzymes in the leukocyte recruitment cascade. In addition to the classical adhesion molecules, the involvement of a number of cell-surface enzymes has been recently implicated in the leukocyte recruitment cascade. Shown here are ectoenzymes that mediate different steps in the recruitment of leukocytes. Cell-surface amine-oxidases such as VAP-1 have been shown to be involve in the rolling, firm adhesion and transmigration of leukocytes, while 5'-nucleotidase such as CD73 has been shown to mediate the activation/arrest and transmigration of leukocytes. Ectopeptidases, such as CD26 have been implicated in the activation of leukocytes. Non-canonical adhesion molecules including the ectoenzymes that mediate each of these steps in the recruitment of neutrophils are summarized in section 1.6 and 1.7.

1.8 Recruitment of monocytes during inflammation.

In addition to the recruitment of neutrophils, migration of other innate immune sentinels such as monocytes has been implicated during the late phase of acute inflammation [146]. Coupled with initial observations made during the late 1980's, recent evidence has suggested that leukocyte infiltration in acute inflammation is predominantly neutrophilic during the initial hours of inflammation, however subsequent recruitment of monocytes during the late phase regulate the progression of an ongoing inflammatory response [147-148]. Besides their physiological similarities with neutrophils, bone marrow and blood monocytes retain the ability to proliferate and differentiate into resident phagocytes known as macrophage in the lungs, liver, spleen and other tissues [149-151]. Based on early observations it was believed that macrophages were derived from mesenchymal tissues, however studies using radioisotope labeling of blood and bone marrow cells later demonstrated that monocytes are the precursors of macrophages in all tissues except the brain [152-154]. More recent studies have also identified monocytes as the precursors for dendritic cells [155].

Recruitment of monocytes at inflammatory sites follows the general scheme of the classical leukocyte recruitment cascade that includes selectin (L and P-selectin) mediated rolling, integrin (VLA-4, LFA-1) mediated adhesion, and junctional adhesion molecule (PECAM-1) mediated transmigration [156]. LY6C^{hi} monocytes, a subset of monocytic innate immune cells that express high levels of CC-chemokine receptor (CCR2) and referred to as inflammatory monocytes, have been shown to express L-selectin and P-selectin glycoprotein ligand (PSGL1) that mediates the rolling of these cells on inflamed endothelium [25, 157]. Expression of VLA4, and Mac-1 on monocytes facilitate firm adhesion [158]. Firmly adhered monocytes then transmigrate via a PECAM-1 dependent manner to an inflammatory tissue [159]. Apart from the role of P and L-

selectins, VCAM-1 was also found to mediate the rolling and adhesion of inflammatory monocytes in inflammation [156, 160]. Using blocking antibodies against ICAM1 or Mac-1, PECAM-1 was also shown to inhibit the recruitment of monocytes during acute inflammation and atherosclerosis [25, 160]. Several studies have identified VLA-4 as the major integrin that mediates firm adhesion of monocytes [160-162]. In addition to VLA-4, recruitment of another subset of monocytes (LY6C^{low}) was shown to be mediated by LFA-1 [163]. In contrast, the deficiency of LFA-1 did not inhibit the recruitment of LY6C^{hi} monocytes at inflammatory sites [164], suggesting a differential mechanism for the recruitment of monocyte subsets in inflammation and this phenomenon was regulated in a tissue and inflammatory stimulus dependent manner. Some studies have suggested that initial recruitment of polymorphonuclear leukocytes (such as neutrophils) can initiate a second phase of cellular recruitment in the form of monocytes [165-166]. For example, Ward et al. showed activated PMN lysates were capable of inducing chemotaxis of monocytes indicating a role of storage granules of polymorphonuclear leukocytes in the chemotactic behaviour of these mononuclear cells [167]. Subsequent studies by Gallin et al. showed that lysates from PMN isolated from 'specific granule deficiency' patients had no effect on monocyte chemotaxis which further suggested a role for PMN granules in monocyte chemotaxis [168]. In line with these observations, reduced number of migrating monocytes in neutropenic septic patients demonstrated the involvement of PMN mediated monocyte recruitment [169]. The role of pro-inflammatory cytokines and chemokines has also been shown to be involved in neutrophil mediated monocyte recruitment in inflammation [166]. For example, Hurst et al. showed a neutrophil derived IL-6 mediated switch/transition of monocyte recruitment in a model of acute inflammation [170]. Also, MCP-1 (monocyte chemoattractant protein-1), a chemoattractant that has been shown to be released by cytokine stimulated neutrophils [171] (in addition to macrophage

and dendritic cells) is one of the crucial mediators for the recruitment of monocytes at inflammatory sites. Collectively, these studies have demonstrated a role for PMN storage granules and activated neutrophil derived cytokines/chemokines in the regulation of monocyte recruitment in inflammation.

Recruitment of monocytes has been implicated in a number of bacterial, fungal (yeast and moulds) and viral infections where CC-chemokine receptor CCR2 plays a central role [172-173]. With regards to the role of adhesion molecules, analogous to neutrophils, the recruitment of monocytes is also understudied in the lungs and liver during an inflammatory response and hence the role of classical leukocyte adhesion receptors such as selectins and integrins in the recruitment of monocytes in these organs is incompletely understood. In addition to the classical adhesion molecules, the involvement of other non-classical adhesion molecules that may mediate monocyte recruitment in inflamed pulmonary and hepatic vasculatures are yet to be identified.

1.9 Inflammation and metastasis.

The concept of inflammation as a critical contributor to cancer was established more than a century ago when Rudolph Virchow hypothesized the origin of cancer at sites of chronic inflammation [174]. Virchow's hypothesis was primarily based on two different experimental observations: first, he observed that certain irritants could induce tissue injury and inflammation and thereby enhance proliferation of cells at the inflammatory site and second, the presence of leukocytes in neoplastic tissues that he described as 'lymphoreticular infiltrate' [175]. Several studies in the last twenty years have supported Virchow's original observations [176-179]. Research aimed to uncover the involvement of inflammation in cancer has not only suggested important links between inflammation and cancer but also provided important insights in targeting inflammation for cancer prevention and therapy [180-182].

Metastasis, the process that defines the spread of a primary tumor to distant organs, is tightly regulated by the interaction of tumor cells with the associated stroma, extracellular matrix, bone marrow derived cells, myeloid derived suppressor cells (MDSC's) and mesenchymal stem cells [183]. The presence of inflammatory cells and their secreted factors within the tumor microenvironment has been suggested to contribute significantly to invasion and metastasis [176, 184]. Although, the involvement of immune cells in primary tumor formation and progression was established over a century ago, a significant number of studies over the past few decades have re-defined the role of different immune cells in cancer progression (reviewed in [185]). Initially, it was believed that the migration of leukocytes towards the primary tumor mass was an attempt to eliminate the tumor cells. Several studies however, have challenged this hypothesis and although, some leukocytes (CTL's and NK cells) possess certain anti-tumor properties, the role of the immune cell infiltrate in tumors is now debatable. For example, studies using antibody mediated neutrophil depletion have suggested that neutrophils may have both pro and anti-tumor roles in cancer formation and progression [186]. Observations in preclinical murine models of lung and liver metastasis have suggested a pro-tumor/tumor promoting phenotype of neutrophils. In these studies, antibody mediated depletion of neutrophils was associated with a reduced tumor burden at metastatic sites (liver, lungs) [187-188]. Interestingly, delivering humanized neutrophils into the preclinical murine models of cancer has been shown to increase melanoma-lung metastasis [189]. In contrast to these observations, Granot et al. showed that tumor entrained neutrophils (TEN) could inhibit the seeding of circulating tumor cells in the lung by producing H_2O_2 and CCL2 in the pre-metastatic lung [190]. In a separate study, Finisguerra et al. showed MET is required for the recruitment and anti-tumor activity of neutrophils where nitric oxide synthase catalyzes a major function [191]. Based on this evidence it can be concluded that the role of neutrophils in cancer

metastasis is highly debatable and at least in part it is microenvironment specific. Thus, further studies will be necessary to provide more insight into the specific role of neutrophils in cancer metastasis.

Emerging evidence from a number of studies over the last decade, indicate the presence of more than one neutrophil population in cancer [192]. Fridlender et al. identified two different subpopulations of neutrophils (N1 and N2) where neutrophil phenotype and polarization was dependent on the release of TGF-β within the tumor microenvironment [193]. Since then several studies were undertaken to identify the different subpopulations of neutrophils in cancer. Most of these studies were dependent primarily on different cell surface proteins markers for the identification of neutrophil subpopulations [192, 194]. However, it is important to mention that none of these protein markers were specific for a particular neutrophil subtype [195-197]. Thus, future studies are necessary to design strategies that can specifically identify diverse neutrophil subpopulations that may exist in cancer. To identify the phenotypic diversity, polarization and plasticity of neutrophils will also be necessary to understand their specific role in cancer progression and metastasis. A recent review highlights some of the major discrepancies in mouse neutrophils compared to human neutrophils in cancer [198].

Apart from the involvement of macrophages and neutrophils, the emerging role of cancer associated fibroblasts in cancer progression has also been identified (CAF's) [199]. Recent studies have demonstrated that CAF's can induce tumor cell invasion by producing pro-inflammatory cytokines such as IL-6 [200]. Moreover, when activated, CAF's can produce growth factors essential for secondary tumor growth at a distant site. Myeloid derived suppressor cells (MDSC), a subpopulation of immune cells from the myeloid lineage, have been shown to produce pro-

inflammatory cytokines and growth factors within the tumor microenvironment that promote chronic inflammation and contribute to metastatic disease [201].

Tumor associated stromal cells and bone marrow derived innate immune cells can educate circulating tumor cells by releasing certain factors within the primary tumor microenvironment to induce metastasis at distant sites [202]. They form a 'pre-metastatic niche' that has been implicated in different cancer metastasis murine models. Kaplan et al. in 2005 observed that the association of VLA-4 in VEGFR1 positive bone marrow pro-genitors and tumor cell specific growth factor mediated upregulation of fibronectin in the ECM within the tumor microenvironment were essential for the formation of pre-metastatic niche [203-204]. A significant number of studies published in recent years, have identified the role of tumor exosomes in initiating the formation of pre-metastatic niche to promote the metastatic behavior of circulating tumor cells [205-206].

The systemic release of cytokines and growth factors by the primary tumor cells, tumor associated stromal cells, endothelial cells and activated immune cells in the tumor microenvironment has been shown to promote the progression of metastatic disease and have been implicated in different events in the metastatic cascade [207]. These small circulating peptides released in the tumor microenvironment can regulate metastasis by both autocrine and paracrine signaling pathways [208-210]. Tumor associated macrophages produce a variety of cytokines and growth factors (TNFα, IL-6, IL-1, FGF, EGF, HGF, PDGF, TGF-β) within the tumor microenvironment that induce adhesion, motility, angiogenesis, invasiveness and secondary growth of disseminated tumor cells. TNF-α and IL-1, in particular, have been shown to increase the incidence of metastatic disease and their presence in the tumor microenvironment has been associated with poor prognosis and outcome [184, 210-211]. TNF-α can activate the vascular endothelium and upregulate the expression of different adhesion molecules (P-selectin, VCAM-1,

E-selectin) that facilitate the binding of circulating tumor cells to the endothelium and supports their subsequent extravasation to a secondary site [202, 212-213] [214]. The metastasis promoting effects of TNF-α are facilitated largely by its ability to signal through NFκB, a potent regulator of inflammatory response. Similar to TNF-α, the release and presence of IL-1 within the tumor microenvironment has also been shown to be associated with more aggressive metastatic phenotype [211, 215]. The precise molecular mechanisms of how IL-1 mediates cancer progression remains to be understood, however several studies have indicated that IL-1 can upregulate matrix metalloproteases and angiogenic growth factors such as the vascular endothelial growth factor (VEGF) [211, 216]. IL-1β has also been shown to upregulate endothelial adhesion receptors (such as VCAM-1 in the hepatic endothelium) to enhance melanoma-liver metastasis [217]. Apart from these two pleotropic cytokines, IL-6, IL-8, TGF-β, CSF-1, induce and promote cancer progression and metastasis [218-222].

Related to the cytokines, chemokines, a subclass of chemotactic cytokines released within the tumor microenvironment are also potent mediators of metastatic disease [223]. Specifically, CCL2, CCL5, and CXCL12 and their corresponding receptors have been shown to have roles in promoting metastasis [224]. These cytokines and growth factors are not only capable of recruiting other immune cells into the tumor but can also trigger different inflammatory signaling pathways that directly provide survival advantages and induce growth of disseminated tumor cells. For example, STAT3 and NFκB signaling have been shown to directly contribute to the metastatic process [181, 225]. Thus akin to classical leukocyte recruitment, different pro-inflammatory cytokine mediated upregulation of endothelial adhesion receptors can promote adhesion and extravasation of metastatic cancer cells within a given organ. These studies may indicate that

similar adhesion molecules can be used/shared by leukocytes and metastatic cancer cells for their organ-specific recruitment.

1.10 Organ-selective cancer dissemination and the metastatic cascade.

In addition to the essential role of the tumor microenvironment and inflammation in determining the spread of cancer to distant organs, the process of metastasis also depends on a number of rate limiting sequence of events where, enhanced invasiveness and increased motility induce cancer cells to leave the primary tumor mass to enter and survive in the circulation (bloodstream or lymphatics) [226-227]. To survive in the circulation and at secondary site, these malignant cells acquire the ability to resist certain stresses, such as selective pressure from the tumor microenvironment, physical damage from shear forces, complement mediated lysis and immune cell mediated killing [228-229]. Once the cell survives in the circulation, these cells exit from the capillary beds and enter into a new tissue in a process termed extravasation, and eventually colonize a distant organ [230-231]. These cells can then travel to virtually any organ in the body. To obtain adequate blood supply and essential nutrients, metastatic cancer cells gain and acquire the ability to form new blood vessels in a region beyond the pre-existing blood vessels [232]. This process is termed 'angiogenic switch' and is a critical step in the process of metastasis of solid tumors [233-234]. Each and every step in the metastasis cascade are rate limiting as disruption of any of the steps can halt the process of secondary tumor formation at a distant site. Although the precise mechanisms that regulate these processes and guides metastatic cancer cells to a particular secondary organ is mostly unknown, recent studies have highlighted the importance of (i) cell of origin, (ii) intrinsic cellular and molecular properties of a tumor (iii) organ and tissue affinities, (iv) circulatory patterns, and (v) invasive and infiltrative nature in determining the organ-

selectivity of metastatic cancer cells [235-236]. Important to mention that this thesis is focused on understanding the adhesion/extravasation step in the metastatic cascade.

The concept of organ-selectivity in cancer metastasis was first demonstrated in the late eighteen hundreds. Stephen Paget's ground-breaking question in 1889 that "What is it that decides what organs shall suffer in a case of disseminated cancer?" and his seminal observations later established the idea of organ-selective metastatic disease when he proposed the 'seed and soil hypothesis' (1889) and suggested that the distribution of disseminated cancer cells (seeds) depends upon particular factors within a specific organ (soil) that allows the colonization of the disseminated cancer cells based on their growth characteristics [237]. In his landmark paper in 1889 working with breast cancer autopsy specimens, Dr. Paget observed that the majority of metastatic occurrence was to the liver, bones, ovary and occasionally in the spleen. This observation contradicted a prevailing view by Virchow where he proposed that metastatic disease was the result of arrest of tumor cell emboli in a vasculature [238]. Dr. Paget stated "remote organs cannot be altogether passive or indifferent regarding embolism". He explained the principle of his 'seed and soil hypothesis' by stating: "When a plant goes to seed, its seeds are carried in all directions, but they can only live and grow if they fall on congenial soil." This hypothesis was again questioned many years later (1928) by James Ewing who proposed that the mechanical factors and the direct circulatory routes between a primary tumor and specific secondary organ are sufficient to drive organ selective metastasis [239]. Observations during the 1970's by Isaiah Fidler and colleagues using syngeneic mouse models showed although tumor cells traveled through the circulation to the majority of the organs and mechanically trapped in the vascular beds of these distant organs, subsequent proliferation and growth of disseminated cancer cells in a secondary organ was influenced by congenial organ vasculature and organ specific cells thus suggested a

49

selective nature to metastasis and reconfirmed Stephen Paget's original observation [240-242]. In a study using B16-F10 murine immunocompetent melanoma model *in vivo*, Fidler and Kripke showed significant variation exist in a heterogeneous population of tumor cells in their ability to produce metastatic lesions to the lungs and that parental population of metastatic cancer cells contains the metastasis producing clones [243]. A number of ground-breaking research questions by different groups around this time provided some important insights in areas such as the i) pathogenesis of metastasis, ii) organ-tropism, iii) local tumor microenvironment or niche and iv) metastatic heterogeneity. Independent observations identified lungs and liver as the two major sites of organ-selective metastatic disease. Clinically as well as studies in murine models of metastasis have shown that breast, melanoma, colorectal, pancreatic, sarcomas have high propensity to colonize the lungs and liver [244-246]. Uveal melanoma, a form of cancer that happens in the uvea of the eye, has a significantly high propensity to colonize the liver with approximately 50% of the patients developing liver metastasis 10-15 years after the initial diagnosis [247-248]. Together, these observations re-defined Paget's hundred-year-old 'seed and soil' hypothesis that certain tumors will grow to specific organ-microenvironments that are compatible with their growth characteristics. Focusing primarily on the nature of genetic signatures in the metastatic cells (seeds), a number of studies in the last two decades by Joan Massague and colleagues have provided substantial evidence that further validated the organ-selective nature of metastatic cancer cells [84, 249-254].

1.11 Epithelial to mesenchymal transition in organ-selective cancer dissemination.

One of the crucial processes that underlies cancer progression and metastatic dissemination is the transition of polarized non-motile epithelial cells to a motile mesenchymal phenotype, a phenomenon known as epithelial to mesenchymal transition (EMT) [255]. Although, EMT was

originally identified and described as a key process during the development of embryonic structures, morphogenesis and tissue remodeling, studies over the last two decades has demonstrated an important involvement of EMT in cancer cell invasion and metastasis to distant organs [256]. It has been observed in the majority of solid tumors (mice and humans) that loss of cellular adhesion and the gain of invasive and motile properties during EMT regulate the metastatic spread to the lungs and liver [255, 257]. The absence in expression of an adhesion molecule known as E-cadherin (epithelial cadherin) has been shown to play a fundamental role in the regulation of EMT during the metastasis of solid tumors to the lungs and liver in both mice and humans and that ectopic expression of E-cadherin in cancer cells has been shown to inhibit the invasive and migratory properties of these breast cancer cells *in vitro* and *in vivo* [258-259]. A number of transcription factors such as Snail, Slug, dEF1, SIP1, Twist1, FOXC2 have been identified and shown to regulate the transition of epithelial cells to a mesenchymal phenotype [260-263]. A large number of studies implicate the TGF-β signaling pathway as one of the major regulators of EMT during embryogenesis and metastasis [264-266]. Activation of TGF-β signaling has been shown to induce EMT and enable these cells to invade the extracellular matrix in *in vitro* cell-based systems and promote metastasis to the lungs and liver in mice [267-268]. Induction of the transcription factors Snail, Slug, and SIP1 by TGF-β has been shown to repress the expression of E-cadherin within the adherent junctions resulting in the loss of cell adhesion [269]. Although, all these transcription factors were found to repress/suppress EMT either directly or through indirect mechanisms (interaction/signaling pathways) *in vitro*, how they regulate mesenchymal differentiation, migration and invasion during EMT is not completely understood. Despite this compelling evidence, the contributing role of EMT in the metastatic process of human cancers remains controversial. A large part of this can be attributed to the fact that majority of the protein

markers being used to assess EMT are either expressed on the epithelial or the mesenchymal cell and hence cells that are undergoing the transition from an epithelial to a mesenchymal phenotype are difficult to investigate. Although, studies have indicated the existence of an EMT like phenotype in cancer cells within the primary tumor, the role of EMT in the progression and dissemination of cancer cells to distant organs is highly debatable. In fact, a number of clinical observations found that the majority of the human breast metastatic tumors express normal levels of E-cadherin and maintain their epithelial polarity and morphology suggesting that these cells have metastasized to distant organs (lungs, liver and bone) without undergoing EMT [270-271].
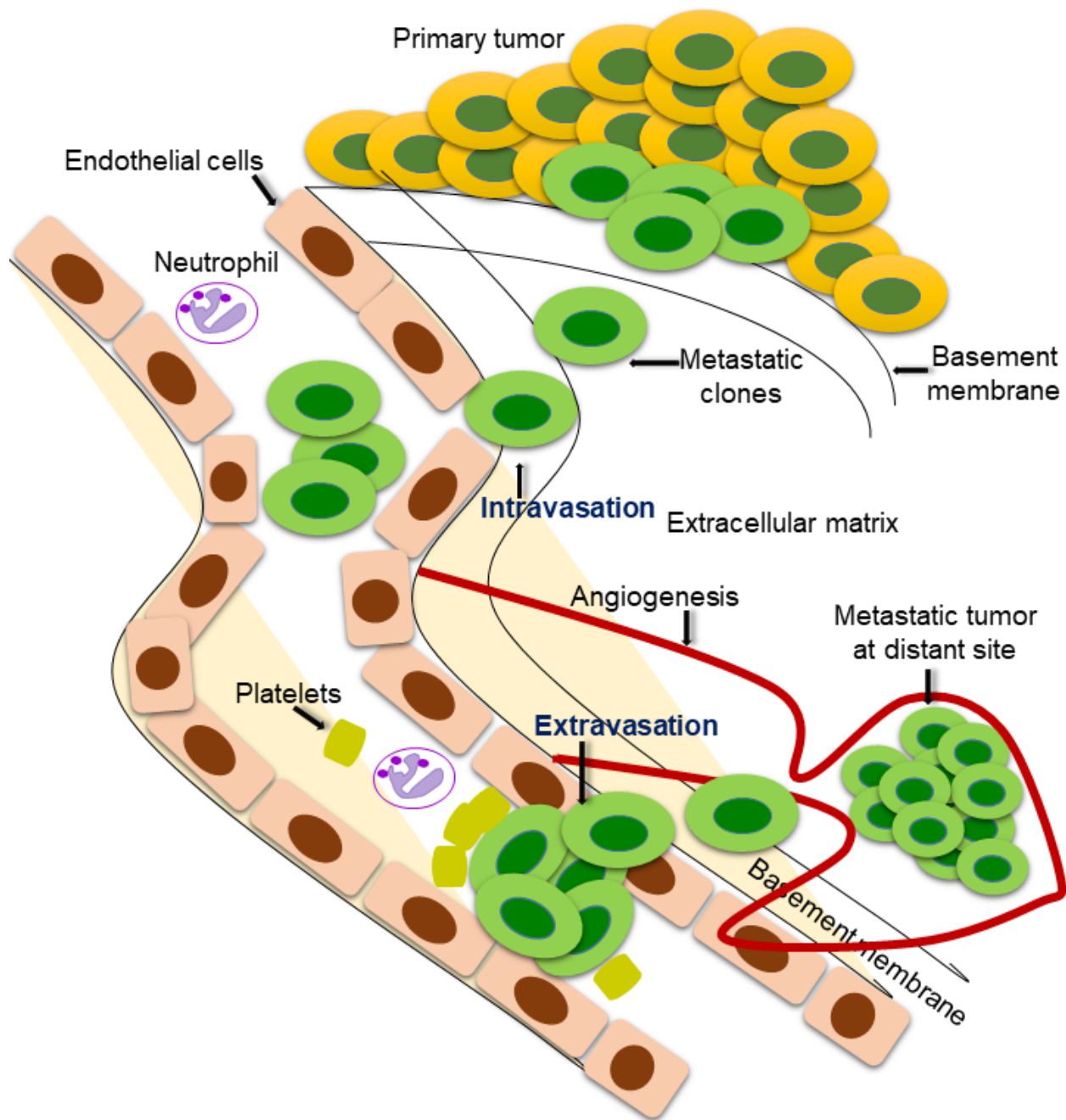
Figure 1.4: Schematic representation of the metastatic cascade. Loss of adhesion and enhanced invasiveness and motility trigger the release of metastatic clones from the primary tumor to enter and survive in the circulation. Metastatic tumor cells finally extravasate to colonize a distant organ.

1.12 Common features in organ-selective cell recruitment to distant organs- a process shared by leukocytes and metastatic cancer cells?

Adhesive cellular and molecular interactions between disseminated tumor cells and the vascular endothelium defines the spread of metastatic disease [272]. Based on a number of clinical observations, it has been found that some cancers metastasize to distant sites in an organ-selective manner and leukocytes and disseminated cancer cells have been found to use common recruitment processes during their transit from the circulation to the tissues [273-274]. These two different cell types have been found to utilize some common adhesion molecules for organ-selective endothelial binding. For example, similar to leukocyte recruitment, the role of selectins and integrins, have been implicated in lung and liver metastasis [275-280].

As mentioned earlier, neutrophil-CD44 and endothelial-HA interaction in the liver sinusoids is an example of a non-canonical recruitment mechanism. CD44 has also been shown to play a dual role (tumor suppression and tumor aggressiveness/promotion) in the progression of cancer and metastases [281]. This transmembrane glycoprotein has been shown to mediate the migration and adhesion of circulating tumor cells [282]. Unlike leukocytes, few studies were designed to identify novel adhesion molecules that mediate extravasation of disseminating cancer cells. In this regard, cell surface adhesion molecules such as metadherin have been shown to be important in the homing and adhesion of disseminated breast cancer cells and have been identified as determinants of organ selective recruitment of metastatic cancer cells to the lungs [91]. Other non-canonical molecules identified thus far include VAP-1 and CD73 that have been implicated in lung metastasis [283-284]. Cell surface peptidases have also been shown to facilitate the adhesion of metastatic cancer cells in an organ-selective manner. For example, Pauli and colleagues found that Lu-ECAM-1 (Lung Endothelial Dipeptidyl Peptidase IV), a lung endothelial

cell surface protein, mediates adhesion of B16-F10 metastatic melanoma cells to the lungs in a Ca^{2+} dependent manner [285] and metastasis of rat breast cancer cells to the lungs [286].

1.13 A putative role for membrane dipeptidase in the recruitment of neutrophils and metastatic cancer cells to the lungs and liver.

Membrane dipeptidase (EC 3.4.13.19), also known as Dipeptidase 1 (DPEP1) and membrane bound dipeptidase-1, is a cell surface GPI (glycosyl-phosphatidyl-inositol)-anchored zinc metalloprotease, first isolated from the brush border membrane of the kidney [287-288]. Although it was originally isolated as a renal enzyme, DPEP1 has been shown to be expressed in other organs including the lungs and liver [289-290]. The molecular mass of DPEP1 ranges from 48 to 59 kilodalton depending on the species, and is expressed as a 63-kilodalton glycosylated form. Dipeptidases are unique peptidases as they have no homology to other metallopeptidases and the amino acid sequence His-Glu-X-X-His common in zinc proteases is absent [291]. Zinc ions are essential for the hydrolytic action of the enzyme and a number of independent site directed mutagenesis studies have shown that Glu125, His152, His198, and His219 are crucial for the catalytic activity of the enzyme [291-293]. Histidine152 is also involved in substrate and inhibitor binding although the exact mechanism is not clear [293].

The mature DPEP1 protein contains seven cysteine residues per subunit six of which are conserved in the human enzyme, and it acts as a homodimer of two identical subunits linked by di-sulfide bridges. Site directed mutagenesis studies demonstrated that the cysteine residues are not involved in enzyme activity [294]. DPEP1 consists of 411 amino acids in humans, while 409 in pig and 410 in mouse and rat. Human DPEP1 is 74% identical to the mouse and rat and 82% identical to pig. DPEP1 has four possible N-glycosylation sites (Asn57, Asn279, Asn332, Asn358) and has been cloned from a number of species including human, pig, rabbit, rat, mouse, and sheep

[295-297]. Membrane dipeptidase hydrolyzes a wide range of dipeptides (including unsaturated dipeptides and dehydropeptides) and has been shown to be involved in the renal metabolism of glutathione and its conjugates (where membrane dipeptidase metabolizes cystinyl-bis-glycine into constituent amino acids) [298]. A major function of the enzyme is to convert leukotriene D4 to leukotriene E4 in the leukotriene biosynthesis pathway. Membrane dipeptidase-2 (also known as DPEP2 and membrane bound dipeptidase-2) and membrane dipeptidase-3 (a.k.a. DPEP3 and membrane bound dipeptidase-3), two other members of the membrane-bound dipeptidase (EC 3.4.13.19) family (M19) have also been identified [290]. Although DPEP2 and DPEP3 have some overlapping functions to DPEP1, DPEP1 is only 51% identical with DPEP2 and 48% with DPEP3. All three genes are located on the same chromosome (chromosome-16) but have diverse tissue expression and functional activity. DPEP1 and DPEP2 are expressed in heart, liver and lungs; DPEP2 and DPEP3 are expressed in the testis; and DPEP1 is expressed in the kidney. Functionally, DPEP1 cleaves both LTD4 and cytinyl-bis-glycine; DPEP2 cleaves LTD4 but not cystinyl-bis-glycine while DPEP3 cleaves cystinyl-bis-glycine and not LTD4 [290].

1.14 Thesis rationale and hypothesis.

Based on compelling evidence that suggested that the LSALT peptide inhibits neutrophil recruitment and cancer metastasis to the lungs and liver of mice by binding to DPEP1, we hypothesized that:

 'LSALT peptide, identified by in vivo phage display, binds to dipeptidase-1 (DPEP1) and inhibits the recruitment of neutrophils and metastatic cancer cells to the lungs and liver'.

The three following aims were proposed to test this hypothesis:

Aim-1 To functionally characterize a lung and liver targeting peptide (LSALT peptide).

Aim-2: To identify the role of DPEP1 in cell recruitment to the lungs and liver.

Aim-3: To validate DPEP1 as an adhesion receptor for neutrophils and metastatic melanoma cells *in vivo*.
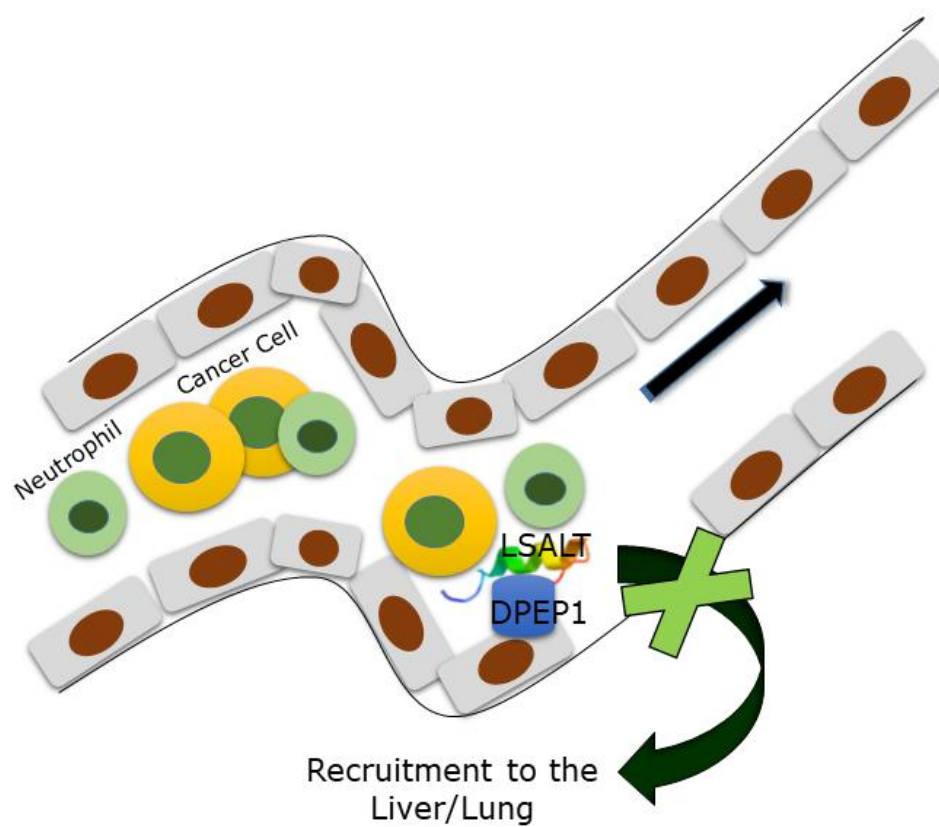
Figure 1.5: Scientific rationale and hypothesis: LSALT peptide, identified by *in vivo* phage display, binds to DPEP1 and inhibits cell recruitment to the lungs and liver.

Chapter Two: Materials and Methods

2.1 Mice:

Six to ten week old C57BL/6 mice were obtained from Charles River (Charles River Laboratories, Shrewsbury, MA, USA) and were housed in groups of five mice and maintained on a 12 hour light/dark schedule with a temperature of 22 °C ± 1 °C and a relative humidity of 50% ± 5%. LysMeGFP mice and *CD44-/-* mice were obtained from Jackson laboratories. All mice weighed between 20-30 grams when they were used for experiments. DPEP1 Knockout (*DPEP1-/-*) mice were generated as described in figure 3.21 by Horizon Discovery (Saint Louis, MO, 63146, USA). Briefly, CRISPR/Cas-9 reagents, including all 5 small guiding RNAs (sgRNA), targeting the mouse DPEP1 gene (renal) [Mus musculus (house mouse); Gene ID: 13479] were designed by bioinformatic analysis. CRISPR/Cas-9 vectors were established based on the genomic DNA sequence of DPEP1. CRISPR/Cas-9 DPEP1 sgRNAs were validated in cultured cell based assays *in vitro* for the identification of the best sgRNA that targeted DPEP1 for subsequent embryo injection. Based on the validation of the CRISPR/Cas-9 DPEP1 sgRNAs constructs *in vitro*, CRISPR/Cas-9 DPEP1 sgRNA, with or without donors were microinjected (pronuclear) into fertilized mouse embryos. These embryos were subsequently transferred to pseudopregnant females. Founder mice were identified by performing PCR and sequencing based genotyping analysis. Mice were genotyped for DPEP1 by using the following primers in a single PCR: Forward primer: 5′-TAGCCTTGAGCTGTGGGAGT-3′, Reverse primer: 5′-GGCATCTTTGTTTTGGGTGT-3′. The expected amplicon sizes were 498 bp, and 229 to 269 bp for the wildtype and null alleles, respectively. Four independent DPEP1 heterozygous knockout mouse lines were generated i.e: 1 bp insertion C, 11 bp deletion-1 bp insertion T, 141 bp deletion and 6 bp deletion. Germline transmission and identification of F1 heterozygous mutant mice were

validated based on genotype analysis by the Centre for Genome Engineering at the University of Calgary. Generation of DPEP1 knockout mice (homozygous, *DPEP1-/-*) in the C57BL/6 background strain were generated by intercrossing the F1 heterozygous mice (*DPEP1+/-*) under the specific breeding guidelines set out by the University of Calgary's animal resource facility. *DPEP1-/-* mice were maintained in a specific pathogen free facility at the University of Calgary's Health Sciences Animal Resource Center. All procedures and protocols (AC16-0183 – breeding protocol and AC13-0323, AC16-0148, AC14-0198 – experimental protocols) regarding animal experiments were reviewed and approved by the University of Calgary Animal Care Committee. The majority of the experiments in this study were performed using the 1bp (C) insertion and 11 bp deletion and 1 bp (T) insertion DPEP1 knockout mouse lines. For melanoma lung metastasis experiments using human cell lines, six to eight week old CB17-SCID mice obtained from Charles River were used.

2.2 Antibodies and reagents:

Antibodies against Ly6G (clone: 1A8) were obtained from Biolegend, while F4/80 (BM8), CD31 (PECAM-1, 390) were obtained from ebioscience. DPEP1 antibodies were purchased from Abcam, Sigma and Proteintech. β-actin antibody was obtained from Milipore EMD. LSALT, KGAL and GFE1 peptides were synthesized by CanPeptide (Pointe-Claire, QC). DPEP1 cDNA's corresponding to mouse, rat or human DPEP1 gene were obtained from GE Dharmacon and OriGene. Human DPEP2 and DPEP3 cDNA's were obtained from OriGene. Sulfo-SBED Biotin Label Transfer Reagent was purchased from Thermo Fisher Scientific. Lipofectamine 2000 and optiMEM medium for transient transfections were purchased from Invitrogen. Lipopolysaccharide (Escherichia coli 111B4) was obtained from the List Biological Laboratories. For the metastasis studies, anti-Gr-1 (clone: RB6 8C5) obtained from Bio-X-cell. Human anti-nucleolin antibody was

purchased from Abcam (Cat. No. ab13541). D-Luciferin was purchased from PerkinElmer. A detailed description of all the chemicals, antibodies, plasmids, primers and other reagents can be found in the key resource table in the appendix section of this thesis.

2.3 *In vivo* imaging studies to investigate neutrophil recruitment to the lungs and liver by spinning disk confocal microscopy:

Six to ten week old C57BL/6 wild type or LysMeGFP mice on the C57BL/6 strain background were injected either with LSALT or control peptide by tail vein five minutes after an intraperitoneal injection of 0.5 mg/kg LPS. Liver and lungs were imaged four hours after LPS injection by spinning disk intravital microscopy (inverted or upright). Mice were anesthetized using Ketamine/Xylazine. Liver and lungs were prepared for imaging according to the principles and protocols established previously [299-300]. Antibodies were administered via jugular vein cannulation. Additional anesthetics were provided by jugular vein catheterization during imaging. Lungs and liver were imaged for at least 30 minutes. In some experiments, imaging was done for an hour. For *in vivo* experiments using Cilastatin, LysMeGFP mice were pre-injected with a 20 mM dose of Cilastatin 12 hours before the injection of LPS and re-injected with Cilastatin 10 minutes before the intraperitoneal injection of 0.5 mg/kg of LPS. Intravital microscopy was performed exactly as described previously [13, 299]. For the assessment of DPEP1 expression in tissues, organs (lungs, liver and kidney) were harvested from five to six week old *DPEP1-/-* or *DPEP1+/+* mice in the C57BL/6 strain and tissues were processed using paraffin embedding for histology. Lungs, liver and kidney sections were stained with DPEP1 antibody (Abcam) using the DAB method to assess DPEP1 expression. To measure endogenous DPEP1 activity in *DPEP1-/-* mice *in vivo,* organs (lungs, liver, spleen and kidney) were harvested from five to six week old DPEP1 null mice and their corresponding wild type mice. Proteins were isolated from tissues using

RIPA/Octyl-glucopyranoside in the absence of protease inhibitors using a tissue homogenizer. 10 µl of the protein lysate from each condition was used to perform DPEP1 enzyme activity exactly as described later in the method section. For the detection of neutrophils in tissue sections four hours after LPS injections, paraffin embedded lungs or liver sections were stained with Ly6G (clone: 1A8) antibody using the DAB method for immunohistochemistry. Lungs and liver of *DPEP1-/-* and *DPEP1+/+* mice were imaged by spinning disk confocal microscopy (inverted or upright) four hours after LPS treatment.

2.4 Image processing and analysis for neutrophil recruitment studies:

Movies and images were captured and processed using Volocity software. For some lung intravital imaging, movies and images were processed by LIF software and then converted to Volocity files for analysis. Neutrophils that were stationary in the liver sinusoids and post-capillary venules of the lungs for more than 1 minute were counted as adherent cells. Total number of neutrophils that were present four hours following LPS treatment were also counted, in the case of pulmonary capillaries. Neutrophils that moved within the liver sinusoids and did not remain stationary after they were firmly adhered, were defined as crawling neutrophils in the liver microvasculature.

2.5 Tissue culture and treatments:

COS1 cells were a kind gift from Dr. Karl Riabowol at the University of Calgary and were maintained in Dulbecco's modified eagle's medium supplemented with 10% fetal bovine serum with non-essential amino acids, L-glutamine and penicillin-streptomycin. Cells were incubated in a humidified 5% CO_2 incubator at 37˚C. COS1 cells grown in Dulbecco's modified eagle's medium supplemented with 10% fetal bovine serum with non-essential amino acids, L-glutamine and penicillin-streptomycin, were treated with LSALT (1mM) before the addition of human

neutrophils in the static binding assays. For the *in vitro* biotin transfer experiments, COS1 cells were treated with Sulfo-SBED-biotin labeled LSALT, GFE1 or control peptide for 10 minutes after 48 hours of transient transfection with human DPEP1. Human neutrophils were isolated from healthy human donors according to the procedures described by Chakrabarti and Patel [301] and were used fresh in static adhesion assays. Protocols for the isolation of human neutrophils was approved by the Conjoint Health Research Ethics Board at the University of Calgary and Alberta Health Services. Transient transfections were performed using OptiMEM medium without additional serum.

70W human melanoma cells were established from parental MeWo cell line in the laboratory of Dr. Robert Kerbel at the University of Toronto. 70W cells were cultured and maintained in Dulbecco's modified eagle's medium (Gibco-BRL, Bethesda, MD, USA) supplemented with 10% fetal bovine serum (Gibco-BRL) with non-essential amino acids, l-glutamine and penicillin-streptomycin. 70W human metastatic melanoma cells were engineered to express GFP-luciferase by stable transfection with a GFP-luciferase dual fusion plasmid under neomycin resistance. GFP-luciferase dual fusion plasmid was a kind gift from Dr. Frank Jirik at the University of Calgary. 70W GFP-luciferase cells were cultured under the selection of 400 µg/ml concentration of genticin (G418) and were incubated in a humidified 5% CO_2 incubator at 37˚C. All cells tested negative for mycoplasma.

2.6 Site directed mutagenesis and transfection:

Human DPEP1 cDNA was purchased from Dharmacon (pCMV-Sport 6 human DPEP1, MHS6278-202756036) and cloned into pcDNA 3.1+ vector (pcDNA DPEP1). To generate the catalytically inert mutant of DPEP1 (E141D), site directed mutagenesis was performed according to the manufacturer's instructions (#200523, Agilent Technologies, Santa Clara, CA, USA). Single

amino acid mutation in the catalytic domain of DPEP1 (E>D) was generated in the pcDNA 3.1 vector backbone. Mutants were obtained by PCR using pcDNA 3.1 DPEP1 as a template and were verified by DNA sequencing. All primer sequences are listed in the key resources table. Transient transfections of COS1 cells were performed by using the lipofectamine 2000 reagent. Briefly, 65-70% confluent COS1 monolayers were transfected with pcDNA DPEP1 or catalytically inert (E141D; pcDNA DPEP1 E>D) mutant construct (3 µg DNA). 48 hours later, cells were washed with PBS and proteins were isolated using RIPA buffer and Western blot analysis was performed to assess DPEP1 expression. For the DPEP1 enzyme activity assay, proteins were isolated in the absence of protease inhibitors. Western blot analysis and DPEP1 enzyme activity assay was performed to assess DPEP1 expression and activity

2.7 Tissue processing and Immunohistochemistry:

Lungs, liver and kidney were harvested from *DPEP1-/-* or *DPEP1+/+* mice either in the absence or presence of LPS and tissues were processed using paraffin embedding for histology. In some experiments, lungs were harvested by PBS perfusion through the right ventricle. For the inflation, lungs were flushed through the right ventricle with an excess amount of PFA (1 ml). 0.075% H_2O_2/methanol was used to inactivate endogenous peroxidases and nonspecific binding was blocked with Rodent Block M (Biocare Medical, Concord, CA, USA). Lung, liver and kidney sections were stained with rabbit-anti-DPEP1 (Abcam) (1/100 dilution). Sections were stained with appropriate secondary antibodies conjugated with a fluorophore or peroxidase for detection by immunofluorescence or conventional immunohistochemistry method to assess DPEP1 expression. Sections were counterstained with hematoxylin and mounted with Eco-mount. To detect the presence of neutrophils in the lungs and liver, tissue sections were stained with anti-Ly6G (clone: 1A8) using the DAB method for immunohistochemistry.

For the Immunohistochemical analysis to assess tumor burden, at the end of each experimental end point, four or six weeks post-injection, mice were sacrificed (anesthetized by IP injection of a mixture of ketamine (100 mg/kg) and xylazine (5 mg/kg) (Vetalar) followed by cervical dislocation), and all five lobes of the lungs were harvested, fixed in 10% formalin, and embedded in paraffin. Paraffin blocks were sectioned to generate 5 non-sequential lung sections (5 μm thick), 100 μm apart, and mounted on glass slides. To quantify metastatic burden, the total number of metastatic lesions was quantified in 5 non-sequential sections of all 5 lobes stained with hematoxylin and eosin (H&E), visualized at 2X magnification. The number of metastatic lesions with a diameter of < 1 mm and > 1 mm was also quantified. To assess the tumor area in each lobe of the lungs, Cell Scan software was used to manually measure the tumor area in three non-sequential lungs sections stained with hematoxylin and eosin.

2.8 *In vitro* biotin transfer and immunoprecipitation assays:

COS1 cells were transiently transfected with 3μg of DPEP1 encoding the human DPEP1 gene. Transfected cells were serum starved in OptiMEM for 2 hours and treated with methyl-beta-cyclodextrin for 30 minutes. After incubation, cells were washed with PBS and treated with 3.3mg/ml biotin transfer peptide (LSALT, GFE1 or control peptide) for 10 minutes. Cells were then washed with PBS and biotin transfer was enabled by UV activation of the aryl azide groups (non-specific binding to nearby proteins) for 15 minutes at 363 nm. Residual fluid was removed and monolayers were lysed with RIPA/ octyl-glucopyranoside (100 mM octyl-glucopyranoside in RIPA buffer). Entire cell lysates were rotated with 50 μl of neutravidin agarose beads at 4°C for 24 hours. Beads were washed with 8M urea buffer, boiled in Laemmli buffer and analysed by Western blotting using a DPEP1 antibody (Proteintech).

2.9 Immunoblot analysis and immunofluorescence studies:

Proteins from human DPEP1 transfected cells were isolated 48 hours after transient transfection using octyl-glucopyranoside/RIPA lysis buffer and Western blot analysis was performed to assess DPEP1 expression using DPEP1 antibody diluted in 1/1000 in 5% milk/TBST. For the detection of human DPEP2 and DPEP3, membranes were immunoblotted with a human specific DPEP2 antibody (Abcam) and DPEP3 antibody (Santa Cruz Biotechnology). For immunofluorescence studies, COS1 cells were transiently transfected with either 3 or 5 µg of dipeptidase-1 (DPEP1) cDNA corresponding to rat or human DPEP1 gene using lipofectamine 2000 (Invitrogen) reagent in OptiMEM medium. 24 hours after transfection, DPEP1 expressing cells were re-seeded on collagen coated (neutralized) cover slips in 24 well plates and allowed to grow for 24 hours at 37°C. 24 hours after seeding, media was removed and cells were washed with PBS. Cells were blocked with FBS/BSA/Tween in PBS for 30 minutes on ice. After incubation, cells were washed with PBS and incubated with LSALT, GFE1, control peptide conjugated with Alexa-488 (green) or with DPEP1 antibody (1/100) (Sigma) on ice for 30 minutes. DPEP1 antibody incubated cells were washed with PBS and incubated with fluorescently conjugated anti-rabbit secondary antibody (1/500 in PBS) for 30 minutes on ice. After incubation, cells were washed with PBS and stained with DAPI for 5 minutes on ice. Cells were then washed with PBS and fixed using 4% paraformaldehyde and immunofluorescence microscopy was performed to assess binding. Peptides were labeled using Alexa fluorophores according to manufactures instructions (Molecular Probes, Thermo Scientific).

2.10 Static adhesion assays *in vitro*:

COS1 cells were transiently transfected with 3 µg of human DPEP1 cDNA using lipofectamine 2000 in OptiMEM media. Transfected cells were re-seeded 24 hours after either on

a 12 well or 24 well plate. Human neutrophils isolated from healthy human donors were labelled with CFDA (CFSE) (Thermo Scientific) according to manufactures instructions. Once labelled, neutrophils were either treated with LPS (100 ng/ml) for 30 minutes at 37˚C or left untreated. 200 µl from ($1X10^6$) cells stock were added to each well containing DPEP1 expressing COS1 cell monolayers. Cells were incubated for 30 minutes at 37°C. After incubation, cells were vigorously washed two times with PBS. Cells were then fixed using para-formaldehyde (4%). The number of neutrophils bound on DPEP1 expressing COS1 monolayers were counted under 10X magnification over 10 different field of views using an inverted fluorescence microscope.

Similar experimental procedures were followed for the static adhesion assays using the 70W GFP-luciferase melanoma cells. Briefly, COS1 cells were transfected with 3 ug of human DPEP1 cDNA. Transfected cells were re-seeded 24 hours after either on a 12 well or 24 well plate. 70W melanoma cells expressing stable GFP-luciferase were harvested using Puck's EDTA and $10x10^3$ cells were seeded on the top of DPEP1 expressing COS1 cell monolayer after 48 hours. Cells were incubated for either 1 or 4 hours at 37˚C. After incubation cells were vigorously washed twice with PBS and fixed using para-formaldehyde (4%). The number 70W melanoma cells bound/adhered to DPEP1 expressing COS1 monolayers were counted under 10X magnification over 10 different field of views using an inverted fluorescence microscope. To determine the role of DPEP2 and DPEP3 in static adhesion assay *in vitro*, similar experimental parameters were followed. Briefly, COS1 cells were transiently transfected with 3 ug of either DPEP1, DPEP2 or DPEP3 cDNA using lipofectamine 2000 reagent (Invitrogen). After 24 hours, transfected cells were re-seeded either on a 12 well or 24 well plate. 70W melanoma cells expressing stable GFP-luciferase were harvested using Puck's EDTA and $10x10^3$ seeded on the top of DPEP1, DPEP2, DPEP3 expressing COS1 cell monolayers after 48 hours. Cells were incubated for either 1 or 4

hours at 37˚C. After incubation cells were vigorously washed twice with PBS. Cells were then fixed using para-formaldehyde (4%). The number 70W melanoma cells bound/adhered were counted under 10X magnification over 10 different fields of view using an inverted fluorescence microscope.

To determine the catalytic activity of DPEP1 for the binding of either human neutrophils or 70W human melanoma cells *in vitro*, COS1 cells were transiently transfected with either the wild type dipeptidase-1 (DPEP1), catalytically inert mutant (E>D) or mutant control (H>R) corresponding human DPEP1 gene using lipofectamine 2000 (Invitrogen) reagent. CFDA labeled human neutrophils or 70W melanoma cells expressing stable GFP-luciferase were seeded on the top of DPEP1 expressing COS1 cell monolayer after 48 hours. After incubation (30 minutes for human neutrophils and 4 hours for 70W GFP-luciferase cells) cells were vigorously washed twice with PBS. Cells were then fixed using para-formaldehyde (4%). The number human neutrophils or 70W melanoma cells bound/adhered on DPEP1 expressing COS1 monolayers were counted under 10X magnification over 10 different fields of view using an inverted fluorescence microscope.

2.11 Fluorometric assay for DPEP1 catalytic activity:

Fluorometric detection of membrane dipeptidase enzyme activity was performed as originally established by Heywood and Hooper and Rajotte et al, with some necessary modifications [302-303]. In brief, COS1 cells were transiently transfected with 3 µg of either human, mouse or rat dipeptidase-1 (DPEP1) cDNA using lipofectamine 2000 reagent. 48 hours after transfection, media was removed and cells were washed with PBS. Proteins were isolated using octyl-glucopyranoside/RIPA in the absence of protease inhibitors. Proteins were first incubated with dipeptidase-1 substrate Gly-D-Phe either in the presence or absence of two specific

69

inhibitors of DPEP1 ie Cilastatin (1 mM) and L-Penicillamine (1 mM) or LSALT, GFE1 and control peptide (1mM) at 37˚C for 1 hour and 40 minutes. After incubation, reaction assay buffer (50 µl/well) was added and the plate was incubated at 37˚C for 40 minutes in the dark. The fluorescence signal generated from the conversion of D-Phe to 6, 69-dihydroxy-(1, 19-biphenyl)-3, 39-diacetic acid in the presence of D-amino acid oxidase and peroxidase was measured using a fluorescence plate reader.

2.12 Myeloperoxidase activity assay *in vivo*:

For the detection of myeloperoxidase activity *in vivo*, lungs were first perfused through the heart using sterile PBS (5 ml) four hours after LPS treatment. Lungs were harvested from *DPEP1-/-* or *DPEP1+/+* mice homogenized in HTAB buffer (5 gram of HTAB in 1 liter of MPO buffer) using a mechanical tissue homogenizer. After homogenization, organ-extracts were mixed thoroughly using a vortex and centrifuged at 5000 rpm at 4˚C for four minutes. Samples were placed on ice and 7 µl of the organ-extract supernatant was assayed in a 96 well microplate in the presence of 200 µl/condition o-dianisidine hydrochloride solution. Absorbance was recorded at 530 nm using a softmax PRO software compatible for microplate reading.

2.13 Cytokine profile *in vivo*:

Six to eight week old SCID, C57/BL6 or *DPEP1 -/-* mice were injected either in the presence or absence of 1mM LSALT (intravenous by tail vein) or control peptide (KGAL) five minutes after the injection of 0.5 mg/kg LPS (i.p). Mice were anesthetized four hours later with ketamine/Xylazine (i.p). Whole blood was collected by cardiac puncture. Blood was incubated at room temperature for 30 minutes and centrifuge at 1000 ×g at 4°C for 10 minutes to obtain the serum in the resulting supernatant. Serum samples were then sent to Eve Technologies at University of Calgary for luminex analysis to determine the presence of cytokines and chemokines

released in the serum. Similar experimental procedures were followed for the detection of serum cytokines in *DPEP1+/+* or *DPEP1-/-* mice treated with 15mg/kg LPS. For the cytokine profile in the tissue homogenate, organs (lungs and liver) were collected and homogenized (using a tissue homogenizer) in 500 µl cold PBS with protease inhibitor cocktail per 200 mg of tissue on ice. To obtain tissue homogenate, homogenized lung and liver tissue samples were centrifuged at 10,000 × g at 4°C for 10 minutes. The resulting supernatant was assayed to determine the released cytokines and chemokines by Luminex analysis. In some experiments, six to eight week old SCID mice were injected with anti-Gr-1 (Clone: RB6 8C5) to deplete circulating leukocytes 24 hours prior to LPS injection to assess the cytokines and chemokines released in the absence of circulating leukocytes.

2.14 Sepsis survival studies:

For the survival studies using LPS, 5 to 7 mice/group were used. *DPEP1+/+* and *DPEP1-/-* mice were administered with 15mg/kg LPS and monitored over a period of seven days. LSALT peptide was injected intravenously into the tail vein of *DPEP1+/+* mice 5 minutes and 18 hours after the LPS injection. Kaplan Meier survival analysis was performed to assess overall survival. Clinical scores in survival studies using LPS were defined based on the criterion originally described by Shrum et al. to score sepsis severity in mice [304].

2.15 *In vivo* melanoma-lung metastasis model:

For the establishment of a human metastatic melanoma mouse model *in vivo*, two different cell numbers were used ($1x10^6$ and 500,000). Preliminary experiments were performed using $1x10^6$ cells in 200 ul of PBS/ mouse while majority of the *in vivo* studies in the human xenograft model was performed using an optimized cell number of 500,000 in 200 ul PBS. GFP-luciferase expressing 70W human melanoma cells cultured in DMEM in the presence of G418, dissociated

from the dish using Puck's EDTA once they reached to 70% confluency. Cells were washed with PBS, counted and injected into six to ten week old immunocompromised mice (CB17-SCID) intravenously by tail vein. LSALT, GFE1 or KGAL peptide (1mM) in 200 ul of PBS was injected intravenously by tail vein into the SCID mice five minutes prior to the injection of 70W GFP-luciferase expressing cells. Mice were monitored on alternate days and imaged by bioluminescence xenoxen IVIS 200 once every week post-injection up to six weeks. Tumor burden was also assessed by immunohistochemistry post-sacrificing the mice.

For the B16-10 murine melanoma-lung metastasis studies *in vivo*, an optimized cell number of 100,000 cells in 200 µl was injected intravenously into the tail vein of eight-ten week old C57BL/6 mice five minutes after the injection of either LSALT or control peptide (1 mM). Mice were monitored on alternate days and sacrificed two weeks post-injection to assess the tumor burden. Metastatic tumor burden was measured based on the presence of black surface nodules/lesions on the surface of lungs and by performing immunohistochemistry on paraffin embedded lung tissue sections.

2.16 Antibody mediated leukocyte depletion in melanoma lung metastasis studies:

For leukocyte depletion studies, six to eight week old CB17-SCID mice were injected with anti-Gr-1 antibody (150 ul from 1mg/ml stock solution) 24 hours prior the injection of LSALT peptide or 70W GFP-luciferase melanoma cells. Mice were injected with anti-Gr-1 antibody for additional five days to maintain a leukocyte depleted situation. For the B16/F10 syngeneic melanoma-lung metastasis model, mice were pre-injected with Ly6G (clone: 1A8) (150 ul of 1mg/ml stock) antibody (i.p) 24 hours before the injection of B16-F10 melanoma cells intravenously by tail vein. LSALT, GFE-1 peptide (1 mM) was injected five minutes before the

injection of melanoma cells. Mice were injected with antibody for two additional days after the injection of peptides and melanoma cells.

2.17 Bioluminescence imaging *in vivo*:

Bioluminescence imaging of mice were performed using a xenozen IVIS 200 optical imaging system in Living Image 3.0 software. Mice were injected intraperitoneally with D-luciferin (150 mg/kg) (PerkinElmer) and allowed to circulate for ten minutes. Mice were anesthetized using isoflurane. Images were captured at 1 second, 30 seconds, 45 seconds and 1 minute exposure time. Total flux of photons were determine by ROI quantification.

2.18 Flow cytometry *in vitro:*

COS1 cells were transiently transfected with DPEP1 cDNA corresponding to the human DPEP1 gene using optiMEM medium and lipofectamine 2000 in the absence of serum. Transfected cells were washed with PBS and dissociated from the Petri dishes 48 hours after transfection using Puck's EDTA. Cells were then incubated in the presence of either secondary only control or anti-DPEP1 antibody (Sigma) (1/100 in PBS) for 30 minutes on ice. Cells were washed with PBS by centrifugation at 1000 rpm for 3 to 5 minutes. An Alexa-488 conjugated anti-rabbit secondary antibody (1/500 in PBS) was then added to cells and incubated for 30 minutes. Cells were then washed with PBS. Washed cells were then filtered through the filter containing specialized FACS tube and 300-500 µl of the cell suspension containing at least $1x10^6$ cells were analyzed by flow cytometry to assess DPEP1 expression.

2.19 Survival assay in melanoma-lung metastasis studies:

Median survival time were determined in mice treated either with LSALT peptide or with 70W melanoma cells alone. Behavior of mice were monitored on alternate days and body weight was measured. Mice were sacrificed based on any of the end-point criterion: i) inefficiency to eat

and drink properly, ii) groom themselves, iii) lack of mobility iii) becoming scruffy or when iv) body weight drops >20%. Kaplan Meier survival analysis was performed to assess overall survival.

2.20 Statistical analysis:

All data were analyzed by either one- way ANOVA or an unpaired students t-test using GraphPad Instat3 software (La Jolla, CA, USA) and are presented here as ±SEM. $P<0.05$ was considered statistically significant.

Chapter Three: Results

3.1 Isolation and screening of a peptide-displaying bacteriophage library *in vivo*.

At the beginning of this study, the mechanisms that govern the recruitment of neutrophils to the lungs and liver were unknown. Therefore, the initial impetus for this thesis was to identify the mechanism(s) by which neutrophils are recruited to the lungs and liver during inflammation. Although, studies in the last three decades have identified the selectins and integrin family members (a group of proteins categorized as classical adhesion molecules) as essential mediators for the recruitment of neutrophils to the mesentery, skin and cremaster muscle, (summarized in [25, 305] , [27-29, 46, 49, 51, 306-307]), observations in recent years have suggested that none of these 'known classical adhesion molecules' are involved in neutrophil recruitment to the inflamed hepatic and pulmonary vasculatures[44-45, 106]. Identification of the interaction between CD44-HA as a mechanism for the adhesion of neutrophils in inflamed hepatic sinusoids by McDonald et al. was the first non-conventional adhesion mechanism described [3]. However, as this interaction was demonstrated as 'a predominant mechanism' in neutrophil adhesion within the liver sinusoids, it was apparent that additional/alternate adhesion molecule(s) utilized for the recruitment of neutrophils were present on the vasculature of this organ. Akin to the liver, molecules involved in the recruitment of neutrophils within the lung have yet to be identified. Thus, to identify cell surface molecules that mediate neutrophil recruitment to the lungs and liver, our research group led by Dr. Jennifer Rahn embarked on an unbiased *in vivo* approach based on the pioneering work of Ruoslahti and colleagues [89]. A combinatorial phage display library was used to isolate and identify peptide displaying bacteriophage that homed to the lungs and liver of mice in response to the gram negative bacterial endotoxin, lipopolysaccharide (LPS), a toxin previously shown to induce a robust systemic inflammatory response in both mice and humans [308]. For this strategy, a phage display library was generated to express peptides produced from cDNA converted from

neutrophil RNA. The neutrophil derived cDNAs were fused to the coat protein gene of T7 bacteriophage and a library called T7N was generated (**Figure 3.1A**). By establishing a phage peptide library using neutrophil RNA we anticipated that isolated phage peptides would reflect proteins present on the neutrophils. Next, to select bacteriophage that home preferentially to the lungs and liver *in vivo*, neutrophils were depleted from C57BL/6 mice using a leukocyte specific antibody (anti-GR-1 clone: RB6 8C5) prior to the injection of the potent inflammatory stimulus LPS. Since the premise of this study was to identify molecules on the endothelium, neutrophil depletion was utilized so that the putative adhesion receptor(s) on the endothelium would not be sterically hindered by the presence of bound neutrophils. Next, to isolate phage that homed specifically to the lungs and liver, the T7N peptide expressing bacteriophage library was injected via the tail vein (intravenous) of the neutrophil depleted mice. Phage were allowed to circulate for ten minutes, the liver and lungs were harvested and phage bound to these organs were isolated and phage that had homed to the liver and lungs were recovered by infecting a host bacterial culture (**Figure 3.1A**). This procedure was repeated five times to enrich for organ specific homing phage. In order to prioritize our efforts on the numerous phage (phage were split into two pools) that were isolated a functional screen was performed based on their ability to inhibit neutrophil recruitment in the liver sinusoids in the presence of LPS. Intravital microscopy was performed to visualize neutrophil behavior in the liver sinusoids *in vivo* and to assess the ability of the isolated bacteriophage to inhibit the recruitment of neutrophils to the liver microvasculature. Among the many lung and liver homing phage isolated, a number of phage were functionally screened for their ability to inhibit neutrophil adhesion by intravital microscopy. A specific peptide displaying phage subclone was found to inhibit the adhesion of neutrophils to the liver sinusoids (LPS: 18.67± 2.49, LPS + phage: 8.16± 0.60) (**Figure 3.1B**). Although the phage display library was generated

from neutrophil RNA in anticipation of identifying peptides that correspond to neutrophil proteins, the inhibitory phage identified encoded a peptide for the out of frame gene sequence of Ube2n. The translated peptide sequence of this bacteriophage subclone was LSALTPSPSWLKYKAL and is referred to in this thesis as LSALT. The LSALT peptide has been patented under the name Metablok (J.J.R., P.K., S.M.R, D.L.S.) and has been assigned to Arch Biopartners.

A

Isolate Neutrophils from mouse → Isolate mRNA Construct cDNA → Insert cDNA into T7 Phage Coat Protein Gene

Pool of T7 Phage Displaying Random Neutrophil Peptides

<u>Subtraction</u> – Depletion of phage that bind to "background cells" (primary fetal mouse lung endothelia, unstimulated)

Selection – Isolation of phage that bind to "target" cells.

Deplete Neutrophils (anti-Ly6G 1 mg/mL) —24 hrs→ Treat with LPS (0.5 mg/kg) —4 hrs→ —10 min→ Cardiac Perfusion (15 mL PBS)

Harvest Organs Titre Phage — Lungs / Liver — Reinject phage 5X → T7N Lung Library / T7N Liver Library

B

** / ***

Adhered neutrophils/FOV

Control Phage | LSALT Phage

LPS

Figure 3.1: Isolation and screening of a peptide displaying bacteriophage library *in vivo*. A. Neutrophils were depleted from (C57BL/6) mice using a leukocyte specific antibody (anti-Gr-1; clone: RB6 8C5) prior to the injection of a potent bacterial inflammatory stimulus (Lipopolysaccharide; LPS 0.5 mg/kg). The T7N peptide displaying bacteriophage library (see materials and methods section for the generation of T7N phage display library) was injected intravenously into the tail vein of mice and allowed to circulate for 10 minutes. Mice were then perfused with PBS and the organs (liver and lungs) were harvested. Phage that homed to the liver and lungs were recovered by infecting a host bacterial culture. This procedure was repeated five times to enrich for specific homing phage, and lung and liver targeting peptide libraries were generated. After purification and isolation, phage were screened for their ability to inhibit neutrophil adhesion in the liver sinusoids and a specific peptide-displaying-phage (LSALT) was isolated. **B.** Six to eight week old C57BL/6 mice were injected either with blocking or control phage (A-stop) in the presence of LPS and the liver was imaged using intravital microscopy four hours later. Neutrophils that were stationary (adhered on the endothelium) were counted as adherent cells. Values shown are the mean ±SEM from two independent experiments; asterisks (**) indicate $P<0.01$ as compared with LPS treated mice and *** indicate $P<0.001$ as compared to the control phage treated mice (one-way ANOVA with the Neuman-Keuls post-test). N=2 (This data was contributed by Dr. Jennifer Rahn).

Since the initial functional studies were performed using bacteriophage that itself contains endotoxin impurities, the corresponding displayed peptide (H-LSALTPSPSWLKYKAL-NH-2) was commercially synthetized and assessed for its functional blocking activity. This LSALT peptide was assessed using intravital spinning disk confocal microscopy in a series of *in vivo* experiments in collaboration with Dr. Paul Kubes at the University of Calgary. When a 500 µM dose of this synthetic peptide (LSALT) was injected intravenously into the tail vein of LysMeGFP mice, similar to the bacteriophage, a significant inhibition in the adhesion and recruitment of LysMeGFP neutrophils in the liver sinusoids was observed (LPS: 137.3±11.52, LPS+ LSALT peptide: 71.14±1.98, LSALT phage: 79.75±4.97) (**Figure 3.2A**), thus validating the initial observations *in vivo*. As the lysozyme M promoter can drive the expression of the green fluorescent protein in monocytes in addition to the neutrophils in LysMeGFP mice [309], the effect of the LSALT peptide was also assessed for its ability to specifically inhibit the adhesion of neutrophils in the liver sinusoids in response to LPS. To assess this, intravital spinning disk microscopy was performed to image the liver of C57BL/6 mice that were injected with the LSALT peptide in the presence of LPS. To visualize the neutrophils in these experiments, Ly6G antibody (clone: 1A8) was used that specifically labels neutrophils [310]. A significant reduction in the adhesion of 1A8 specific neutrophils was observed in the hepatic sinusoids of mice that were treated with the LSALT peptide as compared to the LPS alone treated C57BL/6 mice (LPS: 112.2± 8.83, LPS+LSALT:55.89±5.69) (**Figure 3.2B**). This observation, in combination with the results obtained in the LysMeGFP mice, suggests that the LSALT peptide specifically inhibits the recruitment of neutrophils in the liver microvasculature in response to LPS. In addition, the LSALT peptide was shown to significantly reduce the crawling of firmly adhered 1A8 specific neutrophils in the hepatic sinusoidal endothelium (LPS:16.17±1.40,LPS+LSALT: 9.23±1.31)

further supporting a role for the LSALT peptide in two distinct steps (adhesion and crawling) in the neutrophil recruitment cascade (**Figure 3.2B**). The molecular basis of crawling under shear is one of the least understood processes in the neutrophil adhesion cascade with only one known interaction (Mac-1-ICAM-1) shown to mediate luminal crawling of neutrophils under shear in response to an inflammatory stimulus [33]. As other molecular players that mediate crawling of neutrophils under shear are yet to be identified, LSALT peptide mediated inhibition of neutrophil crawling within the hepatic sinusoids provides a tool to uncover some of the fundamental basis of this event in inflamed microvasculature.

A

Sham LPS LSALT Peptide Phage

Adhered neutrophils/FOV

*** ***

Sham LSALT Phage LSALT Peptide

LPS

B

LPS

Sham ContP LSALT

Neutrophils Ly6G/1A8 Kupffer Cells (F4/80) Vasculature (CD31)

Adhesion

Adhered neutrophils/FOV

*** ***

Sham ContP LSALT Peptide

LPS

Crawling

Crawling neutrophils/FOV

**

LSALT

LPS
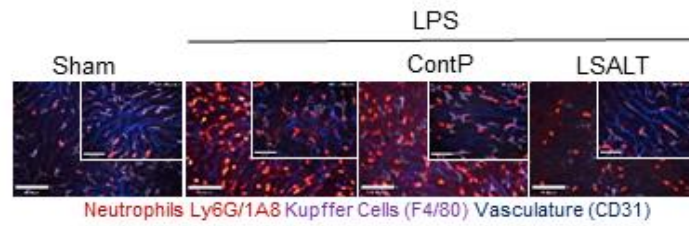
Figure 3.2. LSALT phage/peptide inhibits neutrophil adhesion in the liver sinusoids in response to LPS. A. Six to eight week old LysMeGFP mice were injected either with the LSALT phage or peptide intravenously five minutes after LPS injection. The livers were imaged using intravital spinning disk confocal microscopy. Shown here are representative intravital spinning disk confocal images of neutrophils (GFP, green) and Kupffer cells (F4/80, purple) in the liver sinusoids (CD31, blue) (upper panel). Neutrophils that were stationary in the liver sinusoids for more than one minute were counted as adherent cells. Scale bar: 150 μm. Values shown are the means ±SEM from at least three independent experiments; asterisks (***) indicate P<0.001 when compared to LPS treated mice (one-way ANOVA with the Neuman-Keuls post-test). **B.** Eight to ten week old C57BL/6 mice were injected either with LSALT peptide or control peptide (KGAL) intravenously via the tail vein five minutes after an intraperitoneal injection of 0.5 mg/kg LPS (i.p). Intravital microscopy was performed on the liver four hours later. Shown here are neutrophils (Ly6G, clone: 1A8, red) and Kupffer cells (F4/80, purple) in the liver sinusoids (CD31, blue). Neutrophils that were stationary for more than one minute in the liver sinusoids were counted as adherent cells. Inset shows a separate image captured under 20X objective. Scale bar: 90 μm. Crawling of neutrophils were also monitored and firmly adhered cells with elongated behavior indicative of transmigration were counted as crawling neutrophils (right panel). The graph shows the mean ±SEM from two independent experiments; asterisks (***) indicate P<0.001 when compared to LPS treated control mice (one-way ANOVA with the Neuman-Keuls post-test). (Experiments performed in collaboration with Dr. Liane Babes).

3.2 LSALT peptide inhibits neutrophil adhesion in the liver sinusoids in *CD44 -/-* mice *in vivo*.

CD44, a transmembrane glycoprotein expressed on a wide variety of cell types in the hematopoietic lineage, has been shown to be involved in a number of different cellular and physiological processes in health and disease [311]. However, the role of this protein in the recruitment of neutrophils in inflammatory diseases, in particular endotoxmeia/sepsis was unknown prior to 2008 when McDonald et al. showed that CD44 expressed on the surface of neutrophils binds to hyaluronic acid (HA) expressed on the sinusoidal endothelium of the liver and through this interaction mediates neutrophil adhesion and sequestration within the liver microvasculature in an LPS-induced model of endotoxemia [3, 312]. Interestingly, this mechanism was found to be restricted to the sinusoidal endothelium as no significant reduction in neutrophil adhesion was observed in the post-capillary venules when this interaction was disrupted either by the use of monoclonal antibodies to CD44 or CD44 knockout mice. Moreover, using bone marrow transplantation to generate chimeric animals, the investigators showed that CD44 expressed by the neutrophil and not the endothelial CD44 was required for neutrophil adhesion in vascular beds of the liver.

Based on the identified role for CD44-HA in the liver, experiments were performed to determine if LSALT mediated inhibition of neutrophil recruitment resulted due to the binding of the LSALT peptide to CD44. To address this, we first assessed the recruitment of neutrophils in the liver of *CD44 -/-* mice in the presence of LPS. Indeed, (*CD44+/+*: 71.66 ± 2.60 , *CD44-/-*: 36.33 ± 2.18) reduction in the adhesion of 1A8 specific neutrophils in the liver of *CD44-/-* mice was observed compared to the wild type C57BL/6 mice in the presence of LPS (**Figure 3.3A-B**). This observation was consistent with the results published by McDonald et al.[3]. Next,

85

experiments were performed to assess the potential of CD44 as the receptor of the LSALT peptide. Six-eight week old *CD44 -/-* mice were injected with the LSALT peptide (1mM) in the presence of LPS. Intravital spinning disk confocal microscopy of the liver of these mice revealed a significant inhibition (*CD44-/-*LPS*:* 84.66±10.36, *CD44-/-*LPS+LSALT: 32.11±5.58) in the adhesion of 1A8 specific neutrophils in the presence of LSALT peptide compared to the LPS treated *CD44-/-* mice (**Figure 3.3C-D**). These observations not only suggested that CD44 was not the functional receptor for the LSALT peptide but also support the idea that a second adhesion molecule in addition to CD44 is involved in the recruitment of neutrophils in the inflamed hepatic sinusoids.

A

Sham   LPS (CD44+/+)   LPS (CD44-/-)

Neutrophils (Ly6G/1A8) Kupffer Cells (F4/80) Vasculature (CD31)

B

***

Adhered neutrophils/FOV

Sham   CD44 +/+   CD44 -/-

LPS

C

LPS

Sham   ContP   LSALT

CD44 -/-

Neutrophils (Ly6G/1A8) Kupffer Cells (F4/80) Vasculature (CD31)

D

**
**

Adhered neutrophils/FOV

Sham   ContP   LSALT

LPS
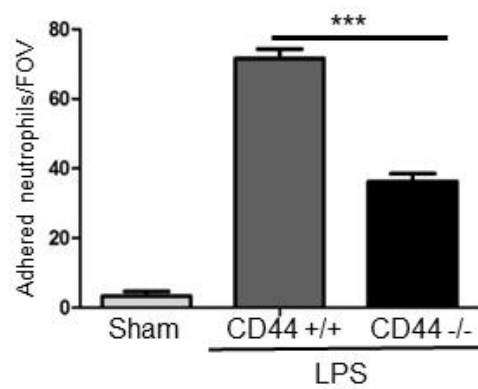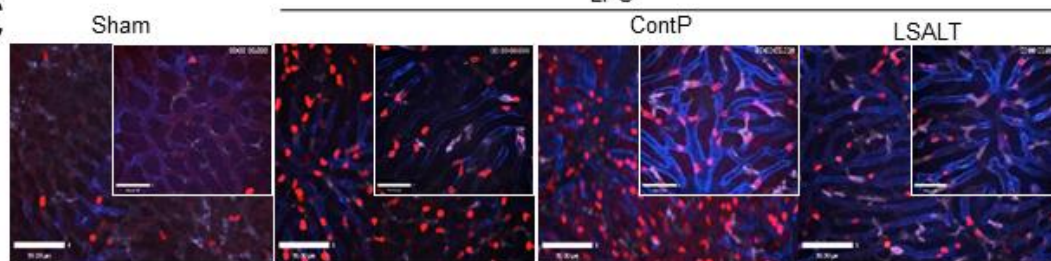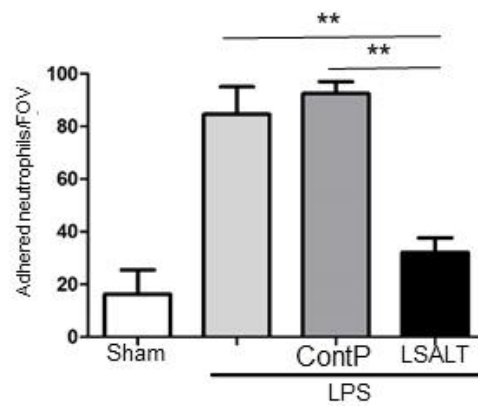
Figure 3.3: LSALT peptide inhibits neutrophil adhesion in the liver sinusoids in *CD44-/-* mice in the presence of LPS. A. Six to eight week old *CD44+/+* mice or *CD44-/-* mice were injected with 0.5 mg/kg LPS (i.p) and the liver was imaged using intravital spinning disk confocal microscopy. Shown here are the presence of neutrophils (Ly6G, clone: 1A8, red) and Kupffer cells (F4/80, purple) in the liver sinusoids (CD31, blue) (upper panel). **B**. Graph shows the number of neutrophils that were stationary for more than one minute within the liver sinusoids. A separate 20X image is shown in the inset. Scale bar: 100 μm. **C-D.** Six to eight week old CD44 deficient (*CD44 -/-*) mice in the C57BL/6 background strain were injected intravenously via the tail vein with LSALT or control peptide (KGAL) (1mM) five minutes after the administration of 0.5 mg/kg LPS (i.p). Shown here are intravital spinning disk confocal images of neutrophils (Ly6G, clone: 1A8, red) and Kupffer cells (F4/80, purple) in liver sinusoids (CD31, blue). Adhered neutrophils were counted as described previously. Inset shows a separate image captured under 20X objective. Scale bar: 90 μm. **D.** Graph shows the mean ±SEM. from three independent experiments; asterisks (***) indicate $P<0.001$ as compared to the LPS treated *CD44-/-* mice (one-way ANOVA with the Neuman-Keuls post-test). (Experiments performed in collaboration with Dr. Liane Babes).
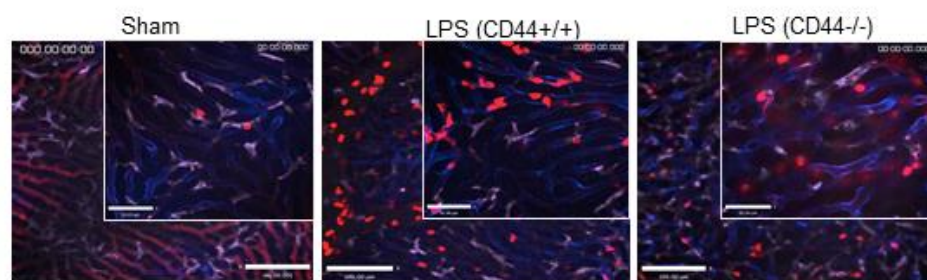
3.3 LSALT peptide inhibits neutrophil recruitment in the pulmonary microvessels.

As the LSALT displaying phage was also found to bind the endothelium within the lungs, we next wanted to assess the effect of the LSALT peptide on the recruitment of neutrophils to the inflamed pulmonary vasculature. To date, the molecular mechanisms underlying neutrophil recruitment within the inflamed pulmonary microvasculature is unknown. The absence of current understanding has been in part attributed to the lack of imaging strategies/techniques sophisticated enough to visualize neutrophil behavior under physical shear within the tiny capillary networks in the lungs. Coupled with the challenge of constant movement from the breathing and respiratory actions of a live mouse studies directly investigating the underlying mechanisms have been limited. In addition, the lack of evidence supporting the involvement of known adhesion molecules within the pulmonary vascular beds suggests the presence of other yet to be identified adhesion receptors. Recently the obstacles hindering intravital imaging within the lung were overcome by Mathew Krummel's group at the University of California, San Francisco [313]. Adopting similar technical parameters, in collaboration with Drs. Bryan Yipp and Paul Kubes, intravital confocal microscopy was performed to assess the effect of the LSALT peptide on neutrophil recruitment to the lungs of C57BL/6 mice in the presence of LPS. A significant inhibition in the recruitment of 1A8 specific neutrophils in two distinct vascular compartments of the lungs (capillaries and medium sized vessels) was observed in mice that were treated with the LSALT peptide compared to the LPS alone treated control mice (capillaries: LPS: 127.6 ±10.05, LPS+ LSALT: 74.11±8.67, medium size vessels: LPS: 11.11±1.52, LPS+LSALT: 3.60±1.03) (**Figure 3.4A-B**). Since in addition to the lungs, LSALT also inhibited neutrophil recruitment to the liver sinusoids, this observation strengthened our pre-existing idea that lungs and liver may use a common adhesion molecule for cellular recruitment to pulmonary and hepatic vasculatures, a notion that is consistent

with our original hypothesis and supports the possibility that LSALT binds to a previously unknown adhesion molecule in both the lungs and liver microvasculature. Of note, in collaboration with Dr. Daniel Muruve in the Snyder Institute at the University of Calgary, the LSALT peptide has also been shown to significantly inhibit the recruitment of LysMeGFP neutrophils to the inflamed renal vascular beds in an ischemia reperfusion model (Lau and Muruve, unpublished).

A

Capillaries

LPS   LPS+LSALT

Neutrophils (Ly6G/1A8) Vasculature (CD31)

***

Neutrophils/FOV

LPS   LSALT

B

Post-capillary venules

**   ***

Neutrophils/FOV   Adhered neutrophils/FOV

LPS   LSALT   LPS   LSALT
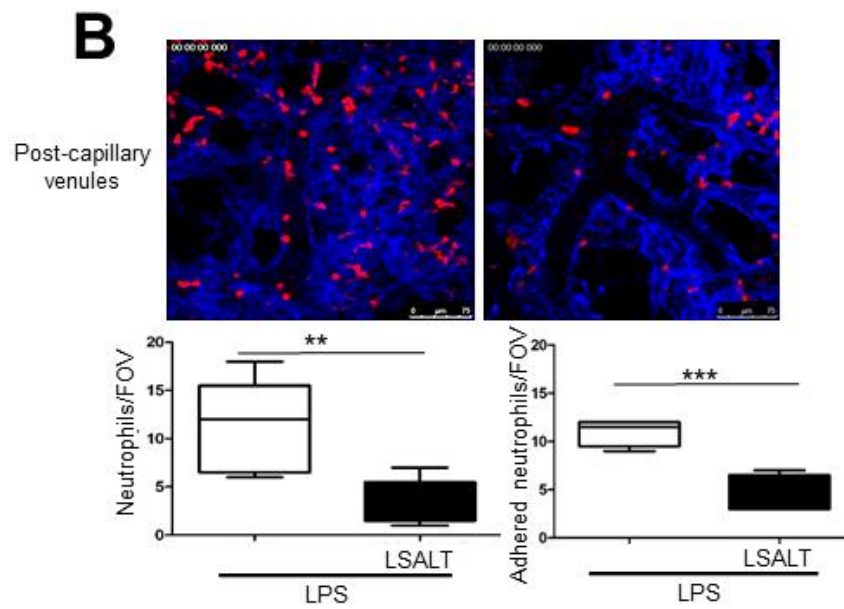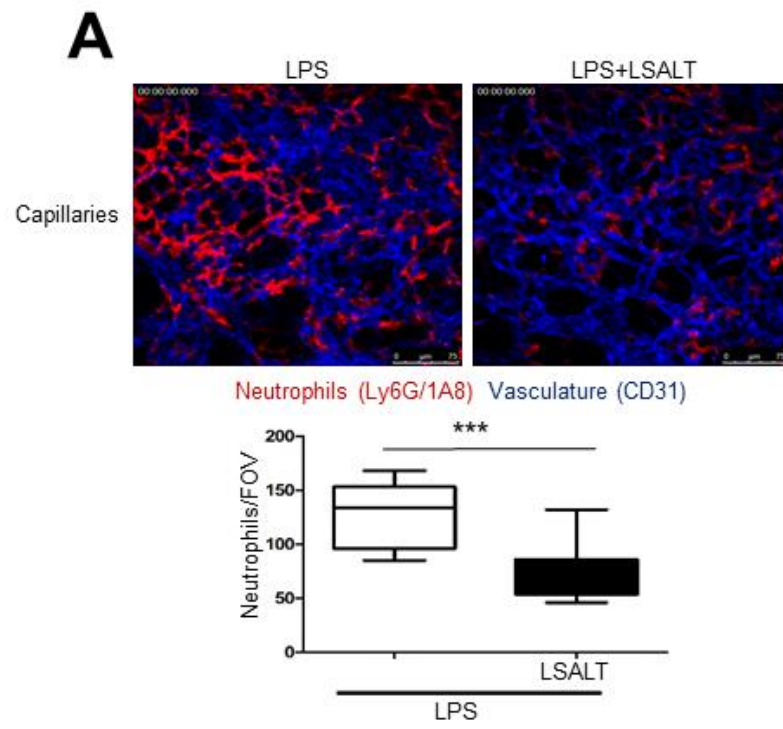
Figure 3.4: LSALT peptide inhibits neutrophil recruitment to the lungs in response to LPS.

A-B. Eight to ten week old C57BL/6 mice were injected with LSALT peptide (i.v.) in the presence of 0.5 mg/kg of LPS (i.p) and the lungs were imaged using intravital microscopy four hours later. Shown here are intravital spinning disk confocal images of neutrophils (Ly6G, clone: 1A8, red) in the lung vasculature (CD31, blue). Numbers of neutrophils present in the lung vasculature, capillaries **(A)** and medium sized vessels **(B)** were counted four hours following LPS treatment. Graph shows the mean ±SEM. from two independent experiments; asterisks (**) indicate $P<0.01$ as compared with LPS treated control mice. (***) indicate $P<0.001$ as compared to the LPS treated mice (one-way ANOVA with the Neuman-Keuls post-test) Neutrophils that were stationary for more than one minute within the medium sized vessels/post capillary venules of the lungs were counted and plotted (lower right panel). Scale bar: 75 μm. (Lung imaging was performed by Dr. Bryan Yipp, mouse injections and data analysis was done by myself).

3.4 LSALT peptide inhibits cancer metastasis to the lungs and liver *in vivo*.

Based on the literature that neutrophils and metastatic cancer cells may use/share common adhesion molecules for organ-specific endothelial binding/extravasation and as LSALT peptide inhibited the recruitment of neutrophils to the liver and lungs, we hypothesized that treatment of mice with the LSALT peptide will inhibit the recruitment of metastatic cancer cells to the lungs and liver. To address this question *in vivo*, two melanoma lung metastasis models were used. The first is a highly metastatic human melanoma-lung metastasis (70W) model and the second is an immunocompetent melanoma-lung metastasis murine model (B16/F10). MeWo derived 70W human melanoma cells were a kind gift from Dr. Robert Kerbel at the University of Toronto. To establish a cell line compatible for *in vivo* imaging, 70W melanoma cells were engineered to stably express a fusion GFP-luciferase plasmid construct. Next to address the effect of the LSALT peptide in melanoma lung metastasis, initial experiments were performed using the 70W human melanoma model. Briefly, SCID mice were intravenously administered 70W GFP-luciferase cells five minutes following a 500 μM dose of the LSALT peptide (i.v.). A dramatic reduction in the melanoma-lung metastatic tumor burden as assessed by bioluminescent imaging was observed in mice treated with the LSALT peptide compared to the mice that were injected with 70W melanoma cells alone (70W alone: 2.867e+006±907718, 70W+LSALT: 649167±294055 photons/s/cm^2) (**Figure 3.5A-B**). In addition, tumor burden was validated by immunohistochemical assessment using human specific anti-nucleolin to visualize the human cancer cells (**Figure 3.5C**). These observations support the hypothesis that neutrophils and metastatic melanoma cells may use/share common adhesion molecules for organ-selective recruitment to the lungs. Next, based on this striking observation, the potential of the LSALT peptide to block metastasis in a syngeneic B16/F10 melanoma-lung metastasis murine model was assessed and similar to the human

xenograft model, the LSALT peptide inhibited melanoma lung metastasis (B16/F10 alone: 4.750±1.652, B16/F10+LSALT: 2.500±0.6455) (**Figure 3.5D**). These observations further reinforced the idea that common adhesion molecules may be used/shared for organ specific recruitment of neutrophils and metastatic cancer cells to the lungs and liver. Further, in collaboration with Dr. Peter Siegel at the McGill University, the LSALT peptide was assessed in a breast cancer-liver metastasis model. Using a 4T1 derived liver aggressive breast cancer cell line in an immunocompetent murine model (BalbC) a striking reduction was also observed in breast cancer-liver metastases when either the LSALT phage or a 500 µM dose of the LSALT peptide was injected intravenously into the tail vein of BalbC mice following splenic injections of 4T1 murine breast cancer cells (Tabariès and Siegel, unpublished). Taken together, these observations suggested that in addition to neutrophil recruitment, the LSALT peptide reduces the metastatic tumor burden in the lungs and liver in human xenograft and immunocompetent mouse models *in vivo* further suggesting the involvement of common adhesion molecules that mediate recruitment of cells to the lungs and liver. Based on the fact that metastases are largely governed by the adhesive cellular and molecular interactions between proteins expressed on the surface of circulating tumor cells and the endothelium, these observations may have clinical applications. First, targeting of adhesion molecules that mediate organ-selective metastatic disease to the lungs and liver with pharmacological inhibitors may prevent metastatic spread and second, our results in the pre-clinical mouse models, suggest the LSALT peptide may have direct therapeutic applications. For example, it has been postulated that the endothelium of a given organ may exhibit unique vascular addresses or zip codes. As such studies have been devoted to identifying these addresses using a similar phage-display strategy described in this thesis [89, 314-315]. Of the

94

peptides identified that recognize organ-specific vascular signatures a few are currently being

developed as cancer therapeutics and imaging agents [316-318].

A

LSALT

0 μM   50 μM   500 μM   Normal

B

Control   LSALT

70W Human Melanoma

Luciferase Activity

8.0×10⁸
6.0×10⁸
4.0×10⁸
2.0×10⁸

*

LSALT

70W Human Melanoma

C

H and E   Human Nucleolin

Control

LSALT

70W Human Melanoma

D

Control   LSALT

Number of metastatic lesions>500 mm

5
4
3
2
1
0

LSALT

B16-F10
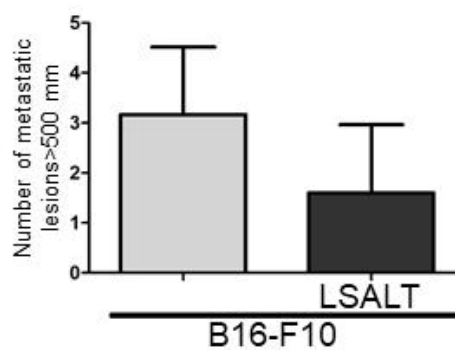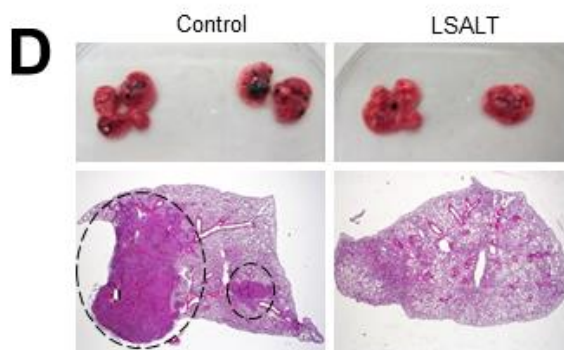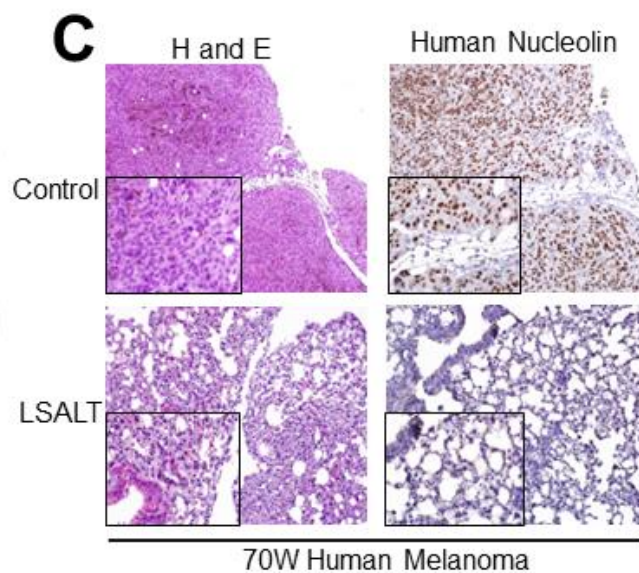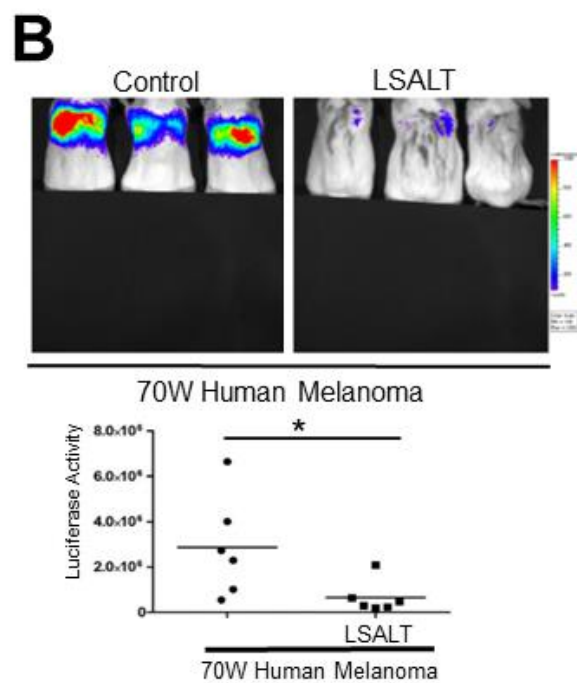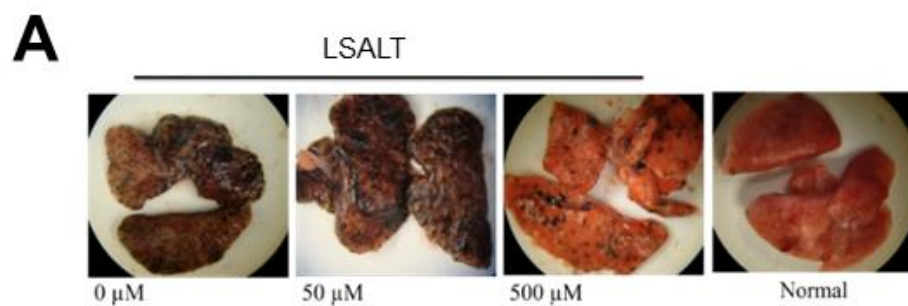
Figure 3.5: LSALT peptide inhibits melanoma-lung metastasis. A. 70W GFP-luciferase human melanoma cells were injected in six to eight week old immunocompromised SCID mice five minutes after the injection of a 500 µM dose of LSALT peptide (i.v.) and the lungs were harvested four weeks later to assess tumor burden. **B.** SCID mice were injected with LSALT peptide (i.v.) five minutes prior to the injection of 70W GFP-luciferase human melanoma cells (i.v.). Mice were imaged six weeks later using bioluminescence imaging (IVIS 200). Graph shows quantification of tumor burden as assessed by luciferase activity measured using Xenogen optical *in vivo* imaging system. An unpaired student's t-test was performed to compare the LSALT treated group with the control group. (*) indicate $P<0.05$ as compared to control group. N=5 **C.** Lungs harvested from either LSALT or 70W GFP-luciferase human melanoma cells injected SCID mice, were harvested, fixed, paraffin embedded and assessed by immunohistochemistry using hematoxylin and eosin (left panel) and human anti-nucleolin (right panel). Scale bar 20µm **D.** Lungs harvested from C57BL/6 mice injected with B16/F10 (100,000 cells/mouse) murine melanoma cells either in the presence or absence of 1 mM LSALT peptide (i.v.) were photographed (upper panel) and assessed by immunohistochemistry using hematoxylin and eosin (lower panel). Tumor burden was measured by the quantification of number of metastatic lesions that were more than 500 µm on the surface of the lungs (lower right panels). Scale bar: 20 µm. (tail vein injections were performed by Dr. Xiaoguang Hao).

3.5 Leukocytes (Gr-1+) are not required for melanoma-lung metastasis *in vivo*.

Since the LSALT peptide blocks neutrophil recruitment it is possible that the recruitment of neutrophils is required for the initial seeding and extravasation of the cancer cells. Alternatively, the cancer cells may use the same receptor as the neutrophils for recruitment and binding within the lungs and liver. Based on the emerging role of leukocytes in the metastatic spread of cancer, the requirement of leukocyte recruitment in the initial seeding and establishment of melanoma metastasis to the lungs was investigated. To assess this, an antibody (anti-Gr-1) mediated leukocyte depletion strategy was used. The conditions required for leukocyte depletion *in vivo* was first determined and a single intraperitoneal injection of anti-Gr-1 antibody (150µl from 1mg/ml stock) was found to deplete neutrophils significantly from the circulation after 24 hours. (**Figure 3.6A-B**). Thus immunocompromised mice (SCID) were injected with anti-Gr-1 antibody (clone: RC6 8C5) 24 hours prior to the injection of 70W GFP-luciferase human melanoma cells to deplete the circulating leukocytes. In addition, to ensure depletion of the Gr-1+ cells over a sufficient timeframe the mice were injected with repeated doses of anti-Gr-1 for an additional five days. Bioluminescence imaging revealed a significant increase in tumor burden in the lungs of mice that were depleted for circulating leukocytes (control group: 581950±182733, Gr-1 group: 2.266e+006±450030 photons/s/cm^2) (**Figure 3.6C**). This observation was unexpected as the role of leukocytes in cancer metastasis has largely been associated with their "metastatic promoting" phenotype although some studies have shown an anti-metastatic role of leukocytes [187, 190, 319]. For example, a significant reduction in cancer metastasis was seen in liver and lung metastasis mouse models following a similar depletion of leukocytes/neutrophils using Gr-1 antibody [187-188]. In contrast, also using antibody mediated depletion strategies, Granot et al. showed that tumor entrained neutrophils possessed anti-metastatic potential in pre-metastatic lungs [190].

Independent of these contrasting roles, the data presented here suggests that Gr-1+ cells are not required for the initial establishment of 70W metastasis in the lungs and thus the effect of the LSALT peptide was assessed in this experimental setting. Irrespective of the presence of circulating leukocytes, the LSALT peptide was found to inhibit melanoma-lung metastasis *in vivo* (Figure 3.6D-E). In addition, although the LSALT peptide abrogated metastasis to the lungs in both the presence and absence of circulating leukocytes (control group: 70W alone: $2.867e+006\pm 907718$, 70W+LSALT: 649167 ± 294055 photons/s/cm^2), the inhibition was more significant when the circulating leukocytes were absent (Gr-1 group: 70W alone: $1.225e+007\pm1.471e+006$, 70W+LSALT: 118000 ± 50123 photons/s/cm^2) suggesting a possible competition for a single endothelial receptor between leukocytes and metastatic cancer cells. Moreover, injection of a single dose of the LSALT peptide dramatically increased the overall survival of mice irrespective of the presence of circulating leukocytes (**Figure 3.6 D-E**). Together, these results support the idea that the inhibition by LSALT is the result of inhibition of a common mechanism utilized by both neutrophils and melanoma cancer cells.
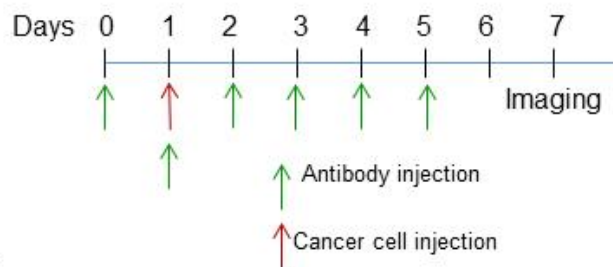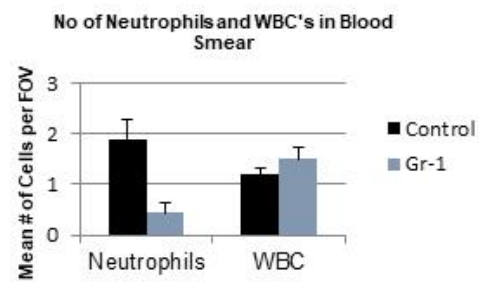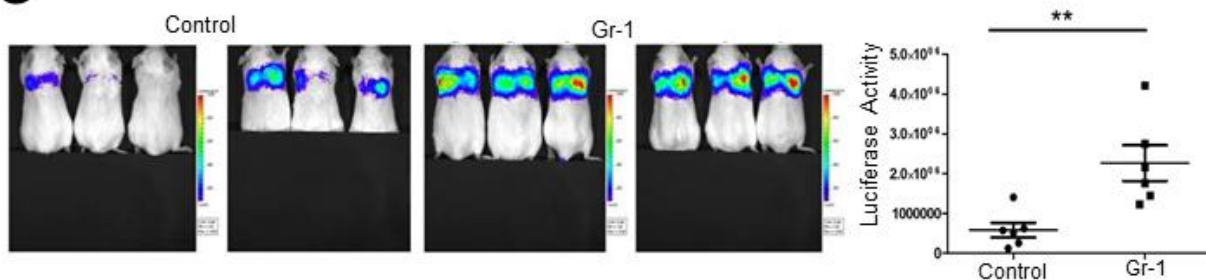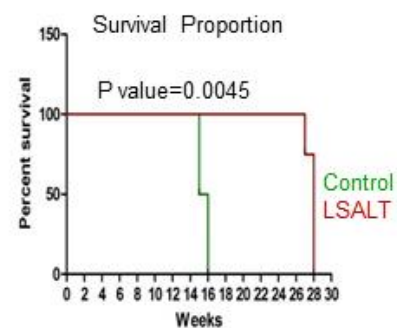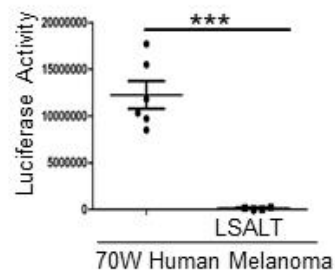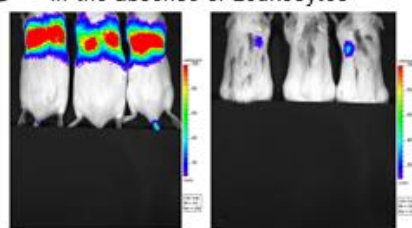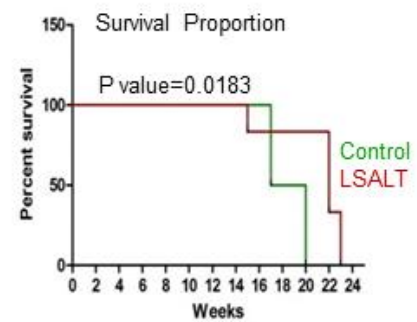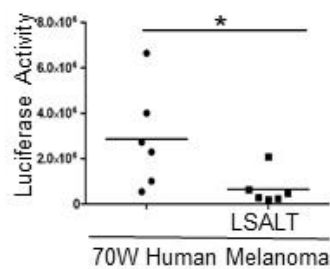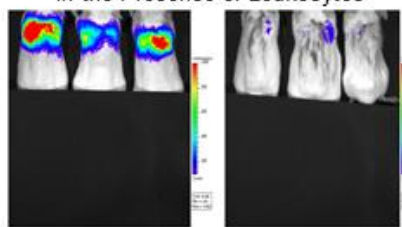
Figure 3.6: Leukocytes (Gr-1 +) are not required for melanoma-lung metastasis *in vivo*. A. Schematic representation of the experimental design of antibody and melanoma cell injection. **B.** Six to eight week old SCID mice were injected with anti-Gr-1 (clone: RB6 8C5) (150 µl from 1mg/kg stock solution) by intraperitoneal injection. Blood was collected from these mice after 18-24 hours and histological analysis was performed to assess the number of circulating leukocytes and white blood cells in blood smears. Graph shows the number of circulating neutrophils and white blood cells in anti-Gr-1 treated mice compared to the control mice. **C.** Leukocytes were depleted using anti-Gr-1 (clone: RB6 8C5) 24 hours prior to intravenous injection of 70W GFP-luciferase human melanoma cells. Mice in the Gr-1 group were injected with anti-Gr-1 for five additional days to maintain a neutrophil depleted situation. Tumor burden was assessed four weeks later using bioluminescence imaging (IVIS 200). Graphs show quantification of tumor burden as assessed by luciferase activity measured using the Xenogen IVIS-200 Optical *in vivo* Imaging system. **D-E.** Six to eight week old SCID mice were injected with 1 mM LSALT peptide (i.v.) five minutes prior to intravenous injection of 70W GFP-luciferase melanoma cells either in the presence or absence of circulating leukocytes. Mice were imaged six weeks later using bioluminescence imaging (IVIS 200). Graphs show quantification of tumor burden as assessed by luciferase activity measured using the Xenogen IVIS-200 Optical *in vivo* Imaging system. Kaplan Meier survival analysis was performed to determine the overall survival. (Dr. Xiaoguang Hao performed tail vein injections).

3.6 LSALT peptide binds to dipeptidase-1 (DPEP1).

Based on the ability of the LSALT peptide to functionally inhibit neutrophil recruitment as well as cancer metastasis to the lungs and liver, we sought to understand the molecular mechanism of this inhibition. One of the central objectives of the project around this time (early 2014) was to identify the functional receptor of LSALT peptide on the endothelium of lungs and liver. As we were determining strategies to identify the receptor for the LSALT peptide, we discovered a study that was published by Errki Ruoslahti's group at the Burnham Institute in California (1999) that isolated and identified two lung homing peptides by *in vivo* phage display they called GFE1 and GFE2 based on a common tripeptide "GFE" motif [303]. Using *in vivo* biotinylation, affinity purification and protein sequencing, the authors of this study identified a 55-kilodalton-lung cell surface protein called 'membrane dipeptidase' as the receptor for both of these GFE peptides. In this study these two GFE-peptide displaying phage were shown to bind selectively to lung primary cells and membrane dipeptidase transfected COS1 cells *in vitro*. In addition, GFE1 peptide was also shown to inhibit the enzymatic activity of dipeptidase-1 in a dose dependent manner in dipeptidase-1 transfected COS1 cells.

Although, the sequence of LSALT has no similarity to the two GFE peptides, based on their ability to home to the lungs, we asked if GFE1 peptide could functionally inhibit melanoma-lung metastasis *in vivo*. Surprisingly, a single intravenous injection of GFE1 peptide (1 mM) significantly reduced metastasis of human melanoma cells to the lungs, similar to the LSALT peptide in the same experimental paradigm (70W alone: 287610±103032, 70W+LSALT: 5882±3101, 70W+GFE1: 2072±693.8 photons/s/cm^2) (**Figure 3.7A-B**).

A

Control | LSALT Peptide (i.v) | GFE-1 Peptide (i.v)

70W Human Melanoma

B

Control | LSALT | GFE1

B16-F10 murine melanoma

103
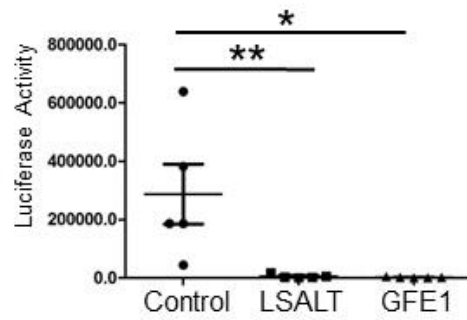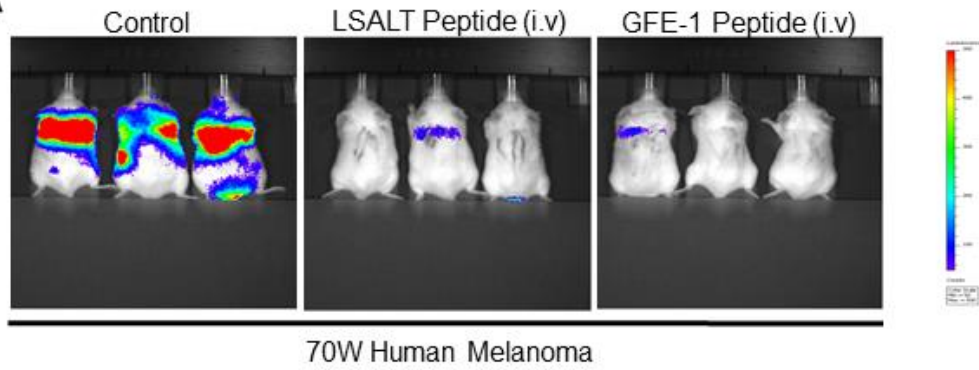
Figure 3.7. DPEP1 specific peptide (GFE1) inhibits melanoma metastasis to the lungs in human xenograft and syngeneic mouse models *in vivo*. A. 70W human melanoma cells expressing GFP-luciferase were injected in immunocompromised mice (SCID) five minutes after the injection of LSALT and GFE1 peptide. Mice were imaged five weeks later using bioluminescence imaging (IVIS 200). Graph shows quantification of tumor burden as assessed by luciferase activity measured using the Xenogen IVIS-200 optical *in vivo* imaging system. Values shown are the mean ±SEM, asterisks (**) indicate $P<0.01$ as compared with control mice (one-way ANOVA with the Neuman-Keuls post-test). **B.** Representative lung sections from mice injected with B16/F10 murine melanoma cells either in the presence or absence of LSALT and GFE1 peptide were assessed by immunohistochemistry (stained with hematoxylin and eosin) to assess tumor burden. Scale bar: 20 µm. N=2 (Dr. Xiaoguang Hao performed tail vein injections).

Although the LSALT and GFE1 peptides share similarities in their ability to home to the lungs, this functional resemblance of both peptides surprised us. Thus, experiments were performed to assess if GFE1 could also inhibit LPS induced infiltration of neutrophils in the sinusoidal endothelium of the liver. To investigate this, the liver of LysMeGFP mice bearing GFP neutrophils (high) and monocytes (low) in the presence of the GFE1 peptide was imaged by intravital spinning disk confocal microscopy. Similar to the LSALT peptide, the GFE1 peptide was found to dampen the inflammatory response in the liver by inhibiting neutrophil adhesion in the hepatic sinusoidal endothelium in the presence of LPS (LPS: 110.7±10.73, LPS+ LSALT: 68.33±4.096, LPS+GFE1: 66.00±10.82) (**Figure 3.8**). It is important to mention that the role of GFE1 in the recruitment of cells to the lungs and liver had not been assessed. These two striking *in vivo* observations led us to hypothesize that membrane dipeptidase may be the functional receptor for the LSALT peptide. Thus, to confirm if dipeptidase-1 (DPEP1) was the receptor for the LSALT peptide, *in vitro* peptide binding studies were performed using COS1 cells as a model system. Based on their high transfection efficiency, amenability to work with, and the lack of membrane dipeptidase expression as assessed by Western blot (**Figure 3.10A**), COS1 cells were used as an *in vitro* model for peptide binding assays. Initial experiments were performed to assess if GFE1 and LSALT could recognize dipeptidase-1 (DPEP1). Using similar experimental parameters as described by Rajotte and Ruoslahti, racine DPEP1 was transiently expressed in COS1 cells by transfection and examined fluorescently for the ability of conjugated LSALT and GFE1 peptides to bind to DPEP1. Observations from a series of *in vitro* experiments using fluorescence microscopy showed a significant increase in the binding of both LSALT and GFE1 peptides to the racine DPEP1 expressing COS1 cells (**Figure 3.9A**). In addition, experiments were performed using murine and human DPEP1 transfected COS1 cells and similar results were found

(**Figure 3.9B, 3.10A and 3.10C**). Collectively, these *in vitro* observations further support the idea that DPEP1 is the functional receptor for the LSALT peptide and highlight the conserved newly described function of DPEP1 across species.

To assess if LSALT and GFE1 peptide can bind directly to DPEP1, a second independent peptide binding *in vitro* approach was utilized. A biotin transfer strategy (Sulfo SBED) was used where a biotin moiety is transferred in an unbiased manner to proteins that are in close proximity when activated with UV light. In these experiments DPEP1 expressing COS1 cells were first treated with biotin conjugated LSALT peptide followed by activation of the aryl azide group in the Sulfo-SBED biotin at 363 nanometer wavelength to enable biotin transfer to neighboring proteins. Proteins from these cells were then precipitated with NeutrAvidin-conjugated beads and Western blot analysis was performed to assess the close association of the LSALT and DPEP1. Results from three independent biotin transfer experiments *in vitro*, showed that LSALT and GFE1 both bound to human DPEP1 (**Figure 3.10B**). To further validate DPEP1 as the receptor for the LSALT peptide, mass spectrometry (MS/MS) analysis on LSALT-biotin treated DPEP1 Immunoprecipitates were performed and DPEP1 was identified as a binding partner for the LSALT peptide, further confirming the immunofluorescence and biotin transfer experimental observations.

As DPEP1 belongs to a large group of membrane proteins that includes two closely related family members with overlapping structural and functional similarities, we next asked if LSALT and GFE1 could bind to these protein family members i.e.; DPEP2 and DPEP3. Using a similar *in vitro* experimental paradigm to the one performed for DPEP1, experiments were undertaken using plasmid constructs containing the human DPEP2 and DPEP3. The LSALT and GFE1 peptides were found to be highly specific for DPEP1 as no significant binding of LSALT or GFE1 peptides

was observed on the COS1 cells expressing DPEP2 or DPEP3, thus confirming the specificity of

LSALT and GFE1 for DPEP1 (**Figure 3.11**). Western blot analysis confirmed the expression of

DPEP1, DPEP2 and DPEP3 in these experimental paradigms (**Figure 3.11 lower panel**).

A

Sham | | LSALT | GFE1 | ContP

LPS

Neutrophils (LysMeGFP) Kupffer Cells (F4/80) Vasculature (CD31)

B
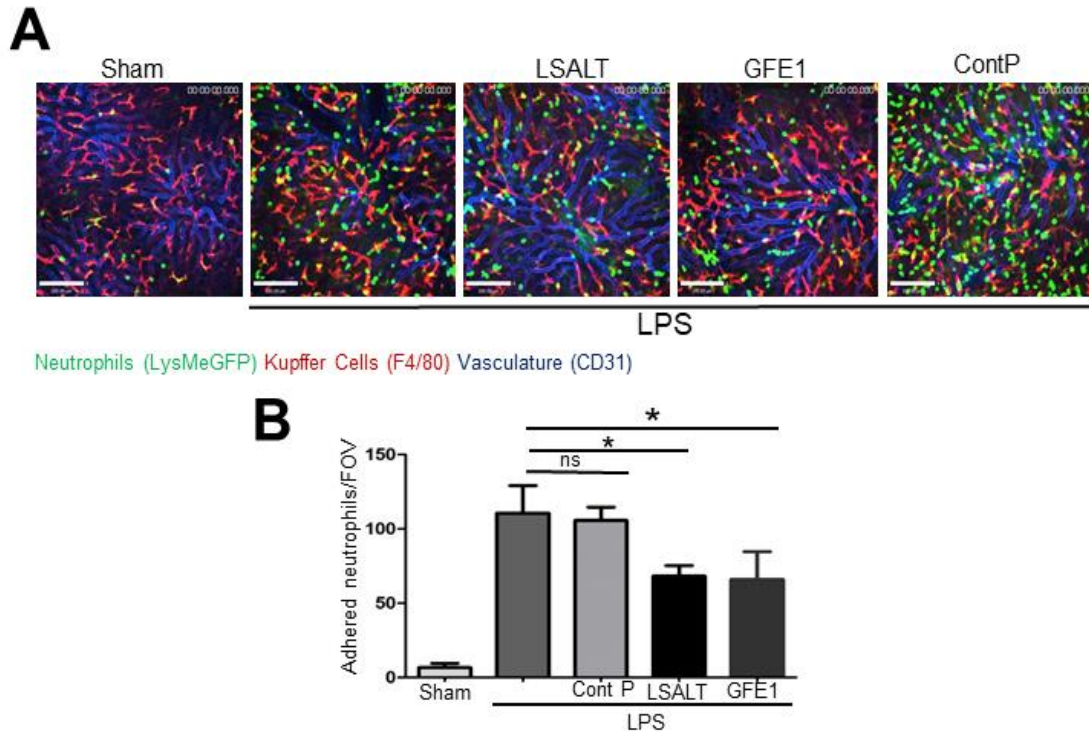
Figure 3.8: DPEP1 specific peptide (GFE1) inhibits neutrophil adhesion in the liver sinusoids in the presence of LPS. A. The functional activity of DPEP1 specific peptide, GFE1 was assessed in neutrophil recruitment *in vivo* in the presence of LPS. Six to eight week old LysMeGFP mice (C57BL/6) were injected either with 1mM LSALT or GFE1 peptide (i.v.) via the tail vein five minutes after the injection of LPS and the liver was imaged using intravital spinning disk microscopy. Shown here are the neutrophils (GFP, green) and Kupffer cells (F4/80, purple) in liver sinusoids (CD31, blue) (upper panel). Neutrophils that remained stationary in the liver sinusoids for more than one minute were counted as adherent cells. **B.** Graph shows the number of adhered neutrophils within the liver sinusoids in the mice treated with GFE1 and LSALT compared to control mice treated with LPS. N=3 (Experiments performed in collaboration with Dr. Liane Babes).
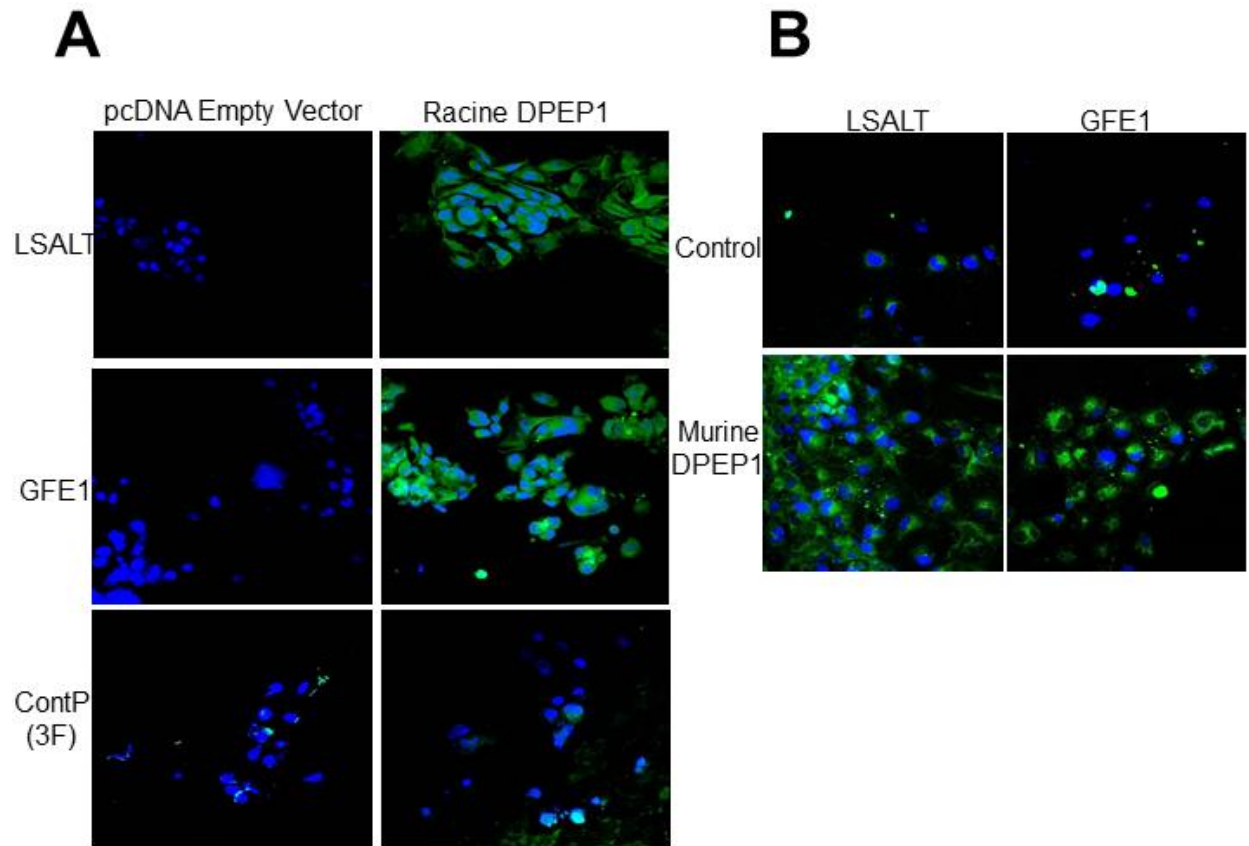
Figure 3.9. LSALT peptide binds to dipeptidase-1 (DPEP1) expressing COS1 cells *in vitro*.
A. COS1 cells were either mock transfected or transiently transfected with 3 or 5 µg of DPEP1 plasmid corresponding to either racine **(A)** or murine **(B)** DPEP1 gene using lipofectamine 2000 (Invitrogen) reagent in OptiMEM medium. Transfected cells were stained with fluorescently conjugated LSALT, GFE1 or control peptide (KGAL) and immunofluorescence microscopy was performed to assess binding. Shown here are representative immunofluorescence images from at least three independent experiments with similar results. Scale bar: 50µM. (N=3)

A

Positive Control | Control | DPEP1

55 —
36 —

DPEP1

B

Control | DPEP1 LSALT | DPEP1 KGAL

55 —
36 —

DPEP1

Inputs

C

DPEP1 antibody | LSALT | DPEP1 specific peptide (GFE1) | Control peptide

DPEP1 (Human) Transfected Cos-1
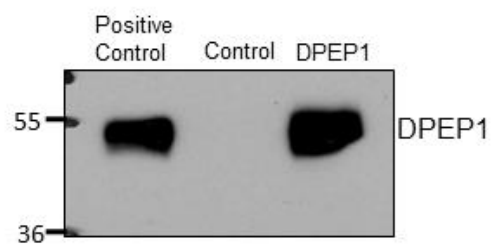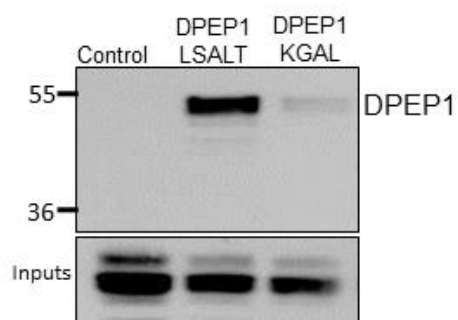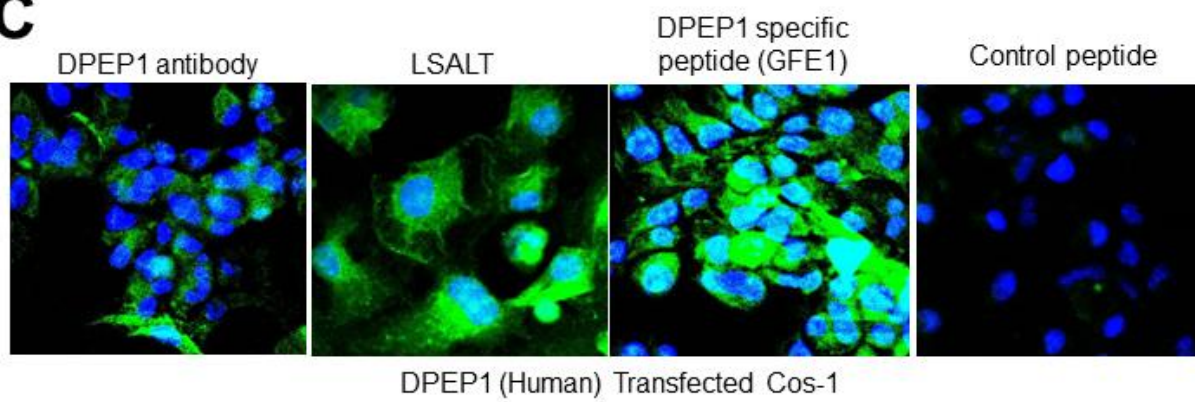
Figure 3.10: LSALT and GFE1 peptide binds to human DPEP1. A. COS1 cells were transiently transfected with 3 µg of plasmid encoding the human DPEP1 gene. Proteins were isolated 48 hours after transient transfection using RIPA/octyl glucoside and Western blot analysis was performed to assess DPEP1 expression. **B.** COS1 cells were transiently transfected with 3 µg of plasmid encoding the human DPEP1 gene and incubated with Sulfo-SBED biotin reagent conjugated LSALT or control peptide and biotin transfer was performed *in vitro*. Mock or DPEP1 transfected cells were precipitated with NeutrAvidin conjugated beads and Western blot analysis was performed using a human specific DPEP1 antibody to demonstrate the direct association of LSALT to DPEP1. A representative Western blot is shown from three independent experiments with similar results. **C.** COS1 cells were transiently transfected with cDNA corresponding to human DPEP1 and peptide-binding assay was performed *in vitro* to assess binding using fluorescently conjugated peptides. Shown are representative photomicrographs of each experimental condition (N=5). (Results in the panel B were contributed by Dr. Jennifer Rahn.)
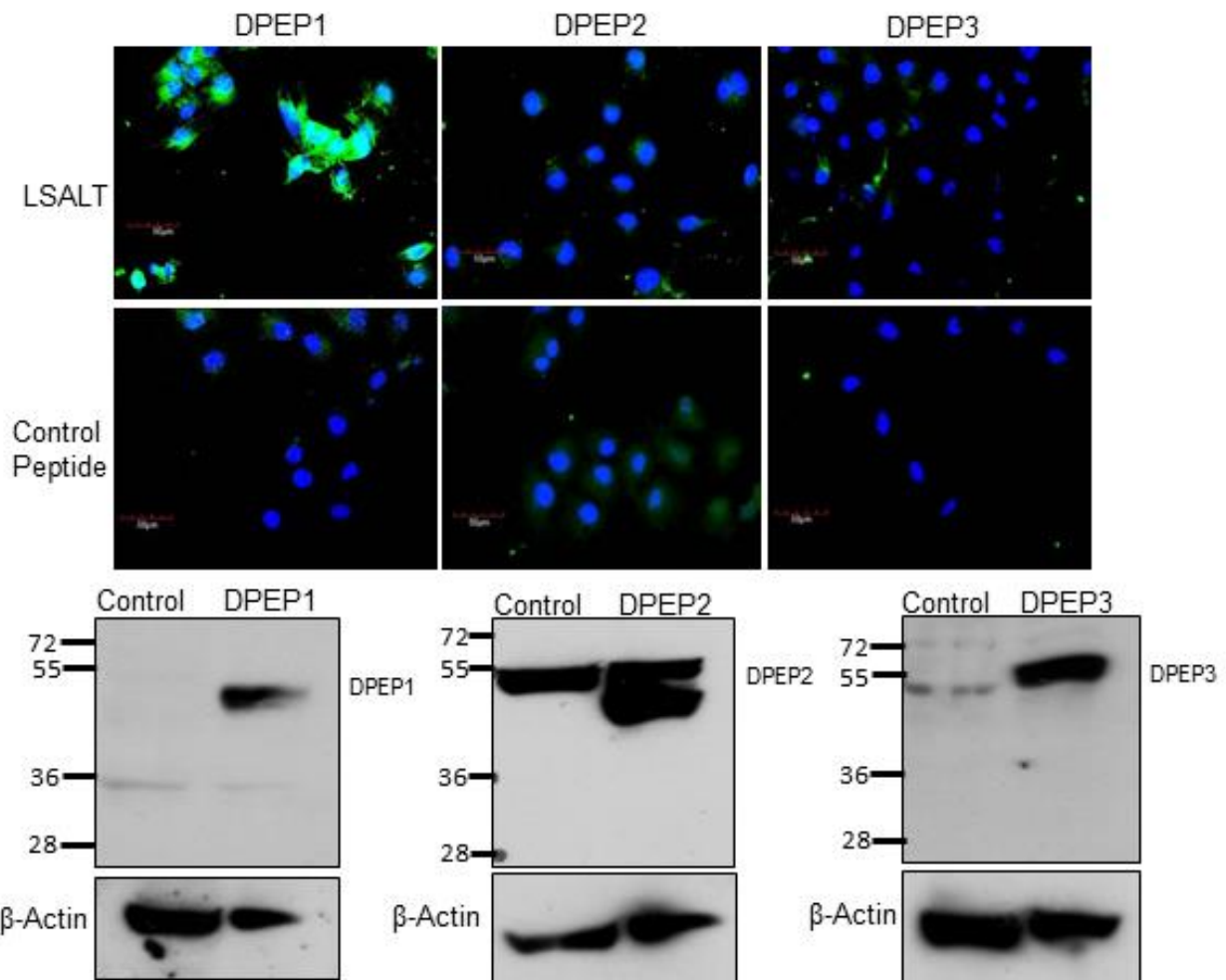
Figure 3.11: LSALT and GFE1 do not bind to DPEP2 and DPEP3 *in vitro*. COS1 cells were either mock transfected or transiently transfected with 3 µg of plasmids encoding the human DPEP1, DPEP2 or DPEP3 gene and *in vitro* peptide binding assays were performed. Shown here are the representative images from at least three independent experiments with similar results (upper panels). Western blot analysis confirmed the expression of DPEP1, DPEP2 and DPEP3 in the same experiment (lower panel). β-actin was used as a loading control (lower panels).

3.7 DPEP1 is an adhesion receptor for neutrophils and metastatic cancer cells.

There is emerging evidence that cell surface enzymes, particularly ectoenzymes (enzymes with catalytic activity in the extracellular space) can play a critical role in mediating adhesion and recruitment of leukocytes to different organs either by acting as an adhesion receptor (by physical binding) or via their catalytic activity. For example, studies have indicated that cell surface ectoenzymes such as VAP-1 (Vascular Adhesion Protein-1), CD73 and CD38 promote leukocyte adhesion during inflammation through their adhesive functions [320-321]. Analogous to these molecules we asked if the ectoenzyme DPEP1 could also mediate the adhesion of neutrophils and metastatic cancer cells. To investigate this, static adhesion assays were performed *in vitro* with DPEP1-expressing COS1 cell monolayers according to the principles and protocols originally established by Chakrabarti and Patel et al. [322]. Neutrophils were isolated from healthy human donors and labeled with carboxyfluorescein diacetate succinimidyl ester-CFDA (CFSE). When these labeled neutrophils were added on the top of DPEP1 expressing COS1 cell monolayers a significant increase in the binding of the neutrophils was observed on the DPEP1-expressing COS1 monolayers compared to the mock-transfected COS1 cells (DPEP1:10.70±1.764, DPEP1+LSALT:5.053±0.9535) . This data suggested that DPEP1 acts as a direct adhesion receptor for human neutrophils (**Figure 3.12A**). In addition, incubation of the LSALT peptide with the DPEP1-expressing COS1 cell monolayer significantly inhibited the binding of the neutrophils thus mirroring our *in vivo* observations. In addition, specificity of the binding was shown as the LSALT peptide only inhibited the DPEP1-specific binding. Western blot analysis confirmed the transient expression of DPEP1 by the COS1 cells in these experiments. To assess if the metastatic melanoma cells can also bind DPEP1, similar experiments were performed. Analogous to the human neutrophils, a significant increase in the binding of 70W (GFP-luciferase) human

melanoma cells was observed compared to the mock-transfected COS1 cells (Control: 3.000±
0.3886, DPEP1: 10.59±0.9310) (**Figure 3.12B**). It is important to note that, this is the same cell
line that was used to model melanoma-lung metastases *in vivo*. Together these observations
identify DPEP1 as a physical adhesion receptor for human neutrophils and metastatic melanoma
cells.

Based on the fact that DPEP1 shares significant structural and functional homology with
DPEP2 and DPEP3, we also asked if metastatic melanoma cells could bind to the other membrane
dipeptidase family members. To address this, similar static adhesion assays were performed *in
vitro* with DPEP2 and DPEP3-expressing COS1 cells. No significant increase in the binding of the
70W-GFP-luciferase melanoma cells was observed on DPEP2 and DPEP3-expressing COS1 cell
monolayers demonstrating selectivity for binding to DPEP1. Together, these *in vitro* observations
show specificity for DPEP1 as an adhesion receptor for metastatic melanoma cells. (**Figure 3.13**).
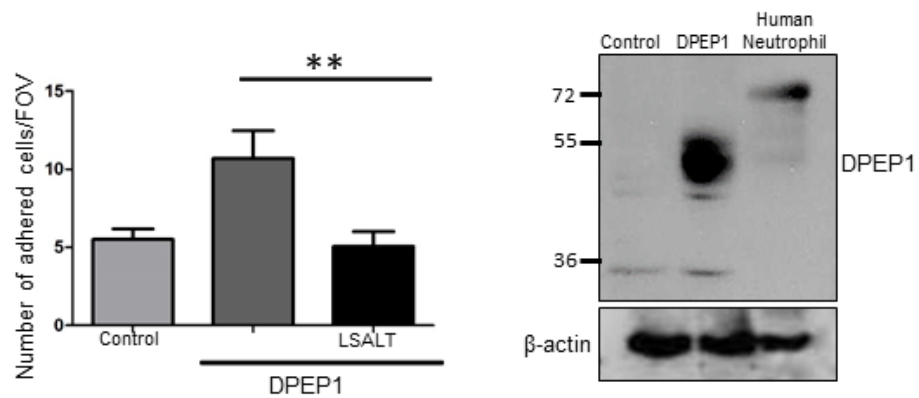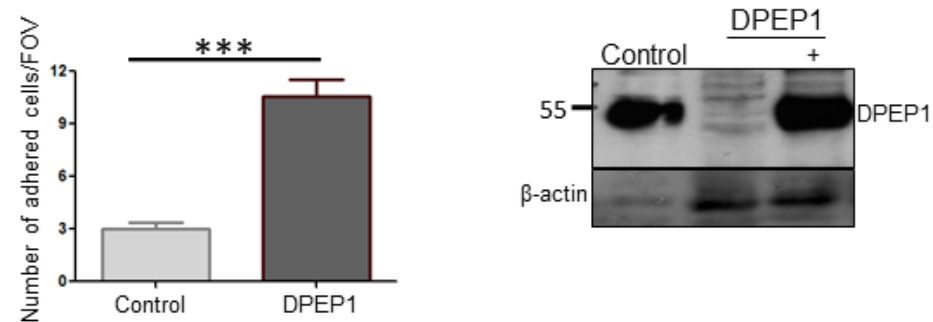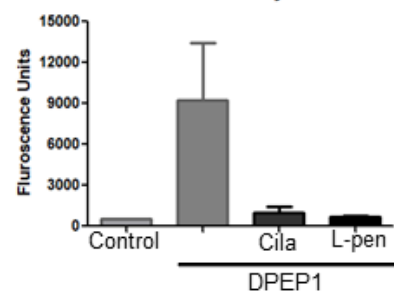
Figure 3.12: DPEP1 is an adhesion receptor for neutrophils and metastatic cancer cells. A. Human neutrophils isolated from healthy donors, were overlaid on the top of COS1 cell monolayers expressing DPEP1 and a neutrophil static adhesion assay was performed. Number of carboxyfluorescein diacetate succinimidyl ester-CFDA labeled neutrophils bound/adhered on DPEP1 expressing COS1 cell monolayers in the presence or absence of LSALT peptide were counted under 10X magnification over ten different fields of views using an inverted fluorescence microscope. Results are shown from two independent experiments. An unpaired student's t-test was performed to compare the LSALT treated group with the non-treated group. Western blot analysis confirmed DPEP1 expression in COS1 cells while no expression of DPEP1 was observed in human neutrophils (right panel). **B.** A static adhesion assay was performed to assess the binding of 70W GFP-luciferase melanoma cells on DPEP1 expressing COS1 cells. The number of 70W melanoma cells bound/adhered on DPEP1 expressing COS1 monolayers were counted under 10X magnification over 10 different field of views using an inverted fluorescence microscope. Proteins from DPEP1 transfected cells were isolated after 48 hours using octyl-glucoside/RIPA lysis buffer and Western blot analysis was performed to assess DPEP1 expression (right panel). An unpaired 2-tailed student's t-test was performed to compare the binding of 70W GFP-luciferase melanoma cells to DPEP1 transfected cells against the control or mock transfected cells. Values shown are from three independent experiments; asterisks (***) indicate $P<0.001$ as compared with mock-transfected cells. **C.** DPEP1 activity assay and the fluorometric detection of D-Phe were performed according to the principles originally established by Heywood and Hooper (1995) to assess DPEP1 enzyme activity.

A

B

Human DPEP1   Human DPEP2   Human DPEP3
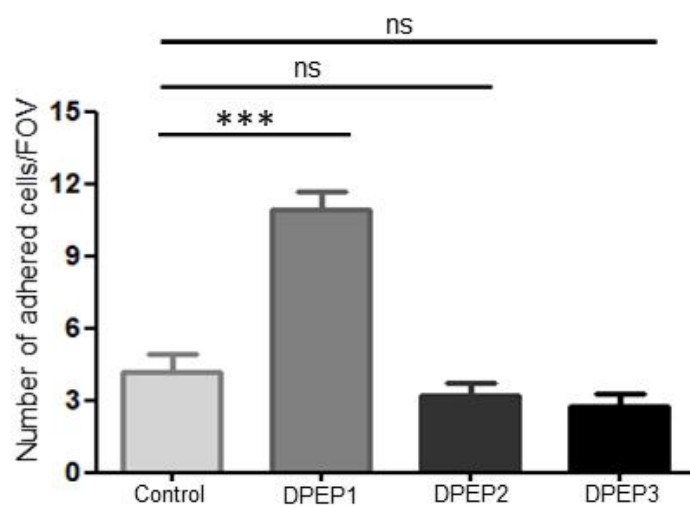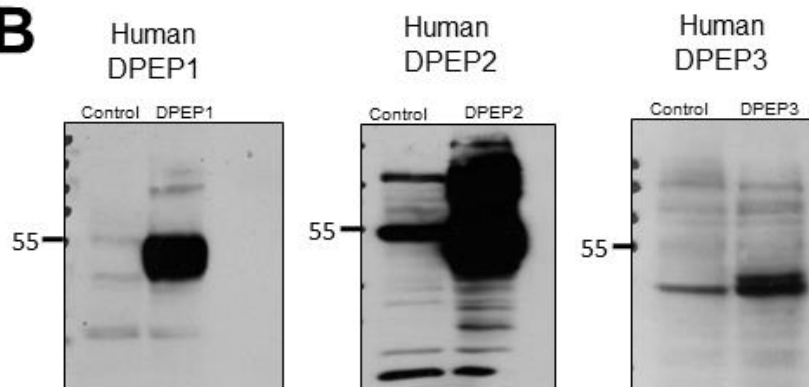
Figure 3.13: 70W human melanoma cells bind specifically to DPEP1 expressing COS1 monolayers *in vitro*. **A.** COS1 cells were transiently transfected with 3 µg of either human DPEP1, DPEP2 or DPEP3 cDNA using lipofectamine 2000 reagent (Invitrogen). 70W melanoma cells expressing stable GFP-luciferase were harvested using Puck's EDTA and $10x10^3$ seeded on the top of DPEP1, DPEP2, and DPEP3 expressing COS1 cell monolayer after 48 hours. Number of 70W melanoma cells bound/adhered was counted under 10X magnification over 10 different field of views using an inverted fluorescence microscope. **B.** Proteins from transfected cells were isolated after 48 hours using octyl-glucoside/RIPA lysis buffer and Western blot analysis was performed to assess protein expression. (N=2)

3.8 Catalytic activity of DPEP1 is not required for binding of human neutrophils and metastatic cancer cells.

As mentioned previously studies in recent years have suggested that increased activity of certain ectoenzymes can regulate leukocyte trafficking at inflammatory sites [117, 323]. As described earlier VAP-1 and CD73 are two examples in this regard as both of these cell surface enzymes were previously shown to play a crucial role in mediating firm adhesion and transmigration of leukocytes in response to an inflammatory response [134, 323-324]. Similar to these molecules, DPEP1 is an ectoenzyme, and based on the data presented in this thesis, it can act as an adhesion receptor for neutrophils and metastatic cancer cells. Thus the requirement of DPEP1's catalytic activity for the adhesion of neutrophils and metastatic melanoma cells was investigated. Experiments were first performed to confirm the activity of DPEP1 in racine, murine or human DPEP1-transfected COS1 cells (**Figure 3.14A**). To do this, a specific fluorometric DPEP1 enzyme assay originally established by Heywood and Hooper in the early 1990's [302] was implemented. Using this assay, a significant increase in DPEP1 enzyme activity in COS1 cells transiently transfected with racine, murine or human DPEP1 was seen. Based on this observation, experiments were then performed to assess if LSALT peptide could inhibit DPEP1 enzyme activity *in vitro*. Previously GFE1, but not GFE2, was shown to inhibit the enzymatic activity of DPEP1 [303]. Therefore, DPEP1 activity was assessed in the presence of LSALT, GFE1 and GFE2. Results from the *in vitro* DPEP1 activity assays showed that although GFE1 inhibited the DPEP1 activity at a dose of 1 mM (consistent with Rajotte et al.), the LSALT and GFE2 peptides had no significant effect on DPEP1 activity (DPEP1: 6653±1153, DPEP1+LSALT: 5189±1089, DPEP1+GFE1: 3563±818.9, DPEP1+GFE2: 4684±1083) (**Figure 3.14B**). To determine if a higher concentration of the LSALT peptide was capable of inhibiting DPEP1 activity, increasing

119

concentrations (100 µm-1 mM) of the LSALT and GFE1 peptides were assessed (**Appendix Figure 3**). Although GFE1 was shown to inhibit DPEP1 activity in a dose dependent manner, no significant inhibition was observed in the presence of the LSALT peptide even at concentrations as high as 6 mM. As anticipated, two known pharmacological inhibitors of DPEP1, Cilastatin and l-penicillamine, were also assessed and found to significantly inhibit DPEP1 enzyme activity in COS1 cells that were transiently transfected with either murine (murine DPEP1: 6991±473.3, murine DPEP1+Cilastatin: 543.3±2.514, murine DPEP1+Penicillamine: 552.4±5.734) or human DPEP1 (human DPEP1: 11815±127.2, human DPEP1+Cilastatin: 660.1±5.310, human DPEP1+Penicillamine: 658.3±71.40) (**Figure 3.14C and 3.14D**).
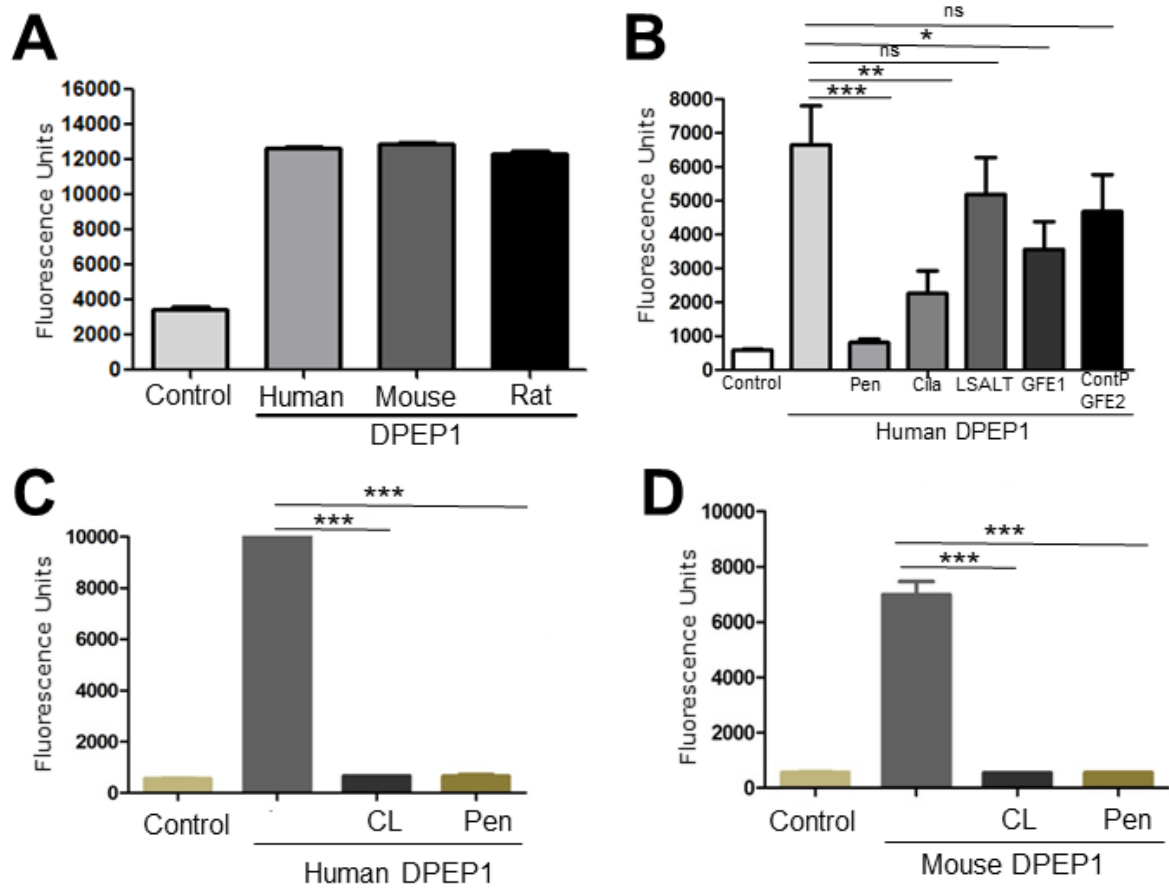
Figure 3.14. LSALT does not inhibit dipeptidase-1 (DPEP1) enzyme activity *in vitro*. A. COS1 cells were transiently transfected with 3µg of either human, mouse or rat membrane di peptidase (DPEP1). Proteins were isolated from transfected cells 48 hours later using octyl-glucoside/RIPA in the absence of protease inhibitors and DPEP1 enzyme activity assay and the fluorometric detection of D-Phe was performed exactly as described by Heywood and Hooper previously. **B.** COS1 cell lysates from DPEP1 (human) transfected cells were assessed for DPEP1 activity in the presence or absence of 1mM LSALT, and the control peptide (GFE2). N=5 **C-D.** COS1 cells were transiently transfected with either human or mouse DPEP1 and cell lysates were assessed for DPEP1 activity in the presence or absence of DPEP1 inhibitors, Cilastatin (1mM) and l-penicillamine (1mM). Values shown are the mean ±SEM from six independent experiments; asterisks (***) indicate $P<0.001$ as compared with DPEP1 transfected cells (one-way ANOVA with the Neuman-Keuls post-test).

The second question with regards to DPEP1 enzyme activity was to assess if the catalytic activity of DPEP1 is required for the adhesion and recruitment of neutrophils and metastatic cancer cells *in vitro* and *in vivo*. Previous studies identified glutamic acid 141 (E141) and histidine 219 (H219) as critical residues in the catalytic domain of DPEP1 [292-293]. To assess the requirement of the catalytic activity in human DPEP1, equivalent residues corresponding to these amino acids (E141D and H215R) were mutated using site directed mutagenesis. DPEP1 enzyme activity was assessed in COS1 cells transfected with the mutant constructs (E141D, H215R). As predicted a significant inhibition of DPEP1 catalytic activity in E141D transfected COS1 cells was observed (DPEP1: 17420 ± 2894, DPEP1 E>141D: 4834 ± 1838, DPEP1H>215R: 14626 ± 4521) (**Figure 3.15A**). Surprisingly however, no reduction in DPEP1 enzyme activity was seen in the DPEP1-H215R transfected COS1 cells (**Figure 3.15A**) and instead the DPEP1 activity was found to be similar to wild type DPEP1. It is important to note that the requirement of this histidine for enzymatic activity was based on mutational analysis in porcine DPEP1 where the equivalent histidine (H219) was shown to ablate enzyme activity. These results therefore suggest a species-specific dependence of H219 (H215 in human DPEP1) on the catalytic activity of DPEP1. This mutant construct of DPEP1 was therefore used as a mutant control as the amino acid substitution was made within the catalytic domain of DPEP1 but did not reduce DPEP1 enzyme activity. In addition to the assessment of the enzyme activity, Western blot analysis was performed to validate the expression of the DPEP1 mutants in the COS1 cells (**Figure 3.15B**). Once the mutant DPEP1 constructs were characterized, the effect of LSALT binding was assessed. *In vitro* peptide binding assays were performed using fluorescently conjugated peptides in COS1 cells transiently transfected with the wild type, H215R and the catalytically inert E141D DPEP1 constructs. Similar to the wild type DPEP1 and the mutant control (H215R), both the LSALT and GFE1 peptide bound

to COS1 cells expressing the catalytically inert DPEP1 mutant E141D. This observation further suggests that the catalytic activity of DPEP1 is not required for the binding of LSALT and GFE1 peptides *in vitro* (**Figure 3.15C**).

Next, to determine if the catalytic activity of DPEP1 is required for DPEP1-mediated adhesion of human neutrophils and metastatic melanoma cells, static adhesion assays were performed *in vitro* using DPEP1 catalytically inert mutant (E141D)-transfected COS1 cell monolayers. Similar to the peptides, neither human neutrophils nor the metastatic melanoma cells required DPEP1 catalytic activity for binding as both of these cell types bound to the catalytically inert (E141D) DPEP1 expressing COS1 cells in a manner similar to both the wild type DPEP1 and the mutant DPEP1 control (H215R) (wild type DPEP1:10.43±0.8959, DPEP1 E141D: 8.571±0.9221, DPEP1 H215R: 10.29± 0.8650) (**Figure 3.16) (Figure 3.17**). Irrespective of the mutational status of DPEP1, the LSALT peptide maintained its capacity to inhibit the binding of 70W (GFP-luciferase) melanoma cells to a monolayer of DPEP1-expressing COS1 cells (**Figure 3.17**). DPEP1 enzyme activity assay and Western blot analysis confirmed the expression and activity of DPEP1 in these experimental paradigms (**Figure 3.16B and Figure 3.17B**).

A

B

C   LSALT   Control Peptide

H-DPEP1

H-DPEP1
(H215)

H-DPEP1
(E141)
Catalytically
inert
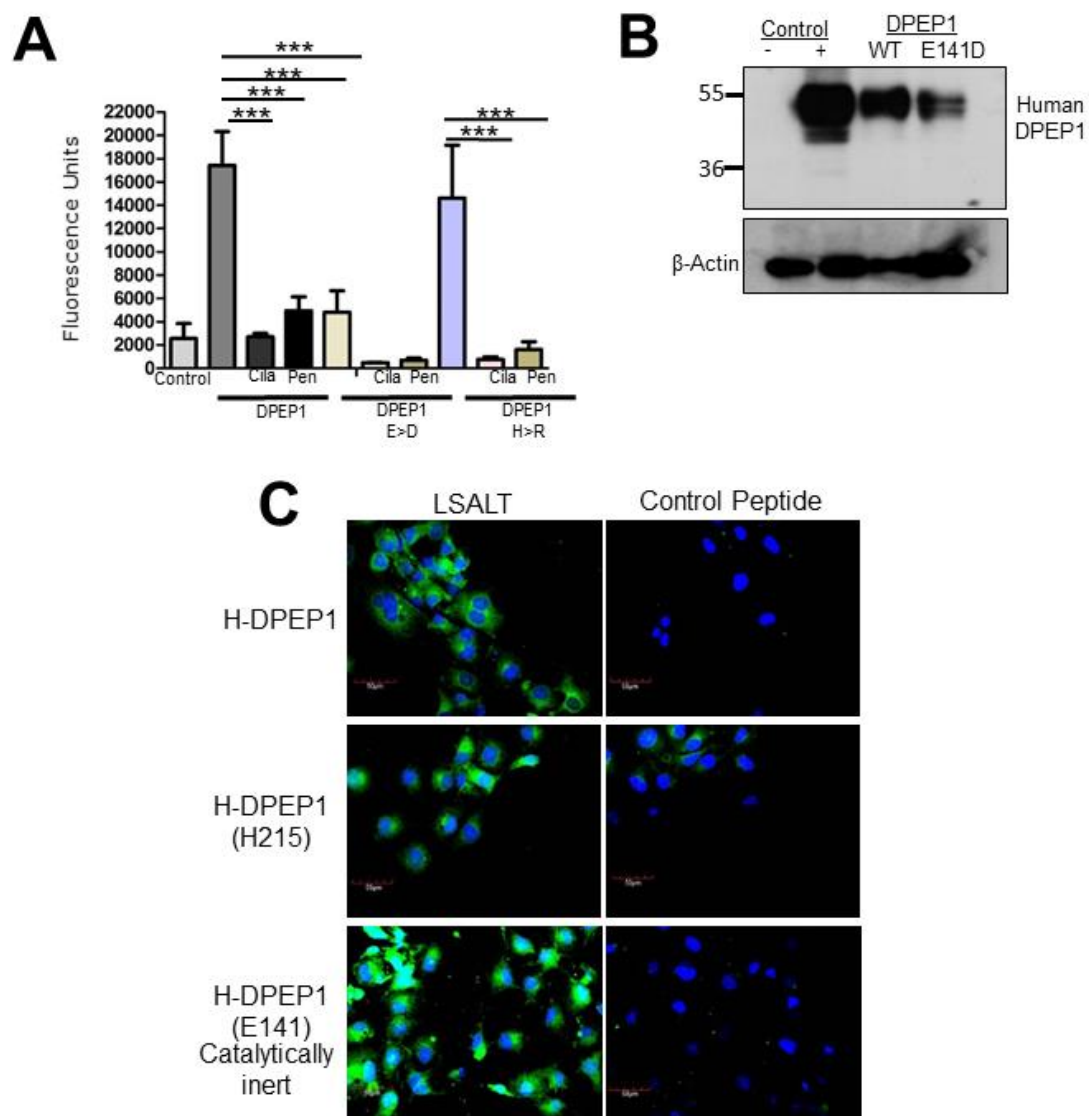
Figure 3.15: Catalytic activity of DPEP1 is not required for binding. A. Proteins were isolated from DPEP1 transfected COS1 cells after 48 hours using octyl-glucoside/RIPA. DPEP1 activity assay and the fluorometric detection of D-Phe were performed to assess DPEP1 enzyme activity. Values shown are the mean ±SEM. from six independent experiments; asterisks (***) indicate $P<0.001$ as compared with DPEP1 transfected cells (one-way ANOVA with the Neuman-Keuls post-test) (N=5). **B.** Proteins from transfected COS1 cells were isolated 48 hours later using octyl-glucoside/RIPA lysis buffer and Western blot analysis was performed to assess DPEP1 expression. **C.** COS1 cells were transiently transfected with 3 µg of either the wild type dipeptidase-1 (DPEP1), catalytically inert DPEP1 mutant (E>D) or mutant control (H>R) and peptide binding assays were performed *in vitro* using fluorescently conjugated peptides. Shown are representative photomicrographs of each experimental condition (N=3).
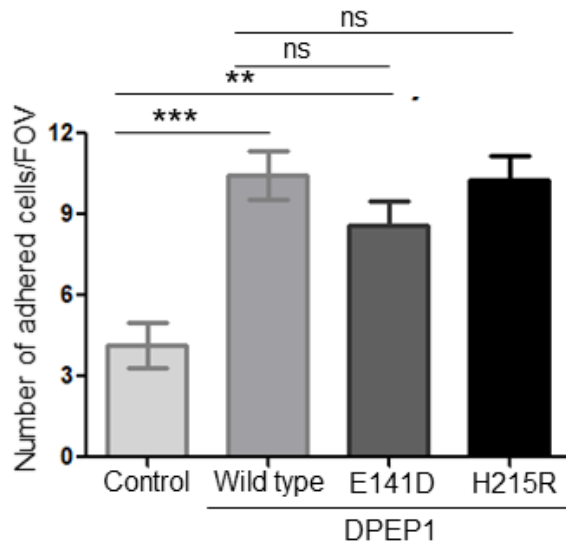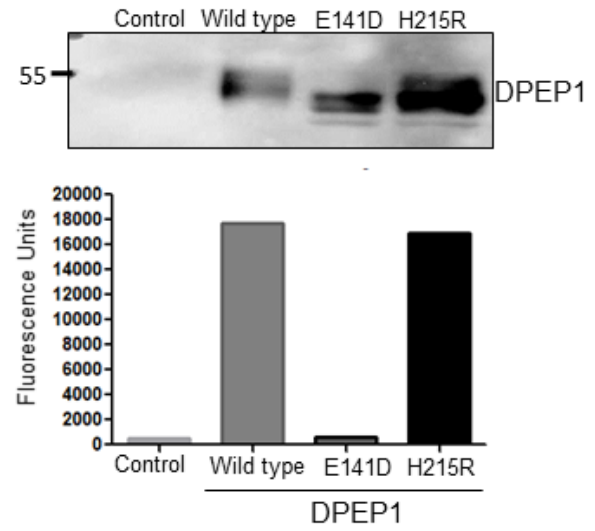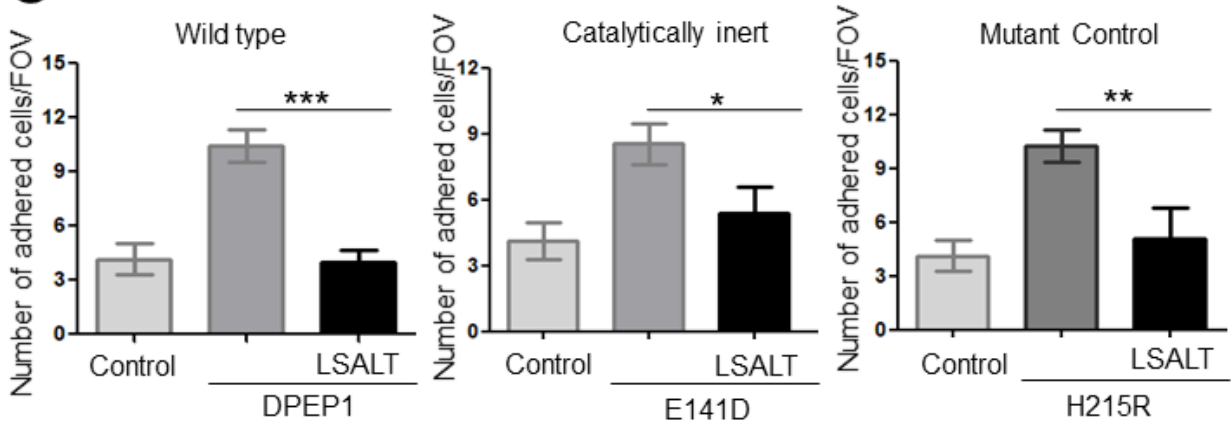
Figure 3.16: Catalytic activity of DPEP1 is not required for the binding of metastatic melanoma cells *in vitro*. A. COS1 cells were transfected either with wild type DPEP1, catalytically inert (E141D) or mutant control (H215R) plasmid constructs and 70W static adhesion assays were performed *in vitro*. The number of adhered cells was counted as described previously. N=2 **B.** A corresponding Western blot and enzyme activity assay is shown that confirmed DPEP1 expression (upper panel) and activity (lower panel) in the static adhesion assay. **C.** 70W static adhesion assay was performed in the presence of LSALT peptide *in vitro* in DPEP1 wild type and mutant expressing COS1 cells. Total number of adhered cells was counted as described previously. Graph shows the total number of adhered cells counted in 10 different field of views.
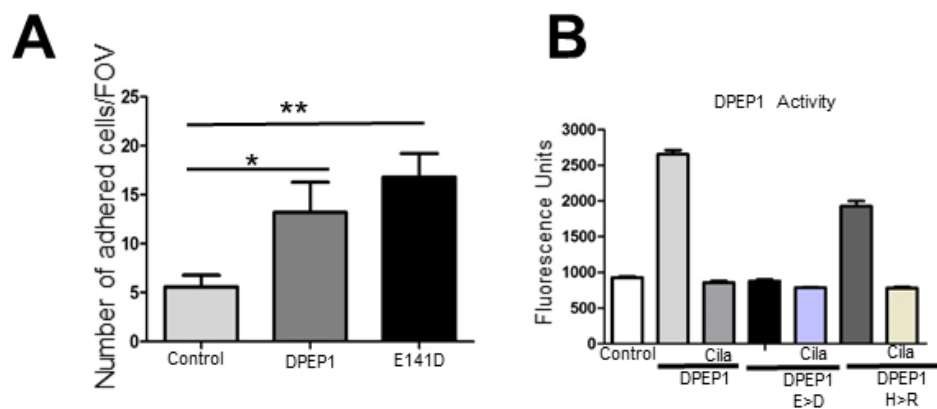
Figure 3.17: Catalytic activity of DPEP1 is not required for neutrophil adhesion *in vitro*. A.

Freshly isolated human neutrophils were labeled with carboxyfluorescein diacetate succinimidyl

ester CFDA and overlaid on the top of DPEP1 expressing wild type and mutant-expressing COS1

cells and a static adhesion assay was performed *in vitro*. Total number of adhered neutrophils was

counted as described previously. **B.** Corresponding DPEP1 activity assay shows an inhibition in

the enzymatic activity of DPEP1 in catalytically inert DPEP1 (E141D) transfected COS1 cells.

As a second approach to assess the requirement of DPEP1 catalytic activity for the binding of metastatic melanoma cells the pharmacological inhibitor, Cilastatin was used. First the required concentration of Cilastatin that could inhibit the cell surface DPEP1 activity *in vitro* was optimized. A 10 mM dose of Cilastatin was found to inhibit 63.81% of cell surface DPEP1 catalytic activity *in vitro* (DPEP1: 5793±105.3, DPEP1+Cilastatin: 2098±52.17) (**Figure 3.18A**). Once the dose of Cilastatin was optimized, experiments were then performed to assess if this inhibition in the catalytic activity at the cell surface plays any role in the adhesion/binding of metastatic cancer cells to the DPEP1 expressing COS1 cell monolayers. Consistent with previous observations using catalytically inert mutants, no inhibition in the binding of 70W (GFP-luciferase) human melanoma cells on DPEP1 expressing COS1 cell monolayers was observed in the presence of Cilastatin, further suggesting that DPEP1 enzyme activity is not required for the adhesion of 70W (GFP-luciferase) cells *in vitro* (**Figure 3.18C**). To investigate if this was validated *in vivo*, LysMeGFP mice were injected with Cilastatin in the presence of LPS and neutrophil adhesion was assessed in the liver sinusoids. Intravital imaging of the liver in these mice revealed no significant difference in the adhesion of neutrophils in the presence of Cilastatin compared to the LPS alone treated mice, indicating that the catalytic activity of DPEP1 is not required for neutrophil adhesion *in vivo*. This was in contrast to the LSALT peptide-treated mice where a significant inhibition in neutrophil adhesion was observed in this series of experiments (LPS: 132.6±7.096, LPS+ Cilastatin: 123.2±20.32, LPS+LSALT: 75.80±1.908) (**Figure 3.18E**). Taken together these observations suggest that the catalytic activity of DPEP1 is not required for adhesion *in vitro* and *in vivo*.
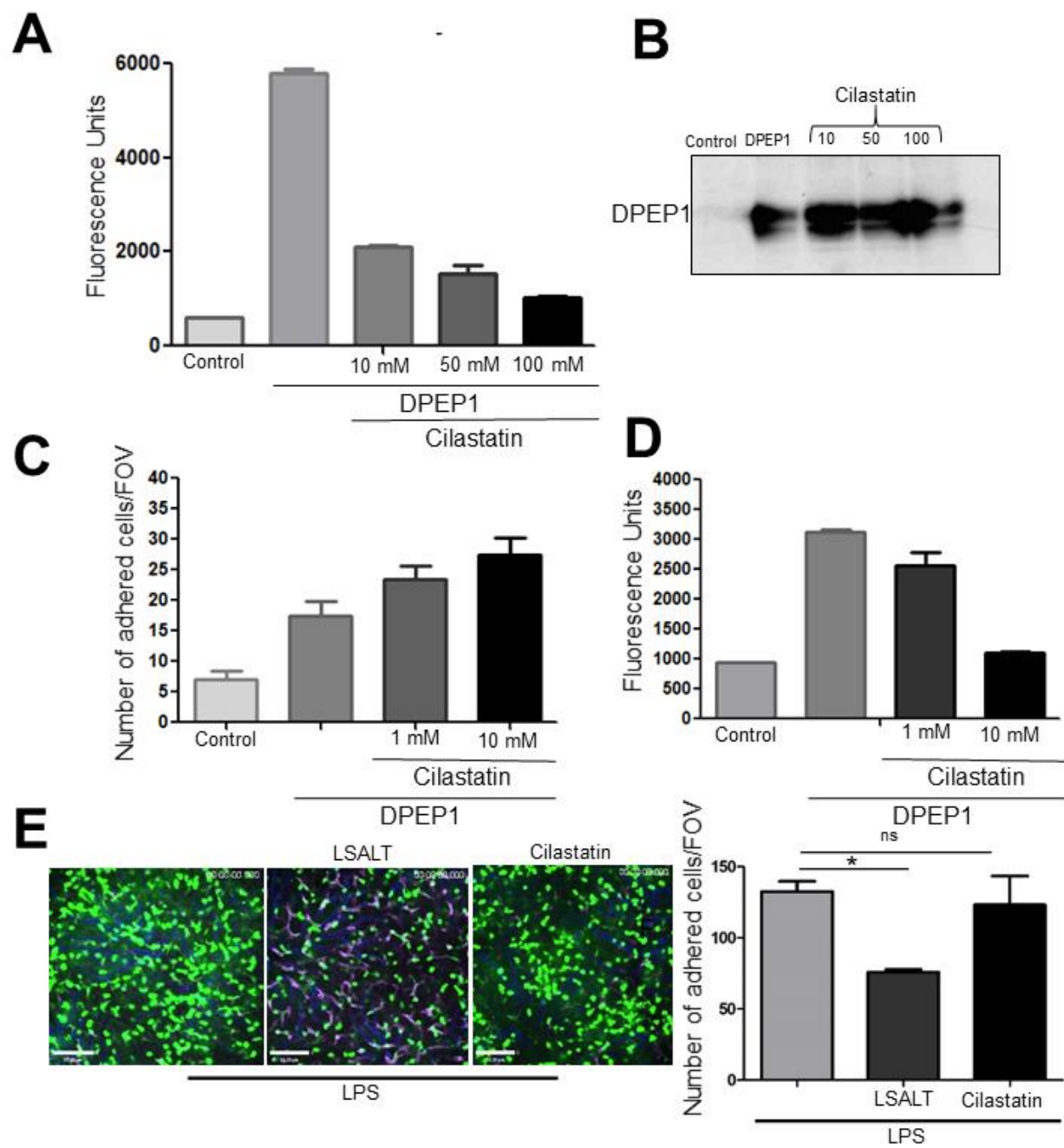
Figure 3.18: Cilastatin does not inhibit adhesion of metastatic melanoma cells and neutrophils. A. Cilastatin at different concentrations was added to DPEP1 expressing COS1 cells 48 hours after transient transfection and incubated for one hour at 37°C. Cells were washed with PBS and proteins were collected using RIPA/octyl-glucoside lysis buffer. Protein lysates treated with Cilastatin were then assessed for DPEP1 activity (by fluorometric DPEP1 activity assay) and expression by Western blot analysis **(B)**. **C.** 70W GFP-luciferase cells were added on the top of DPEP1 expressing COS1 cells five minutes after the treatment of Cilastatin and incubated for one hour at 37°C. The number of adhered cells bound to the DPEP1 expressing COS1 cell monolayer was counted in 10 random field-of-views under 10X objective using an inverted florescent microscope. **D.** DPEP1 activity assay confirmed the inhibition of DPEP1 activity in this set of experiments. **E.** Six to eight week old LysMeGFP mice were treated with either 1mM LSALT or Cilastatin (20 nM) in the presence of LPS and the liver of mice were imaged by intravital spinning disk confocal microscopy. Shown here are the presence of neutrophils (GFP, green) and Kupffer cells (F4/80, purple) in the liver sinusoids (CD31, blue). Neutrophils that remained stationary for more than one minute were counted as adherent cells. (Intravital imaging experiments in panel E were performed in collaboration with Dr. Liane Babes).

3.9 DPEP1 expressed in the lungs, liver and kidney *in vivo*.

DPEP1 was originally isolated from the brush border membrane of the renal tubular epithelial cells in the kidney. Although, a very limited number of studies may have indicated the presence of this GPI-anchored ectoenzyme in the lungs, the expression and activity of DPEP1 in different organ/tissues is largely unknown. Based on this evidence and the results that DPEP1 acts as an adhesion receptor for neutrophils and metastatic melanoma cells *in vivo*, endogenous DPEP1 expression in different organs including the lungs and liver was assessed. Lungs, liver and kidney from six to eight week old C57BL/6 mice were harvested and immunohistological analysis was performed to assess DPEP1 expression in these tissues using a DPEP1 specific antibody. As anticipated, robust expression of DPEP1 in the renal epithelial brush border membrane of the kidney was found along with DPEP1 localized around the endothelial lining of the blood vessels in both lungs and liver (**Figure 3.19A**). In addition to expression, the endogenous DPEP1 activity in different organs was also investigated by performing a fluorometric enzyme assay to measure DPEP1 specific catalytic activity in these tissues. Similar to the expression profiles, kidneys and lungs were found to contain the highest endogenous DPEP1 enzyme activity, while livers expressed lower activity when compared to the lungs and kidneys (**Figure 3.19B**). A minimal level of DPEP1 activity was observed in the spleen. To confirm the specificity of the DPEP1 activity in these tissues, *in vitro* DPEP1 enzyme activity assays were performed in the presence of Cilastatin and a significant reduction in the DPEP1 activity in the lungs, kidney and liver tissue homogenates was observed (**Figure 3.19C**).
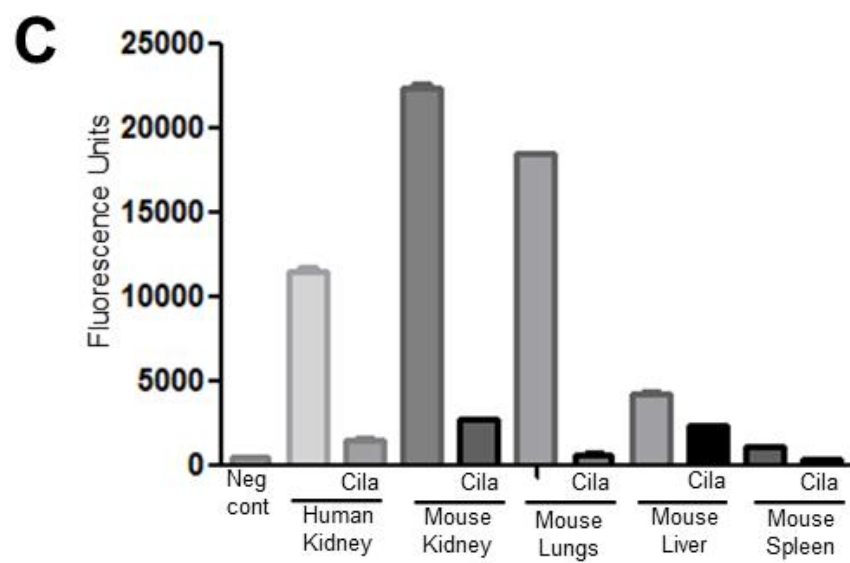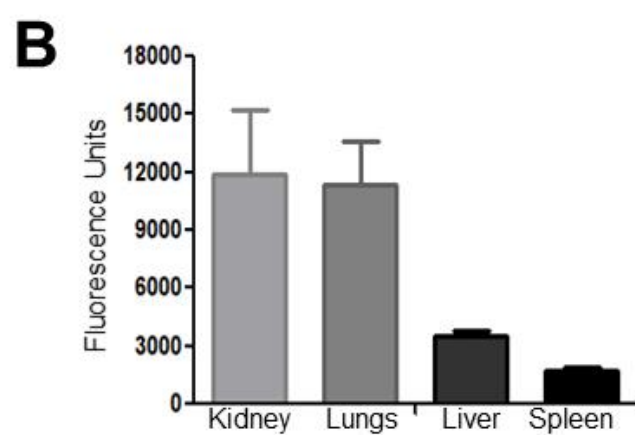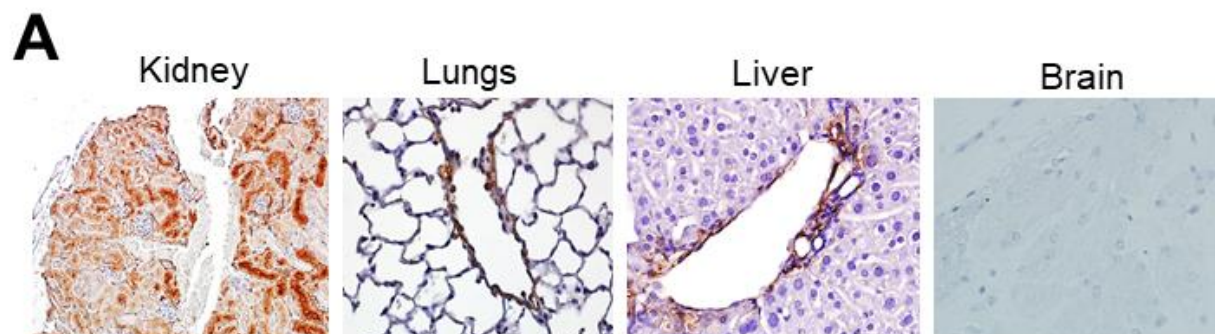
Figure 3.19: Lungs, liver and kidney express functional DPEP1. A. Organs (kidney, lungs liver and brain) were harvested from eight to ten week old C57BL/6 mice and tissues were fixed, paraffin embedded and processed for histology. Immunohistochemistry was performed on the kidney, lung, liver and brain sections using DPEP1 antibody (Abcam) and visualized using the DAB method. (DPEP1 is shown in brown) Scale bar: 20 µm. **B.** Organs (lungs, liver, spleen and kidneys) were harvested from eight to ten-week-old C57BL/6 mice. Proteins were isolated from tissues using RIPA/Octyl-glucoside using a tissue homogenizer. 10 µl of the protein lysate from each experimental condition/organ was used to perform DPEP1 enzyme activity. **C.** Organ extracts were assessed in the presence of Cilastatin (1 mM) to confirm DPEP1 specific activity in the lung, kidney and liver tissue homogenates.

3.10 LPS does not modulate DPEP1 expression and activity.

A number of studies have previously demonstrated increased expression and activity of cell surface adhesion enzymes at sites of inflammation [325-326]. Based on these studies, and since the LSALT peptide was originally isolated from an LPS-inflamed-lung endothelium, experiments were performed to assess if LPS could induce DPEP1 expression and activity in the lungs and liver. We first asked if LPS could induce DPEP1 surface expression *in vitro*. DPEP1 expressing COS1 cells were treated with LPS and flow cytometry was performed to assess DPEP1 surface expression. No significant difference in DPEP1 surface expression was observed on the DPEP1-expressing COS1 cells treated with LPS as compared to untreated DPEP1-expressing COS1 cells (**Figure 3.20A**). One caveat to this experiment is that the lack of increased DPEP1 expression *in vitro* could be a consequence of ectopic expression of DPEP1 by the COS1 cells as both the binding of the LSALT peptide or the human neutrophils/melanoma cells occurred in the absence of additional stimulation, a result in contrast to the *in vivo* studies. Instead, these results suggest that DPEP1 expression on the COS1 cells is already in a confirmation amenable to binding. We therefore asked if LPS could induce DPEP1 expression *in vivo.* C57BL/6 mice were injected with LPS and immunohistological assessment of DPEP1 expression was performed on tissues harvested after four hours. Mirroring the flow cytometry observations *in vitro*, no change in DPEP1 expression in the lungs and liver was observed in the presence of LPS (**Figure 3.20B-C**). Similarly, when DPEP1 enzyme activity was performed in tissue homogenates that were harvested four hours after LPS treatment, no significant difference in the catalytic activity of DPEP1 in the lungs, liver and kidney was observed in the mice treated with LPS compared to the untreated control mice (**Figure 3.20D**). Taken together, these results suggest that LPS does not regulate the expression or activity of DPEP1. Since the original isolation of the LSALT peptide was from an LPS-inflamed

endothelium, LPS may have an alternative role in DPEP1 biology. These observations open a number of possibilities as to how LPS might regulate DPEP1 biology on the endothelium of lungs and liver. These include, i) modifying the affinity of DPEP1, ii) post translational modifications of DPEP1 iii) inducing structural and conformational changes in DPEP1 structure or iv) ectodomain phosphorylation. Also based on the fact that DPEP1 is a GPI-anchored protein, LPS may also regulate DPEP1 biology from a cell signaling/signal transduction aspect as the majority of GPI-anchored proteins signals through an adaptor protein after cleavage by specific phospholipases in the lipid rafts of membrane microdomains. These questions are however open-ended and need further investigation to understand the specific role of LPS in the regulation of DPEP1. In parallel, it is also possible that LPS activates the cognate DPEP1 ligand present on the surface of neutrophils (a mechanism similar to neutrophil integrin activation in response to inflammatory cues that leads to a conformational change that allows binding to the corresponding receptor on the endothelium) and thus regulate DPEP1 mediated recruitment of neutrophils to the inflamed pulmonary and hepatic vasculatures. Conversely, based on the observation that no additional inflammatory stimulus was required for the binding of metastatic cancer cells to DPEP1, the ligand for DPEP1 may not need to be activated on metastatic cancer cells in order to bind to DPEP1 on the lung endothelium. This suggests the possibility that metastatic cancer cells may act as an activated inflammatory cell that is competent to bind DPEP1 without an addtional inflammatory stimulus. Thus, identifying the cognate ligand(s) for DPEP1 present on the neutrophils and metastatic cancer cells would be necessary to address these questions.

A

Mock
DPEP1 Ab

SENGER-ROY-1C-29SEP2015-_003

P4   2.7%

Count
FITC-A

Mock- LPS Treated (100ng/ml)
DPEP1 Ab

SENGER-ROY-1C-29SEP2015-_005

P4   4.1%

Count
FITC-A

Human DPEP1 transfected
DPEP1 Ab

SENGER-ROY-1C-29SEP2015-_008

P4   43.2 %

Count
FITC-A

Human DPEP1 transfected (LPS
Treated-100ng/ml) DPEP1 Ab

SENGER-ROY-1C-29SEP2015-_010

P4   45.6 %

Count
FITC-A

B

PBS   LPS

DPEP1+/+

DPEP1-/-

Lungs

C

PBS   LPS

DPEP1+/-

DPEP1 -/-

Liver

D

Fluorescence Units

LPS   LPS   LPS   LPS
Kidney   Lungs   Liver   Spleen

138

Figure 3.20: LPS does not induce DPEP1 expression or activity *in vitro* and *in vivo*. A. COS1 cells were either transiently transfected with human DPEP1 or mock transfected. 48 hours after transfection, cells were treated with LPS (100 ng/ml) for 30 minutes and stained with a DPEP1 antibody. Flow cytometry was performed to assess DPEP1 surface expression. **B-C.** Lungs and livers were harvested from untreated C57BL/6 mice or C57BL/6 mice treated with LPS (0.5 mg/kg), fixed, paraffin embedded and processed for histology. Immunohistochemistry was performed to assess DPEP1 expression in the lungs and livers and visualize using the DAB reagent. (DPEP1 is shown in brown) Scale bar: 20 µm. **D.** Endogenous DPEP1 activity in different organs were assessed. C57BL/6 mice were treated with PBS or LPS (0.5 mg/kg) for four hours and organs (kidney, lungs, liver, and spleen) were harvested. Proteins were isolated from tissues using RIPA/Octyl-glucoside using a tissue homogenizer. 10 µl of each protein lysate from each experimental condition/organ were used to perform DPEP1 enzyme activity.

3.11 Generation and characterization of a *DPEP1 -/-* transgenic mouse by CRISPR/Cas9.

Our functional and biochemical observations strongly suggested that DPEP1 acts as an adhesion receptor for neutrophils and metastatic melanoma cells. Thus a DPEP1 knockout mouse line was generated to directly assess the role of DPEP1 in the recruitment of neutrophils and metastatic cancer cells to the lungs and liver *in vivo*. Horizon Discovery (Saint Louis, MO, 63146, USA) was contracted to generate heterozygote DPEP1 knockouts using CRISPR/Cas-9 system to mediate the knockdown of DPEP1 gene on chromosome-16 in the mouse genome. A detailed description and schematic representation of the generation of *DPEP1-/-* mice is described in chapter two (materials and method section) of this thesis (**Figure 3.21 and 3.22**). Briefly, using specific CRISPR/Cas-9 constructs, four independent mouse lines deficient for functional DPEP1 protein were generated. These four lines were i) 1base pair insertion of cytosine 'C', ii) 11 base pair deletion and 1 base pair insertion of thymine "T" iii) 6 base pair deletion and iv) 141 base pair deletion. These four mutations were generated in the catalytic domain of murine DPEP1 using specific sgRNA's that selectively targeted DPEP1. Mutations were designed and established in a way that it introduced a pre-mature stop codon resulting in a complete loss of functional DPEP1 protein (**Figure 3.22**). The majority of the results that are presented in this thesis were performed using the 1 bp C insertion and 11 bp deletion and T insertion DPEP1 knockout mouse lines. We are currently in the process of assessing the other lines.

To begin to characterize the *DPEP1-/-* mice, tissues from the C and T *DPEP1-/-* mice were harvested, fixed, paraffin embedded and assessed by immunohistochemistry for DPEP1 expression. Histological analysis revealed a complete absence of DPEP1 expression in the lungs, liver and kidney of *DPEP1-/-* mice compared to DPEP1 wild type mice (*DPEP1+/+*) (**Figure 3.23 left panels**). DPEP1 activity was also absent in the *DPEP1-/-* mice compared to *DPEP1+/+* mice

(**Figure 3.23 right panels**). DPEP1 heterozygous mice (*DPEP1+/-*) were also assessed for the presence of functional DPEP1 activity in the lungs and kidney. Results from a number of *DPEP1+/-* mice from different generations suggested that they all expressed functional DPEP1 activity to a level that was similar to the DPEP1+/+ mice (**Figure 3.23C**). In addition to the 1bp C and T *DPEP1 -/-* mouse lines, a complete inhibition in DPEP1 enzyme activity in the lungs and in the kidney in the two other *DPEP1 -/-* mouse lines were also observed (i.e. 6 bop deletion and 141 bp deletion) (**Figure 3.23B**). Collectively, these results confirmed the absence of functional DPEP1 in the lungs, liver and kidney of the *DPEP1 -/-* mice. The expression of DPEP1 in human lungs and liver tissue was also assessed and as seen in the mouse tissues, DPEP1 was expressed within the human lungs and liver (**Figure 3.23D**).

A DPEP1 NC_000074.6

CRISPR target/PAM site

GATGCTGACTTGAACAAGCTAGCCCAAACACACACCCAACATCCCCAAGCTGAAGGCTGGCTTTGTCGGAGGCCAGTTCTG

B CelF CelR
sgRNA Dpep1

C

D sgRNA, Cas9
Microinjection → Pseudopregnant female → Founder

E

Founder	Genotype	Location	Transmission
#8 F	WT/-141	12454-12594	WT/-141
#18 F	WT/-11/+1(T)	12580-12590	WT/-11, +1(T)
#29 F	WT/+1(C)	12586	WT/+1(C)
#32 M	WT/+48	12586	NA
			WT/-6

F

#8 141bp deletion

#18 11bp del, 1bp(T) insertion

#29 1bp(C) insertion

6bp deletion

G

Wildtype: GAACAAGCTAGCCCAAACACACACCAACATCCCCAAGC-TGAAGGCTGGCTTTGTCGGAGGC
#18: GAACAAGCTAGCCCAAACACACACCAACATC-----------TGCTGGCTTTGTCGGAGGC
#29: GAACAAGCTAGCCCAAACACACACCAACATCCCCAAGCCTGAAGGCTGGCTTTGTCGGAGGC
#: GAACAAGCTAGCCCAAACACACACCAACATCCCCAAG-------GCTGGCTTTGTCGGAGGC

#8:CTAATCCACC--------------------141bp--------------------GGCTTTGTCG

Wild-type:
GAACAAGCTAGCCCAAACACACACCAACATCCCCAAGCTGAAGGCTGGCTTTGTCGGAGGC

#18 Homozygote: 11bp deletion, 1bp (T) insertion
GAACAAGCTAGCCCAAACACACACCAACATCTGGCTGGCTTTGTCGGAGGCCAGGTACATCCTC

#29 Homozygote: 1bp (C) insertion
GAACAAGCTAGCCCAAACACACACCAACATCCCCAAGCCTGAAGGCTGGCTTTGTCGGAGGC

Homozygote: 6bp deletion
CAAGCTAGCCCAAACACACACCAACATCCCCAAGGCTGGCTTTGTCGGAGGCCAGGTAC

142

Figure 3.21: Generation of *DPEP1 -/-* mice by CRISPR/Cas-9. A.CRISPR/Cas-9 target region in murine DPEP1. The sequence highlighted in red is the targeting sequence and the PAM motif is highlighted in blue. **B.** Schematic representation of target sequence insertion into gRNA plasmid. The red highlighted regions are the Cel-1 enzyme sites. **C.** Assessment of CRISPR/Cas-9 efficiency *in vitro*. HEK-293T cells were transfected with the sgRNA-Cas9 targeting DPEP1. A fragment containing the DPEP1 targeting region was PCR amplified from mouse genomic DNA and gel purified. The PCR product was left untreated or incubated with Cel-1.The fragment (498 bp) could be cut into two bands (229 bp and 269 bp). **D.** Schematic representation of microinjection. **E.** A total of four founders were generated for further breeding, transmission and for the establishment of frame shift knockout mouse lines. **F.** An example of a polyacrylamide gel electrophoresis showing genotyping of each homozygote that can be discriminated based on size. The size difference between 1bp (C) insertion homozygote and wild type is too small to be detected by gel electrophoresis. The 1bp (C) insert and 1bp T inserts were confirmed by sequencing. **D.** Mice were identified and confirmed by DNA sequencing. (Figure contributed by Dr. Bo Young Ahn).
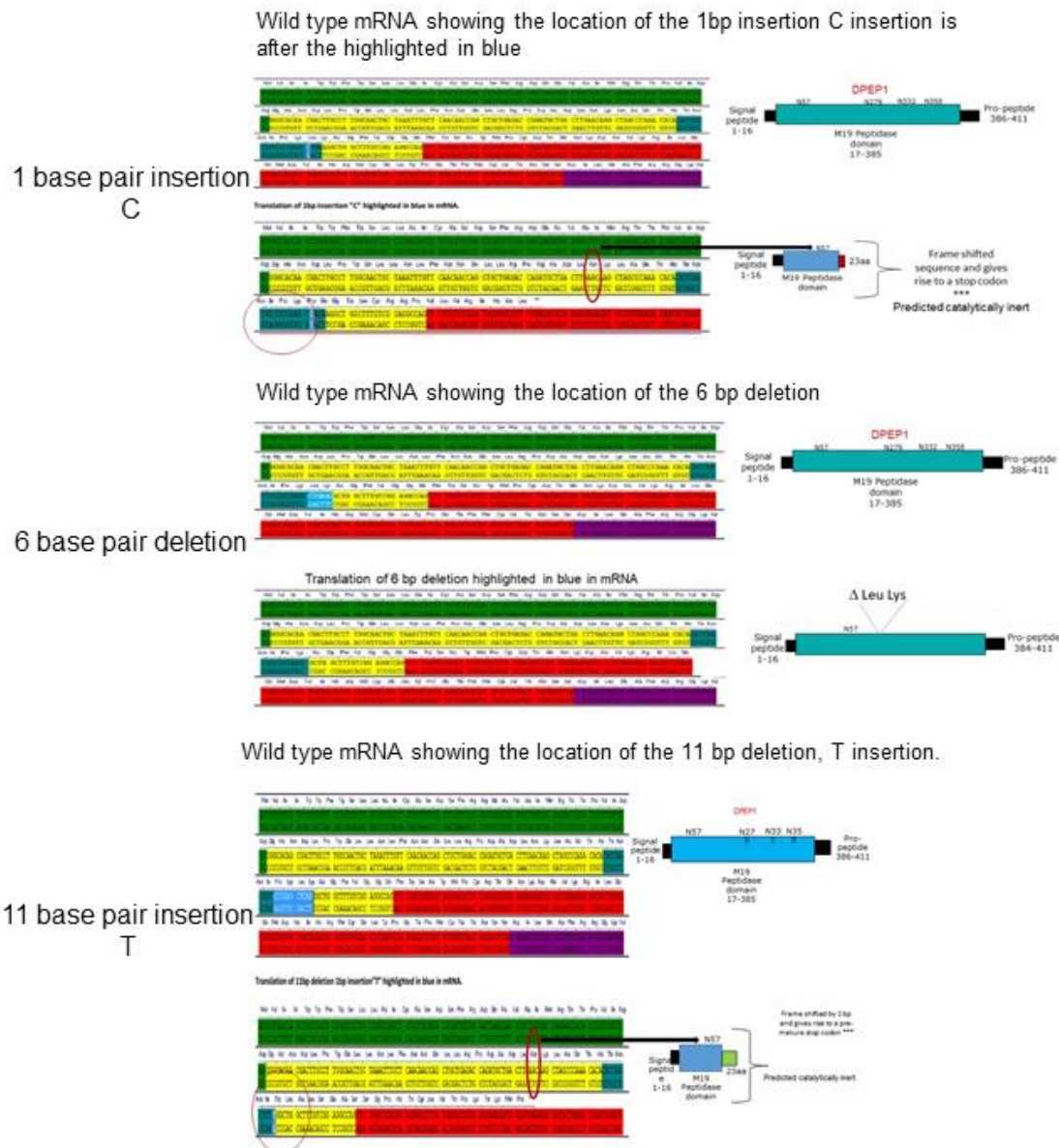
Figure 3.22: Schematic representation/mapping of CRISPR/Cas-9 mediated knockout of DPEP1 in *DPEP1-/-* mice. Schematic representation of three independent *DPEP1-/-* transgenic mouse lines generated by CRISPR/Cas-9. Based on the CRISPR/Cas-9 target region in murine DPEP1, predicted maps were generated to hypothetically predict the consequences of each mutation in the structure of DPEP1 protein in *DPEP1-/-* mice.

144
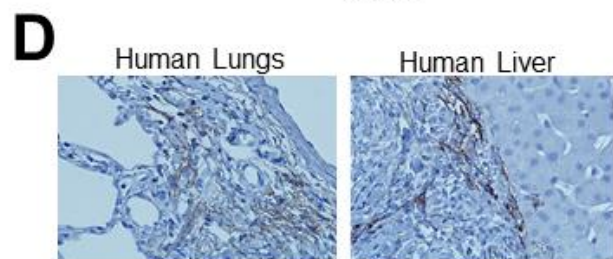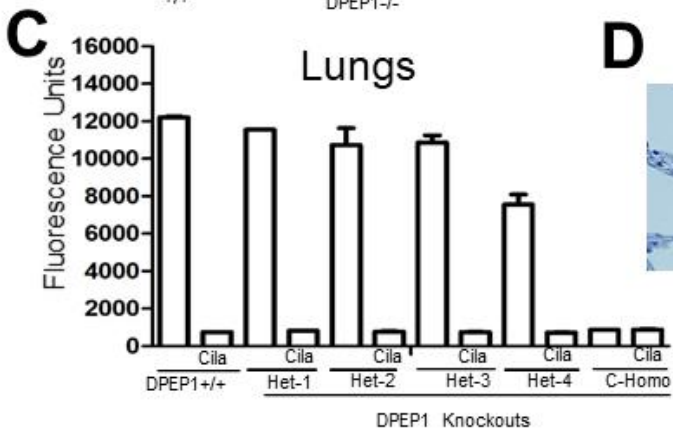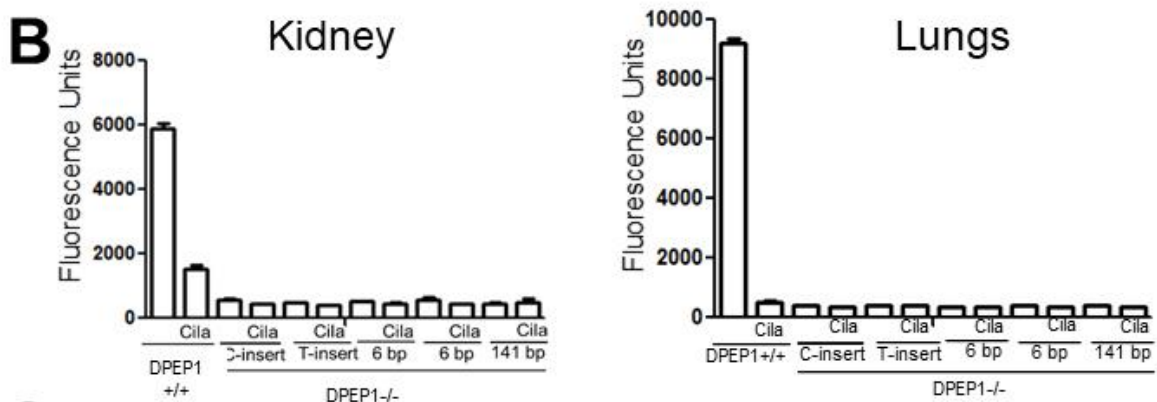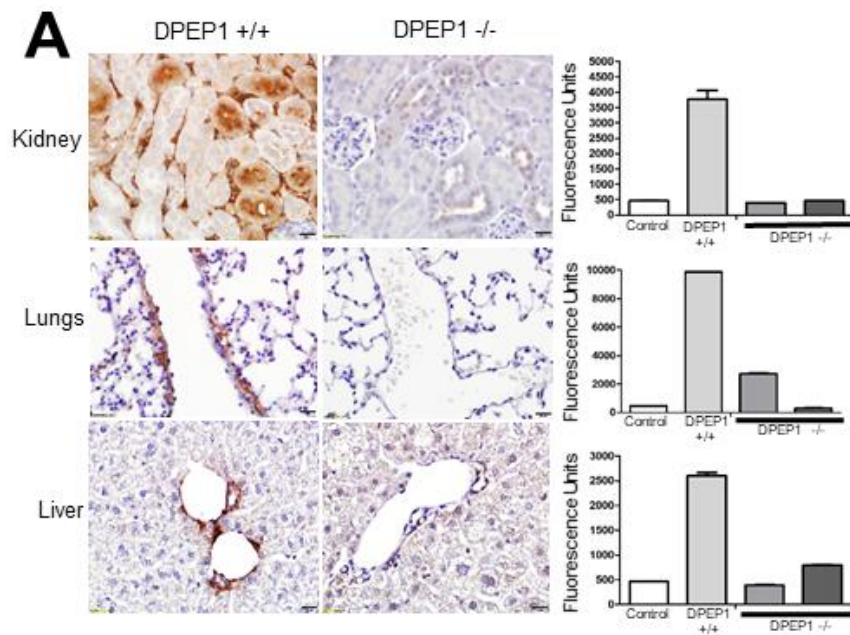
Figure 3.23: Characterization of *DPEP1-/-* mice *in vivo*. A. *DPEP1 -/-* mice were generated as described in the materials and method section using CRISPR/Cas9 technology. Five to six week old *DPEP1 -/-* and *DPEP1+/+* mice were sacrificed and lungs, liver and kidney were harvested to assess DPEP1 expression. Tissues were harvested, fixed and processed using paraffin embedding for histology. Immunohistochemistry was performed on kidney, lung and liver sections using the DAB method to assess DPEP1 expression (brown) (left panel). Scale bar: 20 µm. Proteins were isolated from tissues using octyl-glucoside buffer and DPEP1 enzyme activity assay was performed (right panels). Immunohistological analysis and DPEP1enzyme activity assay confirmed the absence of functional DPEP1 in the tissues of *DPEP1 -/-* mice. **B.** Four independent *DPEP1 -/-* mice lines generated using CRISPR/Cas9 were functionally characterized using DPEP1 enzyme activity assay. Organs were harvested from *DPEP1+/+* or *DPEP1 -/-* mice and proteins were isolated using RIPA/octyl-glucoside lysis buffer. Kidney and lung tissue homogenates from all four *DPEP1 -/-* mice were assessed for DPEP1 enzyme activity. **C.** DPEP1 enzyme activity was assessed in DPEP1 heterozygous (*DPEP1+/-*) mice using DPEP1 activity assay. **D.** Paraffin embedded human lungs and liver sections were stained with anti-DPEP1 to assess DPEP1 expression (brown). Scale bar: 20 µm. Human lung tissues were provided by Dr. Margaret Kelly while the human liver tissues were obtained from Dr. Mark Swain.

3.12 Absence of functional DPEP1 reduced myeloperoxidase activity and recruitment of neutrophils to the pulmonary vasculature of *DPEP1-/-* mice.

Once the absence of functional DPEP1 protein was validated in different tissues of the *DPEP1-/-* mice, the functional role of DPEP1 in neutrophil recruitment to the lungs was investigated *in vivo*. One initial strategy to address this question was to assess the levels of myeloperoxidase activity in lungs of *DPEP1-/-* mice in the presence of LPS. Myeloperoxidase (MPO), an enzyme expressed by activated granulocytes at inflammatory sites, has been shown extensively over the years as a measurement of neutrophil recruitment in organs such as the lungs [327]. Although some studies have indicated that monocytes and other innate granulocytes may also express MPO, based on a large body of evidence it has been well accepted that activated neutrophils are the major granulocytic population among the innate immune cells that express MPO during inflammation. Thus, MPO activity in the lungs of *DPEP1-/-* mice was assessed in the presence of LPS. Strikingly, a significant reduction in MPO activity in *DPEP1-/-* mice in the presence of LPS was observed compared to the *DPEP1+/+* mice. Two different *DPEP1-/-*mice lines (1 bp insertion C and 11 bp deletion-1 bp insertion T) that were deficient of functional DPEP1 protein were used and similar MPO activity were observed (*DPEP1+/+*LPS LPS: 0.3413±0.003250, *DPEP1-/-*C+LPS: 0.2132±0.003750, *DPEP1-/-*T+LPS: 0.1221±0.00155) (**Figure 3.24A**). These results suggested for the first time that DPEP1 is involved in the recruitment of leukocytes/neutrophils to the lungs in response to an LPS induced inflammation. Based on the fact that the LSALT binds to DPEP1 and that DPEP1 is involved in the recruitment of neutrophils/monocytes to the lungs, the effect of LSALT peptide in the recruitment of neutrophils/monocytes to the lungs of *DPEP1-/-*mice was investigated. Briefly, *DPEP1 -/-* mice were injected with the LSALT peptide in the presence of LPS. And an MPO activity assay was

147

performed. A significant reduction in the MPO activity in the lungs of *DPEP1-/-* mice was observed compared to the *DPEP1+/+* mice. Moreover, no reduction in lung MPO activity was observed in the *DPEP1 -/-* mice in the presence of LSALT, further supporting DPEP1 as the sole target for the LSALT peptide (**Figure 3.24B**).

As discussed previously, MPO activity within the lungs can also be contributed by the presence of monocytes and other innate immune cells in the pulmonary vasculatures, thus we next asked if DPEP1 is specifically involved in the recruitment of neutrophils to the lungs. To assess this, lungs from *DPEP1-/-* and *DPEP1+/+* mice were harvested four hours following LPS injection and histology was performed using a ly6G antibody clone called 1A8 that specifically detects neutrophils. Evaluation of a series of lung sections from LPS treated *DPEP1 -/-* mice showed a significant reduction in the number of 1A8 specific neutrophils recruited to the lungs of *DPEP1-/-* mice compared to the *DPEP1+/+* (*DPEP1+/+* LPS: 48.87±3.633, *DPEP1-/-C*+LPS: 33.53±2.147, *DPEP1-/-T*+LPS: 35.53±1.932) (**Figure 3.24C**). Importantly, a second investigator (Dr. Jennifer Rahn) blinded to the experimental conditions, obtained similar results. These observations further suggested a functional role of DPEP1 in the recruitment of neutrophils to the lungs. We also asked if DPEP1 is also involved in the recruitment of other innate immune cells such as monocytes to the lungs. To address this, histological analysis on paraffin embedded lung sections were performed in the lungs of LPS treated *DPEP1 -/-* and *DPEP1+/+* mice using an antibody that detects both neutrophils and monocytes called Gr-1 (Ly6G/Ly6C, clone RB6 8C5). Using this strategy, we observed a significant reduction in the recruitment of Ly6G/Ly6C cell population in the presence of LPS in *DPEP1 -/-* mice compared to the *DPEP1+/+* mice (*DPEP1+/+*LPS: 45.60±4.554, *DPEP1-/-C*+LPS: 23.40±1.524, *DPEP1-/-T*+LPS: 21.93±3.199) (**Figure 3.24D**). These observations suggest that in addition to the neutrophils, DPEP1 may also

act as an adhesion receptor to recruit other innate immune cells such as monocytes during inflammation. However further investigation is required to validate this observation, for example, using a monocyte specific antibody such as Ly6C. Finally to validate the role of DPEP1 in LPS induced recruitment of neutrophils to the lungs, intravital spinning disk microscopy was performed. Mirroring our MPO activity and histological analysis, a significant reduction in the number of neutrophils recruited to the LPS inflamed pulmonary vasculature was observed (*DPEP1+/+*LPS: 81.25±6.780, *DPEP1-/-C*+LPS: 54.47±3.730) (**Figure 3.25A**). In addition, a significant reduction was also observed in the number of neutrophil clusters within the lung capillaries in *DPEP1-/-* mice compared to *DPEP1+/+* mice in the presence of LPS (**Figure 3.28B**). Taken together, these indicate a novel role for DPEP1 in neutrophil recruitment to the inflamed pulmonary vascular beds. This data supports the idea that DPEP1 is the first non-classical adhesion molecule described for neutrophil recruitment to the inflamed pulmonary vasculatures and provides a newly described function for DPEP1.
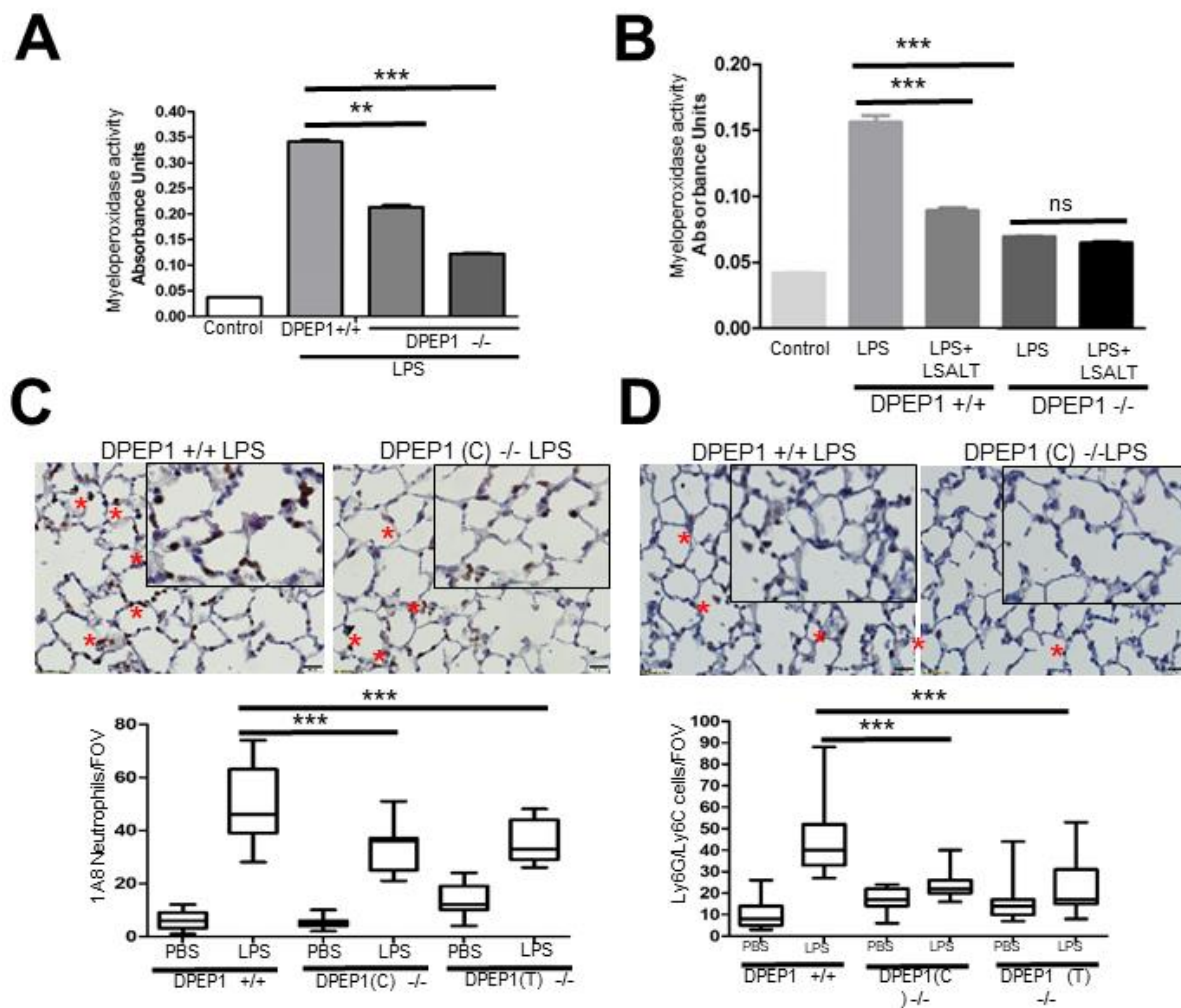
Figure 3.24: Impaired leukocyte/neutrophil recruitment in the lungs of *DPEP1 -/-* mice. A. Five to six week old *DPEP1-/-* (two different *DPEP1 -/-* mice were used i.e., 1 base pair C-insertion and 11 base pair deletion-T-insertion) and *DPEP1+/+* mice were injected with PBS or 0.5 mg/kg LPS (i.p). Lungs were perfused with PBS through the heart and harvested. Tissues were homogenized using the HTAB buffer and myeloperoxidase activity assay was performed. **B.** Five to six week old *DPEP1 -/-* mice or *DPEP1+/+* mice were injected with 1 mM LSALT (i.v.) via the tail vein five minutes after the injection of 0.5 mg/kg LPS (i.p). Lungs were perfused through the heart four hours later and organs were harvested. Myeloperoxidase activity assay was performed as described previously. **C.** Lungs harvested from LPS injected *DPEP1 -/-* mice or *DPEP1+/+* mice were fixed and processed using paraffin embedding for histology. Lung sections were stained with Ly6G (clone 1A8) antibody using the DAB method to detect the presence of infiltrated neutrophils into the lungs in the presence of LPS. Upper panel shows the presence of neutrophils (brown) in a representative lung section from at least three independent experiments with similar results. The number of neutrophils infiltrated to the lungs four hours after LPS injection were counted in 15 different field of views in lung sections stained with the Ly6G (clone: 1A8) antibody (lower panel). Scale bar: 20 μm. Red asterisks indicate the presence of neutrophils. Results are shown from one experiment from at least three independent experiments with similar results. Graph shows an inhibition in the number of neutrophils infiltrated to the lungs in *DPEP1 -/-* mice compared to *DPEP1+/+* mice. **D.** Fixed and paraffin embedded lung sections were assessed by immunohistochemistry and stained with anti-Gr-1 (Ly6G/Ly6C) to assess the presence of neutrophils/monocytes (brown) in the lungs of *DPEP1-/-* mice that were treated with LPS. Number of Ly6G/Ly6C positive cells infiltrated to the lungs four hours later LPS injection were

counted in 15 different field-of-views and quantified (lower panel). Scale bar: 20 µm. Red asterisks indicate the presence of Ly6G/Ly6C cells.

A

DPEP1 +/+ LPS   DPEP1 -/- LPS

Neutrophils (Ly6G/1A8)   Vasculature (CD31)

B
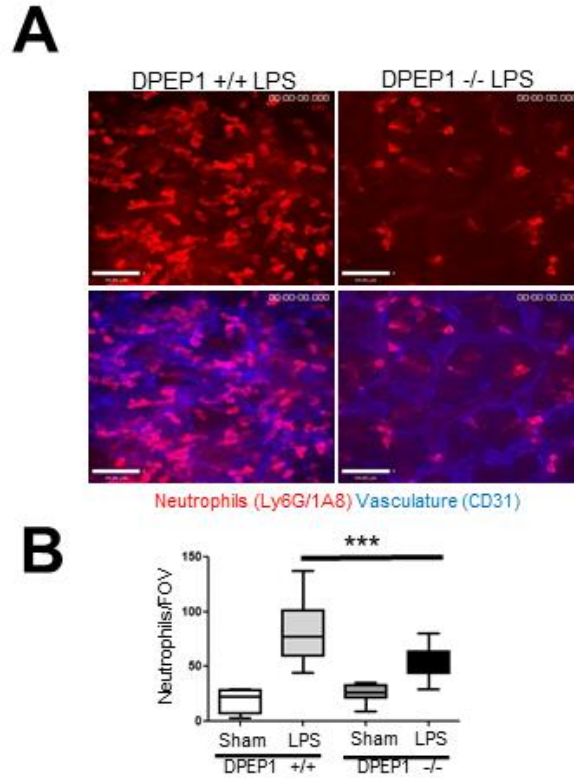
Figure 3.25: Impaired neutrophil recruitment in the lungs of *DPEP1 -/-* mice in the presence of LPS. A. Five to six week old *DPEP1+/+* or *DPEP1-/-* mice were injected with LPS and lungs were imaged using spinning disk confocal microscopy four hours later. Shown here are the neutrophils (Ly6G, clone: 1A8, red, upper panel) in the pulmonary vasculature (CD31, blue) (Lower panel). **B.** Total number of neutrophils were counted four hours after LPS injection from at least four different field-of-views of the lungs of each mouse and graphed. (Lung imaging was performed by Dr. Andrew K. Chojnacki under the supervision of Dr. Ajitha Thanabalasuriar. Mouse injections and data analysis was performed by myself).

3.13 Neutrophil recruitment is compromised in the liver of *DPEP1 -/-* mice.

Based on the original *in vivo* screen where the LSALT peptide functionally inhibited the recruitment of neutrophils to the inflamed hepatic microvasculature (**Figure 3.1B and 3.2**) and the identified role of DPEP1 in the recruitment of neutrophils to the inflamed pulmonary vasculatures, the functional role of DPEP1 in neutrophil recruitment in the inflamed hepatic sinusoids was investigated. Previously a role for CD44-HA was identified in the binding interaction of neutrophils to the liver sinusoids in response LPS-induced endotoxemia [3]. Based on the observations described in this thesis we predicted the existence of a second adhesion molecule in these vascular beds. This rationale was based on the fact that the LSALT peptide inhibited 49.81% of neutrophil adhesion in the liver of C57BL/6 mice in the presence of LPS and that the LSALT peptide could further inhibit the recruitment of neutrophils in an LPS activated sinusoidal endothelium of *CD44 -/-* mice. Thus, experiments were performed to assess if DPEP1 is an alternative neutrophil receptor in the vascular beds of liver. Intravital spinning disk confocal microscopy was used to investigate the behavior of neutrophils in real time and no difference was observed in terms of the recruitment of neutrophils in the liver of *DPEP1 -/-* mice compared to the *DPEP1+/+* mice under normal basal conditions. In contrast, intravital imaging of the liver of *DPEP1 -/-* mice in the presence of LPS revealed a significant reduction in the recruitment of neutrophils in LPS-induced inflamed hepatic vascular beds (*DPEP1+/+*LPS: 10.47±1.091, *DPEP1-/-C*+LPS: 5.556±0.5786) (**Figure 3.26A-C**). 53% reduction in the number of adhered neutrophils was observed in the sinusoidal endothelium of the liver in *DPEP1 -/-* mice compared to the *DPEP1+/+* mice supporting DPEP1 as the second adhesion molecule for neutrophils in these vascular compartments of the liver (**Figure 3.26B**). In addition to adhesion, a profound reduction in the crawling behavior of neutrophils in the liver sinusoids of the *DPEP1-/-* mice was

also observed as compared to the *DPEP1+/+* mice. This data identifies a previously unknown role for DPEP1 in neutrophil crawling in the inflamed hepatic sinusoids. In addition, the LSALT peptide had no effect on the recruitment of neutrophils in inflamed hepatic sinusoids in *DPEP1 -/-* mice validating DPEP1 as the functional receptor for the LSALT peptide (**Figure 3.26D-E**). To further assess the recruitment of neutrophils to the inflamed liver, immunohistological staining was performed using Ly6G antibody clone 1A8 to detect the presence of infiltrated neutrophils in the liver in the presence of LPS. Consistent with our intravital imaging observations, a significant reduction in the number of neutrophils was observed in the liver of *DPEP1 -/-* mice *in vivo* (*DPEP1+/+*LPS: 20.10±1.138, *DPEP1-/-C*+LPS: 11.60±0.9852) (**Figure 3.26F**).

A DPEP1 +/+ LPS   DPEP1 -/- LPS

B Adhesion

C Crawling

D DPEP1 -/- LPS   DPEP1 -/- LPS+LSALT

E

F DPEP1 +/+ LPS   DPEP1 -/- LPS

G DPEP1 +/+ LPS   DPEP1 -/- LPS
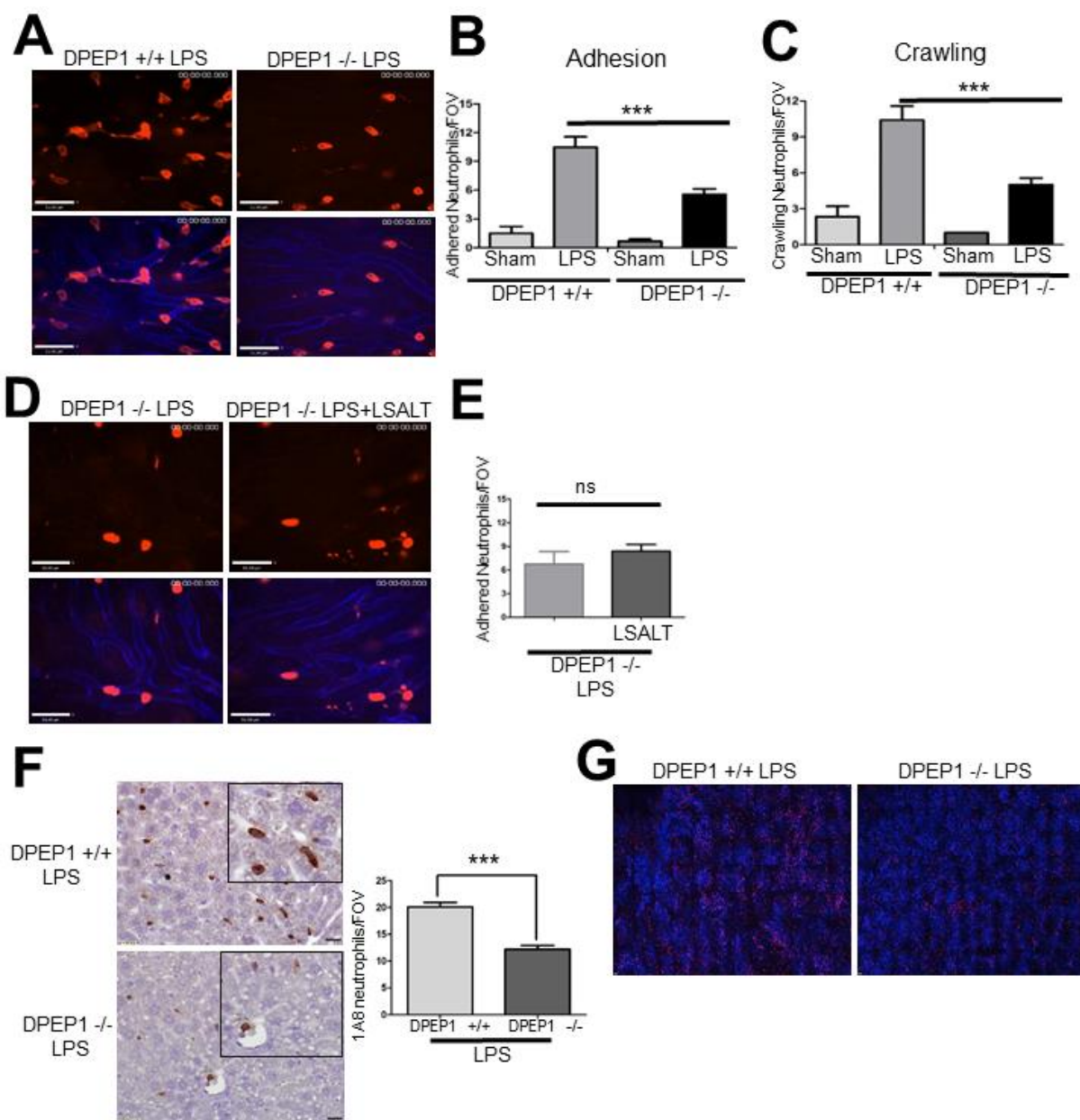
Figure 3.26: Reduced recruitment of neutrophils to the hepatic vascular beds in the presence of LPS in *DPEP1 -/- mice.* A. Six week old *DPEP1 -/-* mice or *DPEP1+/+* mice were injected with LPS and livers were imaged by intravital microscopy four hours later. Shown here are the neutrophils (Ly6G, clone: 1A8, red) in the liver sinusoids (CD31, blue). **B.** Neutrophils that were stationary for more than one minute were counted as adherent cells. Total number of adhered neutrophils present in the sinusoidal endothelium of the liver was counted and graphed **C.** Crawling of neutrophils were also monitored and firmly adhered cells with elongated behavior for transmigration were counted as crawling neutrophils. Values shown are the mean ±SEM from at least three independent experiments; asterisks (***) indicate P<0.001 as compared to LPS treated *DPEP1+/+* mice (one-way ANOVA with the Neuman-Keuls post-test). **D-E.** *DPEP1-/-* mice were injected with LSALT peptide five minutes after the injection of LPS and livers were imaged four hours later using intravital microscopy. **F.** Livers harvested from *DPEP1 -/-* or *DPEP1+/+* mice four hours after LPS injection, were fixed, paraffin-embedded, and processed for immunohistochemistry. Immunohistochemical analysis was performed using Ly6G (clone: 1A8) antibody to detect the presence of infiltrated neutrophils in the liver using the DAB method for visualization. Scale bar: 20 µm. (Neutrophils are shown in brown) G. Stitched images of a liver from *DPEP1 +/+* or *DPEP1 -/-* mice treated with LPS are shown. Neutrophils are red (Ly6G, clone: 1A8) and hepatic sinusoids are blue (CD31). Scale bar: 100 µm. (Experiments performed in collaboration with Dr. Liane Babes).

Since CD44 is a major neutrophil adhesion receptor in the liver sinusoids [3] and based on our findings that DPEP1 is a second adhesion molecule in these vascular beds, we next asked if CD44 and DPEP1 represent the predominate neutrophil adhesion mechanisms within the LPS induced inflamed hepatic sinusoids. To address this question *DPEP1 -/-* mice were treated with an anti-CD44 monoclonal antibody, treated with LPS and assessed for neutrophil recruitment in the liver sinusoids. Strikingly, a further inhibition of neutrophil recruitment and intraluminal crawling in the liver sinusoids was observed (*DPEP1-/-*LPS: 5.000±0.5567, *DPEP1-/-*LPS+CD44 monoclonal antibody: 1.625±0.3239) (**Figure 3.27A-B**). The total number of neutrophils present within the liver sinusoids four hours later LPS treatment was also counted and although there was a significant reduction in the total number of neutrophils present in CD44 monoclonal antibody injected *DPEP1+/+* mice and *DPEP1 -/-* mice, the number of neutrophils was substantially reduced in the presence of CD44 monoclonal antibody in the *DPEP1-/-* mice further suggesting DPEP1 and CD44 represent two dominant mechanisms for the recruitment of neutrophils in the inflamed hepatic vasculatures. Taken together, these observations reveal a crucial and previously unidentified role for DPEP1 in the adhesion and crawling of neutrophils in inflamed hepatic microvasculature in the presence of LPS.
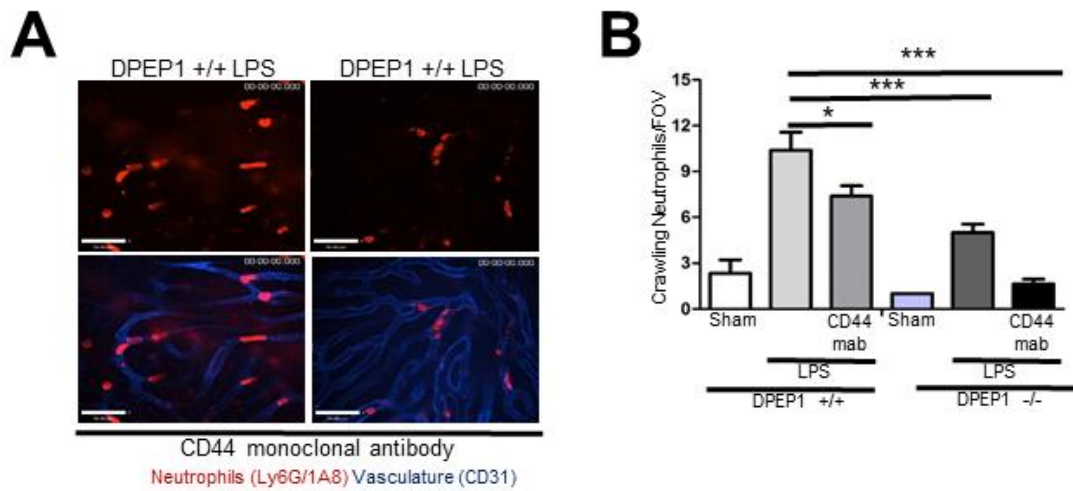
Figure 3.27: CD44 and DPEP1 represent predominant mechanisms for neutrophil adhesion in the liver sinusoids in the presence of LPS. A. *DPEP1+/+* or *DPEP1-/-* mice were injected with CD44 monoclonal antibody in the presence of LPS and the liver was imaged by intravital microscopy. Shown here are the neutrophils (Ly6G, clone: 1A8, red) in the sinusoidal endothelium (CD31, blue). White arrow indicates the presence of crawling neutrophils within the sinusoidal endothelium. **B.** Total number of crawling neutrophils in the liver microvasculature was counted as described earlier and graphed. Scale bar: 45 µm. (Experiments performed in collaboration with Dr. Liane Babes).

3.14 Targeting DPEP1 provides therapeutic benefit from acute lung injury induced endotoxemia.

As sepsis/acute respiratory distress syndrome (ARDS) remains one of the most common causes of mortality in North America and since excessive dysregulated recruitment of neutrophils is a hallmark of endotoxemia, experiments were performed to investigate if targeting DPEP1 could provide therapeutic benefits in LPS-induced endotoxemia. To address the therapeutic role of DPEP1 in LPS induced endotoxemia, *DPEP1 -/-* mice and *DPEP1+/+* mice were injected with a lethal dose (15mg/kg) of the bacterial endotoxin (LPS) and survival was assessed. The absence of DPEP1 significantly increased the survival of mice that were treated with the lethal dose of LPS. In this survival study all mice (6/6) in the *DPEP1+/+* group were sacrificed based on the clinical criteria that were originally established by Shrum et al. [328]. In contrast only one of the *DPEP1 -/-* mouse (1/6) needed to be sacrificed based on the severity of the sepsis specific clinical scores (**Figure 3.28A**). Based on this observation, experiments were next performed to assess if treatment of *DPEP1+/+* mice with the LSALT peptide could also increase the overall survival in the presence of the high-dose LPS. It is important to mention that a single dose of the LSALT peptide was shown to significantly increase the survival of mice bearing melanoma-lung metastasis (**Figure 3.6**). To address the question if LSALT could provide therapeutic benefit in the context of endotoxmeia induced ARDS, *DPEP1+/+* mice were injected with a single dose of LSALT peptide (1mM) in the presence of a lethal dose of LPS (15 mg/kg). Mimicking our earlier observations in the *DPEP1 -/-* mice, treatment of *DPEP1+/+* mice with the LSALT peptide significantly increased the overall survival (4/7) (**Figure 3.28B**). In addition, treatment of *DPEP1+/+* mice with a second dose of the LSALT peptide at 18 hours following LPS treatment further increased survival (6/7) (**Figure 3.28B**). Taken together, these two striking observations

provide strong evidence that in addition to the adhesion function, targeting this GPI-anchored cell surface protein could also provide direct therapeutic benefit in patients with endotoxin induced acute respiratory distress syndrome.

Since one of the major contributing factors of endotoxin induced mortality in patients with systemic inflammatory diseases is acute lung injury that primarily results from the destruction of endothelial barriers, the proinflammatory cytokine mediated recruitment of innate leukocytes in LPS-induced acute lung injury in *DPEP1-/-* mice was investigated. To assess the role of DPEP1 in LPS-induced acute lung injury, *DPEP1-/-* and *DPEP1+/+* mice were injected with LPS (15mg/kg) and the lungs were harvested at 4, 8 and 12 hours. Histological assessment of lung sections from *DPEP1 -/-* mice revealed a significant reduction in inflammation associated cellular features as early as eight hours, a protective feature that was maintained at 12 hours (**Figure 3.28C**). In addition, similar results were observed when *DPEP1+/+* mice were treated with the LSALT peptide (**Figure 3.28D**). These observations, in part, indicate a role for DPEP1 during LPS-induced endotoxemia that can be mitigated in the *DPEP1-/-* mice or LSALT treated *DPEP1+/+* mice (**Figure 3.28**) thus supporting the idea that targeting DPEP1 could provide direct therapeutic benefit in acute lung injury induced endotoxemia.

A

Survival proportions

Percent survival vs Time in hours

P value=0.002

— DPEP1 +/+ LPS
— DPEP1 -/-LPS

B

Survival proportions

Percent survival vs Time in hours

— LPS
— LPS+LSALT Single dose
— LPS+LSALT Double dose

P value =0.004

P value =0.0006

C

	DPEP1 +/+ LPS	DPEP1 -/-LPS
4 hours		
8 hours		
12 hours		

D

	LPS	LPS+LSALT
12 hours		
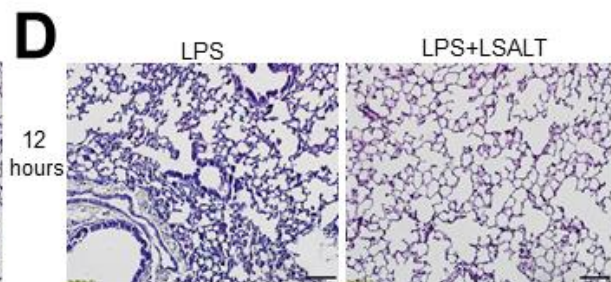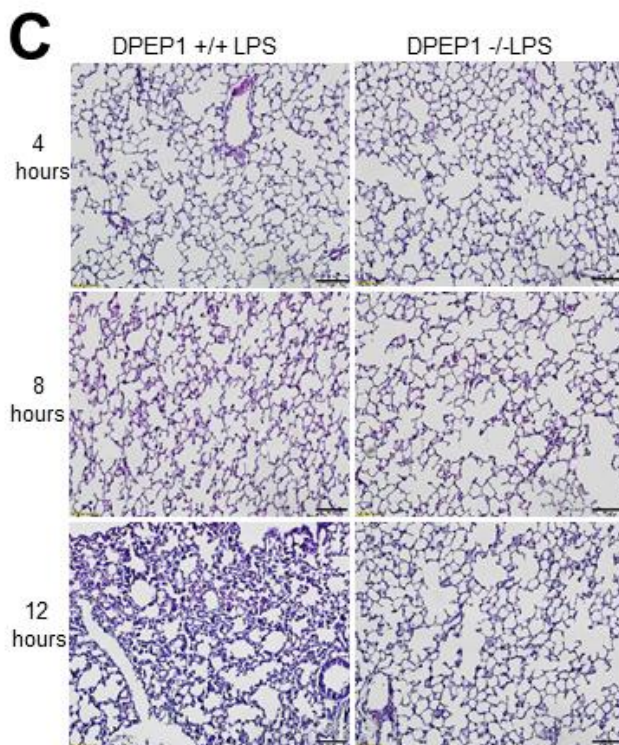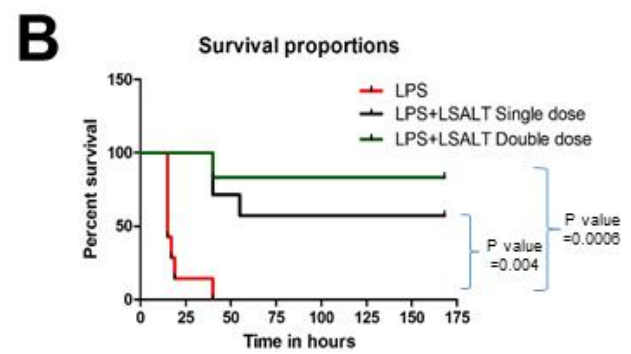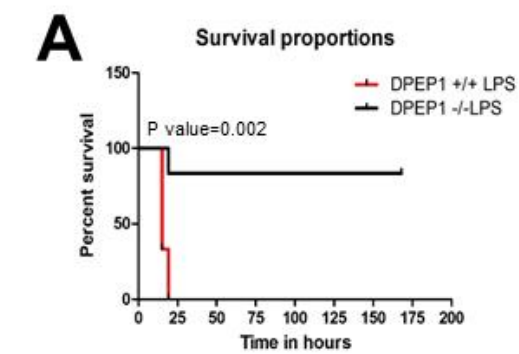
Figure 3.28: Targeting DPEP1 provides therapeutic benefit and increase overall survival in ARDS. A. Graph shows Kaplan Meier survival assessment of *DPEP1+/+* or *DPEP1 -/-* mice injected with 15mg/kg of LPS. The log-rank test was used to compare the distribution of survival times. **B.** Graph shows Kaplan Meier survival assessment of *DPEP1 +/+* mice treated with LPS in the presence or absence of LSALT administered 5 minutes (single dose) or 5 minutes and 18 hours (double dose) following LPS. N=5-7 mice per group. **C.** Histological assessment of lungs harvested at 4, 8 and 12 hours from *DPEP1+/+* or *DPEP1-/-* mice treated with 15mg/kg LPS was performed. Shown are representative H&E images. Scale bar: 100 µm. **D.** Histological assessment of lungs harvested at 12 hours from *DPEP1+/+* mice treated with LPS (15mg/kg) in the presence or absence of LSALT. Shown are representative H&E images. Scale bar: 100 µm. C. *DPEP1 +/+* mice were treated with LPS in the presence or absence of LSALT and Kaplan Meier survival analysis was performed. N=5/6 mice per group was used. Clinical scores were recorded by Dr. Liane babes and myself.

3.15 Genetic or pharmacological inhibition of DPEP1 suppresses systemic release of LPS-induced pro-inflammatory cytokines.

Since the deregulated release of pro-inflammatory cytokines/chemokine mediated inflammatory milieu plays a crucial role in the pathogenesis underlying endotoxin induced ARDS/acute lung injury, the release of different pro-inflammatory mediators in the systemic microenvironment of LPS-induced endotoxemia was investigated. These cytokines/chemokines have the ability to bind to GPCR's present on the surface of neutrophils that allows the adhesion of neutrophils in an integrin dependent manner in response to an inflammatory stimulus or infection. To assess the release of pro-inflammatory mediators in LPS-induced endotoxemia, six to eight week old *DPEP1+/+* mice were injected with the LSALT peptide in the presence of LPS and Luminex analysis was performed. A significant decrease in the systemic release of a number of pro-inflammatory cytokines/chemokines was observed in the *DPEP1 -/-* mice as compared to the *DPEP1+/+* mice. Specifically, a striking reduction in the release of MIP-2, IL-1β, IL-17, IL-5, and IL-6 was noted (**Figure 3.29A**), a result consistent with previous studies where IL-1β, MIP-2 and IL-6 were shown to recruit neutrophils during inflammation [166, 329-330]. In addition, treatment with the LSALT peptide resulted in the release of an anti-inflammatory cytokine IL-10 (**Figure 3.29B**). Together, these observations suggest that the LSALT peptide might exert its anti-inflammatory effect by inhibiting the recruitment of neutrophils partly by: i) inhibiting the release of pro-inflammatory mediators through binding to DPEP1 in the presence of LPS and ii) inducing the systemic release of anti-inflammatory cytokine IL-10. In addition to release of inflammatory mediators systemically, we investigated the local secretome within the lung and liver tissue. Briefly, lungs and liver from LPS injected *DPEP1+/+* and *DPEP-/-* mice were harvested and tissue homogenates were assessed by Luminex analysis for the presence of cytokines and

chemokines. A significant reduction in the levels of IL-6, IP-10, and KC in the lungs and liver tissue homogenates in *DPEP1-/-* mice and LSALT treated *DPEP1+/+* mice were observed (**Figure 3.30**). Based on the above observations, it is evident that DPEP1 mediated recruitment of neutrophils to the lungs and liver regulates the release of pro-inflammatory cytokines and chemokines during inflammation.

Since these cytokines were upregulated in the presence of a sublethal dose of LPS (0.5 mg/kg) that might not directly correlate with the severity of LPS-induced endotoxemia, experiments were also performed to assess the release of cytokines and chemokines in the systemic circulation (serum) of mice treated with a lethal dose of LPS (15mg/kg). Luminex analysis revealed the presence of a LPS induced endotoxemia specific pro-inflammatory cytokine signature in the systemic circulation that included the upregulation of IL-1β, IL-5, IL-6, and IFN-γ, that were reduced in the *DPEP1-/-* mice and LSALT-treated *DPEP1+/+* mice (**Figure 3.29C**). Moreover, LPS-induced systemic upregulation of MIP-2 (macrophage inflammatory protein-2), a chemoattractant that has been shown to be involved in the chemotaxis of neutrophils and contributes to acute lung injury, was also reduced in *DPEP1-/-* mice in the presence of LPS and LSALT treated *DPEP1 +/+* mice. Taken together, these observations suggest a previously unknown role of DPEP1 in the regulation of pro-inflammatory cytokines/chemokines in the presence of LPS that may ultimately lead to acute lung injury induced endotoxemia.

Although, activated (LPS) macrophage have been shown to be one of the major producers of IL-1β and IL-6, some studies have also shown that these cytokines can be released/derived from activated neutrophils in response to certain inflammatory/pathological conditions [170, 331]. Based on previous studies and the observations made in this thesis, it is possible that in addition to the resident macrophage (cells that are not directly affected by the LSALT peptide), LPS-

mediated activation of neutrophils may result in the release of IL-1β and IL-6 in the systemic

circulation and hence mediate a second wave of cellular recruitment in the form of monocytes. It

is important to mention that the recruitment of Ly6G/Ly6C (neutrophil/monocytes) cell

populations were both inhibited in the presence of the LSALT peptide or when the *DPEP1-/-* mice

were treated with LPS (**Figure 3.29**). As mentioned, monocytes have been shown to be recruited

by IL-1β and IL-6 dependent manner [166, 332]. Also in addition to the activated neutrophils, the

presence of IL-5, IL-10, IL-17 and IFN-γ in the systemic circulation may indicate the involvement

of T-helper cells (Th1 and Th2) and type 1 and a type 2 immune response. Nevertheless, it was the

inhibition of neutrophil recruitment that was critical for the reduced lung tissue damage and

increased survival of mice and not the levels of the cytokines/chemokines. Also, the reduced

cytokine levels within the lung and liver tissue secretome (**Figure 3.30**) suggest that dampening

the DPEP1 mediated recruitment of neutrophils to the lungs and liver could have a systemic effect.

Future studies would be required to identify the specific immune cell populations that

secrete/release these cytokines/chemokines. To specifically investigate the role of neutrophils,

Ly6G (clone: 1A8) mediated neutrophil depletion strategy could be utilized before the injection of

LPS and/or the LSALT peptide to assess the cytokines/chemokines by Luminex analysis.

A LPS (0.5 mg/kg) 4 hours

B

C LPS (15 mg/kg)
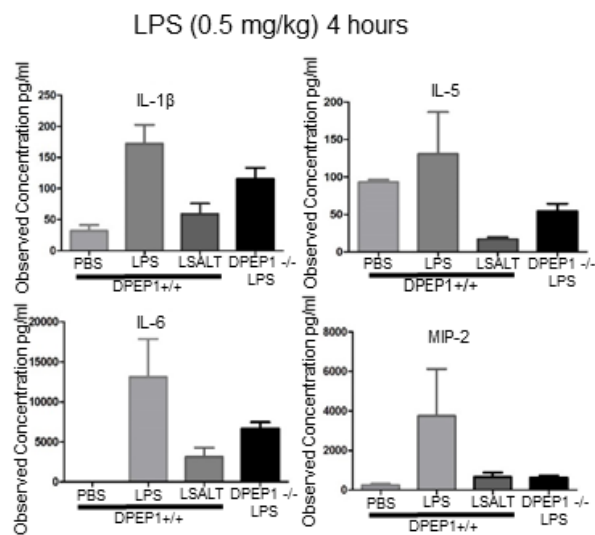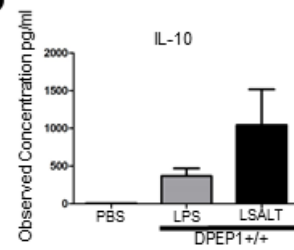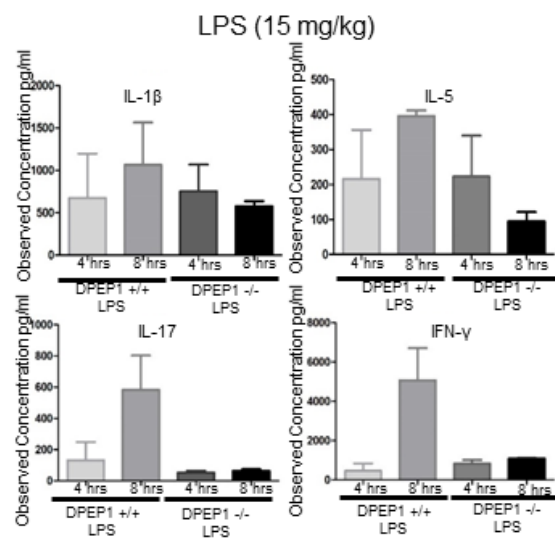
Figure 3.29: Genetic and pharmacological inhibition of DPEP1 regulates the systemic release of inflammatory mediators. A-B. Serum isolated from either *DPEP1 +/+* or *DPEP1 -/-* mice treated with LPS (0.5mg/kg) for four hours and Luminex analysis was performed to assess the release of different inflammatory cytokines and growth factors in the systemic circulation (serum). C. Serum collected from *DPEP1+/+* mice or *DPEP1 -/-* mice treated with 15 mg/kg of LPS and Luminex analysis was performed to assess the presence of cytokines and growth factors.
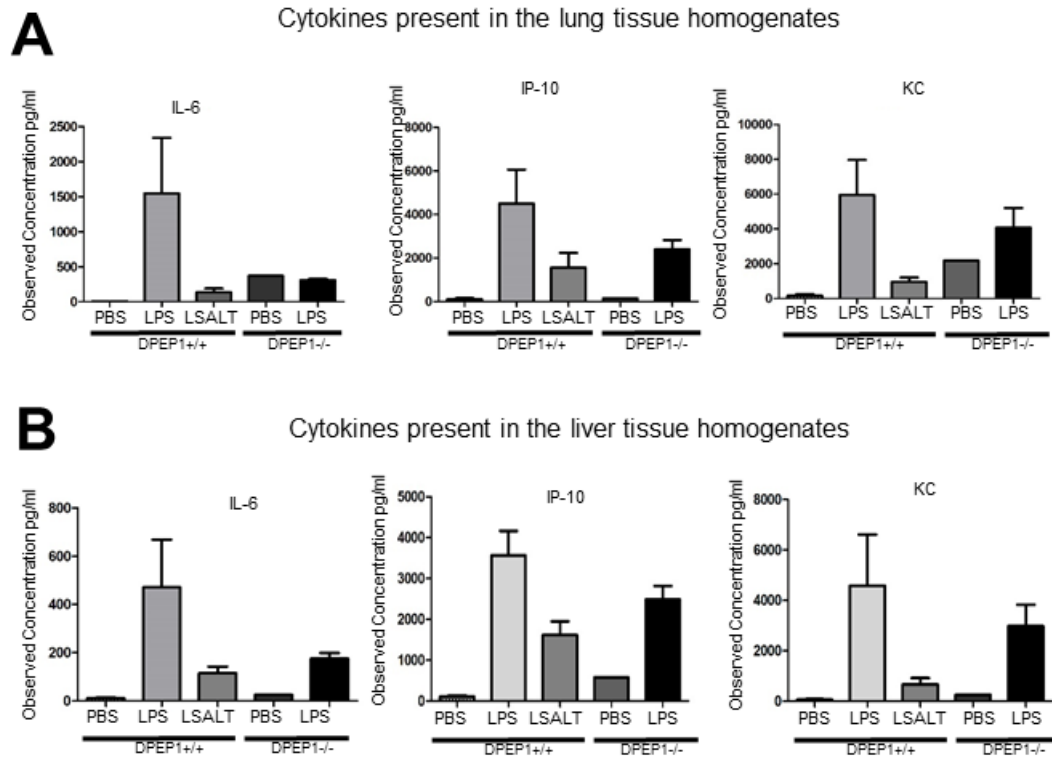
Figure 3.30: Genetic and pharmacological inhibition of DPEP1 regulates the inflammatory microenvironment in the lungs and liver. A-B. Lung and liver tissue homogenates prepared from *DPEP1+/+* and *DPEP1-/-* mice treated with 0.5 mg/kg LPS (four hours following LPS administration) either in the presence or absence of a 1mM dose of LSALT peptide (i.v.) were assessed for the presence of inflammatory mediators by Luminex analysis.

3.16 Reduced melanoma-lung metastasis in the lungs of *DPEP1 -/-* mice.

Since LSALT inhibited cancer metastasis to the lungs and liver and based on the data that DPEP1 mediates the recruitment of neutrophils to the lungs and liver in inflammation, the functional role of DPEP1 in melanoma-lung metastasis was investigated *in vivo*. To address this, a syngeneic melanoma-lung metastasis model was used *in vivo*. B16-F10 murine melanoma cells were injected in eight to ten week old *DPEP1 -/-* mice and *DPEP1 +/-* mice intravenously via the tail vein. Quantification from paraffin embedded lung sections stained with hematoxylin and eosin revealed a reduction in the tumor burden in *DPEP1-/-* mice compared to the *DPEP1 +/-* mice (**Figure 3.31**). This preliminary observation suggests a possible role for DPEP1 in melanoma lung metastasis *in vivo*. Although, these experiments will need to be repeated and evaluated in other metastatic models to conclusively establish a role for DPEP1 in lung and liver metastasis, this initial observation hints at a putative therapeutic role for the targeting of DPEP1 in organ-selective cancer metastasis to the lungs and liver.
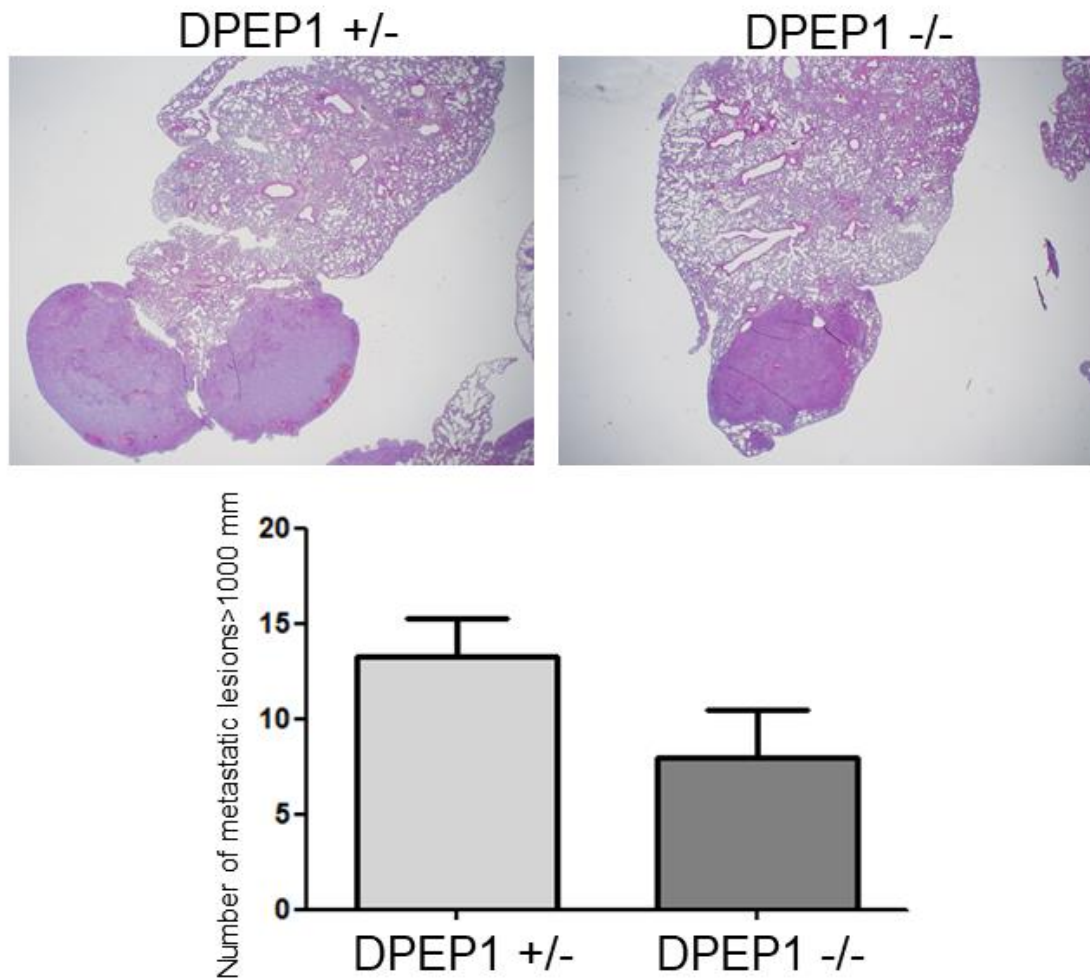
Figure 3.31: Reduced melanoma lung metastasis in *DPEP1 -/-* mice. A-B. Lungs harvested from *DPEP1+/-* and *DPEP1-/-* mice three weeks after the injection of B16-F10 murine melanoma cells were assessed by immunohistochemistry (hematoxylin and eosin) to evaluate tumor burden. Sections from three non-sequential series of lung tissues were analyzed for tumor burden and quantified. Shown here is an example of metastatic tumor lesions in the lungs of *DPEP1+/-* mice (two metastatic lesions >1000 mm are shown in one lobe of the lungs) and *DPEP1-/-* mice (one metastatic lesion >1000 mm is shown in one lobe of the lungs). Scale bar: 100 μm. (Tail vein injections were performed by Dr. Xueqing Lun).

Chapter Four: Discussion and Future Directions

4.1 DPEP1 is an organ-selective adhesion molecule for the recruitment of neutrophils to the lungs and liver during inflammation.

The overall goal of this thesis was to identify novel cell adhesion molecules that mediate organ-selective recruitment of neutrophils and metastatic cancer cells to the lungs and liver. The initial impetus for this study originated from the observation that recruitment of neutrophils to the inflamed hepatic and pulmonary vasculatures appeared independent of classical adhesion molecules such as the selectins and integrins based on the use of knock-out animals and function blocking antibodies. During the course of this thesis CD44-HA interaction was identified as the first non-canonical adhesive mechanism for neutrophils in the inflamed hepatic sinusoids [3]. These primary observations formed the initial foundation of this thesis project as we hypothesized that *'specific molecules expressed on the lungs and liver endothelium mediate the recruitment of neutrophils to the lungs and liver in an organ-selective manner'*.

Adopting the principles originally established by Errki Ruoslahti and colleagues, *in vivo* phage display was used to identify lung and liver 'specific' neutrophil adhesion receptors. This functional screen was unique as intravital spinning disk confocal microscopy combined with *in vivo* phage display was used to screen for lung and liver specific peptides displayed on phage that home to lungs and liver and functionally inhibit the recruitment of neutrophils to these organs in inflammation. A single phage and its corresponding displayed peptide called LSALT, inhibited neutrophil adhesion to the lungs and liver in response to LPS (**Figure 3.1A, 3.2 and 3.4**). This inhibition was found to be independent of CD44 as further inhibition in neutrophil adhesion in the LSALT peptide treated *CD44-/-* mice was observed that indicated the presence of a second adhesion molecule responsible for neutrophil recruitment within the sinusoidal endothelium of the liver (**Figure 3.3**). As the classical adhesion receptors to date have been shown to have minimal

involvement in neutrophil recruitment to the inflamed lungs and liver, these observations were extremely interesting based on the fact that it revealed i) a homing peptide could functionally block neutrophil recruitment within the inflamed pulmonary capillaries and hepatic sinusoids and ii) suggested the existence of an unidentified mechanism of adhesion.

Based on the ability of the LSALT peptide to functionally inhibit neutrophil recruitment to the lungs and liver, we focused on identifying the 'endothelial receptor' of this peptide. Using a series of biochemical, genetic *in vitro* and *in vivo* approaches 'DPEP1' was identified as the functional target for the LSALT peptide (**Figure 3.9 and 3.10**). In addition to the murine and racine DPEP1, binding of the LSALT peptide to the human DPEP1 protein support the human translational capacity of this unique lung and liver homing peptide (LSALT) and demonstrates the evolutionary conservation of the DPEP1 protein across different species. Importantly, this binding was specific to DPEP1 and not to other family members (DPEP2 and DPEP3), suggesting specificity for the LSALT peptide to DPEP1.

As LSALT binds specifically to DPEP1 and since DPEP1 is a GPI-anchored cell surface ectopeptidase, identifying the putative binding site of the LSALT peptide in the extracellular domain of DPEP1 would provide essential insights into the biochemistry of this novel interaction. Important to mention that using the LSALT peptide as a substrate for combinatorial phage display (a strategy we call reverse bio-panning), Dr. Jennifer Rahn has identified unique peptides that each harbor an 'IPK' motif. This approach was based on a modified strategy used to identify the RGD motif for integrin binding [333-334]. This tripeptide IPK motif was found to be present adjacent to the N-terminal extracellular domain (exon 3) of DPEP1 and is conserved from mouse to humans and was absent in DPEP2 and DPEP3. This observation 'may' indicate IPK as the potential binding

Figure 4.1 Schematic representation of the 'IPK' (potential LSALT binding site on DPEP1) motif in the extracellular domain (Exon 3). This figure was contributed by Dr. Bo Young Ahn.

site for the LSALT peptide in the extracellular domain of DPEP1. Thus, *in vitro* binding studies using a fluorescent IPK peptide or mass spectrometry on biotin-LSALT treated DPEP1 immunoprecipitates will uncover the potential of the IPK motif as the binding site for the LSALT peptide to DPEP1. In an alternative gain of function approach, this motif can be added to other family members (DPEP2 and DPEP3) that do not harbor the motif and are devoid of any peptide binding.

Through a series of *in vitro* static adhesion assays this study has demonstrated that human neutrophils bind directly to DPEP1 expressing COS1 cell monolayers, an observation that supports DPEP1 as a physical adhesion receptor for human neutrophils (**Figure 3.13**). This DPEP1 mediated binding of human neutrophils to COS1 cell monolayers were significantly inhibited in the presence of the LSALT peptide and thus mirrored our *in vivo* observations. These results identified a novel role of DPEP1 as a putative adhesion receptor for neutrophils. However, using static *in vitro* adhesion assays in the absence of shear stress does not mimic the more complex *in vivo* scenario. Thus, *in vitro* adhesion assays in the presence of shear flow would provide a more ideal *in vitro* cell based system to assess the adhesion function of DPEP1. It is important to mention that Cinamon et al. showed an important role of shear stress in the transendothelial migration of leukocytes [335]. Also, to determine the ability of human neutrophils to adhere directly on recombinant DPEP1 coated polystyrene plates will provide direct insight into the role of DPEP1 as a physical adhesion receptor.

As discussed previously in addition to their adhesive functions, several cell surface ectoenzymes have been shown to regulate leukocyte recruitment through a function that requires their enzymatic activity [116]. For example, the enzymatic functions of VAP-1, CD73, CD26 and

CD10 have been implicated in the regulation of lymphocytes and leukocytes in response to an inflammatory response [122, 336]. However, in contrast to the role of these ectoenzymes in recruitment, we found that the adhesion function of DPEP1 was independent of its catalytic activity as a catalytically inert DPEP1 mutant or pharmacological inhibitors of DPEP1 had no effect on the binding of human neutrophils on DPEP1 expressing COS1 cells (*in vitro*) and *in vivo* (**Figure 3.16, and 3.18**). These observations further support the role of DPEP1 as a physical adhesion receptor functioning independent of its enzymatic activity. To further demonstrate that the catalytic activity of DPEP1 is not required in the recruitment of neutrophils, a *DPEP1-/-* mouse devoid of enzyme activity using the specific mutation we established *in vitro* (E141D) could be generated. Serendipitously, one of our CRISP/Cas-9 generated *DPEP1-/-* mice has an in-frame 2 amino acid deletion (6 base pair deletion) which appears to lack the catalytic activity and could be used for this purpose (**Figure 3.22**). We are in a process of characterizing these knockout mice.

One issue that remains unresolved is how LPS modulates the ability of neutrophils to bind to an inflamed endothelium in a DPEP1 dependent manner, since we have not observed any alteration in DPEP1 expression and activity in response to LPS (**Figure 3.20**). However, it is important to mention that these observations are primarily based on using a single sublethal dose of LPS (0.5 mg/kg) at a specific time point (four hours). Also, *in vitro* binding studies using DPEP1 expressing COS1 cells suggested no requirement of LPS activation for the binding of the LSALT peptide. These results may also indicate a number of possibilities by which LPS may regulate DPEP1 biology on the endothelium of lungs and liver. As discussed briefly in the results section, these may include: i) structural and conformational changes in DPEP1 to provide an increase in binding availability, ii) enhanced affinity and/or avidity of DPEP1 for neutrophils (similar to integrins) or iii) changes in post-translational modifications (such as phosphorylation,

glycosylation) of DPEP1. Thus, further studies will be necessary to address the specific role of LPS in DPEP1 biology. Consistent with the role of post-translational regulation in adhesion, Yipp et al, showed that ectodomain phosphorylation of a glycoprotein adhesion molecule called CD36 expressed on human dermal microvascular endothelial cells was essential for the adhesion of plasmodium infected erythrocytes [337]. Analogous to CD36, DPEP1 is also a glycoprotein adhesion receptor, it would be interesting to address if a similar mechanisms exists upon LPS induced DPEP1 mediated adhesion and recruitment of neutrophils to the lungs and liver. Glycosylation of classical adhesion molecules such as integrins has been shown to play a crucial role in leukocyte adhesion [338-339]. Moreover, similar to integrins and majority of the leukocyte adhesion receptors identified thus far, DPEP1 is also a glycoprotein and based on our experimental evidence that DPEP1 is highly glycosylated in transiently transfected COS1 cells (appendix), it would be important to assess the requirement for glycosylation in LPS induced DPEP1 mediated adhesion of neutrophils. Site directed mutagenesis could be performed at the N-glycosylation sites of DPEP1 (Asn57, Asn279, Asn332, Asn358) and these mutant constructs could be expressed in COS1 cells *in vitro* to assess adhesion by static binding assays in the presence or absence of LPS. Alternatively, N-glycosidase enzymes such as endo-H and PNGase or chemical inhibitors such as tunicamycin could be used.

The compelling evidence that suggest DPEP1 as the receptor for the LSALT peptide and as an adhesion molecule for the neutrophil recruitment *in vitro*, was supported by the generation of a CRISPR/Cas-9-DPEP1 knockout mouse to validate the functional role of DPEP1 in neutrophil recruitment *in vivo*. Extensive characterization (immunohistochemistry, DPEP1 enzyme activity assay) of *DPEP1-/-* mice demonstrated a successful knockdown of the DPEP1 gene in the kidney, lungs and liver of *DPEP1-/-* mice (**Figure 3.26**). Myeloperoxidase activity assays,

immunohistological analysis and intravital imaging of the lungs of *DPEP1-/-* mice confirmed a role for DPEP1 in the recruitment of neutrophils to the lungs of *DPEP1-/-* mice, further validating DPEP1 as a major adhesion receptor within the inflamed vascular beds of the lungs (**Figure 3.24 and 3.25**). DPEP1 represents the first neutrophil adhesion receptor identified within the inflamed lung vasculature. As the absence of DPEP1 did not result in a complete inhibition in the recruitment of neutrophils to the inflamed pulmonary vasculatures, these observations also indicate the presence of other adhesion molecule(s) within the inflamed vascular beds of the lungs. The generation of the *DPEP1-/-* knockout mice would provide an available tool to use in a similar phage homing strategy to identify the additional adhesion molecules that mediate neutrophil recruitment to the lungs. In this approach, phage that home specifically to the lungs of neutrophil depleted *DPEP1-/-* mice could be isolated similar to our original *in vivo* selection. These specific lung homing (DPEP1 independent) phage can then be screened on the basis of their ability to inhibit neutrophil recruitment to the lungs by either myeloperoxidase activity assays or by using intravital microscopy.

Similar to our observations in the pulmonary vascular beds of the lungs, a significant impairment in neutrophil recruitment was also observed within the sinusoidal endothelium of the liver in *DPEP1-/-* mice (**Figure 3.26**). In addition to adhesion, neutrophils were compromised for crawling within the liver sinusoids of *DPEP1-/-* mice. These results were consistent with the previous observations where a significant reduction in the crawling of neutrophils in LSALT treated *DPEP1+/+* mice was observed. As discussed previously, as the molecular basis of neutrophil crawling under shear is not well understood, LSALT mediated inhibition in neutrophils crawling in *DPEP1+/+* mice and LPS treated *DPEP1-/-* mice, suggests a role in crawling for this

cell surface peptidase. DPEP1 mediated neutrophil crawling however differs from β2 integrin dependent mechanisms where LFA-1 and Mac-1 mediate transluminal crawling of neutrophils [33]. Future studies in this regard will be necessary to understand the mechanisms underlying DPEP1 mediated neutrophil crawling under shear in response to LPS. The inability of the LSALT peptide to further abrogate the recruitment of neutrophils to the lungs and liver of *DPEP1-/-* mice confirmed DPEP1 as the sole target for the LSALT peptide. These results further support our initial hypothesis that a common adhesion molecule is responsible for the recruitment of neutrophils to the inflamed pulmonary and hepatic vascular beds. Based on the study by McDonald et al. that CD44-HA interaction is a predominant mechanism of neutrophil adhesion within the inflamed liver sinusoids, neutrophil recruitment was assessed in *DPEP1-/-* mice in the presence of a CD44 monoclonal antibody. Further reduction was observed as neutrophil recruitment was inhibited to background levels in the hepatic sinusoids of *DPEP1-/-* mice in the presence of CD44 monoclonal antibody (**Figure 3.27**). Together, these observations suggested that CD44-HA and DPEP1 represent the two predominant neutrophil adhesion mechanisms within the liver sinusoids. Based on the fact that no known adhesion receptors are involved in the recruitment of neutrophils to the inflamed pulmonary vasculatures, identification of DPEP1 as a mediator of neutrophil recruitment to the lungs is the first documented observation of a non-canonical neutrophil adhesion receptor in the lungs. Moreover, it is important to mention that apart from CD44-HA (within the liver sinusoids) no known adhesion molecules are involved in neutrophil recruitment to the liver, thus the identification of DPEP1 as a second adhesion receptor for organ-selective neutrophil recruitment to the inflamed hepatic vasculatures will provide insight into the molecular complexities of neutrophil recruitment in these capillary beds.

In contrast to the lungs and liver, neutrophil recruitment appeared not to be compromised in other vascular beds such as the cremaster muscle (where classical adhesion molecules mediate the recruitment of neutrophils) in *DPEP1-/-* mice or when *DPEP1+/+* mice were treated with the LSALT peptide (initial observations by Dr. Bjoern Petri), supporting DPEP1 as an organ-selective adhesion molecule for the recruitment of neutrophils to the lungs and liver. Additional investigation in this regard would be essential to define the role of DPEP1 in other vascular beds such as the mesentery or skin where the classical leukocyte recruitment cascade was originally described, to further establish DPEP1 as a lung and liver specific adhesion molecule. Further the understanding of the signaling events involved in DPEP1-mediated adhesion and crawling of neutrophils on the lung and liver endothelium would be essential to identify the molecular mechanisms underlying DPEP1 mediated neutrophil recruitment. Also, apart from adhesion and crawling, intravital imaging studies in *DPEP1-/-* mice *in vivo* may reveal the specific involvement of DPEP1 in other steps (such as transmigration) in the neutrophil adhesion cascade. Since some studies have indicated stimulus dependent activation and involvement of different adhesion molecules in neutrophil recruitment, assessing the role of DPEP1 in neutrophil recruitment in response to other inflammatory stimuli such as TNFα, IL-1β. LTB4 may provide insight into the role of DPEP1 within the pulmonary and hepatic vascular beds in other inflammatory conditions.

4.2 DPEP1 is an organ-selective adhesion molecule for the metastatic cancer cells to the lungs and liver.

Some studies have indicated similar adhesion/extravasation events associated with the recruitment process of leukocytes and metastatic cancer cells and proposed the concept of sharing common adhesion molecules (reviewed in [272, 340]). In addition to the involvement of classical leukocyte adhesion receptors (such as the selectins and integrins), some of these studies have also

suggested a role for cell surface enzymes (VAP-1, CD73) in the dissemination and progression of cancer metastasis [283, 341-342]. As mentioned, from the original observations of Stephen Paget [237], a significant number of studies combined with clinical observations have redefined the organ-selective nature of metastasis and have identified lungs and liver as the two primary sites for metastatic colonization (reviewed in [84, 343]). The question that why lungs and liver are the two major sites for metastatic colonization remains to be completely understood. According to Paget's seed and soil hypothesis, these organs may consist of 'specific factors' that provide a congenial microenvironment for the growth of secondary tumors. In addition, liver and lungs may express unique vascular signatures that support the growth of metastatic cancer cells in these vascular beds (similar to how leukocytes get recruited via the non-canonical adhesion molecules to these organs during inflammation). Based on these data and the observation that the LSALT peptide inhibited neutrophil recruitment to the lungs and liver by binding to DPEP1, the functional role of the LSALT peptide in the dissemination of metastatic cancer cells was assessed and similar to neutrophil recruitment, LSALT peptide was able to significantly abrogate metastasis of human and murine melanoma cells to the lungs of mice in pre-clinical human xenograft and immunocompetent murine models (**Figure 3.5**), an observation that was not limited to melanoma-lung metastasis as a significant reduction in breast cancer-liver metastasis in a second immunocompetent murine model (collaboration with Dr. Peter Siegel's laboratory at McGill University) was also observed (Tabariès and Siegel, unpublished). In addition to these *in vivo* observations, *in vitro* static adhesion assays using human melanoma cells (70W) demonstrated the adhesion function of the DPEP1 protein and the blocking activity of the LSALT peptide. Collectively, these observations in addition to neutrophil recruitment, identified a functional role of the LSALT peptide in the dissemination of metastatic cancer cells to the lungs and liver and

support the idea that these organs use/share a common adhesion molecule (DPEP1) for the organ-specific endothelial binding of neutrophils and metastatic cancer cells. Since the metastatic model used allowed the assessment (injection of metastatic melanoma cells intravenously into the bloodstream for lung colonization) of the extravasation step in the metastatic cascade, visualization of this specific event by intravital microscopy would provide more insight with regards to the exact step involved in LSALT peptide mediated inhibition and DPEP1 mediated adhesion /extravasation of cancer cells to the lungs and liver. Also, the *in vitro* observations may have suggested that the enzyme activity of DPEP1 may not be required for the adhesion/binding of the 70W melanoma cells (similar to the human neutrophils), performing *in vivo* experiments using Cilastatin would strengthen this claim with regards to organ-selective metastasis to the lungs and liver. To address this, immunocompromised (SCID) or immunocompetent (C57BL/6) mice could be injected with Cilastatin in the presence of human (70W) or murine (B16) melanoma cells and melanoma-lung metastatic tumor burden could be assessed by bioluminescence imaging or immunohistochemistry. Although, phage display has been used extensively to understand the unique vascular addresses, limited number of studies were designed to identify adhesion molecules that mediate organ-selective recruitment of metastatic cancer cells. As mentioned using phage display, metadherin (expressed on breast cancer cells) was identified and demonstrated as a crucial adhesion molecule for the breast cancer metastasis to the lungs [91]. Thus in addition to metadherin, identification of DPEP1 as an adhesion molecule for lung and liver metastasis will provide insights into the molecular mechanisms of how metastatic melanoma and breast cancer cells bind to the capillary beds of the lungs and liver. Furthermore, it may also be interesting to determine if metadherin expressing metastatic cancer cells binds to DPEP1 on the endothelium of lungs to promote

183

metastatic disease. *In vitro* static adhesion assays using metadherin expressing cancer cells and *in vivo* experiments using *DPEP1-/-* mice could be used to address this question.

The initial observation of reduced melanoma lung metastatic tumor burden in *DPEP1-/-* mice (**Figure 3.31**) also indicate that targeting this GPI-anchored adhesion molecule (by pharmacological peptides or genetically) may also provide therapeutic and survival benefits in patients with metastasis to the lungs and liver. These observations are however preliminary and thus further experiments need to be performed with a large number of cohorts to confirm a role of DPEP1 in organ-selective metastatic disease to the lungs. In addition to the melanoma-lung metastasis, it would be essential to determine the involvement of DPEP1 in other cancers (such as osteosarcoma, colorectal, breast) that also have the propensity to colonize and metastasize to the lungs. Since LSALT abrogated breast cancer metastasis to the liver and DPEP1 plays a crucial functional role in neutrophil recruitment in the liver, it would be important to investigate the role of DPEP1 in organ-selective metastasis to the liver. To address this question, C57BL/6 specific B16-F10 melanoma liver metastasis, E0771 breast liver metastasis and MC38-CRC liver metastasis immunocompetent murine models could be developed and assessed. Understanding the role of DPEP1 in the context of other metastatic tumors would be important in order to confirm DPEP1 as a lung and liver specific molecule for metastatic cancer cells. For example, using a human (70W) or murine (B16) melanoma model, the role of DPEP1 could be investigated in brain metastasis. Interestingly, during the course of this thesis using *in vivo* selection, we have developed a 70W human melanoma cell line that has a higher propensity to metastasize to the brain. As this is a human xenograft *in vivo* model, LSALT peptide could be intravenously injected into the SCID (*DPEP1+/+*) mice in the presence of brain-metastatic 70W melanoma cells and tumor burden could be assessed by bioluminescence imaging or histology. In an alternative approach, *DPEP1-*

/- (C57BL/6) mice could be injected with B16-F10 cells to assess the role of DPEP1 in melanoma-brain metastasis. To further investigate the specificity for DPEP1 to mediate liver and lung metastasis, other cancers such as prostate cancer that has a propensity to go to the bone could be studied.

Over the past two decades emerging evidence has suggested the functional involvement of the innate immune system in cancer dissemination and progression [344]. Apart from the involvement of different immune sentinels, the role of neutrophils in the initiation, establishment and progression of cancer is being evaluated [345]. As mentioned, although some studies may have indicated the potential anti-tumor properties of neutrophils, the majority of investigations thus far have supported a pro-tumor function of neutrophils in cancer progression [187-188, 190-191, 346-349]. Studies presented in this thesis using a human melanoma murine xenograft model suggest that Gr-1+ cells/leukocytes may play a protective role against melanoma-lung metastasis as a significant increase in the metastatic tumor burden in the lungs of mice was observed when Gr-1+ cells were depleted (**Figure 3.6**). This observation opposed results published to date with regards to the role of neutrophils in cancer metastasis. In fact, using a different lung metastasis murine model (osteosarcoma) within our laboratory, a decrease in lung metastasis was observed when Gr-1+ cells were depleted (Wierenga and Senger, unpublished). Although, these studies may suggest a differential role of Gr-1+ cells in lung metastasis, using a more specific antibody such as Ly6G (clone: 1A8) to deplete circulating neutrophils would specifically assess the role of neutrophils in lung metastasis. Intravital imaging of the lungs in the presence of melanoma cells may also provide further evidence if a direct interaction between the cancer cells and other innate immune sentinels is required for the seeding or initial establishment of melanoma lung metastasis. Alternatively, the observation that neutrophils and 70W cancer cells both use DPEP1, the increase in metastasis may

result from the loss of competition for the receptor. Thus, further investigation is warranted to delineate the involvement of neutrophils in organ-selective metastatic disease. Importantly irrespective of the presence of circulating leukocytes in preclinical murine models, the LSALT peptide maintained significant reduction in melanoma-lung metastasis suggesting a broad-spectrum biological activity of the LSALT peptide as a potential therapeutic in organ-selective metastatic disease. Although, the mice in the LSALT peptide treated groups were eventually sacrificed based on certain experimental endpoint criterion (such as loss of body weight, having any difficulty ambulating, feeding or grooming or becoming scruffy), injection of a single dose of the LSALT peptide dramatically increased the overall survival of mice irrespective of the presence of circulating leukocytes (**Figure 3.6 D-E**). Based on the observations that the LSALT peptide inhibited the adhesion of 70W melanoma cells *in vitro*, one possible underlying mechanism to explain this observation can be attributed to the fact that the treatment of the LSALT peptide may inhibit the adhesion of metastatic cancer cells and thus disrupt the initial seeding of these cells to the lungs. Alternatively, it could also be possible that, the treatment of the LSALT peptide could result in a dormant metastatic cancer cell population in the lungs that eventually lead to the generation of a slow growing cancer cell population. These possibilities will need to be addressed experimentally in future studies to understand the exact mechanisms underlying the increased overall survival in the presence of the LSALT peptide.

Based on the functional observations that identified and demonstrated DPEP1 as the receptor for the LSALT peptide and an adhesion receptor for the neutrophils and metastatic cancer cells to the lungs and liver, it will be important to identify the cognate DPEP1 ligand/ligands on neutrophils and/or metastatic cancer cells. As mentioned, based on the reverse bio-panning of the LSALT peptide, we hypothesize that the IPK motif (in the extracellular domain of DPEP1) could

be involved in the binding of the LSALT peptide. Thus, the IPK peptide could be used as a 'bait' to identify the ligand of DPEP1. Experiments in this regard could be performed to address if the IPK peptide motif is important for the binding of the LSALT peptide (*in vitro* competitive inhibition assays) and human neutrophils/metastatic cancer cells. MS/MS analysis of IPK-biotin treated neutrophil and/or metastatic cancer cell precipitates could then be used to identify the cognate ligand of DPEP1.

4.3 DPEP1 is a potential therapeutic target in systemic inflammatory diseases and organ-selective metastatic disease.

In spite of intensive investigation, sepsis remains one of the most common causes of admission and readmission to intensive care units and contributes to between 300,000 to 500,000 deaths annually in North America [350-354]. Pulmonary dysfunction, a frequent occurrence in patients with sepsis (especially when combined with Acute Respiratory Distress Syndrome or ARDS) is associated with high mortality rates [355-356]. A common problem associated with these disorders is the excessive recruitment of neutrophils that culminates to multi-organ failure [357]. Molecular mechanisms underlying this deregulated cellular recruitment still remains to be understood. Thus, based on the functional role of DPEP1 in neutrophil recruitment to the lungs and liver in LPS-induced inflammation, we assessed the involvement of DPEP1 in an LPS-induced model of endotoxemia. The ability of the LSALT peptide treated *DPEP1+/+* mice or LPS-treated *DPEP1-/-* mice to withstand a lethal dose of LPS (15mg/kg) suggests that targeting DPEP1 could provide therapeutic benefit in endotoxin induced systemic inflammatory diseases (**Figure 3.28**). In addition to the increase survival in *DPEP1-/-* mice (from 0% to 83%), it is important to mention that although the majority of *DPEP1-/-* mice showed initial clinical symptoms associated with severe sepsis similar to *DPEP1+/+* mice (**Appendix table 1A**), there was a marked reduction in

clinical symptoms in *DPEP1-/-* mice after 48 hours indicating a therapeutic role of DPEP1 inhibition in the recovery of these mice from severe sepsis that may provide direct clinical impact. Similar to the LPS treated (15mg/kg) *DPEP1-/-* mice, a significant increase in the survival of *DPEP1+/+* mice in the presence of the LSALT peptide also provides support that targeting DPEP1 could be a therapeutic option in endotoxemia induced systemic inflammatory diseases. A single dose of the LSALT peptide was able to increase the overall survival of *DPEP1+/+* mice from 0% to 60% where the majority of the mice showed sepsis specific clinical features 24 hours after LSALT administration, a result that indicates that the treatment of mice with multiple doses of the LSALT peptide could enhance its therapeutic effect further. Indeed, treatment of *DPEP1+/+* mice with one additional dose of LSALT peptide at 18 hours further increased overall survival in *DPEP1+/+* mice from 0% to 83%, similar to the LPS treated *DPEP1-/-* mice. More importantly, clinical symptoms associated with LPS induced endotoxemia were not observed in these mice (**Figure 3.28**). These results were consistent with the observation that delivery of a single dose of the LSALT peptide prior to the arrival of cancer cells in the lung could increase overall survival in mice in a human melanoma-lung metastatic model. Previously peptides selected *in vivo* using phage display have been shown to have therapeutic potential either in a combination with another chemotherapeutic or as imaging agents in diseases such as cancer [358], in this thesis it has been demonstrated that a peptide identified using *in vivo* phage display can inhibit excessive recruitment of neutrophils to the lungs and liver in inflammation and increased overall survival. Further, treatment with the LSALT peptide was shown to inhibit neutrophil aggregation (**Appendix figure 2**) and since clustering of neutrophils within the microcappillaries of the lungs and liver is one of the critical clinical features in systemic inflammatory diseases [359-360] this observation provides additional support for the protective nature of the LSALT peptide.

A major cause underlying endotoxemia induced acute lung injury mediated mortality from ARDS is the influx of excessive neutrophils that result in the destruction of the endothelial barrier in part through the release of pro-inflammatory cytokines [361-362]. We observed a significant change in the cellularity and inflammation/acute lung injury associated pathology in the lungs of *DPEP1-/-* mice compared to the *DPEP1+/+* mice 8-12 hours after LPS (15mg/kg) treatment (**Figure 3.28**). In addition, a marked reduction in the release of pro-inflammatory cytokines in the LPS treated *DPEP1-/-* mice and *DPEP1+/+* mice treated with the LSALT peptide was seen (**Figure 3.29**). Since endotoxin-induced systemic release of pro-inflammatory mediators facilitate a cytokine storm in endotoxin induced systemic inflammation [363-364], these data suggest a possible underlying mechanism in the recovery of these mice. Collectively, these observations support DPEP1 as a potential therapeutic target in acute lung injury, ARDS, however, based on the limitations of using LPS as a model of acute lung injury/ARDS it would be important to validate these findings in other murine models of ARDS/acute lung injury (ALI). For example, Oleic acid, a fatty acid that targets the capillary endothelium of the lungs could be used [365]. Intravenous injections of oleic acid is associated with haemorrhage, hyaline membrane formation, and inflammatory cellular infiltration to the lungs [366-367]. Thus, administration of oleic acid in *DPEP1-/-* mice or LSALT peptide treated *DPEP1+/+* mice could be assessed. In addition, understanding the therapeutic role of DPEP1 in other murine models of systemic inflammation such as ischemia reperfusion or cecal ligation and puncture (CLP) would further strengthen these observations. As mentioned, in collaboration with Dr. Muruve at the University of Calgary treatment of mice with the LSALT peptide increased the overall survival in a murine model of cecal ligation and puncture (Lau and Muruve, unpublished).

Based on these observations and since lung dysfunction mediated mortality is one of the major problems associated in patients with endotoxmeia and ARDS, targeting DPEP1 may provide important insights for the development of new therapeutic strategies for other lung inflammatory diseases such as asthma, COPD where chronic inflammation plays a critical role in the pathogenesis. In addition to the lungs, as LPS mediated endotoxemia may induce liver damage [368-369] and a functional role of DPEP1 in neutrophil recruitment to the liver sinusoids has been shown, thus it will be pertinent to assess the effects on liver function and pathology in LPS-treated *DPEP1-/-* mice and LSALT treated *DPEP1+/+* mice. Immunohistochemical assessment of the liver as well determining the levels of liver damage specific enzymes such as aspartate aminotransferase and alanine aminotransferase could be used to address this question.

As this study utilized a bacterial lipopolysaccharide model to induce neutrophil adhesion during inflammation and endotoxemia to investigate the role of the LSALT peptide and DPEP1, limitations of this strategy as an *in vivo* model of sepsis must be considered. A number of studies support the use of this model based on some pathological resemblance with human sepsis, however a growing body of evidence suggests several limitations [370-371] with a major drawback being the early and rapid onset of the disease and the transient release of proinflammatory mediators which is more intense in this context as compared to human sepsis [370]. For example, the quick onset of sepsis related clinical characteristics resulting from a bolus injection of high-dose LPS contributes to a rapid progression of the disease that are characterized by hypothermia, decrease in motor activities and respiratory quality, piloerection and production and release of inflammatory mediators and acute lung injury. In contrast to LPS-induced endotoxemia in mice, the onset of these critical features progress rather gradually in human sepsis patients [371]. Although, some of the pathophysiological clinical characteristics of LPS-induced endotoxemia in mice do represent

similar features associated with acute lung injury and acute respiratory distress syndrome [372-373]. Thus, the observations presented in this thesis may provide insight into our understanding of the LSALT peptide and DPEP1 in LPS-induced endotoxemia mediated acute respiratory distress syndrome/acute lung injury however it will be important to utilize other polymicrobial murine models that more closely mimic human sepsis (such as CLP). Alternatively, administration of a live bacterial strain/inoculum by intravenous injections could be implemented to increase our understanding of the role of the LSALT peptide and DPEP1 during bacterial sepsis. Administration of the LSALT peptide in the presence of live bacterial strains would assess the potential of the LSALT peptide while the use of the *DPEP1-/-* mice in this model would directly assess the role of DPEP1. Interestingly, using a single bolus injection or continuous infusion of live bacterial strains (*Staphylococcus aureus*, *Pseudomonas aeruginosa*, *Pneumococcus*) has been shown previously to closely mimic human sepsis and produce more clinically relevant results [371].

As DPEP1 was originally isolated from the renal brush borders (and based on its heightened expression in the kidney), it would also be important to assess the role of this adhesion molecule in kidney inflammation, acute kidney injury and dysfunction. Radiographic contrast agents represents one of the most common causes of contrast induce acute kidney injury (CI-AKI) with limited understanding underlying pathogenesis [374-375]. The LSALT peptide has been shown to mediate inhibition in the infiltration of LysMeGFP leukocytes to the inflamed renal vascular beds supporting a role for DPEP1 in kidney inflammation (Lau and Muruve, unpublished). In addition, DPEP1 was found to be associated with the tubular reabsorption of contrast agents in CI-AKI (Lau and Muruve unpublished). Thus, based on the high incidence of morbidity and mortality associated with patients that undergo cardiac surgery induced acute kidney injury, it would be essential to understand the role of DPEP1 in kidney diseases.

In addition to the anti-inflammatory properties, the anti-metastatic functional activities of the LSALT peptide in metastatic murine models suggests the therapeutic potential of this anti-inflammatory peptide that may lead to clinically relevant agents that could be used in organ-selective metastatic disease. Functional reduction in cancer progression using peptides is not without precedence as several studies have previously demonstrated the therapeutic use of homing peptides identified by *in vivo* phage display in the progression of breast and ovarian cancers [358, 376]. Also, based on the fact that neutropenia is one of the critical features associated with majority of the patients with metastatic disease [377-378], LSALT peptide may be very effective clinically as it significantly inhibited metastasis to the lungs and increased overall survival in preclinical murine model in the absence of leukocytes. Although, it may be an open ended question of whether the LSALT peptide can be developed as a therapeutic in the context of organ-selective metastatic disease, based on our observations in murine models, LSALT may function as an effective therapeutic if given in patients after the resection of the primary tumor in a neoadjuvant setting. Based on the inhibitory effects of LSALT peptide we would also hope that multiple dosing of this peptide could enhance the translational potential of this novel anti-inflammatory peptide in organ-selective cancer metastasis. It is important to mention, that a second dose of the LSALT peptide significantly increased overall survival and reduced severe sepsis associated clinical features in the LPS-induced model of lethal endotoxemia and ARDS. In addition, it would be crucial to assess the therapeutic role of the LSALT peptide in primary tumor growth. From a therapeutic point of view, it would be extremely important to determine the pharmacokinetic properties of the LSALT peptide. One of the key pharmacokinetic characteristics would be to assess the half-life/bioavailability of the LSALT peptide in the circulation *in vivo*. Two different strategies could be employed to address this question. First, intravital imaging of the liver and lung with

fluorescently labelled LSALT peptide over time and second, immunohistochemical analysis of the lungs and liver sections from mice after the administration of the fluorescent/biotin labeled LSALT peptide *in vivo*. As albumin was shown to increase the half-life of short lived proteins in the circulation [379] similar strategies could be used to stabilize and extend the half-life of the LSALT peptide *in vivo*. Additionally, to determine other pharmacokinetic properties such as MTD, absorption, toxicity would also be necessary in order to develop and establish the LSALT peptide as a therapeutic.

Primary observations with respect to the role of LSALT and DPEP1 in this study are based on the use of a single human melanoma xenograft and the B16-F10 immunocompetent model. As there are multiple limitations associated with the ability of these models to recapitulate and mimic the human disease in mice [380-381], future studies need to be performed to validate these observations using additional lung and liver metastatic models. One major limitation of using high passage cancer cell lines is that the cells acquire multiple genetic and phenotypic diversities that are distinct from the original parental clones. These include acquiring more genetic mutations, resistant properties, poor tropism, altered invasive potential and infiltrative abilities that eventually lead to a heterogeneous cancer cell population. Since both the human and murine melanoma (B16-F10 and MeWo derived 70W) lung metastatic models used in this study were established at least two decades ago, using alternative cancer cell lines and patient-derived cultures that metastasize to the lungs and liver would be helpful in determining the efficacy of the LSALT peptide and the role of DPEP1 in organ-selective metastasis to the lungs and liver. Patient-derived metastatic tumor cells could be isolated from the primary cultures by their propensity to colonize the lung and liver in mice *in vivo*. In addition, future studies should aim to assess the effects of the LSALT peptide in spontaneous metastatic murine models. Breast cancer cell lines (such as 4T1 and LM2)

can be orthotopically implanted into the mammary fat pad of mice and the effect of the LSALT peptide can be assessed after the resection of the primary tumor (when the tumors reach a size of 400 mm^3). Similarly, E0771 breast or MC38 colorectal liver metastatic murine cancer cells derived from C57BL/6 mice could be assessed for their metastatic potential in *DPEP1-/-* mice. In addition, patient-derived organoid cultures could be used to study the development and pathogenesis of cancer [382-383]. Thus, in addition to the spontaneous and patient derived metastatic models, investigating the functional role of the LSALT peptide and the adhesive function of DPEP1 in patient-derived organoid cultures may provide direct insights into the involvement of this interaction in conditions that may mimic the clinical situation better. Melanoma and/or breast-lung and liver metastatic cells could be isolated from the tumor biopsy and established to assess these questions *in vitro* and *in vivo* (xenografts).

Emerging evidence from recent studies have suggested involvement of the microbiome in neutrophil biology, inflammation and cancer progression [384-386]. Based on the existing role of toll-like receptors in microbiota [387] and the observation that DPEP1 mediates adhesion of neutrophils in the presence of bacterial lipopolysaccharide, it would be interesting to determine the role of the microbiome in DPEP1 mediated neutrophil recruitment in ARDS/acute lung injury. These questions could be addressed employing more than one comprehensive experimental strategies that could include i) antibiotic-mediated depletion of microbiota ii) housing *DPEP1-/-* mice in a more sterile facility such as germ free facility and also iii) housing *DPEP1-/-* mice in a facility that provides more wild microenvironment and is more relevant clinically. Although, no noticeable/visible differences were observed with regards to infection and/or other abnormalities on housing the DPEP1 wild-type and *DPEP1-/-* mice in two different animal facilities (CCCMG and Biohazard level II) at the University of Calgary, determining the gut microbial composition

and their influence in neutrophil recruitment in these mouse colonies in future studies would assist in understanding the involvement of microbiota in DPEP1 mediated recruitment of neutrophils. Alternatively, antibiotic-mediated depletion of microbiota could be utilized to study basal neutrophil recruitment to the lungs and liver of *DPEP1-/-* mice in the presence or absence of LPS. As mentioned, some recent studies have indicated a possible mechanistic role of the microbiome in the cancer progression and dissemination [386]. Thus, in addition to neutrophil recruitment and inflammation it would also be important to assess the possible role (if any) of DPEP1 in the metastasis of melanoma and breast cancer cells to the lungs and liver.

Akin to organ-specific vasculatures, a significant number of studies in the past few years have suggested a diverse structural and functional heterogeneity within the lymphatic vascular system as a contributor to inflammatory disorders and cancer dissemination [388-389]. These studies have suggested that lymphatic vasculatures may also have unique molecular addresses [390]. Based on these organ-specific molecular signatures, and since cells recruited via the lymphatic circulation could drive inflammatory responses and metastatic progression to distant organs, it may be important to identify molecules expressed within the lymphatic vascular beds. Using a similar phage display strategy as described in this thesis could provide a useful tool. Assessing the expression of DPEP1 within the lymphatic vessels may also provide insights into identifying the requirement/involvement of specific circulatory patterns in the progression of organ-selective metastatic disease.

Overall, the key findings of this thesis suggest that i) LSALT peptide isolated by *in vivo* phage display blocks cancer metastasis and neutrophil recruitment to the lungs and liver and ii) DPEP1 the sole target of the LSALT peptide, is a cell surface GPI-anchored glycoprotein,

expressed on the vascular endothelium of lungs and liver and mediates organ-selective recruitment of neutrophils and metastatic cancer cells.

APPENDIX A:
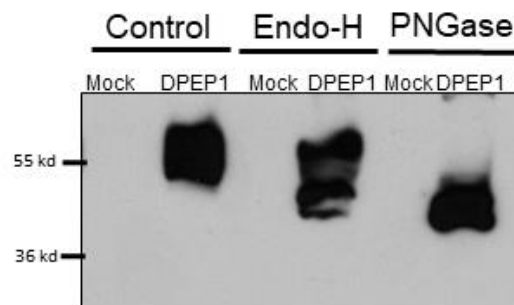
Appendix Figure 1: DPEP1 is glycosylated in transiently transfected COS1 cells. COS1 cells transiently transfected with human DPEP1. Proteins were isolated from transfected cells 48 hours later and treated with glycosidase enzymes: Endo-H and PNGase to assess DPEP1 expression by Western blot analysis.

Neutrophil Aggregates in Hepatic Sinusoids

Neutrophil clusters
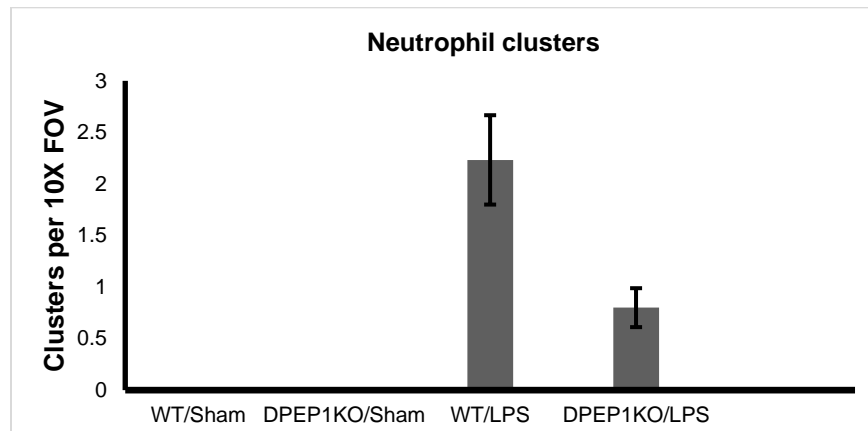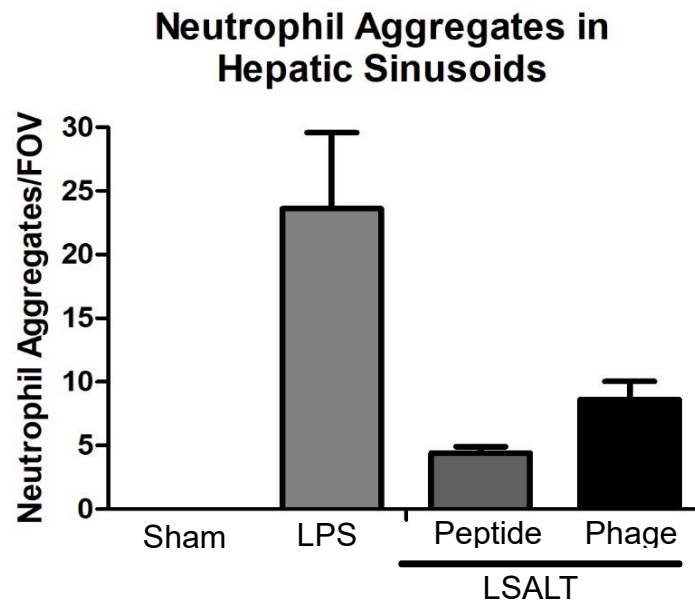
Appendix Figure 2: Inhibition of neutrophil aggregates/clusters in LSALT treated *DPEP1+/+* mice and *DPEP1-/-* mice in the liver (upper panel) and lungs (lower panel). Neutrophil aggregates (four or more neutrophils bound together) were counted in liver sinusoids in the LPS treated mice (upper panel). Neutrophil clusters were counted in the pulmonary vasculatures in the *DPEP1+/+* (WT) and *DPEP1-/-* mice treated with LPS.
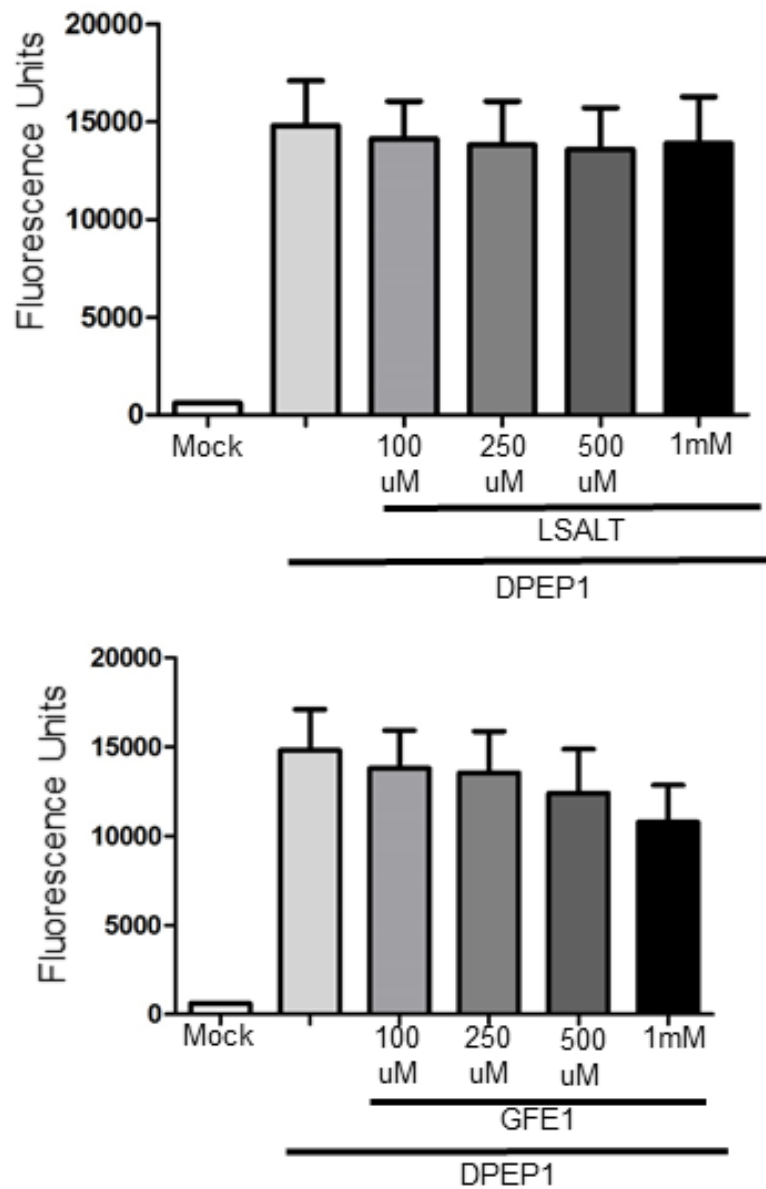
Appendix Figure 3: GFE1 inhibits DPEP1 enzyme activity in a dose dependent manner.

Proteins from DPEP1 transfected COS1 cells were assessed for DPEP1 activity in the presence

of either LSALT or GFE1 peptide.

Table 1(A) Summary of clinical scores from *DPEP1+/+* and *DPEP1-/-* mice treated with 15 mg/kg LPS.

	DPEP1+/+ LPS					*DPEP1-/-* LPS				
Time hours	Mouse 1	Mouse 2	Mouse 3	Mouse 4	Mouse 5	Mouse 1	Mouse 2	Mouse 3	Mouse 4	Mouse 5
12	15	17	11	2	3	15	1	10	7	4
15	20/4	20/4	19/4	1	2	14	1	11	5	4
19				14/4	19/4	17/3	10	15	11	5
20							9	18	15	7
22							5	15	12	3
24							9	15	13	8
26							8	14	12	3
28							3	14	11	4
40							0	10	8	4
44							2	14	9	3
50							1	6	4	1

(A) Table summarizes the clinical scores from *DPEP1+/+* and *DPEP1-/-* mice treated with 15 mg/kg LPS.

Table 1(B) Summary of clinical scores from *DPEP1+/+* and *DPEP1-/-* mice treated with 15 mg/kg LPS in the presence or absence of LSALT.

	DPEP1+/+ LPS							*DPEP1+/+* LPS+LSALT Single dose							*DPEP1+/+* LPS+LSALT Double dose					
Time in hours	Mouse 1	Mouse 2	Mouse 3	Mouse 4	Mouse 5	Mouse 6	Mouse 7	Mouse 1	Mouse 2	Mouse 3	Mouse 4	Mouse 5	Mouse 6	Mouse 7	Mouse 1	Mouse 2	Mouse 3	Mouse 4	Mouse 5	Mouse 6
15	13	6	14/3	15/4	16	20/4	20/4	0	6	5	7	10	2	7	0	1	0	0	0	8
17	17	9			14			2	6	2	2	12	3	5	0	2	0	1	0	10
19	15	4			20/3			1	7	2	3	9	3	4	0	1	0	1	0	10
22	23	12						3	8	1	8	5	3	10	2	1	2	2	3	12
24		12						2	6	4	4	5	3	11	2	3	0	0	2	10

26		9					2	3	1	4	2	3	14	1	2	1	1	0	12
40		16/**3**					12	12	13	/**3**	15	4	18/**3**	0	1	3	0	0	17/**3**
48							11	11	8	11/**3**	2		1	1	2	0	0	

Table 1 (B): Table summarizes the clinical scores that were recorded from *DPEP1+/+* mice treated with LPS either in the presence or absence of LSALT. Clinical scores were defined based on the criterion originally described by Shrum et al. (2014) to score sepsis severity in mice. Numbers highlighted in red were the respiratory quality/respiratory rate scores calculated/measured in mice at different time points. Mice were sacrificed when they either reached an overall score of 21 or their respiration rate/respiratory quality score reached to 3 or more.

Key resources table

Reagent or Recourse	Source	Identifier
Antibodies		
Rat-anti-mouse LY6G	Biolegend	Clone 1A8 (Catalog number 127601/127602)
Rat-anti-mouse F4/80 Monoclonal Antibody	eBioscience™	Clone BM8 (Catalog Number 14-4801-82)
Rat-anti-mouse CD31 (PECAM-1) Monoclonal Antibody	eBioscience™	Clone 390 (Cat# 14-0311-82)
Rabbit-anti- human DPEP1 polyclonal antibody	Atlas antibodies	Cat#HPA012783
Rabbit-anti-human/mouse DPEP1 polyclonal antibody	Proteintech	Cat# 12222-1-AP
Rabbit-anti-human DPEP1 polyclonal antibody	Abcam	Cat#ab121308
Rabbit-anti-human DPEP2 polyclonal antibody	Abcam	Cat#ab125516

Goat-anti-human DPEP3 polyclonal antibody	Santa Cruz Biotechnology	Clone N-16 Cat#sc-164219
Mouse anti-actin monoclonal antibody	Milipore EMD	Clone C4 MAB 1501
Rat-anti-mouse Gr-1 monoclonal antibody	BioXcell	Clone RB6-8C5 Cat#BE0075
Goat-anti-rabbit secondary antibody, Alexa Fluor 488	Invitrogen	Cat# A11034
Goat-anti-rabbit secondary antibody HRP(For IHC)	Dako	Cat# K4011
Goat-anti-rabbit secondary antibody, HRP (For Western Blot analysis)	Santa Cruz Biotechnology	Cat# sc-2054
Goat-anti mouse secondary antibody, HRP (For Western Blot analysis)	Santa Cruz Biotechnology	sc-2055
Goat-anti-rat secondary antibody,Biotylated	Vector Laboratories	Cat#BA-9401
Plasmids and ORF's		
MGC Human DPEP1 cDNA	GE-Dharmacon (Thermo scientific)	Clone ID:3846046 Accession:BC017023 Cat#MHS6278-202756036

Mouse DPEP1 cDNA	GE-Dharmacon (Thermo scientific)	Clone ID:2812088 Accession: BC003492 Cat# MMM1013-202760787
Rat DPEP1 cDNA	GE-Dharmacon (Thermo scientific)	Clone ID:7100683 Accession:BC072476 Cat# MRN4770-202780294
Human DPEP2	Origene	Accession: NM_022355 Cat# SC122933
Human DPEP3	Origene	Accession: NM_022357 Cat# SC125567
Peptides chemicals and other reagents		
LSALT peptide (H-LSALTPSPSWLKYKAL-NH2)	This paper (Canpeptide)	NA
KGAL peptide (H-KKGALWGRQKQHQGCLGEDWWPWC-NH2)	This paper (Canpeptide)	NA
GFE1 peptide (H-CGFECVRQCPERC-NH2	Canpeptide	NA

GFE2 peptide (H-CGFELETC-NH2)	Canpeptide	NA
Alexa Fluor 488 protein labeling kit	ThermoFisher SCIENTIFIC	Cat#A37570
Alexa Fluor 568 protein labeling kit	ThermoFisher SCIENTIFIC	Cat#A10238
Alexa Fluor 647 protein labeling kit	ThermoFisher SCIENTIFIC	Cat#A20173
Vybrant™ CFDA SE Cell Tracer Kit	ThermoFisher SCIENTIFIC	Cat#V12883
Paraformaldehyde	Sigma Aldrich	Cat#P6148
Ketamine Hydrocloride (Narketan)	Vetoquinol	Code:440894 DIN 02374994
Cilastatin sodium salt	Sigma-Aldrich	Product Number: C5743
L-Penicillamine	Sigma-Aldrich	Product Number: 196312
D-Amino Acid Oxidase from porcine kidney	Sigma-Aldrich	Product Number:A5222

Peroxidase from horseradish	Sigma-Aldrich	Product Number:77332
4-Hydroxyphenylacetic acid	Sigma-Aldrich	Product Number:H50004
Flavin adenine dinucleotide disodium salt hydrate	Sigma-Aldrich	Product Number:F8384
Glycyl-D-Phenylalanine	Sigma-Aldrich	Product Number:S756717
Sulfo-SBED Biotin Label Transfer Reagent	ThermoFisher SCIENTIFIC	Catalog Number: 33033
Lipofectamine® 2000 Transfection Reagent	ThermoFisher SCIENTIFIC (Invitrogen)	Catalog Number: 11668027
OptiMEM I Reduced serum medium	ThermoFisher SCIENTIFIC (Gibco)	Catalog Number: 31985-070
DMEM–high-glucose, no glutamine	ThermoFisher SCIENTIFIC (Gibco)	Catalog Number: 11960-044

Ultrapure LPS (*Escherichia coli* 111B4)	List Biological Laboratories. INC	Catalog Number: 421
Octyl β-D-glucopyranoside	Sigma-Aldrich	Catalog Number: O8001
DAPI	ThermoFisher SCIENTIFIC	Cat#D1306
Fetal bovine serum	ThermoFisher SCIENTIFIC (Gibco)	Cat#12483020
MEM Non-essential amino acids	ThermoFisher SCIENTIFIC (Gibco)	Cat#11140-050
L-glutamine	ThermoFisher SCIENTIFIC (Gibco))	Cat#25030-081
Penicillin-streptomycin	ThermoFisher SCIENTIFIC (Gibco)	Cat#15140-122
Quik Change *II Site-Directed Mutagenesis Kit*	Agilent Technologies, Santa Clara, CA, USA	Cat #200523

pcDNA 3.1(+) vector	ThermoFisher (Invitrogen)	Cat#V79020
Rodent Block M	Biocare Medical, Concord, CA, USA	SKU#RBM9611
Liquid DAB+ substrate chromogen system	Dako	Cat# Code K3468
Rodent-Decloaker	Biocare Medical	SKU#RD913M
Eco-mount	Biocare Medical	SKU#EM897L
Hematoxylin solution, Gill No-2	Sigma-Aldrich	Cat#GHS232
Anatech Eosin-Y	Fisher Scientific	Cat#NC9686037
Methyl-beta-cyclodextrin	Sigma-Aldrich	Cat#C4555
Urea	Sigma-Aldrich	Cat#U0631
Neutr Avidin Agarose	Thermo Fischer SCIENTIFIC Pierce	Cat#29200
Bovine Type 1collagen solution(3mg/ml)	Advanced Biomatrix	Cat#5005
Bovine Serum Albumin	Roche	Cat#10735094001
Tween 20	Sigma-Aldrich	Cat#P7949
Triton X-100	Sigma-Aldrich	Cat#T9284
Hexadecyltrimethylammonium bromide	Sigma Aldrich	Cat# H5882

O-dianisidine hydrochloride	Sigma Aldrich	Cat# D3252
RTU Vectastain ABC reagent kit	Vector Laboratories)	Cat# VectPK7100
Oligo nucleotides/ Primers		
HDPEP1 Forward primer 5'-GGTGGCAGGACTGAACTTGAA - 3' HDPEP1 Reverse primer 5'-AGGAGCCACTCTGCCATGC - 3'	University of Calgary DNA synthesis facility	NA
HDPEP2 Forward primer 5'-CTTGCAGGGGAAACAGCACAC - 3' HDPEP2 Reverse primer 5'-CCCACGAGGCCATCTCTAAG - 3'	University of Calgary DNA synthesis facility	NA
RatDPEP1 Forward primer 5'-CGGAAATCAGAGGCCAACCT- 3' RatDPEP1 Reverse primer 5'-AGTTGTGCGTAAGGGTCAGG- 3'	University of Calgary DNA synthesis facility	NA

human DPEP1 E141D g63t F 5'-tggccgccatccacgccgatcagg-3' human DPEP1 E141D g63t R 5'-cctgatcggcgtggatggcggcca-3'	University of Calgary DNA synthesis facility	NA
Primers used for the identification of DPEP1 mice in genotyping studies Forward primer: 5′-TAGCCTTGAGCTGTGGGAGT-3′, Reverse primer: 5′-GGCATCTTTGTTTTGGGTGT-3′	University of Calgary DNA synthesis facility and Horizon Discovery (Saint Louis, MO, 63146, USA)	NA
Experimental model: Cell lines		
COS1 cells	Gift from Dr. Karl Riabowol University of Calgary	NA
Human Neutrophils	Isolated from healthy human volunteers at the University of Calgary	NA

Experimental model: Organisms/strains		
C57BL/6 mice	Charles River	C57BL/6NCrl
DPEP1-/- mice	Custom Breed Horizon Discovery	NA
LysMeGFP mice	Jackson laboratories	NA
CD44-/- mice	Jackson laboratories	NA
Software's and algorithms		
Statistical Software	Graph Pad Prism (Version 5)	NA
Softmax PRO software	Molecular Devices	NA
LIF Software	Leica Molecular Devices	NA
Volocity Software	Perkin Elmer	NA

References

1.	Kolaczkowska, E. and P. Kubes, *Neutrophil recruitment and function in health and inflammation.* Nat Rev Immunol, 2013. **13**(3): p. 159-75.
2.	Wong, J., et al., *A minimal role for selectins in the recruitment of leukocytes into the inflamed liver microvasculature.* J Clin Invest, 1997. **99**(11): p. 2782-90.
3.	McDonald, B., et al., *Interaction of CD44 and hyaluronan is the dominant mechanism for neutrophil sequestration in inflamed liver sinusoids.* J Exp Med, 2008. **205**(4): p. 915-27.
4.	Mizgerd, J.P., et al., *Neutrophil emigration in the skin, lungs, and peritoneum: different requirements for CD11/CD18 revealed by CD18-deficient mice.* J Exp Med, 1997. **186**(8): p. 1357-64.
5.	Burns, J.A., et al., *The alpha 4 beta 1 (very late antigen (VLA)-4, CD49d/CD29) and alpha 5 beta 1 (VLA-5, CD49e/CD29) integrins mediate beta 2 (CD11/CD18) integrin-independent neutrophil recruitment to endotoxin-induced lung inflammation.* J Immunol, 2001. **166**(7): p. 4644-9.
6.	Doerschuk, C.M., et al., *The role of P-selectin and ICAM-1 in acute lung injury as determined using blocking antibodies and mutant mice.* J Immunol, 1996. **157**(10): p. 4609-14.
7.	Doerschuk, C.M., et al., *CD18-dependent and -independent mechanisms of neutrophil emigration in the pulmonary and systemic microcirculation of rabbits.* J Immunol, 1990. **144**(6): p. 2327-33.
8.	Petrovich, E., et al., *Lung ICAM-1 and ICAM-2 support spontaneous intravascular effector lymphocyte entrapment but are not required for neutrophil entrapment or emigration inside endotoxin-inflamed lungs.* FASEB J, 2016. **30**(5): p. 1767-78.
9.	Maulitz, R., *Rudolf Virchow, Julius Cohnheim, and the Program of Pathology.* Bulletin of the History of Medicine, 1978. **52**(2): p. 162.
10.	Jarcho, S., *Cohnheim on inflammation-II.* The American journal of cardiology, 1972. **29**(4): p. 546-547.
11.	Malkin, H.M., *Julius Cohnheim (1839-1884). His life and contributions to pathology.* Annals of Clinical & Laboratory Science, 1984. **14**(5): p. 335-342.
12.	Yipp, B.G., et al., *The lung is a host defense niche for immediate neutrophil-mediated vascular protection.* Science immunology, 2017. **2**(10).
13.	Wang, J. and P. Kubes, *A Reservoir of Mature Cavity Macrophages that Can Rapidly Invade Visceral Organs to Affect Tissue Repair.* Cell, 2016. **165**(3): p. 668-78.
14.	Sumen, C., et al., *Intravital microscopy: visualizing immunity in context.* Immunity, 2004. **21**(3): p. 315-329.
15.	e Silva, M.R., *A brief survey of the history of inflammation.* Agents and actions, 1978. **8**(1-2): p. 45-49.
16.	Rocha e Silva, M., *A brief survey of the history of inflammation.* Inflammation Research, 1978. **8**(1): p. 45-49.
17.	Scott, A., et al., *What is "inflammation"? Are we ready to move beyond Celsus?* British journal of sports medicine, 2004. **38**(3): p. 248-249.
18.	Smith, S., *Historical survey of definitions and concepts of inflammation*, in *Inflammation*. 1978, Springer. p. 1-4.
19.	Ley, K., *History of inflammation research*, in *Physiology of Inflammation*. 2001, Springer. p. 1-10.

20.   Underhill, D.M., et al., *Elie Metchnikoff (1845-1916): celebrating 100 years of cellular immunology and beyond.* Nat Rev Immunol, 2016. **16**(10): p. 651-656.

21.   Tauber, A.I., *Metchnikoff and the phagocytosis theory.* Nat Rev Mol Cell Biol, 2003. **4**(11): p. 897-901.

22.   Kaufmann, S.H., *Immunology's foundation: the 100-year anniversary of the Nobel Prize to Paul Ehrlich and Elie Metchnikoff.* Nature immunology, 2008. **9**(7): p. 705-712.

23.   Metchnikoff, E., *Lectures on the comparative pathology of inflammation: delivered at the Pasteur Institute in 1891.* 1893: Рипол Классик.

24.   Metchnikoff, E., *Immunity in infectious disease.* 1905, Cambridge University Press Cambridge/London/New York.

25.   Ley, K., et al., *Getting to the site of inflammation: the leukocyte adhesion cascade updated.* Nature Reviews Immunology, 2007. **7**(9): p. 678-689.

26.   Sadik, C.D., N.D. Kim, and A.D. Luster, *Neutrophils cascading their way to inflammation.* Trends in immunology, 2011. **32**(10): p. 452-460.

27.   Mayadas, T.N., et al., *Leukocyte rolling and extravasation are severely compromised in P selectin-deficient mice.* Cell, 1993. **74**(3): p. 541-54.

28.   Ley, K., et al., *Sequential contribution of L-and P-selectin to leukocyte rolling in vivo.* Journal of Experimental Medicine, 1995. **181**(2): p. 669-675.

29.   Ley, K., T.F. Tedder, and G.S. Kansas, *L-selectin can mediate leukocyte rolling in untreated mesenteric venules in vivo independent of E-or P-selectin.* Blood, 1993. **82**(5): p. 1632-1638.

30.   Laszik, Z., et al., *P-selectin glycoprotein ligand-1 is broadly expressed in cells of myeloid, lymphoid, and dendritic lineage and in some nonhematopoietic cells.* Blood, 1996. **88**(8): p. 3010-3021.

31.   Moore, K.L., et al., *P-selectin glycoprotein ligand-1 mediates rolling of human neutrophils on P-selectin.* The Journal of cell biology, 1995. **128**(4): p. 661-671.

32.   Phillipson, M. and P. Kubes, *The neutrophil in vascular inflammation.* Nature medicine, 2011. **17**(11): p. 1381-1390.

33.   Phillipson, M., et al., *Intraluminal crawling of neutrophils to emigration sites: a molecularly distinct process from adhesion in the recruitment cascade.* Journal of Experimental Medicine, 2006. **203**(12): p. 2569-2575.

34.   Phillipson, M., et al., *Vav1 is essential for mechanotactic crawling and migration of neutrophils out of the inflamed microvasculature.* The Journal of Immunology, 2009. **182**(11): p. 6870-6878.

35.   Woodfin, A., et al., *The junctional adhesion molecule JAM-C regulates polarized transendothelial migration of neutrophils in vivo.* Nature immunology, 2011. **12**(8): p. 761-769.

36.   Petri, B., M. Phillipson, and P. Kubes, *The physiology of leukocyte recruitment: an in vivo perspective.* The Journal of Immunology, 2008. **180**(10): p. 6439-6446.

37.   Burns, A.R., et al., *Analysis of tight junctions during neutrophil transendothelial migration.* J Cell Sci, 2000. **113**(1): p. 45-57.

38.   Phillipson, M., et al., *Endothelial domes encapsulate adherent neutrophils and minimize increases in vascular permeability in paracellular and transcellular emigration.* PLoS One, 2008. **3**(2): p. e1649.

39.   Petri, B., et al., *Endothelial LSP1 is involved in endothelial dome formation, minimizing vascular permeability changes during neutrophil transmigration in vivo.* Blood, 2011. **117**(3): p. 942-952.

40.   Kolaczkowska, E., et al., *Neutrophil elastase activity compensates for a genetic lack of matrix metalloproteinase‐9 (MMP‐9) in leukocyte infiltration in a model of experimental peritonitis.* Journal of leukocyte biology, 2009. **85**(3): p. 374-381.

41.   Wang, S., et al., *Venular basement membranes contain specific matrix protein low expression regions that act as exit points for emigrating neutrophils.* Journal of Experimental Medicine, 2006. **203**(6): p. 1519-1532.

42.   Kuckleburg, C.J., et al., *Proteinase 3 contributes to transendothelial migration of NB1-positive neutrophils.* The Journal of Immunology, 2012. **188**(5): p. 2419-2426.

43.   Phillipson, M., et al., *Intraluminal crawling of neutrophils to emigration sites: a molecularly distinct process from adhesion in the recruitment cascade.* J Exp Med, 2006. **203**(12): p. 2569-75.

44.   Lee, W.-Y. and P. Kubes, *Leukocyte adhesion in the liver: distinct adhesion paradigm from other organs.* Journal of hepatology, 2008. **48**(3): p. 504-512.

45.   Wong, J., et al., *A minimal role for selectins in the recruitment of leukocytes into the inflamed liver microvasculature.* Journal of Clinical Investigation, 1997. **99**(11): p. 2782.

46.   Gallatin, W.M., I.L. Weissman, and E.C. Butcher, *A cell-surface molecule involved in organ-specific homing of lymphocytes.* Nature, 1983. **304**(5921): p. 30-4.

47.   Gallatin, W.M., I.L. Weissman, and E.C. Butcher, *A cell-surface molecule involved in organ-specific homing of lymphocytes.* Nature, 1983. **304**(5921): p. 30.

48.   Bevilacqua, M.P., et al., *Identification of an inducible endothelial-leukocyte adhesion molecule.* Proceedings of the National Academy of Sciences, 1987. **84**(24): p. 9238-9242.

49.   Bevilacqua, M.P., et al., *Identification of an inducible endothelial-leukocyte adhesion molecule.* Proc Natl Acad Sci U S A, 1987. **84**(24): p. 9238-42.

50.   Lasky, L.A., *Selectins: interpreters of cell-specific carbohydrate information during inflammation.* Science, 1992. **258**(5084): p. 964-969.

51.   Geng, J.G., et al., *Rapid neutrophil adhesion to activated endothelium mediated by GMP-140.* Nature, 1990. **343**(6260): p. 757-60.

52.   Geng, J.-G., et al., *Rapid neutrophil adhesion to activated endothelium mediated by GMP-140.* Nature, 1990. **343**(6260): p. 757.

53.   Huang, K.-S., B.J. Graves, and B.A. Wolitzky, *Functional analysis of selectin structure.* The selectins: Initiators of leukocyte endothelial adhesion. Harwood Academic, Amsterdam, 1997: p. 1-29.

54.   Varki, A., *Selectin ligands: will the real ones please stand up?* Journal of Clinical Investigation, 1997. **99**(2): p. 158.

55.   Aigner, S., et al., *CD24 mediates rolling of breast carcinoma cells on P-selectin.* The FASEB journal, 1998. **12**(12): p. 1241-1251.

56.   Levinovitz, A., et al., *Identification of a glycoprotein ligand for E-selectin on mouse myeloid cells.* Journal of Cell Biology, 1993. **121**: p. 449-449.

57.   Steegmaier, M., et al., *The E-selectin-ligand ESL-1 is a variant of a receptor for fibroblast growth factor.* Nature, 1995. **373**(6515): p. 615.

58.   Lawrence, M.B. and T.A. Springer, *Leukocytes roll on a selectin at physiologic flow rates: distinction from and prerequisite for adhesion through integrins.* Cell, 1991. **65**(5): p. 859-73.

59.   Mayadas, T.N., et al., *Leukocyte rolling and extravasation are severely compromised in P selectin-deficient mice.* Cell, 1993. **74**(3): p. 541-554.

60.   Sanchez-Madrid, F., et al., *A Human Leukocyte Differentiation Antigen Family With Distinct a-Subunits And a Common 3-Subunit.* J. exp. Med, 1983. **158**: p. 1785-1803.

61.   Anderson, D.C. and T.A. Springer, *Leukocyte adhesion deficiency: an inherited defect in the Mac-1, LFA-1, and p150,95 glycoproteins.* Annu Rev Med, 1987. **38**: p. 175-94.

62.   Kishimoto, T.K., et al., *Cloning of the β subunit of the leukocyte adhesion proteins: homology to an extracellular matrix receptor defines a novel supergene family.* Cell, 1987. **48**(4): p. 681-690.

63.   Tamkun, J.W., et al., *Structure of integrin, a glycoprotein involved in the transmembrane linkage between fibronectin and actin.* Cell, 1986. **46**(2): p. 271-282.

64.   Fitzgerald, L.A., et al., *Protein sequence of endothelial glycoprotein IIIa derived from a cDNA clone. Identity with platelet glycoprotein IIIa and similarity to" integrin".* Journal of Biological Chemistry, 1987. **262**(9): p. 3936-3939.

65.   Fitzgerald, L.A., et al., *Comparison of cDNA-derived protein sequences of the human fibronectin and vitronectin receptor. alpha.-subunits and platelet glycoprotein IIb.* Biochemistry, 1987. **26**(25): p. 8158-8165.

66.   Poncz, M., et al., *Structure of the platelet membrane glycoprotein IIb. Homology to the alpha subunits of the vitronectin and fibronectin membrane receptors.* Journal of Biological Chemistry, 1987. **262**(18): p. 8476-8482.

67.   Law, S., et al., *The primary structure of the beta-subunit of the cell surface adhesion glycoproteins LFA-1, CR3 and p150, 95 and its relationship to the fibronectin receptor.* The EMBO journal, 1987. **6**(4): p. 915.

68.   Hemler, M.E., J.G. Jacobson, and J.L. Strominger, *Biochemical characterization of VLA-1 and VLA-2. Cell surface heterodimers on activated T cells.* Journal of Biological Chemistry, 1985. **260**(28): p. 15246-15252.

69.   Hemler, M.E., C. Huang, and L. Schwarz, *The VLA protein family. Characterization of five distinct cell surface heterodimers each with a common 130,000 molecular weight beta subunit.* Journal of Biological Chemistry, 1987. **262**(7): p. 3300-3309.

70.   Larson, R.S. and T.A. Springer, *Structure and function of leukocyte integrins.* Immunological reviews, 1990. **114**(1): p. 181-217.

71.   Kishimoto, T.K., et al., *The leukocyte integrins*, in *Advances in immunology.* 1989, Elsevier. p. 149-182.

72.   Elices, M.J., et al., *VCAM-1 on activated endothelium interacts with the leukocyte integrin VLA-4 at a site distinct from the VLA-4/fibronectin binding site.* Cell, 1990. **60**(4): p. 577-584.

73.   Marlin, S.D. and T.A. Springer, *Purified intercellular adhesion molecule-1 (ICAM-1) is a ligand for lymphocyte function-associated antigen 1 (LFA-1).* Cell, 1987. **51**(5): p. 813-819.

74.   Dana, N., et al., *Deficiency of a surface membrane glycoprotein (Mo1) in man.* Journal of Clinical Investigation, 1984. **73**(1): p. 153.

75. Kishimoto, T.K., et al., *Heterogeneous mutations in the β subunit common to the LFA-1, Mac-1, and p150, 95 glycoproteins cause leukocyte adhesion deficiency.* Cell, 1987. **50**(2): p. 193-202.

76. Wardlaw, A.J., et al., *Distinct mutations in two patients with leukocyte adhesion deficiency and their functional correlates.* Journal of Experimental Medicine, 1990. **172**(1): p. 335-345.

77. Kishimoto, T., K. O'Conner, and T. Springer, *Leukocyte adhesion deficiency. Aberrant splicing of a conserved integrin sequence causes a moderate deficiency phenotype.* Journal of Biological Chemistry, 1989. **264**(6): p. 3588-3595.

78. Ruoslahti, E. and D. Rajotte, *An Address System in the Vasculature of Normal Tissues and Tumors.* Annual Review of Immunology, 2000. **18**(1): p. 813-827.

79. Folkman, J., *Angiogenic zip code.* Nature biotechnology, 1999. **17**(8): p. 749-749.

80. Ruoslahti, E., *Vascular zip codes in angiogenesis and metastasis*. 2004, Portland Press Limited.

81. Teesalu, T., K.N. Sugahara, and E. Ruoslahti, *2 Mapping of Vascular ZIP Codes by Phage Display.* Methods in enzymology, 2012. **503**: p. 35.

82. Vane, J.R., E.E. Änggård, and R.M. Botting, *Regulatory functions of the vascular endothelium.* New England Journal of Medicine, 1990. **323**(1): p. 27-36.

83. Stoolman, L.M., *Adhesion molecules controlling lymphocyte migration.* 1989.

84. Gupta, G.P. and J. Massague, *Cancer metastasis: building a framework.* Cell, 2006. **127**(4): p. 679-95.

85. Renkonen, J., et al., *Glycosylation might provide endothelial zip codes for organ-specific leukocyte traffic into inflammatory sites.* The American journal of pathology, 2002. **161**(2): p. 543-550.

86. Sixt, M., et al., *β1 integrins: zip codes and signaling relay for blood cells.* Current opinion in cell biology, 2006. **18**(5): p. 482-490.

87. Järvinen, T.A.H. and E. Ruoslahti, *Molecular Changes in the Vasculature of Injured Tissues.* The American Journal of Pathology, 2007. **171**(2): p. 702-711.

88. Ruoslahti, E., *Specialization of tumour vasculature.* Nature Reviews Cancer, 2002. **2**(2): p. 83-90.

89. Pasqualini, R. and E. Ruoslahti, *Organ targeting In vivo using phage display peptide libraries.* Nature, 1996. **380**: p. 364.

90. Pasqualini, R. and E. Ruoslahti, *Organ targeting in vivo using phage display peptide libraries.* Nature, 1996. **380**(6572): p. 364.

91. Brown, D.M. and E. Ruoslahti, *Metadherin, a cell surface protein in breast tumors that mediates lung metastasis.* Cancer cell, 2004. **5**(4): p. 365-374.

92. Looney, M.R., et al., *Stabilized imaging of immune surveillance in the mouse lung.* Nature methods, 2011. **8**(1): p. 91.

93. Worthen, G.S., et al., *Mechanics of stimulated neutrophils: cell stiffening induces retention in capillaries.* Science, 1989. **245**(4914): p. 183-186.

94. Doerschuk, C.M., *The role of CD18-mediated adhesion in neutrophil sequestration induced by infusion of activated plasma in rabbits.* American journal of respiratory cell and molecular biology, 1992. **7**: p. 140-140.

95. Aird, W.C., *Phenotypic Heterogeneity of the Endothelium.* II. Representative Vascular Beds, 2007. **100**(2): p. 174-190.

96.   Fineman, J.R., S.J. Soifer, and M.A. Heymann, *Regulation of pulmonary vascular tone in the perinatal period.* Annual Review of Physiology, 1995. **57**(1): p. 115-134.

97.   Braet, F. and E. Wisse, *Structural and functional aspects of liver sinusoidal endothelial cell fenestrae: a review.* Comparative hepatology, 2002. **1**(1): p. 1.

98.   Simionescu, M., *Lung endothelium: structure-function correlates.* The Lung: scientific foundations. Raven, New York, 1991: p. 301-331.

99.   King, J., et al., *Structural and functional characteristics of lung macro-and microvascular endothelial cell phenotypes.* Microvascular research, 2004. **67**(2): p. 139-151.

100.   Wright, J.R., *Pulmonary surfactant: a front line of lung host defense.* Journal of Clinical Investigation, 2003. **111**(10): p. 1453-1455.

101.   Dockrell, D.H. and M.K. Whyte, *Regulation of phagocyte lifespan in the lung during bacterial infection.* Journal of leukocyte biology, 2006. **79**(5): p. 904-908.

102.   Orfanos, S., et al., *Pulmonary endothelium in acute lung injury: from basic science to the critically ill.* Intensive care medicine, 2004. **30**(9): p. 1702-1714.

103.   Kubes, P. and C. Jenne, *Immune Responses in the Liver.* Annual review of immunology, 2018(0).

104.   Barnes, P.J., *Cellular and molecular mechanisms of asthma and COPD.* Clinical science, 2017. **131**(13): p. 1541-1558.

105.   Basit, A., et al., *ICAM-1 and LFA-1 play critical roles in LPS-induced neutrophil recruitment into the alveolar space.* Am J Physiol Lung Cell Mol Physiol, 2006. **291**(2): p. L200-7.

106.   Mizgerd, J.P., et al., *Neutrophil emigration in the skin, lungs, and peritoneum: different requirements for CD11/CD18 revealed by CD18-deficient mice.* Journal of Experimental Medicine, 1997. **186**(8): p. 1357-1364.

107.   Doerschuk, C.M., et al., *The role of P-selectin and ICAM-1 in acute lung injury as determined using blocking antibodies and mutant mice.* The Journal of Immunology, 1996. **157**(10): p. 4609-4614.

108.   Burns, J.A., et al., *The α4β1 (very late antigen (VLA)-4, CD49d/CD29) and α5β1 (VLA-5, CD49e/CD29) integrins mediate β2 (CD11/CD18) integrin-independent neutrophil recruitment to endotoxin-induced lung inflammation.* The Journal of Immunology, 2001. **166**(7): p. 4644-4649.

109.   Crispe, I.N., *Liver antigen-presenting cells.* Journal of hepatology, 2011. **54**(2): p. 357-365.

110.   Sheth, K. and P. Bankey, *The liver as an immune organ.* Current opinion in critical care, 2001. **7**(2): p. 99-104.

111.   Wisse, E., et al., *The liver sieve: considerations concerning the structure and function of endothelial fenestrae, the sinusoidal wall and the space of Disse.* Hepatology, 1985. **5**(4): p. 683-692.

112.   Kempka, G. and V. Kolb-Bachofen, *Binding, uptake, and transcytosis of ligands for mannose-specific receptors in rat liver: an electron microscopic study.* Experimental cell research, 1988. **176**(1): p. 38-48.

113.   Seki, E. and D.A. Brenner, *Toll-like receptors and adaptor molecules in liver disease: update.* Hepatology, 2008. **48**(1): p. 322-335.

114. Bonder, C.S., et al., *Rules of recruitment for Th1 and Th2 lymphocytes in inflamed liver: a role for alpha-4 integrin and vascular adhesion protein-1.* Immunity, 2005. **23**(2): p. 153-163.

115. Petrovich, E., et al., *Lung ICAM-1 and ICAM-2 support spontaneous intravascular effector lymphocyte entrapment but are not required for neutrophil entrapment or emigration inside endotoxin-inflamed lungs.* The FASEB Journal, 2016. **30**(5): p. 1767-1778.

116. Salmi, M. and S. Jalkanen, *Ectoenzymes controlling leukocyte traffic.* Eur J Immunol, 2012. **42**(2): p. 284-92.

117. Salmi, M. and S. Jalkanen, *Cell-surface enzymes in control of leukocyte trafficking.* Nat Rev Immunol, 2005. **5**(10): p. 760-71.

118. Salmi, M., K. Kalimo, and S. Jalkanen, *Induction and function of vascular adhesion protein-1 at sites of inflammation.* J Exp Med, 1993. **178**(6): p. 2255-60.

119. Salmi, M., et al., *A cell surface amine oxidase directly controls lymphocyte migration.* Immunity, 2001. **14**(3): p. 265-76.

120. Salmi, M. and S. Jalkanen, *A 90-kilodalton endothelial cell molecule mediating lymphocyte binding in humans.* Science, 1992. **257**(5075): p. 1407-9.

121. Salmi, M., K. Kalimo, and S. Jalkanen, *Induction and function of vascular adhesion protein-1 at sites of inflammation.* Journal of Experimental Medicine, 1993. **178**(6): p. 2255-2260.

122. Stolen, C.M., et al., *Absence of the endothelial oxidase AOC3 leads to abnormal leukocyte traffic in vivo.* Immunity, 2005. **22**(1): p. 105-15.

123. Salmi, M. and S. Jalkanen, *Developmental regulation of the adhesive and enzymatic activity of vascular adhesion protein-1 (VAP-1) in humans.* Blood, 2006. **108**(5): p. 1555-61.

124. Kivi, E., et al., *Human Siglec-10 can bind to vascular adhesion protein-1 and serves as its substrate.* Blood, 2009. **114**(26): p. 5385-92.

125. Aalto, K., et al., *Siglec-9 is a novel leukocyte ligand for vascular adhesion protein-1 and can be used in PET imaging of inflammation and cancer.* Blood, 2011. **118**(13): p. 3725-33.

126. Partida-Sanchez, S., et al., *Cyclic ADP-ribose production by CD38 regulates intracellular calcium release, extracellular calcium influx and chemotaxis in neutrophils and is required for bacterial clearance in vivo.* Nat Med, 2001. **7**(11): p. 1209-16.

127. Partida-Sanchez, S., et al., *Regulation of dendritic cell trafficking by the ADP-ribosyl cyclase CD38: impact on the development of humoral immunity.* Immunity, 2004. **20**(3): p. 279-91.

128. Dransfield, I., et al., *Divalent cation regulation of the function of the leukocyte integrin LFA-1.* J Cell Biol, 1992. **116**(1): p. 219-26.

129. Dewitt, S., I. Laffafian, and M.B. Hallett, *Does neutrophil CD38 have a role in Ca++ signaling triggered by beta2 integrin?* Nat Med, 2002. **8**(4): p. 307; author reply 307-8.

130. Funaro, A., et al., *CD157 is an important mediator of neutrophil adhesion and migration.* Blood, 2004. **104**(13): p. 4269-78.

131. Airas, L., M. Salmi, and S. Jalkanen, *Lymphocyte-vascular adhesion protein-2 is a novel 70-kDa molecule involved in lymphocyte adhesion to vascular endothelium.* J Immunol, 1993. **151**(8): p. 4228-38.

132. Airas, L., et al., *CD73 is involved in lymphocyte binding to the endothelium: characterization of lymphocyte-vascular adhesion protein 2 identifies it as CD73.* J Exp Med, 1995. **182**(5): p. 1603-8.

133. Thompson, L.F., et al., *Crucial role for ecto-5'-nucleotidase (CD73) in vascular leakage during hypoxia.* J Exp Med, 2004. **200**(11): p. 1395-405.

134. Koszalka, P., et al., *Targeted disruption of cd73/ecto-5'-nucleotidase alters thromboregulation and augments vascular inflammatory response.* Circ Res, 2004. **95**(8): p. 814-21.

135. Shipp, M.A., et al., *CD10 (CALLA)/neutral endopeptidase 24.11 modulates inflammatory peptide-induced changes in neutrophil morphology, migration, and adhesion proteins and is itself regulated by neutrophil activation.* Blood, 1991. **78**(7): p. 1834-41.

136. Kanayama, N., et al., *Inactivation of interleukin-8 by aminopeptidase N (CD13).* J Leukoc Biol, 1995. **57**(1): p. 129-34.

137. Kirkwood, K.S., et al., *Deletion of neutral endopeptidase exacerbates intestinal inflammation induced by Clostridium difficile toxin A.* Am J Physiol Gastrointest Liver Physiol, 2001. **281**(2): p. G544-51.

138. Struyf, S., P. Proost, and J. Van Damme, *Regulation of the immune response by the interaction of chemokines and proteases.* Adv Immunol, 2003. **81**: p. 1-44.

139. De Meester, I., et al., *CD26, let it cut or cut it down.* Immunol Today, 1999. **20**(8): p. 367-75.

140. Kruschinski, C., et al., *CD26 (dipeptidyl-peptidase IV)-dependent recruitment of T cells in a rat asthma model.* Clin Exp Immunol, 2005. **139**(1): p. 17-24.

141. Busso, N., et al., *Circulating CD26 is negatively associated with inflammation in human and experimental arthritis.* Am J Pathol, 2005. **166**(2): p. 433-42.

142. Peschon, J.J., et al., *An essential role for ectodomain shedding in mammalian development.* Science, 1998. **282**(5392): p. 1281-4.

143. Itoh, Y. and M. Seiki, *MT1-MMP: an enzyme with multidimensional regulation.* Trends Biochem Sci, 2004. **29**(6): p. 285-9.

144. Nakamura, H., et al., *Constitutive and induced CD44 shedding by ADAM-like proteases and membrane-type 1 matrix metalloproteinase.* Cancer Res, 2004. **64**(3): p. 876-82.

145. Suenaga, N., et al., *CD44 binding through the hemopexin-like domain is critical for its shedding by membrane-type 1 matrix metalloproteinase.* Oncogene, 2005. **24**(5): p. 859-68.

146. Ingersoll, M.A., et al., *Monocyte trafficking in acute and chronic inflammation.* Trends in immunology, 2011. **32**(10): p. 470-477.

147. Ryan, G.B. and G. Majno, *Acute inflammation. A review.* The American journal of pathology, 1977. **86**(1): p. 183.

148. Melnicoff, M.J., P.K. Horan, and P.S. Morahan, *Kinetics of changes in peritoneal cell populations following acute inflammation.* Cellular immunology, 1989. **118**(1): p. 178-191.

149. Geissmann, F., et al., *Development of monocytes, macrophages, and dendritic cells.* Science, 2010. **327**(5966): p. 656-661.

150. Cohn, Z.A. and B. Benson, *The differentiation of mononuclear phagocytes: morphology, cytochemistry, and biochemistry.* Journal of Experimental Medicine, 1965. **121**(1): p. 153-170.

151. van Furth, R. and Z.A. Cohn, *The origin and kinetics of mononuclear phagocytes.* Journal of Experimental Medicine, 1968. **128**(3): p. 415-435.
152. Cohn, Z.A., M.E. Fedorko, and J.G. Hirsch, *The in vitro differentiation of mononuclear phagocytes: V. The formation of macrophage lysosomes.* Journal of Experimental Medicine, 1966. **123**(4): p. 757-766.
153. Ecker, J., et al., *Induction of fatty acid synthesis is a key requirement for phagocytic differentiation of human monocytes.* Proceedings of the National Academy of Sciences, 2010. **107**(17): p. 7817-7822.
154. Sheng, J., C. Ruedl, and K. Karjalainen, *Most tissue-resident macrophages except microglia are derived from fetal hematopoietic stem cells.* Immunity, 2015. **43**(2): p. 382-393.
155. Randolph, G.J., et al., *Differentiation of monocytes into dendritic cells in a model of transendothelial trafficking.* Science, 1998. **282**(5388): p. 480-483.
156. Mestas, J. and K. Ley, *Monocyte-Endothelial Cell Interactions in the Development of Atherosclerosis.* Trends in cardiovascular medicine, 2008. **18**(6): p. 228-232.
157. León, B. and C. Ardavín, *Monocyte migration to inflamed skin and lymph nodes is differentially controlled by L-selectin and PSGL-1.* Blood, 2008. **111**(6): p. 3126-3130.
158. Meerschaert, J. and M.B. Furie, *The adhesion molecules used by monocytes for migration across endothelium include CD11a/CD18, CD11b/CD18, and VLA-4 on monocytes and ICAM-1, VCAM-1, and other ligands on endothelium.* The Journal of Immunology, 1995. **154**(8): p. 4099-4112.
159. Shi, C. and E.G. Pamer, *Monocyte recruitment during infection and inflammation.* Nature Reviews Immunology, 2011. **11**(11): p. 762.
160. *The integrin VLA-4 supports tethering and rolling in flow on VCAM-1.* The Journal of Cell Biology, 1995. **128**(6): p. 1243-1253.
161. Ramos, C.L., et al., *Direct demonstration of P-selectin–and VCAM-1–dependent mononuclear cell rolling in early atherosclerotic lesions of apolipoprotein E–deficient mice.* Circulation research, 1999. **84**(11): p. 1237-1244.
162. Huo, Y., A. Hafezi-Moghadam, and K. Ley, *Role of Vascular Cell Adhesion Molecule-1 and Fibronectin Connecting Segment-1 in Monocyte Rolling and Adhesion on Early Atherosclerotic Lesions.* Circulation Research, 2000. **87**(2): p. 153-159.
163. Auffray, C., et al., *Monitoring of blood vessels and tissues by a population of monocytes with patrolling behavior.* Science, 2007. **317**(5838): p. 666-670.
164. Henderson, R.B., et al., *Rapid recruitment of inflammatory monocytes is independent of neutrophil migration.* Blood, 2003. **102**(1): p. 328-335.
165. Soehnlein, O., L. Lindbom, and C. Weber, *Mechanisms underlying neutrophil-mediated monocyte recruitment.* Blood, 2009. **114**(21): p. 4613-4623.
166. Kaplanski, G., et al., *IL-6: a regulator of the transition from neutrophil to monocyte recruitment during inflammation.* Trends in immunology, 2003. **24**(1): p. 25-29.
167. Ward, P.A., *Chemotaxis of mononuclear cells.* Journal of Experimental Medicine, 1968. **128**(5): p. 1201-1221.
168. Gallin, J.I., et al., *Human neutrophil-specific granule deficiency: a model to assess the role of neutrophil-specific granules in the evolution of the inflammatory response.* Blood, 1982. **59**(6): p. 1317-1329.

169. Mokart, D., et al., *Monocyte deactivation in neutropenic acute respiratory distress syndrome patients treated with granulocyte colony-stimulating factor.* Critical Care, 2008. **12**(1): p. R17.

170. Hurst, S.M., et al., *Il-6 and its soluble receptor orchestrate a temporal switch in the pattern of leukocyte recruitment seen during acute inflammation.* Immunity, 2001. **14**(6): p. 705-714.

171. Yamashiro, S., H. Kamohara, and T. Yoshimura, *MCP-1 is selectively expressed in the late phase by cytokine-stimulated human neutrophils: TNF-α plays a role in maximal MCP-1 mRNA expression.* Journal of leukocyte biology, 1999. **65**(5): p. 671-679.

172. Serbina, N.V. and E.G. Pamer, *Monocyte emigration from bone marrow during bacterial infection requires signals mediated by chemokine receptor CCR2.* Nature immunology, 2006. **7**(3): p. 311.

173. Lim, J.K., et al., *Chemokine receptor Ccr2 is critical for monocyte accumulation and survival in West Nile virus encephalitis.* The Journal of Immunology, 2011. **186**(1): p. 471-478.

174. Heidland, A., et al., *The contribution of Rudolf Virchow to the concept of inflammation: what is still of importance?* 2006.

175. Balkwill, F. and A. Mantovani, *Inflammation and cancer: back to Virchow?* The Lancet, 2001. **357**(9255): p. 539-545.

176. Coussens, L.M. and Z. Werb, *Inflammation and cancer.* Nature, 2002. **420**(6917): p. 860-867.

177. Grivennikov, S.I., F.R. Greten, and M. Karin, *Immunity, inflammation, and cancer.* Cell, 2010. **140**(6): p. 883-899.

178. Pikarsky, E., et al., *NF-κB functions as a tumour promoter in inflammation-associated cancer.* Nature, 2004. **431**(7007): p. 461-466.

179. Marx, J., *Inflammation and cancer: the link grows stronger: research into a long-suspected association between chronic inflammation and cancer reveals how the immune system may be abetting tumors.* Science, 2004. **306**(5698): p. 966-969.

180. Baud, V. and M. Karin, *Is NF-κB a good target for cancer therapy? Hopes and pitfalls.* Nature reviews Drug discovery, 2009. **8**(1): p. 33-40.

181. Yamamoto, Y. and R.B. Gaynor, *Therapeutic potential of inhibition of the NF-κB pathway in the treatment of inflammation and cancer.* Journal of Clinical investigation, 2001. **107**(2): p. 135.

182. Sica, A., et al., *Tumour-associated macrophages are a distinct M2 polarised population promoting tumour progression: potential targets of anti-cancer therapy.* European journal of cancer, 2006. **42**(6): p. 717-727.

183. Joyce, J.A. and J.W. Pollard, *Microenvironmental regulation of metastasis.* Nature Reviews Cancer, 2009. **9**(4): p. 239-252.

184. Mantovani, A., et al., *Cancer-related inflammation.* Nature, 2008. **454**(7203): p. 436-444.

185. Gajewski, T.F., H. Schreiber, and Y.-X. Fu, *Innate and adaptive immune cells in the tumor microenvironment.* Nature immunology, 2013. **14**(10): p. 1014.

186. Fridlender, Z.G. and S.M. Albelda, *Tumor-associated neutrophils: friend or foe?* Carcinogenesis, 2012. **33**(5): p. 949-955.

187. Spicer, J.D., et al., *Neutrophils promote liver metastasis via mac-1–Mediated interactions with circulating tumor cells.* Cancer research, 2012. **72**(16): p. 3919-3927.

188. Wculek, S.K. and I. Malanchi, *Neutrophils support lung colonization of metastasis-initiating breast cancer cells.* Nature, 2015. **528**(7582): p. 413-417.

189. Huh, S.J., et al., *Transiently entrapped circulating tumor cells interact with neutrophils to facilitate lung metastasis development.* Cancer research, 2010. **70**(14): p. 6071-6082.

190. Granot, Z., et al., *Tumor entrained neutrophils inhibit seeding in the premetastatic lung.* Cancer cell, 2011. **20**(3): p. 300-314.

191. Finisguerra, V., et al., *MET is required for the recruitment of anti-tumoural neutrophils.* Nature, 2015. **522**(7556): p. 349-353.

192. Sagiv, J.Y., et al., *Phenotypic diversity and plasticity in circulating neutrophil subpopulations in cancer.* Cell reports, 2015. **10**(4): p. 562-573.

193. Fridlender, Z.G., et al., *Polarization of tumor-associated neutrophil phenotype by TGF-β:"N1" versus "N2" TAN.* Cancer cell, 2009. **16**(3): p. 183-194.

194. Sionov, R.V., Z.G. Fridlender, and Z. Granot, *The multifaceted roles neutrophils play in the tumor microenvironment.* Cancer Microenvironment, 2015. **8**(3): p. 125-158.

195. Sagiv, Jitka Y., et al., *Phenotypic Diversity and Plasticity in Circulating Neutrophil Subpopulations in Cancer.* Cell Reports, 2015. **10**(4): p. 562-573.

196. Mishalian, I., Z. Granot, and Z.G. Fridlender, *The diversity of circulating neutrophils in cancer.* Immunobiology, 2017. **222**(1): p. 82-88.

197. Granot, Z. and J. Jablonska, *Distinct functions of neutrophil in cancer and its regulation.* Mediators of inflammation, 2015. **2015**.

198. Eruslanov, E.B., S. Singhal, and S.M. Albelda, *Mouse versus Human Neutrophils in Cancer: A Major Knowledge Gap.* Trends in Cancer. **3**(2): p. 149-160.

199. Erez, N., et al., *Cancer-associated fibroblasts are activated in incipient neoplasia to orchestrate tumor-promoting inflammation in an NF-κB-dependent manner.* Cancer cell, 2010. **17**(2): p. 135-147.

200. Nagasaki, T., et al., *Interleukin-6 released by colon cancer-associated fibroblasts is critical for tumour angiogenesis: anti-interleukin-6 receptor antibody suppressed angiogenesis and inhibited tumour–stroma interaction.* British journal of cancer, 2014. **110**(2): p. 469-478.

201. Ostrand-Rosenberg, S. and P. Sinha, *Myeloid-derived suppressor cells: linking inflammation and cancer.* The Journal of Immunology, 2009. **182**(8): p. 4499-4506.

202. Psaila, B. and D. Lyden, *The metastatic niche: adapting the foreign soil.* Nature Reviews Cancer, 2009. **9**(4): p. 285-293.

203. Kaplan, R.N., et al., *VEGFR1-positive haematopoietic bone marrow progenitors initiate the pre-metastatic niche.* Nature, 2005. **438**(7069): p. 820-827.

204. Hiratsuka, S., et al., *The S100A8–serum amyloid A3–TLR4 paracrine cascade establishes a pre-metastatic phase.* Nature cell biology, 2008. **10**(11): p. 1349-1355.

205. Costa-Silva, B., et al., *Pancreatic cancer exosomes initiate pre-metastatic niche formation in the liver.* Nature cell biology, 2015. **17**(6): p. 816-826.

206. Peinado, H., et al., *Melanoma exosomes educate bone marrow progenitor cells toward a pro-metastatic phenotype through MET.* Nature medicine, 2012. **18**(6): p. 883-891.

207. Dranoff, G., *Cytokines in cancer pathogenesis and cancer therapy.* Nature Reviews Cancer, 2004. **4**(1): p. 11.

208. Nicolson, G.L., *Cancer progression and growth: relationship of paracrine and autocrine growth mechanisms to organ preference of metastasis.* Experimental cell research, 1993. **204**(2): p. 171-180.

209. Balkwill, F., *TNF-α in promotion and progression of cancer.* Cancer and Metastasis Reviews, 2006. **25**(3): p. 409-416.

210. Moore, R.J., et al., *Mice deficient in tumor necrosis factor-α are resistant to skin carcinogenesis.* Nature medicine, 1999. **5**(7): p. 828-831.

211. Voronov, E., et al., *IL-1 is required for tumor invasiveness and angiogenesis.* Proceedings of the National Academy of Sciences, 2003. **100**(5): p. 2645-2650.

212. O'Hanlon, D., et al., *Soluble adhesion molecules (E-selectin, ICAM-1 and VCAM-1) in breast carcinoma.* European Journal of Cancer, 2002. **38**(17): p. 2252-2257.

213. Gout, S., P.-L. Tremblay, and J. Huot, *Selectins and selectin ligands in extravasation of cancer cells and organ selectivity of metastasis.* Clinical & experimental metastasis, 2008. **25**(4): p. 335-344.

214. Mannori, G., et al., *Differential colon cancer cell adhesion to E-, P-, and L-selectin: role of mucintype glycoproteins.* Cancer Research, 1995. **55**(19): p. 4425-4431.

215. Apte, R.N., et al., *The involvement of IL-1 in tumorigenesis, tumor invasiveness, metastasis and tumor-host interactions.* Cancer and Metastasis Reviews, 2006. **25**(3): p. 387-408.

216. John, A. and G. Tuszynski, *The role of matrix metalloproteinases in tumor angiogenesis and tumor metastasis.* Pathology & Oncology Research, 2001. **7**(1): p. 14-23.

217. Vidal-Vanaclocha, F., et al., *IL-18 regulates IL-1β-dependent hepatic melanoma metastasis via vascular cell adhesion molecule-1.* Proceedings of the National Academy of Sciences, 2000. **97**(2): p. 734-739.

218. Chang, Q., et al., *The IL-6/JAK/Stat3 feed-forward loop drives tumorigenesis and metastasis.* Neoplasia, 2013. **15**(7): p. 848IN40-862IN45.

219. Scheibenbogen, C., et al., *Serum interleukin-8 (IL-8) is elevated in patients with metastatic melanoma and correlates with tumour load.* Melanoma research, 1995. **5**(3): p. 179-182.

220. Padua, D. and J. Massagué, *Roles of TGFβ in metastasis.* Cell research, 2009. **19**(1): p. 89-102.

221. Condeelis, J. and J.W. Pollard, *Macrophages: obligate partners for tumor cell migration, invasion, and metastasis.* Cell, 2006. **124**(2): p. 263-266.

222. Chambers, S.K., et al., *Overexpression of epithelial macrophage colony-stimulating factor (CSF-1) and CSF-1 receptor: a poor prognostic factor in epithelial ovarian cancer, contrasted with a protective effect of stromal CSF-1.* Clinical cancer research, 1997. **3**(6): p. 999-1007.

223. Wang, J.M., et al., *Chemokines and their role in tumor growth and metastasis.* Journal of immunological methods, 1998. **220**(1): p. 1-17.

224. Kakinuma, T. and S.T. Hwang, *Chemokines, chemokine receptors, and cancer metastasis.* Journal of leukocyte biology, 2006. **79**(4): p. 639-651.

225. Huber, M.A., et al., *NF-κB is essential for epithelial-mesenchymal transition and metastasis in a model of breast cancer progression.* Journal of Clinical Investigation, 2004. **114**(4): p. 569.

226. Valastyan, S. and R.A. Weinberg, *Tumor metastasis: molecular insights and evolving paradigms.* Cell, 2011. **147**(2): p. 275-92.

227. Chaffer, C.L. and R.A. Weinberg, *A perspective on cancer cell metastasis.* Science, 2011. **331**(6024): p. 1559-64.

228. O'Connell, J., et al., *The Fas counterattack: Fas-mediated T cell killing by colon cancer cells expressing Fas ligand.* J Exp Med, 1996. **184**(3): p. 1075-82.

229. Takeda, K., et al., *Involvement of tumor necrosis factor-related apoptosis-inducing ligand in surveillance of tumor metastasis by liver natural killer cells.* Nat Med, 2001. **7**(1): p. 94-100.

230. Chambers, A.F., A.C. Groom, and I.C. MacDonald, *Dissemination and growth of cancer cells in metastatic sites.* Nat Rev Cancer, 2002. **2**(8): p. 563-72.

231. Gupta, G.P., et al., *Mediators of vascular remodelling co-opted for sequential steps in lung metastasis.* Nature, 2007. **446**(7137): p. 765-70.

232. Folkman, J., *The role of angiogenesis in tumor growth.* Semin Cancer Biol, 1992. **3**(2): p. 65-71.

233. Hanahan, D. and R.A. Weinberg, *Hallmarks of cancer: the next generation.* Cell, 2011. **144**(5): p. 646-74.

234. Hanahan, D. and J. Folkman, *Patterns and emerging mechanisms of the angiogenic switch during tumorigenesis.* Cell, 1996. **86**(3): p. 353-64.

235. Nguyen, D.X., P.D. Bos, and J. Massagué, *Metastasis: from dissemination to organ-specific colonization.* Nature Reviews Cancer, 2009. **9**(4): p. 274-284.

236. Chiang, A.C. and J. Massagué, *Molecular basis of metastasis.* New England Journal of Medicine, 2008. **359**(26): p. 2814-2823.

237. Paget, S., *The distribution of secondary growths in cancer of the breast.* The Lancet, 1889. **133**(3421): p. 571-573.

238. Fidler, I.J. *The biology of cancer metastasis*. in *Seminars in cancer biology*. 2011: Academic Press.

239. Ewing, J., *Neoplastic diseases. A treatise on tumors.* The American Journal of the Medical Sciences, 1928. **176**(2): p. 278.

240. Hart, I.R. and I.J. Fidler, *Role of organ selectivity in the determination of metastatic patterns of B16 melanoma.* Cancer research, 1980. **40**(7): p. 2281-2287.

241. Fidler, I.J., *The relationship of embolic homogeneity, number, size and viability to the incidence of experimental metastasis.* European Journal of Cancer (1965), 1973. **9**(3): p. 223-227.

242. Fidler, I.J., *Tumor heterogeneity and the biology of cancer invasion and metastasis.* Cancer research, 1978. **38**(9): p. 2651-2660.

243. Fidler, I.J. and M.L. Kripke, *Metastasis results from preexisting variant cells within a malignant tumor.* Science, 1977. **197**(4306): p. 893-5.

244. Du, Y.-C.N., et al., *Receptor for hyaluronan-mediated motility isoform B promotes liver metastasis in a mouse model of multistep tumorigenesis and a tail vein assay for metastasis.* Proceedings of the National Academy of Sciences, 2011. **108**(40): p. 16753-16758.

245. Tabaries, S., et al., *Claudin-2 is selectively enriched in and promotes the formation of breast cancer liver metastases through engagement of integrin complexes.* Oncogene, 2011. **30**(11): p. 1318.

246. Tabariès, S., et al., *Claudin-2 promotes breast cancer liver metastasis by facilitating tumor cell interactions with hepatocytes.* Molecular and cellular biology, 2012. **32**(15): p. 2979-2991.

247. Bakalian, S., et al., *Molecular pathways mediating liver metastasis in patients with uveal melanoma.* Clinical Cancer Research, 2008. **14**(4): p. 951-956.

248. Sato, T. *Locoregional management of hepatic metastasis from primary uveal melanoma.* in *Seminars in oncology.* 2010: Elsevier.

249. Gupta, G.P., et al., *Identifying site-specific metastasis genes and functions.* Cold Spring Harb Symp Quant Biol, 2005. **70**: p. 149-58.

250. Kang, Y., et al., *Breast cancer bone metastasis mediated by the Smad tumor suppressor pathway.* Proc Natl Acad Sci U S A, 2005. **102**(39): p. 13909-14.

251. Minn, A.J., et al., *Genes that mediate breast cancer metastasis to lung.* Nature, 2005. **436**(7050): p. 518-24.

252. Minn, A.J., et al., *Distinct organ-specific metastatic potential of individual breast cancer cells and primary tumors.* J Clin Invest, 2005. **115**(1): p. 44-55.

253. Bos, P.D., et al., *Genes that mediate breast cancer metastasis to the brain.* Nature, 2009. **459**(7249): p. 1005-9.

254. Kang, Y., et al., *A multigenic program mediating breast cancer metastasis to bone.* Cancer cell, 2003. **3**(6): p. 537-549.

255. Kalluri, R. and R.A. Weinberg, *The basics of epithelial-mesenchymal transition.* The Journal of clinical investigation, 2009. **119**(6): p. 1420-1428.

256. Thiery, J.P. and J.P. Sleeman, *Complex networks orchestrate epithelial–mesenchymal transitions.* Nature reviews Molecular cell biology, 2006. **7**(2): p. 131.

257. DiMeo, T.A., et al., *A novel lung metastasis signature links Wnt signaling with cancer cell self-renewal and epithelial-mesenchymal transition in basal-like breast cancer.* Cancer research, 2009. **69**(13): p. 5364-5373.

258. Onder, T.T., et al., *Loss of E-cadherin promotes metastasis via multiple downstream transcriptional pathways.* Cancer research, 2008. **68**(10): p. 3645-3654.

259. Cano, A., et al., *The transcription factor snail controls epithelial–mesenchymal transitions by repressing E-cadherin expression.* Nature cell biology, 2000. **2**(2): p. 76.

260. Kudo-Saito, C., et al., *Cancer metastasis is accelerated through immunosuppression during Snail-induced EMT of cancer cells.* Cancer cell, 2009. **15**(3): p. 195-206.

261. Fenouille, N., et al., *The epithelial-mesenchymal transition (EMT) regulatory factor SLUG (SNAI2) is a downstream target of SPARC and AKT in promoting melanoma cell invasion.* PloS one, 2012. **7**(7): p. e40378.

262. Imani, S., et al., *Prognostic value of EMT-inducing transcription factors (EMT-TFs) in metastatic breast cancer: a systematic review and meta-analysis.* Scientific reports, 2016. **6**: p. 28587.

263. Byles, V., et al., *SIRT1 induces EMT by cooperating with EMT transcription factors and enhances prostate cancer cell migration and metastasis.* Oncogene, 2012. **31**(43): p. 4619.

264. Roberts, A.B., et al., *Smad3 is key to TGF-β-mediated epithelial-to-mesenchymal transition, fibrosis, tumor suppression and metastasis.* Cytokine & growth factor reviews, 2006. **17**(1-2): p. 19-27.

265. Xie, L., et al., *Activation of the Erk pathway is required for TGF-β1-induced EMT in vitro.* Neoplasia, 2004. **6**(5): p. 603-610.

266. Kasai, H., et al., *TGF-β1 induces human alveolar epithelial to mesenchymal cell transition (EMT).* Respiratory research, 2005. **6**(1): p. 56.

267. Janda, E., et al., *Ras and TGFβ cooperatively regulate epithelial cell plasticity and metastasis: dissection of Ras signaling pathways.* The Journal of cell biology, 2002. **156**(2): p. 299-314.

268. Oft, M., K.-H. Heider, and H. Beug, *TGFβ signaling is necessary for carcinoma cell invasiveness and metastasis.* Current Biology, 1998. **8**(23): p. 1243-1252.

269. Kang, Y. and J. Massagué, *Epithelial-mesenchymal transitions: twist in development and metastasis.* Cell, 2004. **118**(3): p. 277-279.

270. Tarin, D., *The fallacy of epithelial mesenchymal transition in neoplasia.* Cancer research, 2005. **65**(14): p. 5996-6001.

271. Thompson, E.W. and D.F. Newgreen, *Carcinoma invasion and metastasis: a role for epithelial-mesenchymal transition?* Cancer research, 2005. **65**(14): p. 5991-5995.

272. Bendas, G. and L. Borsig, *Cancer cell adhesion and metastasis: selectins, integrins, and the inhibitory potential of heparins.* International journal of cell biology, 2012. **2012**.

273. Dimitroff, C.J., et al., *Rolling of human bone-metastatic prostate tumor cells on human bone marrow endothelium under shear flow is mediated by E-selectin.* Cancer research, 2004. **64**(15): p. 5261-5269.

274. Barthel, S.R., et al., *Targeting selectins and selectin ligands in inflammation and cancer.* Expert opinion on therapeutic targets, 2007. **11**(11): p. 1473-1491.

275. Albelda, S., *Role of integrins and other cell adhesion molecules in tumor progression and metastasis.* Laboratory investigation; a journal of technical methods and pathology, 1993. **68**(1): p. 4-17.

276. Kim, Y.J., et al., *P-selectin deficiency attenuates tumor growth and metastasis.* Proceedings of the National Academy of Sciences, 1998. **95**(16): p. 9325-9330.

277. Ludwig, R.J., et al., *Endothelial P-selectin as a target of heparin action in experimental melanoma lung metastasis.* Cancer research, 2004. **64**(8): p. 2743-2750.

278. Abdel-Ghany, M., et al., *The breast cancer β4 integrin and endothelial human CLCA2 mediate lung metastasis.* Journal of Biological Chemistry, 2001. **276**(27): p. 25438-25446.

279. Hoshino, A., et al., *Tumour exosome integrins determine organotropic metastasis.* Nature, 2015. **527**(7578): p. 329.

280. Hsu, R.Y., et al., *LPS-induced TLR4 signaling in human colorectal cancer cells increases β1 integrin-mediated cell adhesion and liver metastasis.* Cancer research, 2011. **71**(5): p. 1989-1998.

281. Liu, C., et al., *The microRNA miR-34a inhibits prostate cancer stem cells and metastasis by directly repressing CD44.* Nature medicine, 2011. **17**(2): p. 211-215.

282. Marhaba, R. and M. Zöller, *CD44 in cancer progression: adhesion, migration and growth regulation.* Journal of molecular histology, 2004. **35**(3): p. 211-231.

283. Ferjančič, Š., et al., *VCAM-1 and VAP-1 recruit myeloid cells that promote pulmonary metastasis in mice.* Blood, 2013. **121**(16): p. 3289-3297.

284. Stagg, J., et al., *Anti-CD73 antibody therapy inhibits breast tumor growth and metastasis.* Proceedings of the National Academy of Sciences, 2010. **107**(4): p. 1547-1552.

285. Zhu, D., C.-F. Cheng, and B. Pauli, *Blocking of lung endothelial cell adhesion molecule-1 (Lu-ECAM-1) inhibits murine melanoma lung metastasis.* Journal of Clinical Investigation, 1992. **89**(6): p. 1718.

286. Cheng, H.-C., et al., *Lung endothelial dipeptidyl peptidase IV promotes adhesion and metastasis of rat breast cancer cells via tumor cell surface-associated fibronectin.* Journal of Biological Chemistry, 1998. **273**(37): p. 24207-24215.

287. Hooper, N.M., M. Low, and A.J. Turner, *Renal dipeptidase is one of the membrane proteins released by phosphatidylinositol-specific phospholipase C.* Biochemical Journal, 1987. **244**(2): p. 465-469.

288. PARK, S.W., et al., *Endogenous glycosylphosphatidylinositol-specific phospholipase C releases renal dipeptidase from kidney proximal tubules in vitro.* Biochemical Journal, 2001. **353**(2): p. 339-344.

289. Habib, G.M. and M.W. Lieberman, *Cleavage of leukotriene D4 in mice with targeted disruption of a membrane-bound dipeptidase gene*, in *Eicosanoids and Other Bioactive Lipids in Cancer, Inflammation, and Radiation Injury, 4*. 1999, Springer. p. 295-300.

290. Habib, G.M., et al., *Identification of two additional members of the membrane-bound dipeptidase family.* The FASEB journal, 2003. **17**(10): p. 1313-1315.

291. Nitanai, Y., et al., *Crystal structure of human renal dipeptidase involved in β-lactam hydrolysis.* Journal of molecular biology, 2002. **321**(2): p. 177-184.

292. Adachi, H., et al., *Importance of Glu-125 in the catalytic activity of human renal dipeptidase.* Biochimica et Biophysica Acta (BBA)-Protein Structure and Molecular Enzymology, 1993. **1163**(1): p. 42-48.

293. Keynan, S., N.M. Hooper, and A.J. Turner, *Directed mutagenesis of pig renal membrane dipeptidase His219 is critical but the DHXXH motif is not essential for zinc binding or catalytic activity.* FEBS letters, 1994. **349**(1): p. 50-54.

294. Keynan, S., et al., *Site-directed mutagenesis of conserved cysteine residues in porcine membrane dipeptidase. Cys 361 alone is involved in disulfide-linked dimerization.* Biochemistry, 1996. **35**(38): p. 12511-12517.

295. Adachi, H., et al., *Identification of membrane anchoring site of human renal dipeptidase and construction and expression of a cDNA for its secretory form.* Journal of Biological Chemistry, 1990. **265**(25): p. 15341-15345.

296. Rached, E., et al., *cDNA cloning and expression in Xenopus laevis oocytes of pig renal dipeptidase, a glycosyl-phosphatidylinositol-anchored ectoenzyme.* Biochemical journal, 1990. **271**(3): p. 755-760.

297. Igarashi, P. and L.P. Karniski, *Cloning of cDNAs encoding a rabbit renal brush border membrane protein immunologically related to band 3. Sequence similarity with microsomal dipeptidase.* Biochemical Journal, 1991. **280**(1): p. 71-78.

298. Habib, G.M., et al., *Leukotriene D4 and cystinyl-bis-glycine metabolism in membrane-bound dipeptidase-deficient mice.* Proceedings of the National Academy of Sciences, 1998. **95**(9): p. 4859-4863.

299. Babes, L. and P. Kubes, *Visualizing the Tumor Microenvironment of Liver Metastasis by Spinning Disk Confocal Microscopy.* Methods Mol Biol, 2016. **1458**: p. 203-15.

300. Yipp, B.G., et al., *The Lung is a Host Defense Niche for Immediate Neutrophil-Mediated Vascular Protection.* Sci Immunol, 2017. **2**(10).

301. Chakrabarti, S. and K.D. Patel, *Regulation of matrix metalloproteinase-9 release from IL-8-stimulated human neutrophils.* J Leukoc Biol, 2005. **78**(1): p. 279-88.

302. Heywood, S.P. and N.M. Hooper, *Development and application of a fluorometric assay for mammalian membrane dipeptidase.* Analytical biochemistry, 1995. **226**(1): p. 10-14.

303. Rajotte, D. and E. Ruoslahti, *Membrane dipeptidase is the receptor for a lung-targeting peptide identified by in vivo phage display.* Journal of Biological Chemistry, 1999. **274**(17): p. 11593-11598.

304. Shrum, B., et al., *A robust scoring system to evaluate sepsis severity in an animal model.* BMC Res Notes, 2014. **7**: p. 233.

305. Springer, T.A., *Adhesion receptors of the immune system.* Nature, 1990. **346**(6283): p. 425.

306. Nolte, D., et al., *Leukocyte rolling in venules of striated muscle and skin is mediated by P-selectin, not by L-selectin.* American Journal of Physiology-Heart and Circulatory Physiology, 1994. **267**(4): p. H1637-H1642.

307. Lawrence, M.B. and T.A. Springer, *Leukocytes roll on a selectin at physiologic flow rates: distinction from and prerequisite for adhesion through integrins.* Cell, 1991. **65**(5): p. 859-873.

308. Opal, S.M., *Endotoxins and other sepsis triggers*, in *Endotoxemia and Endotoxin Shock.* 2010, Karger Publishers. p. 14-24.

309. Faust, N., et al., *Insertion of enhanced green fluorescent protein into the lysozyme gene creates mice with green fluorescent granulocytes and macrophages.* Blood, 2000. **96**(2): p. 719-726.

310. Daley, J.M., et al., *Use of Ly6G-specific monoclonal antibody to deplete neutrophils in mice.* Journal of leukocyte biology, 2008. **83**(1): p. 64-70.

311. Schmits, R., et al., *CD44 regulates hematopoietic progenitor distribution, granuloma formation, and tumorigenicity.* Blood, 1997. **90**(6): p. 2217-2233.

312. McDonald, B. and P. Kubes, *Interactions between CD44 and hyaluronan in leukocyte trafficking.* Frontiers in immunology, 2015. **6**.

313. Looney, M.R., et al., *Stabilized imaging of immune surveillance in the mouse lung.* Nature methods, 2011. **8**(1): p. 91-96.

314. Rajotte, D., et al., *Molecular heterogeneity of the vascular endothelium revealed by in vivo phage display.* The Journal of clinical investigation, 1998. **102**(2): p. 430-437.

315. Arap, W., R. Pasqualini, and E. Ruoslahti, *Cancer treatment by targeted drug delivery to tumor vasculature in a mouse model.* Science, 1998. **279**(5349): p. 377-380.

316. Temming, K., et al., *RGD-based strategies for selective delivery of therapeutics and imaging agents to the tumour vasculature.* Drug resistance updates, 2005. **8**(6): p. 381-402.

317. Chen, X., et al., *MicroPET and autoradiographic imaging of breast cancer αv-integrin expression using 18F-and 64Cu-labeled RGD peptide.* Bioconjugate chemistry, 2004. **15**(1): p. 41-49.

318. Garanger, E., D. Boturyn, and P. Dumy, *Tumor targeting with RGD peptide ligands-design of new molecular conjugates for imaging and therapy of cancers.* Anti-Cancer Agents in Medicinal Chemistry (Formerly Current Medicinal Chemistry-Anti-Cancer Agents), 2007. **7**(5): p. 552-558.

319. Wculek, S.K. and I. Malanchi, *Neutrophils support lung colonization of metastasis-initiating breast cancer cells.* Nature, 2015. **528**(7582): p. 413.

320. Airas, L., et al., *CD73 is involved in lymphocyte binding to the endothelium: characterization of lymphocyte-vascular adhesion protein 2 identifies it as CD73.* Journal of Experimental Medicine, 1995. **182**(5): p. 1603-1608.

321. Dianzani, U., et al., *Interaction between endothelium and CD4+ CD45RA+ lymphocytes. Role of the human CD38 molecule.* The Journal of Immunology, 1994. **153**(3): p. 952-959.

322. Chakrabarti, S. and K.D. Patel, *Regulation of matrix metalloproteinase-9 release from IL-8-stimulated human neutrophils.* Journal of leukocyte biology, 2005. **78**(1): p. 279-288.

323. Koskinen, K., et al., *Granulocyte transmigration through the endothelium is regulated by the oxidase activity of vascular adhesion protein-1 (VAP-1).* Blood, 2004. **103**(9): p. 3388-3395.

324. Zernecke, A., et al., *CD73/ecto-5'-nucleotidase protects against vascular inflammation and neointima formation.* Circulation, 2006. **113**(17): p. 2120-2127.

325. Jalkanen, S., et al., *The oxidase activity of vascular adhesion protein-1 (VAP-1) induces endothelial E-and P-selectins and leukocyte binding.* Blood, 2007. **110**(6): p. 1864-1870.

326. Musso, T., et al., *CD38 expression and functional activities are up‑regulated by IFN‑γ on human monocytes and monocytic cell lines.* Journal of leukocyte biology, 2001. **69**(4): p. 605-612.

327. Wu, Q., et al., *IL-23-dependent IL-17 production is essential in neutrophil recruitment and activity in mouse lung defense against respiratory Mycoplasma pneumoniae infection.* Microbes and infection, 2007. **9**(1): p. 78-86.

328. Shrum, B., et al., *A robust scoring system to evaluate sepsis severity in an animal model.* BMC research notes, 2014. **7**(1): p. 233.

329. Greenberger, M.J., et al., *Neutralization of macrophage inflammatory protein-2 attenuates neutrophil recruitment and bacterial clearance in murine Klebsiella pneumonia.* The Journal of infectious diseases, 1996. **173**(1): p. 159-165.

330. Miller, L.S., et al., *MyD88 mediates neutrophil recruitment initiated by IL-1R but not TLR2 activation in immunity against Staphylococcus aureus.* Immunity, 2006. **24**(1): p. 79-91.

331. Scapini, P., et al., *The neutrophil as a cellular source of chemokines.* Immunological reviews, 2000. **177**(1): p. 195-203.

332. Issekutz, T.B., *In vivo blood monocyte migration to acute inflammatory reactions, IL-1 alpha, TNF-alpha, IFN-gamma, and C5a utilizes LFA-1, Mac-1, and VLA-4. The relative importance of each integrin.* The Journal of Immunology, 1995. **154**(12): p. 6533-6540.

333. Ruoslahti, E., *RGD and other recognition sequences for integrins.* Annual review of cell and developmental biology, 1996. **12**(1): p. 697-715.

334. Pasqualini, R., E. Koivunen, and E. Ruoslahti, *A peptide isolated from phage display libraries is a structural and functional mimic of an RGD-binding site on integrins.* The Journal of cell biology, 1995. **130**(5): p. 1189-1196.

335. Cinamon, G., V. Shinder, and R. Alon, *Shear forces promote lymphocyte migration across vascular endothelium bearing apical chemokines.* Nature immunology, 2001. **2**(6): p. 515.

336. Salmi, M., et al., *A cell surface amine oxidase directly controls lymphocyte migration.* Immunity, 2001. **14**(3): p. 265-276.

337. Yipp, B.G., et al., *Src-family kinase signaling modulates the adhesion ofPlasmodium falciparum on human microvascular endothelium under flow.* Blood, 2003. **101**(7): p. 2850-2857.

338. Diamond, M.S., et al., *Binding of the integrin Mac-1 (CD11b/CD18) to the third immunoglobulin-like domain of ICAM-1 (CD54) and its regulation by glycosylation.* Cell, 1991. **65**(6): p. 961-971.

339. Sperandio, M., C.A. Gleissner, and K. Ley, *Glycosylation in immune cell trafficking.* Immunological reviews, 2009. **230**(1): p. 97-113.

340. Strell, C. and F. Entschladen, *Extravasation of leukocytes in comparison to tumor cells.* Cell Communication and Signaling : CCS, 2008. **6**: p. 10-10.

341. Morello, S., et al., *Soluble CD73 as biomarker in patients with metastatic melanoma patients treated with nivolumab.* Journal of translational medicine, 2017. **15**(1): p. 244.

342. Antonioli, L., et al., *Anti-CD73 in cancer immunotherapy: awakening new opportunities.* Trends in cancer, 2016. **2**(2): p. 95-109.

343. Massagué, J. and A.C. Obenauf, *Metastatic colonization by circulating tumour cells.* Nature, 2016. **529**(7586): p. 298.

344. De Visser, K.E., A. Eichten, and L.M. Coussens, *Paradoxical roles of the immune system during cancer development.* Nature reviews cancer, 2006. **6**(1): p. 24-37.

345. Coffelt, S.B., M.D. Wellenstein, and K.E. de Visser, *Neutrophils in cancer: neutral no more.* Nature Reviews Cancer, 2016. **16**(7): p. 431.

346. Tabariès, S., et al., *Granulocytic immune infiltrates are essential for the efficient formation of breast cancer liver metastases.* Breast cancer research, 2015. **17**(1): p. 45.

347. Cools-Lartigue, J., et al., *Neutrophil extracellular traps sequester circulating tumor cells and promote metastasis.* The Journal of clinical investigation, 2013. **123**(8): p. 3446-3458.

348. Cools-Lartigue, J., et al., *Neutrophil extracellular traps in cancer progression.* Cellular and molecular life sciences, 2014. **71**(21): p. 4179-4194.

349. McDonald, B., et al., *Systemic inflammation increases cancer cell adhesion to hepatic sinusoids by neutrophil mediated mechanisms.* International journal of cancer, 2009. **125**(6): p. 1298-1305.

350. Angus, D.C. and R.S. Wax, *Epidemiology of sepsis: an update.* Critical care medicine, 2001. **29**(7): p. S109-S116.

351. Bone, R.C., *The pathogenesis of sepsis.* Annals of internal medicine, 1991. **115**(6): p. 457-469.

352. Cohen, J., et al., *Sepsis: a roadmap for future research.* The Lancet infectious diseases, 2015. **15**(5): p. 581-614.

353. Haycock, J., *Estimating Ten-Year Trends in Septic Shock Incidence and Mortality in United States Academic Medical Centers Using Clinical Data: Kadri SS, Rhee C, Strich JR, et al. Chest 2017; 151 (2): 278-285.* Journal of Emergency Medicine, 2017. **53**(1): p. 153.

354. Rhee, C., et al., *Incidence and trends of sepsis in US hospitals using clinical vs claims data, 2009-2014.* Jama, 2017. **318**(13): p. 1241-1249.

355. Neumann, P., *Lung Dysfunction in the Early Phase of Sepsis*, in *Sepsis and Organ Dysfunction*. 2000, Springer. p. 85-90.

356. Miyashita, T., et al., *A three-phase approach for the early identification of acute lung injury induced by severe sepsis.* in vivo, 2016. **30**(4): p. 341-349.

357. Brown, K., et al., *Neutrophils in development of multiple organ failure in sepsis.* The Lancet, 2006. **368**(9530): p. 157-169.

358. Aina, O.H., et al., *Therapeutic cancer targeting peptides.* Peptide Science, 2002. **66**(3): p. 184-199.

359. Baue, A., et al., *Sepsis and Organ Dysfunction:... from Chaos to Rationale*. 2012: Springer Science & Business Media.

360. Kreisel, D., et al., *In vivo two-photon imaging reveals monocyte-dependent neutrophil extravasation during pulmonary inflammation.* Proceedings of the National Academy of Sciences, 2010. **107**(42): p. 18073-18078.

361. Bhatia, M., R.L. Zemans, and S. Jeyaseelan, *Role of chemokines in the pathogenesis of acute lung injury.* American journal of respiratory cell and molecular biology, 2012. **46**(5): p. 566-572.

362. Grommes, J., et al., *Disruption of platelet-derived chemokine heteromers prevents neutrophil extravasation in acute lung injury.* American journal of respiratory and critical care medicine, 2012. **185**(6): p. 628-636.

363. Schulte, W., J. Bernhagen, and R. Bucala, *Cytokines in sepsis: potent immunoregulators and potential therapeutic targets—an updated view.* Mediators of inflammation, 2013. **2013**.

364. Cohen, J., *The immunopathogenesis of sepsis.* Nature, 2002. **420**(6917): p. 885.

365. Devitt, H.H., et al., *Hemodynamic and pathologic effects of prostacyclin on oleic acid-induced pulmonary injury.* Surgery, 1988. **103**(2): p. 213-220.

366. Beilman, G., *Pathogenesis of oleic acid-induced lung injury in the rat: distribution of oleic acid during injury and early endothelial cell changes.* Lipids, 1995. **30**(9): p. 817-823.

367. Derks, C.M. and D. Jacobovitz-Derks, *Embolic pneumopathy induced by oleic acid. A systematic morphologic study.* The American journal of pathology, 1977. **87**(1): p. 143.

368. Izeboud, C., et al., *Endotoxin-induced liver damage in rats is minimized by β 2-adrenoceptor stimulation.* Inflammation Research, 2004. **53**(3): p. 93-99.

369. Bharrhan, S., K. Chopra, and P. Rishi, *Vitamin E supplementation modulates endotoxin-induced liver damage in a rat model.* Am J Biomed Sci, 2010. **2**(1): p. 51-62.

370. Rittirsch, D., L.M. Hoesel, and P.A. Ward, *The disconnect between animal models of sepsis and human sepsis.* Journal of leukocyte biology, 2007. **81**(1): p. 137-143.

371. Nemzek, J.A., K.M.S. Hugunin, and M.R. Opp, *Modeling Sepsis in the Laboratory: Merging Sound Science with Animal Well-Being.* Comparative Medicine, 2008. **58**(2): p. 120-128.

372. SATO, K., et al., *In vivo lipid-derived free radical formation by NADPH oxidase in acute lung injury induced by lipopolysaccharide: a model for ARDS.* The FASEB Journal, 2002. **16**(13): p. 1713-1720.

373. Mei, S.H., et al., *Prevention of LPS-induced acute lung injury in mice by mesenchymal stem cells overexpressing angiopoietin 1.* PLoS medicine, 2007. **4**(9): p. e269.

374. Azzalini, L., V. Spagnoli, and H.Q. Ly, *Contrast-induced nephropathy: from pathophysiology to preventive strategies.* Canadian Journal of Cardiology, 2016. **32**(2): p. 247-255.

375. James, M.T., et al., *Contrast-induced acute kidney injury and risk of adverse clinical outcomes after coronary angiography: a systematic review and meta-analysis.* Circulation: Cardiovascular Interventions, 2013: p. CIRCINTERVENTIONS. 112.974493.

376. Pasqualini, R., et al., *Aminopeptidase N is a receptor for tumor-homing peptides and a target for inhibiting angiogenesis.* Cancer research, 2000. **60**(3): p. 722-727.

377. Lustberg, M.B., *Management of neutropenia in cancer patients.* Clinical advances in hematology & oncology: H&O, 2012. **10**(12): p. 825.

378. Weycker, D., et al., *Risk and consequences of chemotherapy-induced febrile neutropenia in patients with metastatic solid tumors.* Journal of oncology practice, 2014. **11**(1): p. 47-54.

379. Dennis, M.S., et al., *Albumin binding as a general strategy for improving the pharmacokinetics of proteins.* Journal of Biological Chemistry, 2002. **277**(38): p. 35035-35043.

380. Gómez-Cuadrado, L., et al., *Mouse models of metastasis: progress and prospects.* Disease Models & Mechanisms, 2017. **10**(9): p. 1061-1074.

381. Gillet, J.-P., S. Varma, and M.M. Gottesman, *The Clinical Relevance of Cancer Cell Lines.* JNCI Journal of the National Cancer Institute, 2013. **105**(7): p. 452-458.

382. Gao, D., et al., *Organoid cultures derived from patients with advanced prostate cancer.* Cell, 2014. **159**(1): p. 176-187.

383. Huch, M. and B.-K. Koo, *Modeling mouse and human development using organoid cultures.* Development, 2015. **142**(18): p. 3113-3125.

384. Zhang, D., et al., *Neutrophil ageing is regulated by the microbiome.* Nature, 2015. **525**(7570): p. 528.

385. Honda, K. and D.R. Littman, *The microbiome in infectious disease and inflammation.* Annual review of immunology, 2012. **30**: p. 759-795.

386. Schwabe, R.F. and C. Jobin, *The microbiome and cancer.* Nature Reviews Cancer, 2013. **13**(11): p. 800.

387. Vijay-Kumar, M., et al., *Metabolic syndrome and altered gut microbiota in mice lacking Toll-like receptor 5.* Science, 2010. **328**(5975): p. 228-231.

388. Stacker, S.A., et al., *VEGF-D promotes the metastatic spread of tumor cells via the lymphatics.* Nature medicine, 2001. **7**(2): p. 186.

389. Muller, W.A. and G.J. Randolph, *Migration of leukocytes across endothelium and beyond: molecules involved in the transmigration and fate of monocytes.* Journal of leukocyte biology, 1999. **66**(5): p. 698-704.

390. Petrova, T.V. and G.Y. Koh, *Organ-specific lymphatic vasculature: From development to pathophysiology.* Journal of Experimental Medicine, 2017: p. jem. 20171868.